NTRCI

NATIONAL TRANSPORTATION RESEARCH CENTER, INCORPORATED
University Transportation Center

U08: Finite Element Analysis Crash Model of Tractor-Trailers (Phase B)

This project was funded by the NTRCI University Transportation Center under a grant from the U.S. Department of Transportation Research and Innovative Technology Administration (#DTRT06G-0043) and Federal Highway Administration under Purchase Order # DTFH61-07-P-00235

The contents of this report reflect the views of the authors, who are responsible for the facts and the accuracy of the information presented herein. This document is disseminated under the sponsorship of the Department of Transportation University Transportation Centers Program and Federal Highway Administration, in the interest of information exchange. The U.S. Government assumes no liability for the contents or use thereof.

Chuck Plaxico, Chuck Miele and James Kennedy – Battelle
Srdjan Simunovic – Oak Ridge National Laboratory
Nikola Zisi – University of Tennessee

August, 2009

1. Report No.	2. Government Accession No.	3. Recipient's Catalog No.
4. Title and Subtitle **U08: Enhanced Finite Element Analysis Crash Model of Tractor-Trailers (Phase B)**		5. Report Date **August 2009** 6. Performing Organization Code
7. Author(s) **Chuck Plaxico, Chuck Miele and James Kennedy – Battelle** **Srdjan Simunovic – Oak Ridge National Laboratory** **Nikola Zisi – The University of Tennessee**		8. Performing Organization Report No.
9. Performing Organization Name and Address **National Transportation Research Center, Inc.** **University Transportation Center** **2360 Cherahala Blvd.** **Knoxville, TN 37932**		10. Work Unit No. (TRAIS) 11. Contract or Grant No. **RITA Grant – DTRT06G-0043** **FHWA Purchase Order - DTFH61-07-P-00235**
12. Sponsoring Agency Name and Address **U.S. Department of Transportation** **Research and Innovative Technology Administration and Federal Highway Administration** **1200 New Jersey Avenue, SE** **Washington, DC 20590**		13. Type of Report and Period Covered **Final Report August 2008 – August 2009** 14. Sponsoring Agency Code **RITA/FHWA**
15. Supplementary Notes		

16. Abstract

Improved understanding of truck-infrastructure crashes will enable the highway community to improve barrier design, to further reduce the likelihood of vehicle-infrastructure fatalities and injuries, and to reduce highway congestion resulting from severe accidents. In collaboration with the TFHRC, the National Transportation Research Center, Inc., University Transportation Center (NTRCI) has taken an active role in enhancing industry understanding of truck-infrastructure crash behavior through funding the development and enhancement of advanced finite element (FE) computer simulation models of truck-infrastructure crashes. NTRCI is helping provide highway engineers with data to make better, more well-informed roadside infrastructure decisions that enhance the safety of the traveling public.

The objective of this current investigation is to validate and enhance computer models of a tractor-semitrailer combination that will be used in analysis, design, and evaluation of roadside safety hardware. The research team is enhancing the overall fidelity of the tractor-semitrailer FE model by verifying vehicle failure modes from simulation against those from actual crash tests. This effort will enable the tractor-semitrailer FE model to provide more realistic predictions of crash performance and significantly reduce the need for costly full-scale truck testing. This report summarizes the results of the second phase (Phase B) of a three-phase program. In general terms, the plan for conducting this effort over three phases is as follows:

1. Phase A – Conduct an in-depth evaluation of the NCAC tractor only FE model, implement selected modifications, and develop a new trailer model.
2. Phase B – Complete preliminary modification of combined tractor-semitrailer FE models, provide them to the FHWA Center of Excellence (COE) community for beta testing, and validate them against suitable full-scale crash tests.
3. Phase C – Refine the combined tractor-semitrailer FE models and develop an interactive, online FE model user's website and a User's Manual document to facilitate the use of the model.

17. Key Word	18. Distribution Statement
finite element, crash model, tractor-trailer, crash analysis, National Crash Analysis Center, center of excellence, highway infrastructure, roadside safety hardware	**No restrictions**

19. Security Classif. (of this report)	20. Security Classif. (of this page)	21. No. of Pages	22. Price
Unclassified	**Unclassified**	**210**	

Table of Contents

EXECUTIVE SUMMARY **1**
CHAPTER 1 – INTRODUCTION **9**
ROADMAP FOR THIS REPORT 10
CHAPTER 2 – SYNTHESIS OF TRACTOR-SEMITRAILER CRASH TESTS **13**
SUMMARY OF TEST VEHICLE PROPERTIES 17
Test Vehicle Dimensions 18
Test Vehicle Mass 21
SUMMARY OF TEST RESULTS 21
Data Collection Methods 21
Accelerometer Results 23
CHAPTER 3 – SEMITRAILER MODEL DEVELOPMENT **51**
DESCRIPTION OF PHYSICAL TRAILER UPON WHICH THE MODEL IS BASED 51
DESCRIPTION OF THE TRAILER FE MODEL 53
Model Size Data 53
Time Step 54
Material Summary 54
Element Types Used 55
Connection Schemes Used 55
Accelerometers 56
Model Check Statistics 57
Any Sources of Possible Numerical Instabilities 57
FINITE ELEMENT MESHING AND MODELING APPROACH DETAILS FOR MAJOR COMPONENTS 57
Kingpin Box 57
Main Lateral Cross-Beams 60
Side-Walls 63
Upper and Lower Side Rails 66
Floor 71
Rear Bumper 73
Rear Frame and Bogie 76
CHAPTER 4 – SEMITRAILER MATERIAL PROPERTIES AND MATERIAL MODELS **83**
DRY FREIGHT TRAILER STRUCTURE 83
MATERIAL ASSIGNMENTS TO TRAILER PARTS 85
MATERIAL PROPERTIES AND MECHANICAL MODELS 96
CHAPTER 5 – AUTOMATED DIMENSIONAL ADJUSTMENTS TO THE TRACTOR AND TRAILER MODELS **97**
TRACTOR MODEL MODIFICATION STEPS 97
TRAILER FE MODEL MODIFICATIONS 111

Table of Contents (Continued)

CHAPTER 6 – ASSESSMENT OF TRACTOR-SEMITRAILER FE MODEL SIMULATION RESULTS 113
OVERVIEW OF THE MWRSF CRASH TEST TL5CMB-2 113
FINITE ELEMENT MODEL FOR TL5CMB-2 SIMULATION 116
SUMMARY OF KEY PHENOMENOLOGICAL EVENTS FROM THE TRACTOR-TRAILER FE MODEL SIMULATION 120
QUALITATIVE ASSESSMENT OF TRACTOR-TRAILER FE MODEL SIMULATION RESULTS 121
Qualitative Comparison of Simulation Results with Test TL5CMB-2 121
Qualitative Comparison of Simulation Results with Other Similar Tests 156
QUANTITATIVE ASSESSMENT OF TRACTOR-TRAILER FE MODEL SIMULATION RESULTS 164
Quantitative Validation Approach 164
Quantitative Evaluation Results 169
CHAPTER 7 – SUMMARY AND DISCUSSION OF RESULTS 171
MODEL ENHANCEMENT 171
MODEL VALIDATION 172
CHAPTER 8 – CONCLUSIONS AND RECOMMENDATIONS FOR FUTURE RESEARCH 175
RECOMMENDATIONS FOR FUTURE WORK 175
Interactive Tractor-Semitrailer Web Site 175
Users Handbook 176
Part Contact Survey 176
Trailer Suspension Properties 176
Extended Validation 177
Trailer Materials Testing 177
Leaf Spring Suspension for Semitrailer Model 177
Standard Trailer Lengths 177
Model Sensitivity Analysis and Uncertainty Quantification 177
More Extensive Literature Review 178
Model Evaluation for Other Impact Conditions 178
Conduct Full Scale Crash Test for FE Model Validation 179
APPENDIX A – VALIDATION/VERIFICATION REPORT FOR FE MODEL SIMULATION OF MWRSF TL5CMB-2 ..... A-1
APPENDIX B – REFERENCES B-1

List of Figures

Figure 1. Chart. Summary of wheelbase lengths of tractors and trailers used in full-scale tests. 19
Figure 2. Chart. Summary of axle loads of tractor-trailer vehicles used in full-scale crash tests. 20
Figure 3. Illustration. General EDR locations and nomenclature used in test reports. 23
Figure 4. Chart. Summary of peak 0.010-seconds average accelerations from accelerometer located inside tractor cabin near the tractor center of gravity..... 30
Figure 5. Chart. Summary of peak 0.010-seconds average accelerations from accelerometer located inside tractor cabin near the tractor fifth-wheel. 30
Figure 6. Chart. Summary of peak 0.010-seconds average accelerations from accelerometer located near the center of gravity of the trailer ballast. 31
Figure 7. Chart. Summary of peak 0.010-seconds average accelerations from accelerometer located near the trailer tandem axle. 31
Figure 8. Chart. Summary of peak 0.050-seconds average accelerations from accelerometer located inside tractor cabin near the tractor center of gravity..... 32
Figure 9. Chart. Summary of peak 0.050-seconds average accelerations from accelerometer located inside tractor cabin near the tractor fifth-wheel. 32
Figure 10. Chart. Summary of peak 0.050-seconds average accelerations from accelerometer located near the center of gravity of the trailer ballast. 33
Figure 11. Chart. Summary of peak 0.050-seconds average accelerations from accelerometer located near the trailer tandem axle..... 33
Figure 12. Chart. Summary of peak ASI values computed from accelerometer data. 34
Figure 13. Chart. Summary of peak 0.01-second moving average acceleration from full-scale tests..... 36
Figure 14. Chart. Summary of peak 0.05-second moving average acceleration from full-scale tests..... 36
Figure 15. Chart. Summary of peak ASI from full-scale tests..... 37
Figure 16. Chart. X-channel 0.050-seconds average acceleration-time history from accelerometer located inside tractor cabin near the tractor center of gravity (for 80,000-lb test vehicles)..... 37
Figure 17. Chart. Y-channel 0.050-seconds average acceleration-time history from accelerometer located inside tractor cabin near the tractor center of gravity (for 80,000-lb test vehicles)..... 38
Figure 18. Chart. ASI-time history from accelerometer located inside tractor cabin near the tractor center of gravity (for 80,000-lb test vehicles). 38
Figure 19. Chart. X-channel 0.050-seconds average acceleration-time history from accelerometer located inside tractor cabin near the tractor center of gravity (for 50,000-lb test vehicles)..... 39
Figure 20. Chart. Y-channel 0.050-seconds average acceleration-time history from accelerometer located inside tractor cabin near the tractor center of gravity (for 50,000-lb test vehicles)..... 39
Figure 21. Chart. ASI-time history from accelerometer located inside tractor cabin near the tractor center of gravity (for 50,000-lb test vehicles). 40
Figure 22. Chart. X-channel 0.050-seconds average acceleration-time history from accelerometer located near the tractor fifth-wheel (for 80,000-lb test vehicles). 40
Figure 23. Chart. Y-channel 0.050-seconds average acceleration-time history from accelerometer located near the tractor fifth-wheel (for 80,000-lb test vehicles). 41

List of Figures (Continued)

Figure 24. Chart. ASI-time history from accelerometer located near the tractor fifth-wheel (for 80,000-lb test vehicles). 41
Figure 25. Chart. X-channel 0.050-seconds average acceleration-time history from accelerometer located near the tractor fifth-wheel (for 50,000-lb test vehicles). 42
Figure 26. Chart. Y-channel 0.050-seconds average acceleration-time history from accelerometer located near the tractor fifth-wheel (for 50,000-lb test vehicles). 42
Figure 27. Chart. ASI-time history from accelerometer located near the tractor fifth-wheel (for 50,000-lb test vehicles). 43
Figure 28. Chart. X-channel 0.050-seconds average acceleration-time history from accelerometer located near the center of gravity of the trailer ballast (for 80,000-lb test vehicles). 43
Figure 29. Chart. Y-channel 0.050-seconds average acceleration-time history from accelerometer located near the center of gravity of the trailer ballast (for 80,000-lb test vehicles). 44
Figure 30. Chart. ASI-time history from accelerometer located near the center of gravity of the trailer ballast (for 80,000-lb test vehicles). 44
Figure 31. Chart. X-channel 0.050-seconds average acceleration-time history from accelerometer located near the center of gravity of the trailer ballast (for 50,000-lb test vehicles). 45
Figure 32. Chart. Y-channel 0.050-seconds average acceleration-time history from accelerometer located near the center of gravity of the trailer ballast (for 50,000-lb test vehicles). 45
Figure 33. Chart. ASI-time history from accelerometer located near the center of gravity of the trailer ballast (for 50,000-lb test vehicles). 46
Figure 34. Chart. X-channel 0.050-seconds average acceleration-time history from accelerometer located near the trailer tandem axle (for 80,000-lb test vehicles). 46
Figure 35. Chart. Y-channel 0.050-seconds average acceleration-time history from accelerometer located near the trailer tandem axle (for 80,000-lb test vehicles). 47
Figure 36. Chart. ASI-time history from accelerometer located near the trailer tandem axle (for 80,000-lb test vehicles). 47
Figure 37. Chart. X-channel 0.050-seconds average acceleration-time history from accelerometer located near the trailer tandem axle (for 50,000-lb test vehicles). 48
Figure 38. Chart. Y-channel 0.050-seconds average acceleration-time history from accelerometer located near the trailer tandem axle (for 50,000-lb test vehicles). 48
Figure 39. Chart. ASI-time history from accelerometer located near the trailer tandem axle (for 50,000-lb test vehicles). 49
Figure 40. Photograph. Stoughton 14.6-m (48-ft) semi trailer. 52
Figure 41. Photograph / Illustration. Kingpin box in place in the (a) physical trailer and the (b) FE model. 58
Figure 42. Photograph / Illustration. (a) Isolated view of the kingpin box after it was removed from the physical trailer and (b) the finite element model of the kingpin box. 58
Figure 43. Photograph / Illustration. (a) The kingpin box with material cut away to gain access to the inside structure (b) the finite element model of the kingpin box showing internal structure. 59
Figure 44. Illustration. Kingpin box showing internal plates and geometric detail. 60
Figure 45. Photograph / Illustration. View of the lower-rear section of the (a) physical trailer and (b) FE model showing structural detail. 61
Figure 46. Illustration. Lateral cross beams. 62

List of Figures (Continued)

Figure 47. Illustration. Lateral cross beams orientation with lower side rail. 62
Figure 48. Photograph / Illustration. View of the inside of the trailer box of (a) the physical trailer and (b) the FE model. 63
Figure 49. Photograph / Illustration. Cut section of the side-wall showing detail of sidewall components for (a) physical trailer and (b) FE model. 64
Figure 50. Illustration. Side-wall section detail. 64
Figure 51. Illustration. Side-wall section detail with plywood removed to show vertical steel hat-sections. 65
Figure 52. Illustration. Top side-wall connection showing CNRBs. 66
Figure 53. Photograph / Illustration. Cut section of the upper side rail of the trailer box of (a) the physical trailer and (b) the FE model showing the structural detail and connection methods. 67
Figure 54. Photograph / Illustration. Cut section of the lower side rail of the trailer box of (a) the physical trailer and (b) the FE model showing the structural detail and connection methods. 67
Figure 55. Illustration. Upper side rail model. 68
Figure 56. Illustration. Upper side rail to side-wall connection details. 69
Figure 57. Illustration. Lower side rail model. 70
Figure 58. Illustration. Lower side rail to side-wall connection details. 71
Figure 59. Photograph. Wooden floor cut section. 72
Figure 60. Illustration. Wooden floor FE model. 73
Figure 61. Illustration. Wooden floor FE model showing slanted plank interfaces. 73
Figure 62. Photograph. Rear bumper showing sectioned area. 74
Figure 63. Illustration. Rear bumper area FE model. 74
Figure 64. Illustration. Rear bumper area parts only. 75
Figure 65. Illustration. *Mat_Spotweld weld elements in rear bumper. 76
Figure 66. Photograph. Front view of trailer vehicle frame and bogie. 77
Figure 67. Illustration. Front view of trailer FE vehicle model of frame and bogie. 77
Figure 68. Photograph. Rear view of trailer vehicle frame and bogie. 78
Figure 69. Illustration. Rear view of trailer FE vehicle model of frame and bogie. 78
Figure 70. Illustration. Rear view of trailer suspension airbag and shock elements. 79
Figure 71. Illustration. Rear frame / bogie part thicknesses. 80
Figure 72. Illustration. Rear frame / bogie part thicknesses. 80
Figure 73. Illustration. Tire and wheel thicknesses. 81
Figure 74. Illustration. Parts identification for Stoughton trailers. 84
Figure 75. Illustration. Original sleeper-cab style tractor FE model. 99
Figure 76. Illustration. Initial removal of parts in the cut region. 100
Figure 77. Illustration. Cut sleeper-cab off. 101
Figure 78. Illustration. Addition of the new back of cabin. 101
Figure 79. Illustration. Tractor model with new cabin. 102
Figure 80. Illustration. Removal of middle set of fairings and exhaust stack. 103
Figure 81. Illustration. Cut frame rails to the desired wheelbase length. 104
Figure 82. Illustration. Cut fairings to match cut distance of frame rails. 105
Figure 83. Illustration. Scale (shorten) drive-shaft parts to match cut from frame rails. 106

List of Figures (Continued)

Figure 84. Illustration. Scales fairings and their support rails to match at their front counterparts. 106
Figure 85. Illustration. Front section translated to meet the back section. 107
Figure 86. Illustration. Close-up of the model with translated front. 107
Figure 87. Illustration. Final configuration after merging cut sections and adding the exhaust stack..... 108
Figure 88. Illustration. Cabin reconnected to frame rails. 109
Figure 89. Illustration. Overall bottom view of the final model. 109
Figure 90. Illustration. Close-Up bottom view of the final model. 110
Figure 91. Illustration. Detail view of the fairings fit. 110
Figure 92. Illustration. Fairing support rails and brackets. 111
Figure 93. Photograph. (a) Tractor-semitrailer vehicle and (b) 1.067 m tall concrete median barrier used in MwRSF Test No. TL5CMB-2. 114
Figure 94. Illustration. Dimensions of the MwRSF Test No. TL5CMB-2 test vehicle. 115
Figure 95. Photograph / Illustration. (a) Tractor test vehicle and (b) tractor FE model. 117
Figure 96. Illustration. Dimensions of the tractor-semitrailer FE vehicle model. 118
Figure 97. Illustration. Comparison of FE vehicle model dimensions to those of the test vehicle..... 119
Figure 98. Photograph / Illustration. Sequential views of MwRSF Test TL5CMB-2 and FE model simulation from a downstream viewpoint. 122
Figure 99. Photograph / Illustration. Sequential views of MwRSF Test TL5CMB-2 and FE model simulation from an upstream viewpoint. 128
Figure 100. Photograph / Illustration. Sequential views of MwRSF Test TL5CMB-2 and FE model simulation from an isometric viewpoint. 134
Figure 101. Illustration. Pertinent accelerometer locations in the FE model. 139
Figure 102. Chart. Longitudinal acceleration-time history plot from *accelerometer 14* inside the tractor cabin (10-millisecond and 50-millisecond moving averages)..... 141
Figure 103. Chart. Transverse acceleration-time history plot from *accelerometer 14* inside the tractor cabin (10-millisecond and 50-millisecond moving averages)..... 141
Figure 104. Chart. Transverse acceleration-time history plot from *accelerometer 14* inside the tractor cabin (10-millisecond and 50-millisecond moving averages)..... 141
Figure 105. Chart. ASI-time history plot from *accelerometer 14* inside the tractor cabin. 141
Figure 106. Chart. ASI-time history plot (excluding z-acceleration data) from *accelerometer 14* inside the tractor cabin. 142
Figure 107. Chart. Roll, pitch and yaw-time history plot from *accelerometer 14* location inside the tractor cabin. 142
Figure 108. Chart. Longitudinal acceleration-time history plot from *accelerometer 15* near the tractor fifth-wheel (10-millisecond and 50-millisecond moving averages). 142
Figure 109. Chart. Transverse acceleration-time history plot from *accelerometer 15* near the tractor fifth-wheel (10-millisecond and 50-millisecond moving averages). 143
Figure 110. Chart. Transverse acceleration-time history plot from *accelerometer 15* near the tractor fifth-wheel (10-millisecond and 50-millisecond moving averages). 143
Figure 111. Chart. ASI-time history plot from *accelerometer 15* near the tractor fifth-wheel. 143
Figure 112. Chart. ASI-time history plot (excluding z-acceleration data) from *accelerometer 15* near the tractor fifth-wheel. 144
Figure 113. Chart. Roll, pitch and yaw-time history plot from *accelerometer 15* near the tractor fifth-wheel. 144

List of Figures (Continued)

Figure 114. Chart. Longitudinal acceleration-time history plot from *accelerometer 15* near the tractor fifth-wheel (10-millisecond and 50-millisecond moving averages). 145
Figure 115. Chart. Transverse acceleration-time history plot from *accelerometer 15* near the tractor fifth-wheel (10-millisecond and 50-millisecond moving averages). 145
Figure 116. Chart. Transverse acceleration-time history plot from *accelerometer 15* near the tractor fifth-wheel (10-millisecond and 50-millisecond moving averages). 145
Figure 117. Chart. ASI-time history plot from *accelerometer 15* near the tractor fifth-wheel. 146
Figure 118. Chart. ASI-time history plot (excluding z-acceleration data) from *accelerometer 15* near the tractor fifth-wheel. 146
Figure 119. Chart. Roll, pitch and yaw-time history plot from *accelerometer 15* near the tractor fifth-wheel. 146
Figure 120. Chart. Longitudinal acceleration-time history plot from the FE simulation and Test TL5CMB-2 from accelerometer at the trailer tandem (50-millisecond moving averages). .. 148
Figure 121. Chart. Lateral acceleration-time history plot from the FE simulation and Test TL5CMB-2 from accelerometer at the trailer tandem (50-millisecond moving averages). 148
Figure 122. Chart. Vertical acceleration-time history plot from the FE simulation and Test TL5CMB-2 from accelerometer at the trailer tandem (50-millisecond moving averages). 149
Figure 123. Chart. ASI-time history plot from the FE simulation and Test TL5CMB-2 from accelerometer at the trailer tandem. 149
Figure 124. Chart. Roll angle-time history plot of the rear section of the trailer from the FE simulation and Test TL5CMB-2. 150
Figure 125. Photograph. Post test view of test vehicle illustrating excessive damage after secondary impact. 151
Figure 126. Photograph. Post test view of the trailer showing damage to sidewall and external ribs. ... 152
Figure 127. Illustration. Contour of effective plastic strain (with contours cut-off at 10%) used to identify areas of the tractor model that sustained damage during simulated impact. 153
Figure 128. Illustration. Contour of effective plastic strain (with contours cut-off at 10%) used to identify areas of the tractor model that sustained damage during simulated impact. 153
Figure 129. Illustration. Contour of effective plastic strain (with contours cut-off at 10%) used to identify areas of the tractor model that sustained damage during simulated impact. 154
Figure 130. Illustration. Contour of effective plastic strain (with contours cut-off at 10%) used to identify areas of the trailer model that sustained damage during simulated impact. 154
Figure 131. Illustration. Contour of effective plastic strain (with contours cut-off at 10%) used to identify areas of the trailer model that sustained damage during simulated impact. 155
Figure 132. Illustration. Contour of effective plastic strain (with contours cut-off at 10%) used to identify areas of the trailer model that sustained damage during simulated impact. 155
Figure 133. Chart. Results of FE simulation compared to full-scale crash tests regarding peak 0.01-second moving average of the three accelerometer channels at four locations on the vehicle. 157
Figure 134. Chart. Results of FE simulation compared to full-scale crash tests regarding peak 0.05-second moving average of the three accelerometer channels at four locations on the vehicle. 158
Figure 135. Chart. Results of FE simulation compared to full-scale crash tests regarding peak ASI values at four locations on the vehicle. 158

List of Figures (Continued)

Figure 136. Chart. X-channel 0.050-seconds average acceleration-time history from accelerometer located inside tractor cabin near the tractor center of gravity from simulation and full-scale test Group A. 159
Figure 137. Chart. Y-channel 0.050-seconds average acceleration-time history from accelerometer located inside tractor cabin near the tractor center of gravity from simulation and full-scale test Group A. 160
Figure 138. Chart. ASI-time history from accelerometer located inside tractor cabin near the tractor center of gravity from simulation and full-scale test Group A. 160
Figure 139. Chart. X-channel 0.050-seconds average acceleration-time history from accelerometer located near the tractor fifth-wheel from simulation and full-scale test Group A. 161
Figure 140. Chart. Y-channel 0.050-seconds average acceleration-time history from accelerometer located near the tractor fifth-wheel from simulation and full-scale test Group A. 161
Figure 141. Chart. ASI-time history from accelerometer located near the tractor fifth-wheel from simulation and full-scale test Group A. 162
Figure 142. Chart. X-channel 0.050-seconds average acceleration-time history from accelerometer located near the trailer tandem axle from simulation and full-scale crash tests Group A. .. 162
Figure 143. Chart. Y-channel 0.050-seconds average acceleration-time history from accelerometer located near the trailer tandem axle from simulation and full-scale crash tests Group A. .. 163
Figure 144. Chart. ASI-time history from accelerometer located near the trailer tandem axle from simulation and full-scale crash tests Group A. 163

List of Tables

Table 1. Summary of Full Scale Tractor-Semitrailer Crash Tests. 15
Table 2. Summary of Full Scale Tractor-semitrailer Dimensions and Mass Properties. 16
Table 3. Summary of EDR Type and Placement used in Full-scale Crash Tests. 22
Table 4. Summary of Peak 0.010-second Average Accelerations and ASI from Accelerometers Located on Tractor. 24
Table 5. Summary of Peak 0.010-second Average Accelerations and ASI from Accelerometers Located on Trailer. 25
Table 6. Summary of Peak 0.050-second Average Accelerations from Accelerometers Located on Tractor. 26
Table 7. Summary of Peak 0.050-second Average Accelerations from Accelerometers Located on Trailer. 27
Table 8. Acceleration Severity Index (ASI) Standards. 28
Table 9. Summary of the Highest, Lowest and Average of the Peak Values for Each Test Group at each Accelerometer Location. 34
Table 10. Summary of the Highest, Lowest and Average of the Peak Values for Each Test Group at Each Accelerometer Location. 35
Table 11. Material Abbreviations. 86
Table 12. Material Assignments for Semitrailer Parts. 87
Table 13. FE Model Part List and Material Assignment 93
Table 14. Summary of Phenomenological Events that Occurred during Full-scale Test and FE Model Simulation. 138
Table A-1. Analysis Solution Verification Table. A-3
Table A-2a. Roadside Safety Validation Metrics Rating Table – Time History Comparisons. A-5
Table A-2b. Roadside Safety Validation Metrics Rating Table – Time History Comparisons (Multiple channels). A-7
Table A-3. Evaluation Criteria Test Applicability Table. A-8
Table A-4. Roadside Safety Phenomena Importance Ranking Table. A-10

List of Equations

Equation 1. Equation for calculating the acceleration severity index (ASI) 28
Equation 2. Equations for calculating the Sprague & Geers metrics 166
Equation 3. Equations for calculating the ANOVA metrics 166

Executive Summary

While many highway crashes involve vehicle-to-vehicle impacts, a substantial number of injuries and fatalities result from single vehicle impacts with roadside infrastructure such as guardrails, protective barriers, roadway signs and other fixed objects. The design and engineering of these structures strongly influence the injury-causing g-forces experienced by vehicle occupants and whether or not vehicles are redirected back into traffic.

The U.S. Department of Transportation (USDOT) and state Departments of Transportation have conducted extensive, full-scale passenger car-barrier crash tests to better understand crash performance of guardrails and barriers and to improve their design. However, very limited work has been conducted on crash performance of barriers when impacted by medium and heavy duty trucks due to the cost and the complexity of full scale truck testing. Substantially more data and better understanding of truck-infrastructure crashes would enable the highway community to improve barrier design, to further reduce the likelihood of vehicle-infrastructure fatalities and injuries and to reduce highway congestion resulting from severe accidents.

In collaboration with the TFHRC, the National Transportation Research Center, Inc., University Transportation Center (NTRCI) has taken an active role in enhancing industry understanding of truck-infrastructure crash behavior through funding the development and enhancement of advanced finite element (FE) computer simulation models of truck-infrastructure crashes. Recent NTRCI funded work on refinement and enhancement of models of single unit truck crashes into concrete barriers has demonstrated the ability of this advanced computer simulation technology to provide sorely needed high quality data and analysis results at substantially lower cost than full-scale crash tests. NTRCI is helping provide highway engineers with data to make better, more well-informed roadside infrastructure decisions that enhance the safety of the traveling public.

To build upon its success with single-unit truck crash simulation and analysis, NTRCI has funded the research team of Battelle, Oak Ridge National Laboratory (ORNL) and the University of Tennessee at Knoxville (UTK) to conduct a three-phase investigation to enhance and refine a FE model for simulating tractor-semitrailer crash events involving barriers and roadside safety hardware such as bridge rails and median barriers. The tractor model was originally developed by the National Crash Analysis Center (NCAC) of George Washington University (GWU) and requires refinement and testing before it can be used by the engineering community for infrastructure design.

The objective of this current investigation led by Battelle is to validate and enhance computer models of a tractor-semitrailer combination that will be used in analysis, design, and evaluation of roadside safety hardware.

Phase A was completed in Year 1of the project and was documented in the Phase A Final Report[i]. Phase B was completed in Year 2 of the project and the results of that effort are documented herein. The tasks completed in Phase B include:

- A synthesis of the full-scale tractor-semitrailer crash tests from the literature
- Completing the semitrailer FE model development, including assignment of material properties obtained through ORNL's research
- Development of Automated Dimensional Adjustment Programs (ADAP) that facilitate modifications to the tractor FE model to produce various wheelbase and cab styles to accommodate closer comparison with the variety of crash test vehicles.
- Release of the combined tractor-semitrailer FE model to the FHWA Finite Element Centers of Excellence (COE) community for beta testing and comment
- Evaluation of the combined tractor-semitrailer FE model by comparison of computer simulation results to full-scale tractor-semitrailer crash test results

Following is a brief summary of the research conducted in Phase B and associated results.

Synthesis of Full-Scale Tractor-Semitrailer Crash Tests. Chapter 2 of the Phase B report is a synthesis of the full-scale crash test data gathered from the literature search in Phase A. The purpose of this synthesis was to provide an understanding of vehicle kinematic behavior and vehicle accelerations (via on-board vehicle acceleration data) during impact in order to assess the general reasonability and fidelity of the tractor-semitrailer vehicle FE model.

The data that were used in the synthesis were from full-scale crash tests that were conducted for the purpose of evaluating the crashworthiness of roadside safety barriers (e.g., bridge rails and roadside median barriers) for use on the National Highway System (NHS). As such, they were conducted under the testing procedures and evaluation guidelines required by the Federal Highway Administration (FHWA). The test guidelines do not require a specific make or model for the test vehicle, but rather provide recommended properties for test vehicles which are representative of various classes of vehicles. The tests were conducted over a span of 26 years, beginning in 1981 and encompass a wide range of vehicle makes, models and overall dimensions. None of the test vehicles were consistent with the properties of the 1992 Freightliner FLD120 tractor upon which the FE model was based.

Because the tests were focused on performance of the barrier, very little information was provided in the reports regarding damage and response of the vehicle. For the purposes of FE model validation, it was necessary to obtain the electronic data (e.g., accelerometer, rate gyros,

[i] Plaxico, C., Kennedy, J., Simunovic, S., and Zisi, N, Enhanced Finite Element Analysis Crash Model of Tractor-Trailers (Phase A), National Transportation Research Center, Inc., Knoxville, TN, 2008.

photos, videos, etc.) corresponding to these tests and to discern as much information as possible relating to the vehicle's response during impact, and then reduce, or synthesize all the data into a useable form for the purpose of general comparison of FE model with the crash test results.

The result of this effort was an extensive set of tables and figures that summarize the general response of tractor-semitrailer vehicles impacting road-side safety barriers based on impact conditions, vehicle properties, and barrier height. This information was used as a gauge to assess the validity of the results from the finite element model.

Semitrailer Model Development. Chapter 3 of the Phase B report describes the continued, more detailed development of the semitrailer FE model. In order to obtain the most accurate geometric and structural properties of the trailers components for FE model development, a 14.6-m (48-foot), dual-tire, tandem axle 1990 Stoughton box trailer was purchased for purposes of disassembling, sectioning and measuring key trailer model components. The methodology and FE modeling implementation details of the specific structural features that were included in the semitrailer FE model are discussed in this chapter. The result of this effort was a more comprehensive and accurate finite element model of the semitrailer leading to better overall fidelity of the tractor-semitrailer FE model, as compared to full-scale crash test results.

Semitrailer Material Properties and Material Models. Chapter 4 of the Phase B report describes the process of obtaining material property data from the open literature and from semitrailer manufacturer's information. It describes and lists the actual material property assignments in the FE model for each part in the semitrailer FE model.

The material assignment for the semitrailer model consisted of three tasks. The first task was to determine the list of structural parts in the semitrailer and their organization as functional groups. The next task was to determine the types of materials and their designation for each of the parts. As different manufacturers have different trailer designs and employ different materials, the first two steps resulted in several part and material assignment schemes. Trailer manufacturers generally do not reveal the specific material grades used for specific parts, so the search had to include original and aftermarket parts suppliers. The third step was to determine elastic and elastic-plastic mechanical properties for each material. The properties were then formatted in the input form for constitutive material models used in LS-DYNA.

The result of this effort was a more accurate and comprehensive materials database for use in the finite element model of the semitrailer. The materials database was implemented as a separate file included in the overall model. This simplifies material management, and provides for easier reformulation of material properties in the model.

Automated Dimensional Adjustments to the Tractor-Semitrailer Models. Tractors and semitrailers are available in many different sizes based on model options, so they vary widely in their dimensional, inertial and impact characteristics. Those basic dimensional differences make it difficult to compare simulations and experiments with only one make and model of tractor and

semitrailer available. It would be beneficial to researchers to be able to adjust existing models without having to build a new vehicle model for each new vehicle configuration.

In addition, all roadside safety hardware used on the National Highway System (NHS) must meet the testing requirements of National Cooperative Highway Research Program (NCHRP) Report 350 Recommended Procedures for the Safety Performance Evaluation of Highway Appurtenances[ii]. This document contains recommended procedures for evaluating the safety performance of various highway safety features. The vehicle dimensions in the original tractor vehicle FE model need to be altered to meet NCHRP Report 350 requirements before being applied in the analysis of roadside safety structures. NCHRP Report 350 does not require a specific make or model for the test vehicle, but rather provides recommended properties for the test vehicles to represent various classes of vehicles. NCHRP Report 350 Test Level 5 requires that the maximum tractor wheelbase not exceed 189 inches for the 36000V vehicle (79,366-lb tractor/van-semitrailer), whereas the current FE model's wheelbase length is 217.2 inches (5.52 m) and includes a sleeper-cab.

Chapter 5 of the Phase B report describes a set of model modification "scripts" called ADAP (Automated Dimensional Adjustment Program) developed to facilitate modification of the tractor and semitrailer FE models (e.g., remove sleeper cabin and shorten wheelbase length). ADAP provides researchers a larger variety of tractor-semitrailer vehicle models to use in their crash simulations. For this project, ADAP provided the research team a means of modifying the dimensions of the vehicle model to match those of previous full-scale crash tests for model validation purposes.

Assessment of Tractor-Semitrailer Simulation Results. The performance of the tractor-semitrailer FE model was assessed by comparing simulation results to data obtained from full-scale crash tests. Of the twelve full-scale tractor-semitrailer crash tests identified in the literature summary, five of them involved a day-cab style tractor pulling a 12.2 to 14.6 m (40 to 48-ft) box-semitrailer impacting a 1,067 mm (42 in) tall barrier at a nominal speed of 80 km/hr at 15 degrees. The most recent of these tests was conducted at the Midwest Roadside Safety Facility on July 12, 2007 (Test No. TL5CMB-2). For evaluation purposes, the finite element analysis was set up to emulate the impact conditions and test vehicle dimensions of that particular test.

Chapter 6 of the Phase B report presents a summary of the tractor-semitrailer FE model and an evaluation of the results of the model compared to the full-scale crash test TL5CMB-2. A qualitative and a quantitative evaluation of the FE model simulation results are presented; however, the overall evaluation is largely qualitative, because the only quantitative data from test TL5CMB-2 was from a single triaxial accelerometer located on the floor of the trailer near the

[ii] Ross, H.E., D.L. Sicking, and H.S. Perrara, "Recommended Procedures for the Safety Performance Evaluation of Highway Appurtenances," *National Cooperative Highway Research Program Report No. 350*, Transportation Research Board, Washington, D.C., 1993.

tandem axle. A general assessment of the model's results is also presented based on a comparison to results of similar tests in the literature.

Chapter 7 of the report discusses the detailed results of the evaluation of the tractor-semitrailer FE model's performance in comparison with full-scale tractor-semitrailer crash test results from MwRSF Test No. TL5CMB-2. In the qualitative assessment, the general response of the modified FE model compared well to test TL5CMB-2; the simulation results replicated the basic timing and magnitudes of phenomenological events that occurred in the full-scale test. A comparison of sequential views of the test and simulation showed that the attitudes (e.g., roll and pitch) of both the tractor and the semitrailer models were consistent with the behavior of the vehicle in the full-scale crash test.

A more general qualitative assessment of the FE model's results was made based on a comparison with additional similar full-scale tests from the literature. In particular, the FE simulation was compared to tests that involved a tractor-semitrailer ballasted to a nominal weight of 36,287 kg (80,000 lb) impacting a 1,067 mm (42-inch) tall barrier at a nominal speed and angle of 80 km/hr and 15 degrees. In that assessment, the peak values of the 0.05-seconds moving average acceleration compared reasonably well in all locations where data were collected, except for the vertical component of acceleration at the tractor cabin.

The response of the tractor-semitrailer FE model was also assessed by a quantitative comparison of the simulation results with those from test TL5CMB-2 using computer software that calculates validation metrics that quantify the similarity of acceleration time-history data between a simulation and test.

The quantitative evaluation provided mixed results. Based on one of the metrics, a comparison of the individual components of acceleration indicated that the simulation was not in agreement with the test, but the comparison of the ASI (Acceleration Severity Index)-time history, which is a composite of the x-, y-, and z-accelerations, indicated that the simulation and test were in very good agreement. Based on another metric, the simulation was shown to be in good agreement with the test regarding comparison of the individual components of acceleration as well as the ASI-time history.

The quantitative metrics and the validation criteria used in this assessment are consistent with those *currently* suggested by the NCHRP 22-24 project team. The NCHRP project is still underway, thus the validation procedures used in this report are tentative and will be finalized in Phase C.

Current Status of Model Development. The overall development of the finite element model of a tractor-semitrailer was completed in Phase B. The model has been reasonably validated based on comparison with full-scale crash tests results. More specifically, the general response of the FE model replicates the basic timing and magnitudes of phenomenological events that occurred in full-scale crash tests of tractor-semitrailer impacts with rigid longitudinal barriers. The quantitative validation, which was based on a comparison of a triaxial accelerometer data at

a single location on the tractor-semitrailer vehicle, provided mixed results based on currently suggested metrics.

All validation so far on this tractor-semitrailer FE model has been done by comparison to redirective impact type crash tests into rigid barriers consistent with the test requirements of NCHRP Report 350 Test 5-12 (e.g., impact speed and angle of 80 km/hr and 15 degrees, respectively). The research team believes that this tractor-semitrailer FE model is reasonably valid for this type of crash simulation and that it will provide useful results in general barrier design evaluation work, regarding impact loads and vehicle-barrier interaction. However, the model has not been assessed for use in other applications such as high-energy impacts (e.g., full frontal impact with bridge pier), general vehicle dynamics (e.g., vehicle response due to steer maneuvers) or vehicle-to-vehicle impacts, to name a few.

Online User Manual and Website. Modern vehicle FE models contain a large of number of submodels, parts, components, and systems with complex properties, interaction, connectivity, spatial and functional relations that are best described using interactive, cross-linked web-based documentation that mimics the relations in the model. A database linked to a web site enables interactive documentation and analysis of the FEA model. In addition to the model development described above, this project includes development of an online User Manual for the tractor-trailer FE model which generates content dynamically based on user selections and inquiries. A preliminary version of the online manual has been developed in Phase B, described in Chapter 8 of the report.

Over the course of Phase B UTK, in collaboration with ORNL, developed a database and associated software that enable interactive documentation and understanding of the tractor-trailer FE model. The package was built around a database management system that incorporated the tractor-trailer database. This database was populated directly from the FE model with a Perl code procedure, and it has the capability to generate content dynamically based on user selections and inquiries. Incorporated Perl based web technologies facilitated the development of a dynamic web server system that can continuously be updated in a speedy fashion as new versions of the FE model evolve, or enhanced display and inquiry options are being sought from the end users.

The design process took several steps to complete. A comprehensive look in the structure of the LS-DYNA FE model input file and the composition of the web site yielded into identification of entities and their attributes that required storage. The subsequent data structure normalization resulted with table identification, definition of columns in these tables, assignment of optimal data types to the columns, and establishment of primary keys. Table relationships were then identified and implemented with creation of foreign keys. The data model was finally refined with inclusion of junction tables that reduced many-to-many relationships to two one-to-many relationships. The database creation act was instigated with a written SQL script, which can

easily be expanded to accommodate future demand. Code was then written in Perl to populate the tractor database with:

- Lookup tables for three part affiliations, sections, materials, constraints, contacts, and sets
- Brief definition tables for parts, sections, materials, tables, curves, constraints, contacts, and sets
- Data definition tables for sections, materials, tables, curves, constrains, contacts, sets, hourglass, and input FE model file lines
- Junction tables for three part affiliations

The tractor web server was built on Perl scripts that receive user requests, interact with the database and serve requested content. The current display capability includes briefs for parts, sections, materials, tables, curves, constrains, and contacts. The data are neatly stored in tables and cross linked appropriately. A more detailed data view of the selected entity offers the user an opportunity to launch a popup window to glimpse the excerpt of the FE model file that served as a source for populating the database.

Plans for Phase C of the Investigation. The goal of the NTRCI FEA Research Team's proposed third phase of this effort is to complete the evaluation, enhancement and validation of the tractor-semitrailer model for redirective impact type crash tests into rigid barriers. The goals of Phase C will be addressed through three specific objectives:

1. Provide a validated generic tractor-semitrailer model to NTRCI for use in analyses of redirective -type crash tests into rigid barriers by the roadside safety research community,
2. Create a User Handbook to facilitate use of the model and document the methodology of model development
3. Implement a user's interactive website and User Manual for the tractor-semitrailer FE model.

At the conclusion of Phase C, the tractor-semitrailer FE model will be suitable for use in crash barrier design and evaluation according to industry best practices such as National Cooperative Highway Research Program (NCHRP) Report 350. Details of the planned effort are described in the NTRCI FEA Research Team's proposal for Phase C.

Chapter 1 – Introduction

In recent decades, the highway community, including the U.S. Department of Transportation (USDOT), the Federal Highway Administration (FHWA), the Turner Fairbank Highway Research Center (TFHRC), and state Departments of Transportation have supported and conducted extensive full-scale passenger car-barrier crash tests to better understand crash performance of guardrails and barriers and to improve their design and to reduce the likelihood of vehicle-infrastructure crash fatalities and injuries.

Improved understanding of truck-infrastructure crashes will enable the highway community to improve barrier design, to further reduce the likelihood of vehicle-infrastructure fatalities and injuries, and to reduce highway congestion resulting from severe accidents. In collaboration with the TFHRC, the National Transportation Research Center, Inc., University Transportation Center (NTRCI) has taken an active role in enhancing industry understanding of truck-infrastructure crash behavior through funding the development and enhancement of advanced finite element (FE) computer simulation models of truck-infrastructure crashes. NTRCI is helping provide highway engineers with data to make better, more well-informed roadside infrastructure decisions that enhance the safety of the traveling public.

NTRCI has funded the research team of Battelle, Oak Ridge National Laboratory (ORNL), and the University of Tennessee at Knoxville (UTK) to conduct a three-phase investigation to enhance and refine a FE model for simulating tractor-semitrailer crash events involving barriers and roadside safety hardware such as bridge rails and median barriers. The tractor model was originally developed by the National Crash Analysis Center (NCAC) of George Washington University (GWU) and requires refinement and testing before it can be used by the engineering community for infrastructure design.

The objective of this current investigation led by Battelle is to validate and enhance computer models of a tractor-semitrailer combination that will be used in analysis, design, and evaluation of roadside safety hardware. The research team is enhancing the overall fidelity of the tractor-semitrailer FE model by verifying vehicle failure modes from simulation against those from actual crash tests. This effort will enable the tractor-semitrailer FE model to provide more realistic predictions of crash performance and significantly reduce the need for costly full-scale truck testing. This report summarizes the results of the second phase of a three-phase program. In general terms, the plan for conducting this effort over three phases is as follows:

4. Phase A – Conduct an in-depth evaluation of the NCAC tractor only FE model, implement selected modifications, and develop a new trailer model.

5. Phase B – Complete preliminary modification of combined tractor-semitrailer FE models, provide them to the FHWA Center of Excellence (COE) community for beta testing, and validate them against suitable full-scale crash tests.

6. Phase C – Refine the combined tractor-semitrailer FE models and develop an interactive, online FE model user's website and a User's Manual document to facilitate the use of the model.

Phase A was completed in Year 1of the project and was documented in the Phase A Final Report [1]. Phase B was completed in Year 2 of the project and the results of that effort are documented herein.

The intended application of the tractor-semitrailer model is to evaluate the crash performance of roadside safety features based on the crash test guidelines of National Cooperative Highway Research Program (NCHRP) Report 350 Recommended Procedures for the Safety Performance Evaluation of Highway Appurtenances for Test Level 5 [2]. In such applications, the tractor serves as a "bullet" vehicle, so model performance is judged by accuracy of load transfer of the vehicle to the barrier and accuracy in simulating the kinematic behavior of the tractor during and after impact.

Roadmap for this Report

This report covers a range of technical issues required for development and refinement of the tractor-semitrailer combination vehicle FE model. The report is organized into 9 chapters as follows.

- **Chapter 2. Synthesis of Full-Scale Tractor-Semitrailer Crash Tests –** A synthesis of the full-scale crash test data gathered from the literature search in Phase A. The purpose of this synthesis was to provide an understanding of vehicle kinematic behavior and vehicle accelerations (via on-board vehicle acceleration data) during impact in order to assess the general reasonability and fidelity of the tractor-semitrailer vehicle FE model.

- **Chapter 3. Semitrailer Model Development –** A summary of the methodology and FE modeling implementation details of the specific structural features of the semitrailer FE model.

- **Chapter 4. Semitrailer Material Properties and Material Models –** A summary of the process of obtaining material property data, description of the actual material property assignments, and a material database that includes detailed material property definitions for each component part of the semitrailer model.

- **Chapter 5. Automated Dimensional Adjustments to the Tractor-Semitrailer Models –** A summary of the development and application of a set of model modification "scripts" called ADAP (Automated Dimensional Adjustment Program) developed to facilitate the basic changes to the tractor and semitrailer FE models (e.g., remove sleeper cabin and shorten wheelbase length).

- **Chapter 6. Assessment of Tractor-Semitrailer Simulation Results –** A summary of the tractor-semitrailer FE model and an evaluation of the results of the model compared to a full-scale crash test. A qualitative and a quantitative evaluation of the FE model simulation results are presented.

- **Chapter 7. Summary and Discussion of Results –** A summary and discussion of the results of the evaluation of the tractor-semitrailer FE model's performance in comparison with a full-scale tractor-semitrailer crash test.

- **Chapter 8. Conclusions and Recommendations for Future Research –** Summarizes the general conclusions regarding the development, model enhancements, the qualitative and quantitative validations of the tractor-semitrailer FE model and provides recommendations for additional research to further improve the accuracy, robustness, and applicability of the tractor-semitrailer FE model.

Chapter 2 – Synthesis of Tractor-Semitrailer Crash Tests

A literature review was performed to acquire information regarding the dynamic response of tractor-trailer vehicles during impact with roadside barriers. The results of this review are a synthesis and a documentation of the test data applicable to the tractor-semitrailer FE model. The purpose of this synthesis was to provide an understanding of vehicle kinematic behavior and vehicle accelerations (via on-board vehicle acceleration data) during impact in order to assess the general reasonability and fidelity of the tractor-semitrailer vehicle FE model.

All of the tests used in the synthesis were conducted for the purpose of evaluating bridge rails and roadside median barriers for use on the National Highway System (NHS), and as such, these tests were conducted under the testing procedures and evaluation guidelines required by FHWA. The current test procedures are documented in NCHRP Report 350, which contains recommended procedures for evaluating the safety performance of various highway safety features [2].

NCHRP Report 350 presents uniform guidelines for the crash testing of both permanent and temporary highway safety features and recommended evaluation criteria to assess test results. These guidelines and criteria incorporate current technology and the collective judgment and expertise of professionals in the field of roadside safety design. They provide (1) a basis on which researchers and user agencies can compare the impact performance merits of candidate safety features, (2) guidance for developers of new safety features, and (3) a basis on which user agencies can formulate performance specification for safety features. Test Levels 4, 5 and 6 in Report 350 are intended to evaluate strength of safety barriers for containing and redirecting heavy vehicles such as single-unit trucks and tractor-trailer vehicles. Report 350 does not require a specific make or model for the test vehicle, but rather provides recommended properties for test vehicles for representing various classes of vehicles.

The purpose of most of the crash tests reviewed was not to track the vehicles' response, but rather to evaluate the performance of roadside barriers. On-vehicle instrumentation was intended to obtain occupant impact data and accident severity caused by impact with a particular barrier. The one exception was the NCAC crash test of a tractor-only which was used to validate the FE tractor model.

Meaningful comparisons to the test data were made at the qualitative and quantitative level (refer to Chapter 6). Generally, the kind of data available from the crash tests was better for making qualitative comparisons (overall observed vehicle behavior) than it was for the more absolute quantitative comparisons involving event-timing, acceleration-time histories, and acceleration values. Nonetheless, some reasonable quantitative comparisons were made and are reported in this section.

Crash test reports were obtained for 12 crash tests involving tractor-semitrailer impacts into roadside safety barriers [3, 4, 5, 6, 7, 8, 9, 10, 11, 12, 13, 14]. These tests were conducted over a

span of 26 years beginning in 1981. Of those tests, nine were conducted at the Texas Transportation Institute (TTI) in College Station, Texas; one test was conducted at the Federal Outdoor Impact Facility (FOIL) in McLean, Virginia by the NCAC; and two were conducted at the Midwest Roadside Safety Facility (MwRSF) in Lincoln, Nebraska. These tests typically involved tractor-semitrailers with a nominal weight of either 50,000 lbs or 80,000 lbs impacting a barrier at a nominal speed and angle of 50 mph and 15 degrees. Table 1 provides a summary of test information and impact conditions for each test.

Table 2 contains information related to test vehicle dimensions and mass.

The data obtained from these reports was used as a gauge to measure model fidelity; however, there were some associated challenges:

- The vehicles used in those tests encompassed a wide range of vehicle makes and dimensions, and none were consistent with the properties of the 1992 Freightliner FLD120 tractor on which the FE model was based.

- Because the tests were focused on performance of the barrier, very little information was provided in the reports regarding damage and response of the vehicle. In cases where detailed vehicle damage was reported, it was unclear how much of the damage was caused from impact with the test article and how much was due to secondary impact or roll-over.

- Most of the tests were very old and only limited data still existed or could be readily accessed. The tests for which electronic data was accessible is noted in the tables.

- The tests involved several different types of barriers ranging in height and stiffness.

Nine of the crash tests were qualification tests for concrete bridge rails and median barriers, which are classified as rigid-barriers in terms of roadside safety devices. The concrete barriers were typically 1.067 m (42 inches) tall, except in two cases where a steel tube rail was installed on top of the concrete barrier to increase overall barrier height. Two of these tests were on “aesthetic” or open-faced, post-and-beam style designs. In most cases, barrier deflections were negligible except for the post-and-beam style designs. Damage to the barriers was reported as being only cosmetic except for the cases involving a steel rail installed on top of the concrete barrier and for the post-and-beam style designs.

Two tests were conducted on an instrumented vertical wall to measure impact forces from tractor-trailer impacts. This type of data can be very useful for verification of the FE model results; however, the results also showed that the magnitude of force was very dependent on the type of tractor and trailer used in the tests. Neither case corresponded to the FE model.

Table 1. Summary of Full Scale Tractor-Semitrailer Crash Tests.

Test No.	Test Agency	Electronic Data Available	Test Date	Vehicle Description				Barrier Description		Impact Conditions		
				Tractor		Trailer						
				Make	Type	Make	Type	Barrier Type	Barrier Height (in.)	Impact Speed (mph)	Impact Angle (deg)	Test Inertial Weight (lbs)
3008	FOIL	**Y**	8/28/2003	1992 Freightliner FLD120	Conventional	N/A	N/A	F-Shape Concrete Safety Shape	32	31.3	25	14,683
405511-2	TTI	**N**	12/12/1995	1983 Freightliner	Conventional	1984 Great Dane	Van	Vertical Concrete Bridge Railing	42	49.8	14.5	79,366
TL5CMB-2	MwRSF	**Y**	7/12/2007	1991 White/GMC	Conventional		48-ft Van	Vertical slope Concrete Median Barrier	42	52.7	15.5	79,705
7162-1	TTI	**Y**	8/9/1990	1980 International	Conventional	1973 Trailmobile	45-ft Van	Ontario Un-Reinforced Concrete Median Barrier	42	49.6	15.1	80,000
ACBR-1	MwRSF	**Y**	8/28/2003	1989 General Motors Brigadier	Conventional		45-ft Van	Aesthetic Open Concrete Bridge Rail	42	49.4	16.3	78,975
7069-13	TTI	**Y**	7/11/1988	1979 International TranStar 4200	Conventional	1977 Pullman	45-ft Van	Vertical Concrete Bridge Railing	42	51.4	16.2	50,050
7069-10	TTI	**Y**	3/3/1988	1979 International TranStar 4200	Conventional	TransStar	45-ft Van	F-Shape Concrete Bridge Railing	42	52.2	14	50,000
4798-13	TTI	**N**	5/26/1983	1974 International	Cab-Over	Fruehauf	40-ft Van	New Jersey Concrete Safety Shape	42	52.1	16.5	80,180
2416-1	TTI	**N**	9/18/1984	1981 Kenworth	Conventional	?	40-ft Van	Texas T5 Concrete Bridge Railing (NJ Shape) w/ Texas C4 Steel Rail	50	48.4	14.5	80,080
6	TTI	**N**	1981	1978 Auto Car	Conventional	Auto Car	40-ft Van	Texas C202 Concrete Parapet w/ Texas C4 Steel Rail	54	49.1	15	79,770
7046-9	TTI	**Y**	5/27/1988	1979 International	Conventional		45-ft Van	Vertical Instrumented Tall Wall	90	50.4	14.6	50,000
7046-3	TTI	**Y**	4/7/1987	1973 White Freightliner	Cab-Over	1966 Fruehauf	40-ft Van	Vertical Instrumented Tall Wall	90	55	15.3	80,080
7046-4	TTI	**N**	5/8/1987	1971 Peterbilt	Conventional	1968 Fruehauf	36.5-ft Tanker	Vertical Instrumented Tall Wall	90	54.8	16	79,900

Table 2. Summary of Full Scale Tractor-semitrailer Dimensions and Mass Properties.

Test No.	Barrier Height (in.)	Trailer Type	Vehicle Dimensions				Vehicle Mass						
			Tractor Wheelbase (ft)	Trailer Wheelbase (ft)	Nominal Trailer Length (ft)	Overall Tractor-Trailer Length (ft)	Tractor Front Axle (lbs)	Tractor Rear Tandem Axle (lbs)	Trailer Rear Tandem Axle (lbs)	Tractor (lbs)	Trailer (lbs)	Ballast (lbs)	Test Inertial Weight (lbs)
4798-13	42	1	12.29	30.71	40	50.2	12,150	34,010	34,020	15,840	13,760	50,580	80,180
7162-1	42	1	14.25	35.8	45	57.4	11,580	34,350	34,070	17,200	12,510	50,290	80,000
TL5CMB-2	42	1	12.91	37.67	48	62.1	9,791	37,516	32,399	*	*	*	79,705
405511-2	42	1	15.50	34.42		58.3	11,210	34,249	33,907	*	*	*	79,366
ACBR-1	42	1	14.22	31.51	45	53.1	8,475	36,725	33,775	*	*	48,450	78,975
7069-13	42	1	14.08	36.5	45	58.2	7,920	22,250	19,880	15,010	12,680	22,360	50,050
7069-10	42	1	15.17	36.17	45	59.2	9,400	21,760	18,840	16,900	13,000	20,100	50,000
2416-1	50	1	16.63	31.48	40	57.1	12,020	34,170	33,890	18,320	13,760	48,000	80,080
6	54	1	13.50	29.25	40	53.9	11,490	33,760	34,520	*	*	47,100	79,770
7046-3	90	1	13.71	30.23	40	51.1	11,680	34,140	34,260	*	*	*	80,080
7046-9	90	1	14.08	35.88	45	58.6	8,540	19,790	21,670	*	*	22,800	50,000
7046-4	90	2	19.67	29.17	36.5	55.4	11,840	33,570	34,490	*	*	53,090	79,900
3008	32	3	17.87	N/A	N/A	N/A	3,744	2,916	NA		N/A	*	14,683

Two tests (i.e., 7162-1 and 405511-2) resulted in unusual failures in major structural components of the trailer. In Test 7162-1, the rear tandem axle assembly separated from the trailer during impact and the trailer box went over the barrier. It was reported that the tandem assembly was poorly constructed, which led to the failure of the tandem assembly. In Test 405511-2, the trailer box fractured early in the impact event. The trailer box split just behind the kingpin box at 0.283 seconds after impact. The fractured trailer managed to remain intact and the test was successful.

NCAC conducted a test specifically for the purpose of collecting crash performance data to use for validation of the NCAC tractor FE model. The test involved a 1992 Freightliner FLD120 tractor impacting an F-shape concrete safety barrier at an impact speed of 52 km/hr (31.25 mph) at an angle of 25 degrees. A crash test report was not written, but accelerometer data was collected at several locations throughout the tractor, rate gyros were mounted near the center of gravity, and high-speed video was captured from several viewpoints. The low mass and low impact speed of this test resulted in a relatively low impact severity compared to other tests that included a tractor-semitrailer combination vehicle, but the data collected in the NCAC test provided very useful information for validation of the tractor FE model because the tractor was isolated and the damage was only moderate. The results of the tractor validation study were reported in the Phase A Report for this program [1].

Summary of Test Vehicle Properties

Figure 1 shows a graphical summary of the wheelbase lengths of the tractors and the trailers used in the tests.

Figure 2 shows a graphical summary of the “axle loads” of the test vehicles. The following is a synthesis of the data presented in these two figures, excluding the two tests that did not involve a box-trailer; i.e., 3008 (tractor-only) and 7046-4 (tanker trailer).

Test Vehicle Dimensions

- Tractor wheel-base lengths ranged from 12.29 ft to 16.63 ft. The average wheel-base length of the tractors was 14.2 ft with a standard deviation of 1.2 ft.

- Trailer wheel-base lengths ranged from 29.25 ft to 37.67 ft. The average wheel-base length of the trailers was 33.6 ft with a standard deviation of 3.0 ft.

- Overall tractor-trailer lengths in all tests ranged from 50.2 ft to 62.1 ft. The average length of the tractor-trailer vehicles was 56.3 ft with a standard deviation of 3.7 ft.

- For tests involving 40-ft trailers, the overall length ranged from 50.2 ft to 57.1 ft. The average length of the vehicles was 53.1 ft with a standard deviation of 3.1 ft.

- For test involving 45-ft trailers, the overall length ranged from 53.1 ft to 59.2 ft. The average length of the vehicles was 57.3 ft with a standard deviation of 2.4 ft.

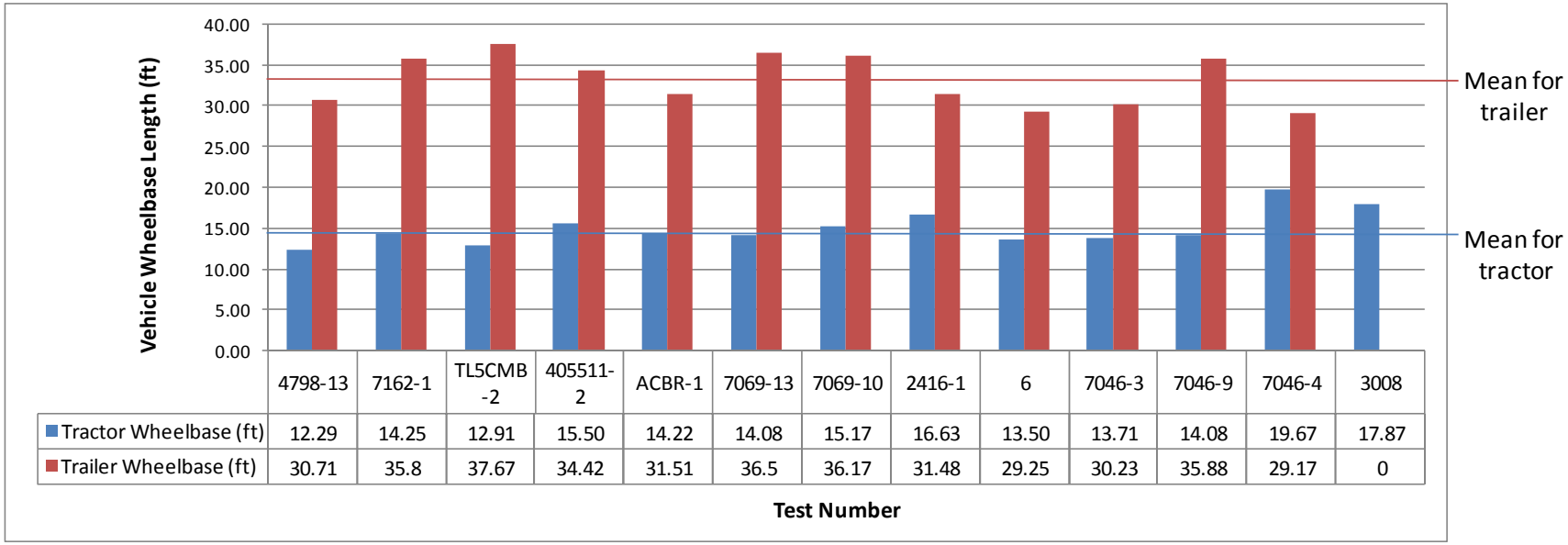

	4798-13	7162-1	TL5CMB-2	405511-2	ACBR-1	7069-13	7069-10	2416-1	6	7046-3	7046-9	7046-4	3008
Tractor Wheelbase (ft)	12.29	14.25	12.91	15.50	14.22	14.08	15.17	16.63	13.50	13.71	14.08	19.67	17.87
Trailer Wheelbase (ft)	30.71	35.8	37.67	34.42	31.51	36.5	36.17	31.48	29.25	30.23	35.88	29.17	0

Figure 1. Chart. Summary of wheelbase lengths of tractors and trailers used in full-scale tests.

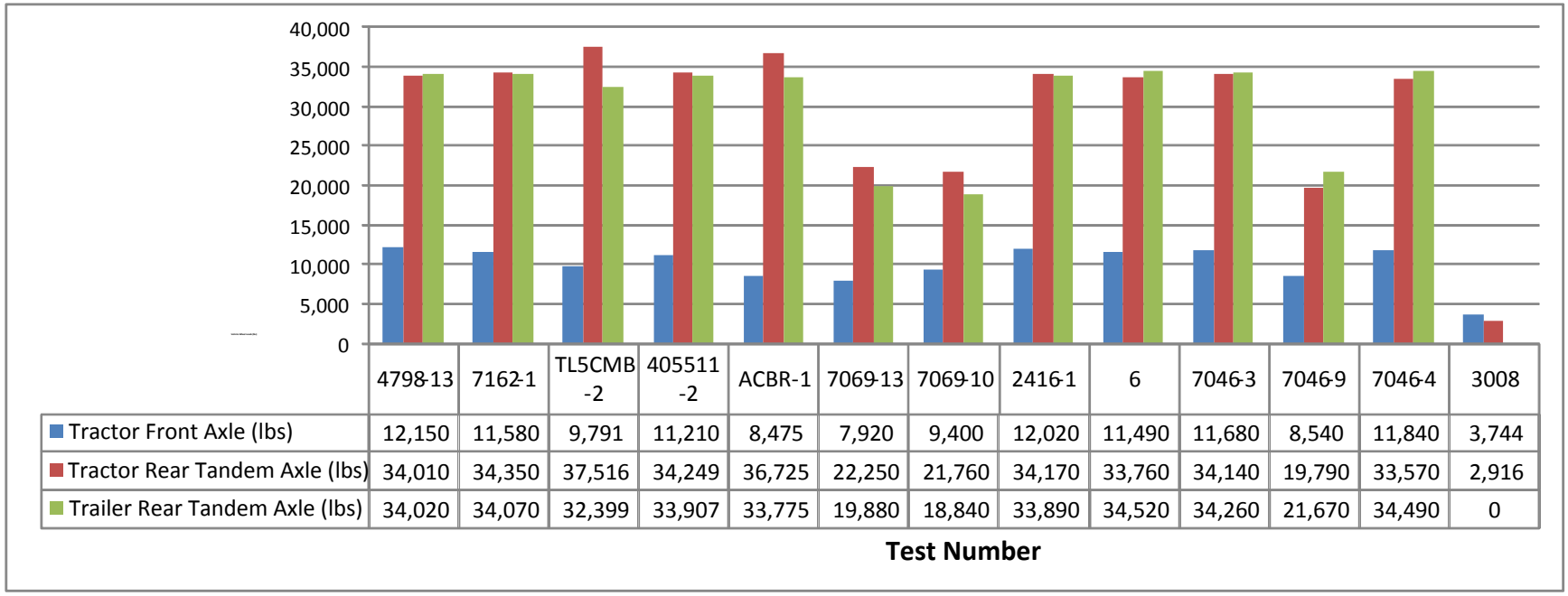

	4798-13	7162-1	TL5CMB-2	405511-2	ACBR-1	7069-13	7069-10	2416-1	6	7046-3	7046-9	7046-4	3008
Tractor Front Axle (lbs)	12,150	11,580	9,791	11,210	8,475	7,920	9,400	12,020	11,490	11,680	8,540	11,840	3,744
Tractor Rear Tandem Axle (lbs)	34,010	34,350	37,516	34,249	36,725	22,250	21,760	34,170	33,760	34,140	19,790	33,570	2,916
Trailer Rear Tandem Axle (lbs)	34,020	34,070	32,399	33,907	33,775	19,880	18,840	33,890	34,520	34,260	21,670	34,490	0

Figure 2. Chart. Summary of axle loads of tractor-trailer vehicles used in full-scale crash tests.

Test Vehicle Mass

- For tractor-trailer test vehicles ballasted to a nominal mass of 80,000 lb:
  - The total test inertial weight of the tractor-trailer vehicle ranged from 78,975 to 80,180 lb. The mean was 79,770 with a standard deviation of 416 lb.
  - The load on the front axle ranged from 8,475 lb to 12,150 lb. The mean was 11,049 lb with a standard deviation of 1,268 lb.
  - The load on the tractor tandem axle ranged from 33,516 lb to 37,516 lb. The mean was 34,865 lb with a standard deviation of 1,418 lb.
  - The load on the trailer tandem axle ranged from 32,399 lb to 34,520 lb. The mean was 33,855 lb with a standard deviation of 634 lb.
- For tractor-trailer test vehicles ballasted to a nominal mass of 50,000 lb:
  - The total test inertial weight of the tractor-trailer vehicle ranged from 50,000 to 50,050 lb. The mean was 50,025. Not enough data to compute standard deviation.
  - The load on the front-axle ranged from 7,920 lb to 9,400 lb with a mean of 8,620. Insufficient data to compute standard deviation.
  - The load on the tractor tandem axle ranged from 19,790 lb to 22,250 lb with a mean of 21,267 lb. Insufficient data to compute standard deviation.
  - The load on the trailer tandem axle ranged from 18,840 lb to 21,670 lb with a mean of 20,130 lb. Insufficient data to compute standard deviation

Summary of Test Results

Data Collection Methods

High-speed video and electronic data recorders (EDRs), such as accelerometers and angular rate transducers, were the primary types of data collection methods used in the full-scale tests. The number, type, and location of the EDRs varied from test to test; however, the most common locations were: 1) inside the tractor cabin near the center of gravity of the tractor, 2) on the tractor near the fifth-wheel, 3) at the front of the trailer near the fifth-wheel, 4) at the center of gravity of the trailer ballast, and/or 5) on the trailer near the trailer tandem axle. Table 3 is a summary of the type and location of EDRs used in each of the full-scale crash tests. Figure 3 shows the general locations of the EDRs, and the nomenclature used in referring to them in this report. The term “fifth-wheel” in this report generally does not discriminate between the tractor and trailer components.

Table 3. Summary of EDR Type and Placement used in Full-scale Crash Tests.

Test No.	Instrumentation					
	Cabin	Tractor Fifth-Wheel	Trailer Fifth Wheel	Trailer Ballast C.G.	Trailer Tandem	Additional Instrumentation
3008	Tri-axial acc. and rate transducer		N/A	N/A	N/A	19 uniaxial acc.
405511-2	Tri-axial acc. and rate transducer	Tri-axial acc.		Tri-axial acc.		11 uniaxial acc. and two string potentiometers
TL5CMB-2					Tri-axial acc.	
7162-1	Bi-axial acc.	Tri-axial acc. and rate transducer	Bi-axial acc.		Bi-axial acc.	
ACBR-1		Tri-axial acc.		Tri-axial acc. and rate transducer		
7069-13	Tri-axial acc. and rate transducer	Bi-axial acc.	Bi-axial acc.	Angular rate transducer	Bi-axial acc.	
7069-10	Tri-axial acc. and rate transducer	Bi-axial acc.	Bi-axial acc.	Angular rate transducer	Bi-axial acc.	
4798-13		Tri-axial acc. and rate transducer				
2416-1		Tri-axial acc. and rate transducer				
6		Tri-axial acc. and rate transducer				
7046-9	Tri-axial acc.	Bi-axial acc.		Bi-axial acc.	Bi-axial acc.	
7046-3	Bi-axial acc.	Tri-axial acc.		Bi-axial acc. and rate transducer	Bi-axial acc.	
7046-4	Bi-axial acc.	Tri-axial acc.		Bi-axial acc. and rate transducer	Bi-axial acc.	

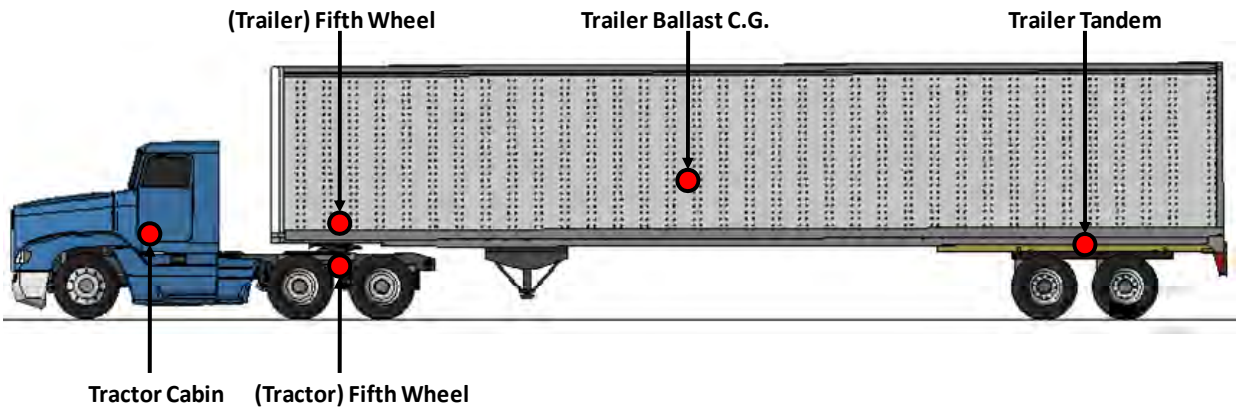

Figure 3. Illustration. General EDR locations and nomenclature used in test reports.

Accelerometer Results

Tables 4 through 7 provide summaries of the peak acceleration values measured in the full-scale tests. These tables are arranged into six groups according to: trailer type, nominal barrier height, and nominal gross static weight of the test vehicle. The six groups are as follows:

- Group A: Tests that involve a tractor with box-trailer ballasted to a nominal weight of 36,287 kg (80,000 lb) impacting a 1,067 mm (42 inches) tall barrier [5, 7, 10, 12, 14].
- Group B: Tests that involve a tractor with box-trailer ballasted to a nominal weight of 22,680 kg (50,000 lb) impacting a 1,067 mm (42 inches) tall barrier [8, 9].
- Group C: Tests that involve a tractor with box-trailer ballasted to a nominal weight of 36,287 kg (80,000 lb) impacting "taller" barriers ranging in height from 1,270 mm (50 inches) to 2,286 mm (90 inches) [3, 4, 6].
- Group D: Tests that involve a tractor with box-trailer ballasted to a nominal weight of 22,680 kg (50,000 lb) impacting a 2,286 mm (90 inches) tall barrier [13].
- Group E: Tests that involve a tractor with tanker-trailer ballasted to a nominal weight of 36,287 kg (80,000 lb) impacting a 2,286 mm (90 inches) tall barrier [6].
- Group F: Test that involved tractor with no trailer impacting a 813 mm (32 inches) tall barrier [10].

None of these tests were identical; however, the groups listed above represent six general categories to facilitate analyzing the test data and to determine the range of expected response. There are, of course, other parameters of a test that can affect results, such as tractor make and model, tractor wheelbase length, trailer make and model, trailer length, weight distribution of the test vehicle, type of ballast, and how the ballast is fastened to the trailer. Quantifying the effects of each of these very specific parameters on impact response was outside the scope of this study.

Table 4. Summary of Peak 0.010-second Average Accelerations and ASI from Accelerometers Located on Tractor.

Group	Test No.	Electronic Data Available	Barrier Height (in.)	Trailer Type	Test Inertial Weight (lbs)	Peak 0.01-second average acceleration						Peak ASI	
						Tractor Cabin			Tractor Fifth-Wheel			Tractor Cabin	Tractor Tandem
						Long.	Lat.	Vert.	Long.	Lat.	Vert.		
						Calc.	Calc.	Calc.	Calc.	Calc.	Calc.	Calc.	Calc.
A	4798-13	-	42	Box	80,180	*	*	*	-	-	-	*	-
	7162-1	**Y**	42	Box	80,000	4.8	6.9	*	4.0	11.6	9.1	0.85	0.50
	TL5CMB-2	**Y**	42	Box	79,705	*	*	*	*	*	*	*	*
	405511-2	-	42	Box	79,366	5.0	10.0	-	4.5	15.0	-	-	-
	ACBR-1	**Y**	42	Box	78,975	*	*	*	6.3	11.8	4.8	*	0.82
B	7069-13	**Y**	42	Box	50,050	6.7	7.1	5.4	4.4	10.4	-	0.49	0.55
	7069-10	**Y**	42	Box	50,000	5.3	6.9	7.2	7.1	11.4	-	0.55	0.84
C	2416-1	-	50	Box	80,080	*	*	*	-	-	-	*	-
	6	-	54	Box	79,770	*	*	*	-	-	-	*	-
	7046-3	**Y**	90	Box	80,080	3.6	14.4	*	3.9	15.5	-	0.76	1.09
D	7046-9	**Y**	90	Box	50,000	5.0	14.1	7.3	4.6	19.6	-	-	-
E	7046-4	-	90	Tanker	79,900	-	-	*	-	-	-	-	-
F	3008	**Y**	32	N/A	14,683								
Mean Values						**5.1**	**9.9**	**6.6**	**5**	**13.6**	**7**	**0.66**	**0.76**

* NOT APPLICABLE
\- DATA NOT AVAILABLE

Table 5. Summary of Peak 0.010-second Average Accelerations and ASI from Accelerometers Located on Trailer.

Group	Test No.	Electronic Data Available	Barrier Height (in.)	Trailer Type	Test Inertial Weight (lbs)	Peak 0.01-second average acceleration						Peak ASI	
						Trailer C.G.			Trailer Tandem			Trailer Ballast C.G.	Trailer Tandem
						Long.	Lat.	Vert.	Long.	Lat.	Vert.		
						Calc.	Calc.	Calc.	Calc.	Calc.	Calc.	Calc.	Calc.
A	4798-13	-	42	Box	80,180	*	*	*	*	*	*	*	*
	7162-1	**Y**	42	Box	80,000	*	*	*	5.8	36.7	*	*	1.1
	TL5CMB-2	**Y**	42	Box	79,705	*	*	*	5.3	29.2	9.2	*	1.4
	405511-2	-	42	Box	79,366	-	-	-	*	*	*	-	*
	ACBR-1	**Y**	42	Box	78,975	3.1	11.1	5.7	*	*	*	0.5	*
B	7069-13	**Y**	42	Box	50,050	*	*	*	2.5	29.9	*	*	0.8
	7069-10	**Y**	42	Box	50,000	*	*	*	5.4	26.5	*	*	1.2
C	2416-1	-	50	Box	80,080	*	*	*	*	*	*	*	*
	6	-	54	Box	79,770	*	*	*	*	*	*	*	*
	7046-3	**Y**	90	Box	80,080	3.5	11.5	*	3.3	12.6	*	0.8	1.1
D	7046-9	**Y**	90	Box	50,000	4.9	17.9	*	5.0	6.6	*	0.6	0.4
E	7046-4	-	90	Tanker	79,900			*			*	-	*
F	3008	**Y**	32	N/A	14,683	*	*	*	*	*	*	*	*
Mean Values						**3.8**	**13.5**	**5.7**	**4.6**	**23.5**	**9.2**	**0.63**	**1**

* NOT APPLICABLE
\- DATA NOT AVAILABLE

Table 6. Summary of Peak 0.050-second Average Accelerations from Accelerometers Located on Tractor.

Group	Test No.	Electronic Data Available	Barrier Height (in.)	Trailer Type	Test Inertial Weight (lbs)	Peak 0.050-second average accelerations (G's)											
						Tractor Cabin						Tractor Fifth-Wheel					
						Longitudinal		Lateral		vertical		Longitudinal		Lateral		Vertical	
						Reported	calc.	Reported	Calc.	Reported	Calc.	Reported	Calc.	Reported	Calc.	Reported	Calc.
A	4798-13	-	42	Box	80,180	*	*	*	*	*	*	6.5	-	3.1	-	9.3	-
	7162-1	Y	42	Box	80,000	1.6	1.6	4.4	4.4	*	*	1.2	1.4	7.9	7.6	3.2	-
	TL5CMB-2	Y	42	Box	79,705	*	*	*	*	*	*	*	*	*	*	*	*
	405511-2	-	42	Box	79,366	1.9	-	5.9	-	4.0	-	1.1	-	8.2	-	3.0	-
	ACBR-1	Y	42	Box	78,975	*	*	*	*	*	*	1.3	1.3	7.4	7.4	3.9	3.1
B	7069-13	Y	42	Box	50,050	3.3	3.2	3.7	4.0	-	3.1		1.6	5.0	4.9	*	*
	7069-10	Y	42	Box	50,000	2.2	2.1	4.7	4.7	-	3.4		2.2	7.5	7.4	*	*
C	2416-1	-	50	Box	80,080	*	*	*	*	*	*	2.4	-	5.5	-	-	-
	6	-	54	Box	79,770	*	*	*	*	*	*	1.7	-	5.9	-	-	-
	7046-3	Y	90	Box	80,080		1.7		6.7	*	*	3.2	2.4	9.7	9.7	-	-
D	7046-9	Y	90	Box	50,000	2.4	2.4	6.8	6.7	-	1.6		2.9		9.1	*	*
E	7046-4	-	90	Tanker	79,900		-		-	*	*	2.1	-	12.3	-	-	-
F	3008	Y	32	N/A	14,683												
Mean Values						2.2		5.4		3.0		2.4		7.4		4.8	

Table 7. Summary of Peak 0.050-second Average Accelerations from Accelerometers Located on Trailer.

Group	Test No.	Electronic Data Available	Barrier Height (in.)	Trailer Type	Test Inertial Weight (lbs)	Peak 0.050-second Average Accelerations (G's)								
						Trailer C.G.						Trailer Tandem		
						Longitudinal		Lateral		Vertical		Long.	Lat.	Vert.
						Reported	Calc.	Reported	Calc.	Reported	Calc.	Calc.	Calc.	Calc.
A	4798-13	-	42	Box	80,180	*	*	*	*	*	*	*	*	*
	7162-1	**Y**	42	Box	80,000	*	*	*	*	*	*	1.9	9.5	*
	TL5CM B-2	**Y**	42	Box	79,705	*	*	*	*	*	*	1.4	12.7	2.8
	405511-2	-	42	Box	79,366	1.3	-	1.8	-	1.3	-	*	*	*
	ACBR-1	**Y**	42	Box	78,975	0.9	0.9	4.1	4.1	5.7	5.7	*	*	*
B	7069-13	**Y**	42	Box	50,050	*	*	*	*	*	*	1.2	7.2	*
	7069-10	**Y**	42	Box	50,000	*	*	*	*	*	*	1.8	10.8	*
C	2416-1	-	50	Box	80,080	*	*	*	*	*	*	*	*	*
	6	-	54	Box	79,770	*	*	*	*	*	*	*	*	*
	7046-3	**Y**	90	Box	80,080	-	2.1	-	6.9	*	*	2.0	9.6	*
D	7046-9	**Y**	90	Box	50,000	-	2.3	-	5.5	*	*	2.6	3.4	*
E	7046-4	-	90	Tanker	79,900	-	-	-	-	*	*	-	-	*
F	3008	**Y**	32	None	14,683	*	*	*	*	*	*	*	*	*
Mean Values						**1.7**		**4.6**		**3.5**		**1.8**	**8.7**	**2.8**

* NOT APPLICABLE
\- DATA NOT AVAILABLE

Several of the tables and figures presented in this section include tests results in terms of the acceleration severity index (ASI). The ASI provides a measure of the severity of vehicle motion during an impact relative to acceptable limits of acceleration for vehicle occupants. The ASI is computed using the equation below:

$$ASI(t) = \sqrt{\frac{\bar{a}_x}{\hat{a}_x} + \frac{\bar{a}_y}{\hat{a}_y} + \frac{\bar{a}_z}{\hat{a}_z}}$$

Equation 1. Equation for calculating the acceleration severity index (ASI)

Where, $\bar{a}_x$, $\bar{a}_y$, and $\bar{a}_z$ are the components of acceleration along the body axes x, y and z at a point on the vehicle average over a moving 0.050-second time interval; $\hat{a}_x$, $\hat{a}_y$, and $\hat{a}_z$ are limit-values for the components of acceleration based on acceptable occupant risk criteria. Note, that if the limit values are set to 1, the ASI is the resultant acceleration. Each ratio in the ASI equation represents a component of acceleration normalized with the corresponding maximum acceptable acceleration magnitude; therefore, values of ASI greater than 1 indicate that there is unacceptable risk to vehicle occupants. The limit-values used in this study correspond to the European standards which are:

Table 8. Acceleration Severity Index (ASI) Standards.

$$\hat{a}_x = 12 \text{ G}$$
$$\hat{a}_y = 9 \text{ G}$$
$$\hat{a}_z = 10 \text{ G}$$

Further details on the procedure for computing the ASI can be found in the literature [2].

Table 4 lists the peak 0.010-second average acceleration and peak ASI values from accelerometers located inside the tractor cabin near the center of gravity of the tractor and from accelerometers located near the tractor's fifth-wheel. Table 5 lists the peak 0.010-second average acceleration and peak ASI values from accelerometers located at the center of gravity of the trailer ballast and from accelerometers located near the tandem axle of the trailer. Table 6 lists the peak 0.050-second average acceleration from accelerometers located inside the tractor cabin near the center of gravity of the tractor and from accelerometers located near the tractor's fifth-wheel. Table 7 lists the peak 0.050-second average acceleration from accelerometers located at the center of gravity of the trailer ballast and from accelerometers located near the tandem axle of the trailer.

Since vertical acceleration data was not available in all cases, the peak ASI values were computed using only the longitudinal and lateral acceleration data so that a reasonable comparison of the results could be made. Furthermore, all calculations of ASI in this study used the same limit-values for acceleration in order to obtain a relative comparison of results. For example, the ASI values computed at the trailer tandem location were in most cases higher than

1, which would indicate that the accelerations were unacceptable; however, this part of the vehicle is not expected to carry vehicle occupants.

The data presented in these tables represent the peak value of each acceleration-time history. The peak 0.010-second average acceleration is not to be confused with the peak 0.010-second average occupant ride-down acceleration (ORA), which is often provided in the test report under occupant risk assessment. The ORA only measures peak values after the time of occupant impact with the interior of the vehicle. In most cases, the maximum accelerations occur prior to occupant impact and, for assessing vehicle response and corresponding barrier loading, it is important to capture the maximum values whenever they may occur.

As mentioned previously, electronic data were not available for all tests; those tests for which electronic data were available are identified in the tables with a "Y" in the third column. There were some cases where some, but not all data were available. In those cases a dash (-) is placed in the table cell to indicate that accelerometer data was collected for that particular data channel in the test, but the data was not available to the NTRCI team. An asterisk (*) in the table cells indicates that data was not collected for that particular data channel. For example, Test 7046-9 has an asterisk in the table cell representing the vertical data channel at the tractor's fifth-wheel; a bi-axial (horizontal-plane only) accelerometer was used at that location and no vertical data was recorded.

The peak values were calculated by the NTRCI team for tests where electronic data were available. These calculated values are denoted in the tables by the sub-heading "Calc." Values taken directly from the test report are denoted in the tables by the sub-heading "Reported." As shown in Table 6, the values computed by the NTRCI team differed in some cases from the values reported in the test report, thus both values are listed.

The data in Tables 4 through 7 are also presented graphically in Figures 4 through 12. Figures 4 through 7 show a summary of the peak 0.010-second average acceleration at the center of gravity of the tractor, at the fifth-wheel, at the center of gravity of the trailer ballast, and at the tandem axle of the trailer, respectively. Figures 8 through 10 show a summary of the peak 0.050-second average acceleration at the center of gravity of the tractor, at the fifth-wheel, at the center of gravity of the trailer ballast, and at the tandem axle of the trailer, respectively. Figure 12 shows a summary of the peak ASI values at each accelerometer location.

Table 9 provides a summary of the highest, lowest, and average of the peak values of ASI for each test group at each accelerometer location, and Table 10 provides a similar summary for the peak values of acceleration. The data in Table 9 and Table 10 are also shown graphically in Figures 13 through 15. These figures provide the most useful format for summarizing the data.

For reference, the 0.05-second moving average acceleration-time histories and the ASI-time histories for all tests (for which electronic data were available) are shown in Figures 16 through 39.

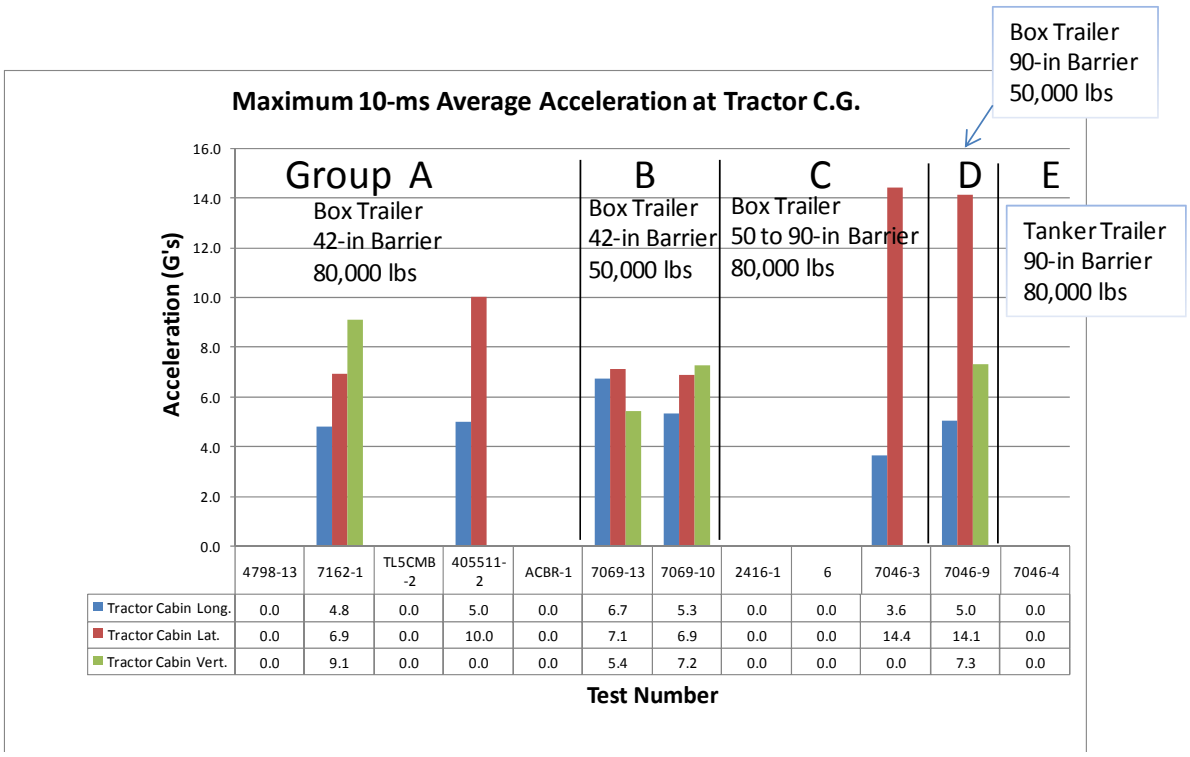

	4798-13	7162-1	TL5CMB -2	405511-2	ACBR-1	7069-13	7069-10	2416-1	6	7046-3	7046-9	7046-4
Tractor Cabin Long.	0.0	4.8	0.0	5.0	0.0	6.7	5.3	0.0	0.0	3.6	5.0	0.0
Tractor Cabin Lat.	0.0	6.9	0.0	10.0	0.0	7.1	6.9	0.0	0.0	14.4	14.1	0.0
Tractor Cabin Vert.	0.0	9.1	0.0	0.0	0.0	5.4	7.2	0.0	0.0	0.0	7.3	0.0

Figure 4. Chart. Summary of peak 0.010-seconds average accelerations from accelerometer located inside tractor cabin near the tractor center of gravity.

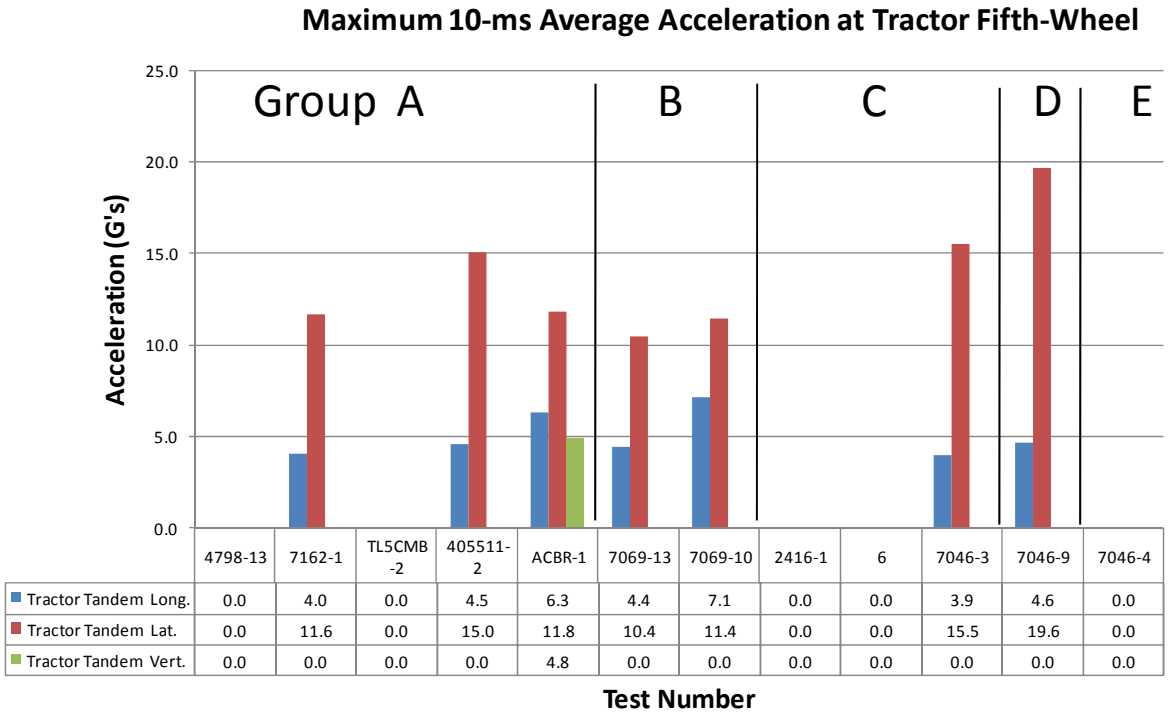

	4798-13	7162-1	TL5CMB -2	405511-2	ACBR-1	7069-13	7069-10	2416-1	6	7046-3	7046-9	7046-4
Tractor Tandem Long.	0.0	4.0	0.0	4.5	6.3	4.4	7.1	0.0	0.0	3.9	4.6	0.0
Tractor Tandem Lat.	0.0	11.6	0.0	15.0	11.8	10.4	11.4	0.0	0.0	15.5	19.6	0.0
Tractor Tandem Vert.	0.0	0.0	0.0	0.0	4.8	0.0	0.0	0.0	0.0	0.0	0.0	0.0

Figure 5. Chart. Summary of peak 0.010-seconds average accelerations from accelerometer located inside tractor cabin near the tractor fifth-wheel.

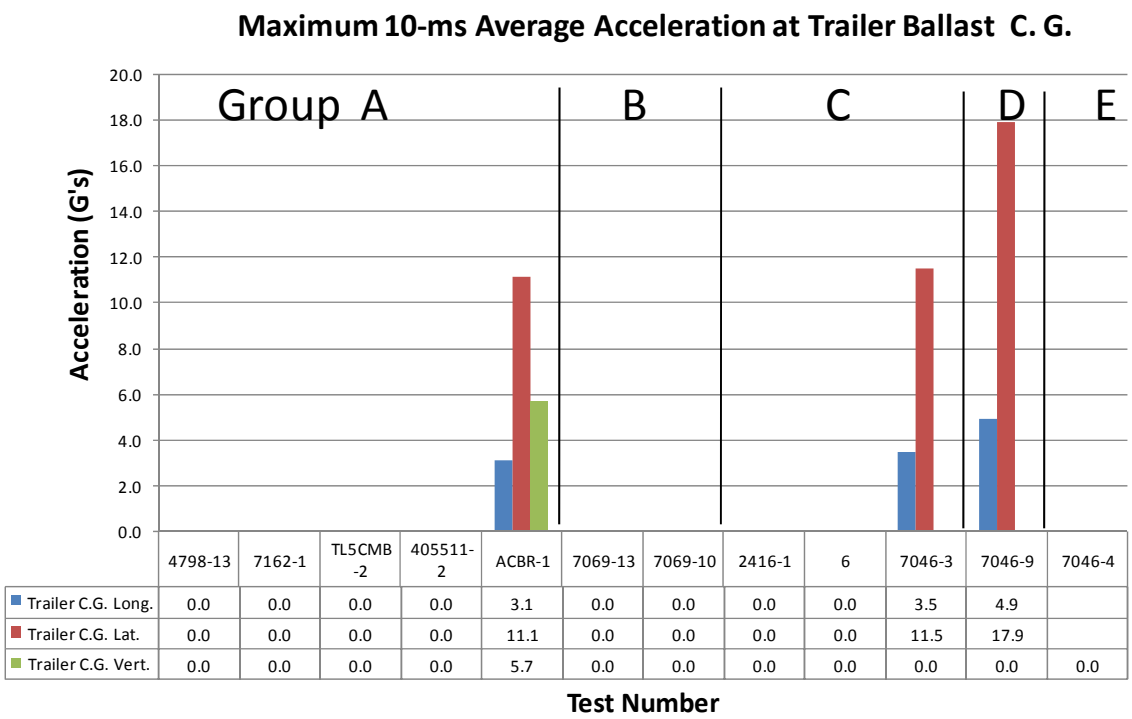

	4798-13	7162-1	TL5CMB -2	405511-2	ACBR-1	7069-13	7069-10	2416-1	6	7046-3	7046-9	7046-4
Trailer C.G. Long.	0.0	0.0	0.0	0.0	3.1	0.0	0.0	0.0	0.0	3.5	4.9	
Trailer C.G. Lat.	0.0	0.0	0.0	0.0	11.1	0.0	0.0	0.0	0.0	11.5	17.9	
Trailer C.G. Vert.	0.0	0.0	0.0	0.0	5.7	0.0	0.0	0.0	0.0	0.0	0.0	0.0

Figure 6. Chart. Summary of peak 0.010-seconds average accelerations from accelerometer located near the center of gravity of the trailer ballast.

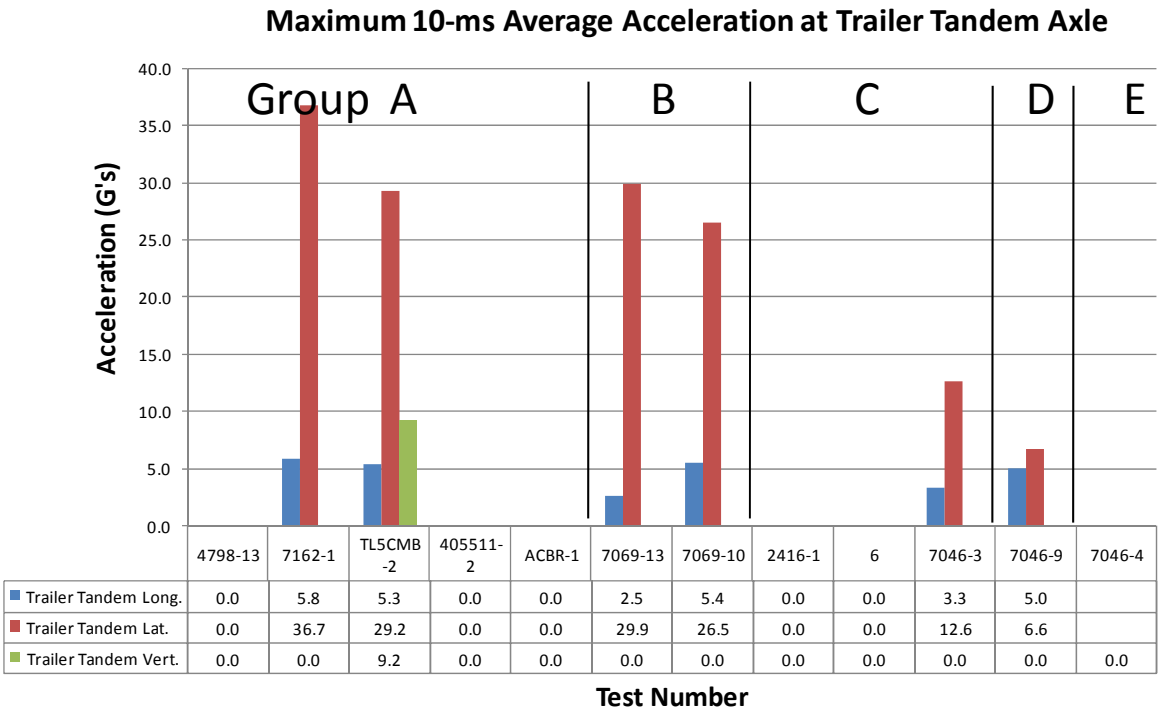

	4798-13	7162-1	TL5CMB -2	405511-2	ACBR-1	7069-13	7069-10	2416-1	6	7046-3	7046-9	7046-4
Trailer Tandem Long.	0.0	5.8	5.3	0.0	0.0	2.5	5.4	0.0	0.0	3.3	5.0	
Trailer Tandem Lat.	0.0	36.7	29.2	0.0	0.0	29.9	26.5	0.0	0.0	12.6	6.6	
Trailer Tandem Vert.	0.0	0.0	9.2	0.0	0.0	0.0	0.0	0.0	0.0	0.0	0.0	0.0

Figure 7. Chart. Summary of peak 0.010-seconds average accelerations from accelerometer located near the trailer tandem axle.

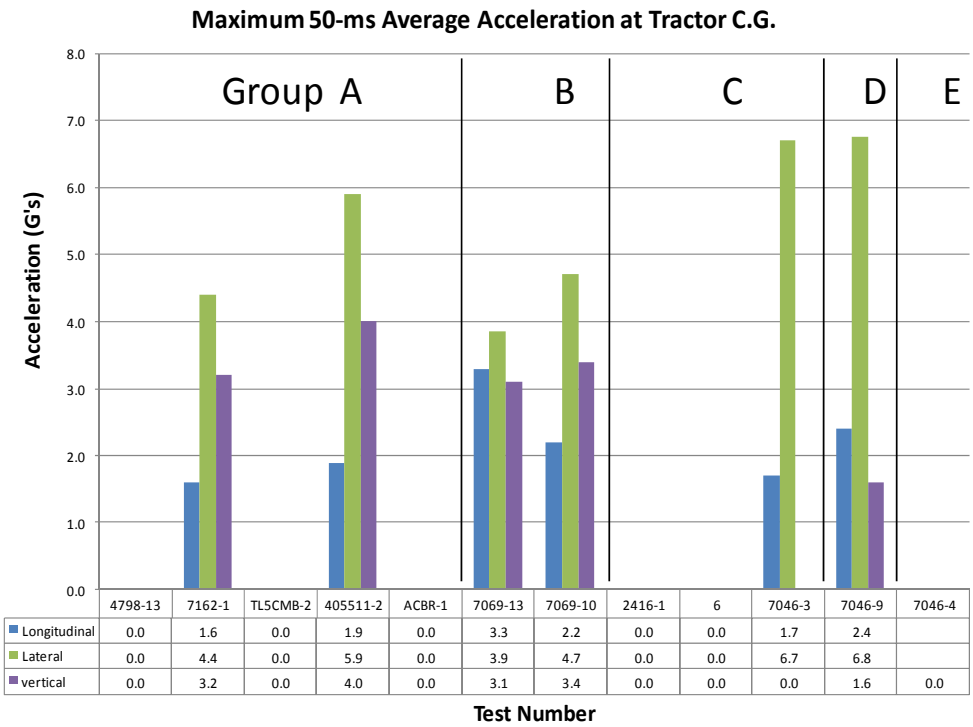

	4798-13	7162-1	TL5CMB-2	405511-2	ACBR-1	7069-13	7069-10	2416-1	6	7046-3	7046-9	7046-4
Longitudinal	0.0	1.6	0.0	1.9	0.0	3.3	2.2	0.0	0.0	1.7	2.4	
Lateral	0.0	4.4	0.0	5.9	0.0	3.9	4.7	0.0	0.0	6.7	6.8	
vertical	0.0	3.2	0.0	4.0	0.0	3.1	3.4	0.0	0.0	0.0	1.6	0.0

Figure 8. Chart. Summary of peak 0.050-seconds average accelerations from accelerometer located inside tractor cabin near the tractor center of gravity.

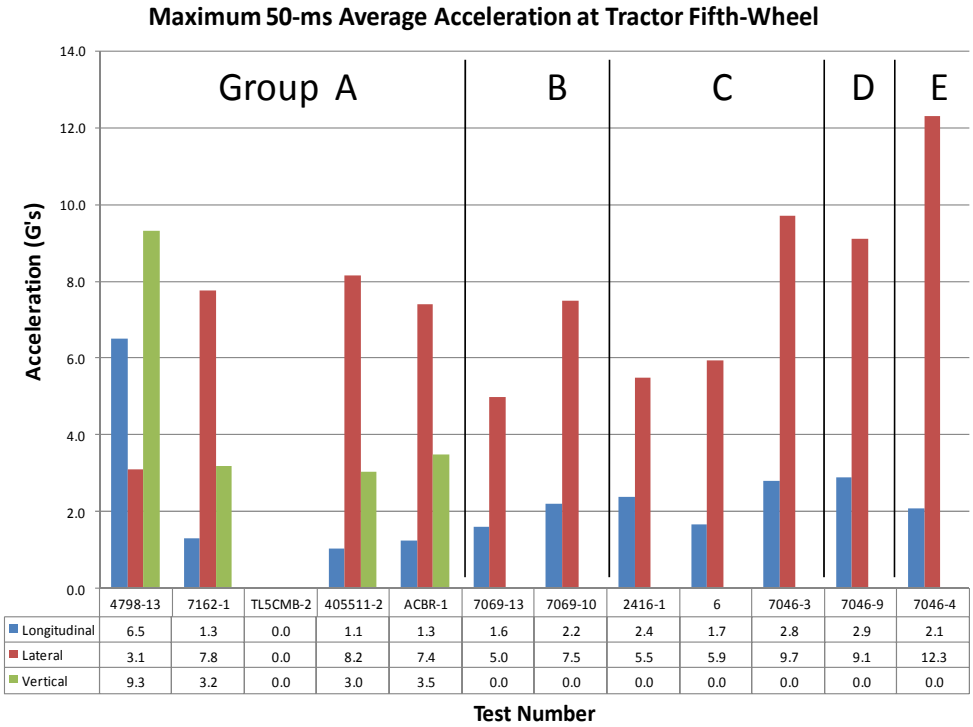

	4798-13	7162-1	TL5CMB-2	405511-2	ACBR-1	7069-13	7069-10	2416-1	6	7046-3	7046-9	7046-4
Longitudinal	6.5	1.3	0.0	1.1	1.3	1.6	2.2	2.4	1.7	2.8	2.9	2.1
Lateral	3.1	7.8	0.0	8.2	7.4	5.0	7.5	5.5	5.9	9.7	9.1	12.3
Vertical	9.3	3.2	0.0	3.0	3.5	0.0	0.0	0.0	0.0	0.0	0.0	0.0

Figure 9. Chart. Summary of peak 0.050-seconds average accelerations from accelerometer located inside tractor cabin near the tractor fifth-wheel.

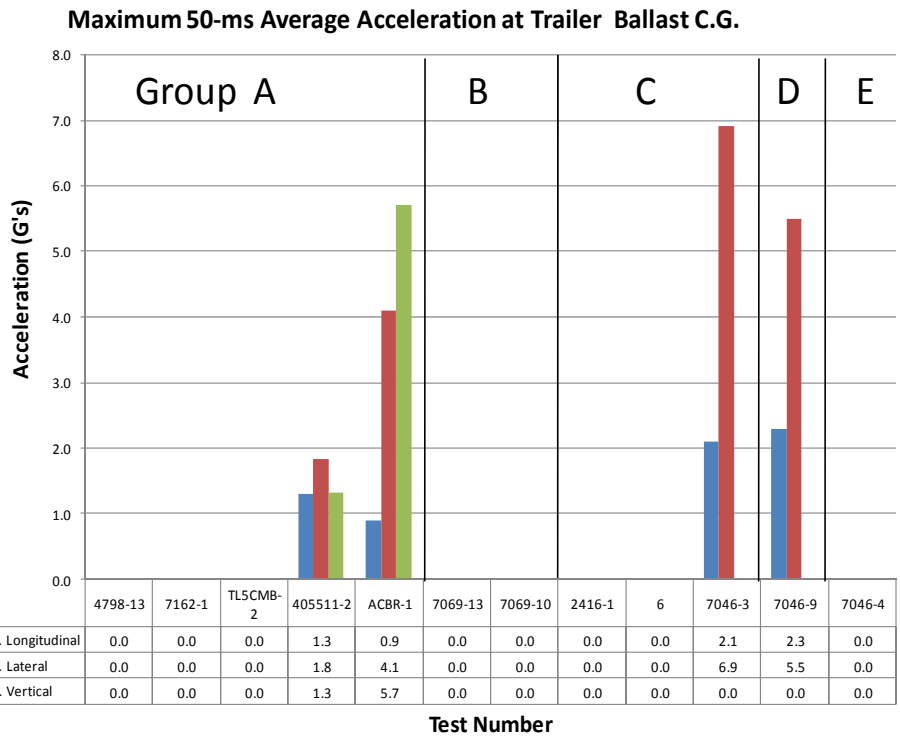

	4798-13	7162-1	TL5CMB-2	405511-2	ACBR-1	7069-13	7069-10	2416-1	6	7046-3	7046-9	7046-4
Trailer C.G. Longitudinal	0.0	0.0	0.0	1.3	0.9	0.0	0.0	0.0	0.0	2.1	2.3	0.0
Trailer C.G. Lateral	0.0	0.0	0.0	1.8	4.1	0.0	0.0	0.0	0.0	6.9	5.5	0.0
Trailer C.G. Vertical	0.0	0.0	0.0	1.3	5.7	0.0	0.0	0.0	0.0	0.0	0.0	0.0

Figure 10. Chart. Summary of peak 0.050-seconds average accelerations from accelerometer located near the center of gravity of the trailer ballast.

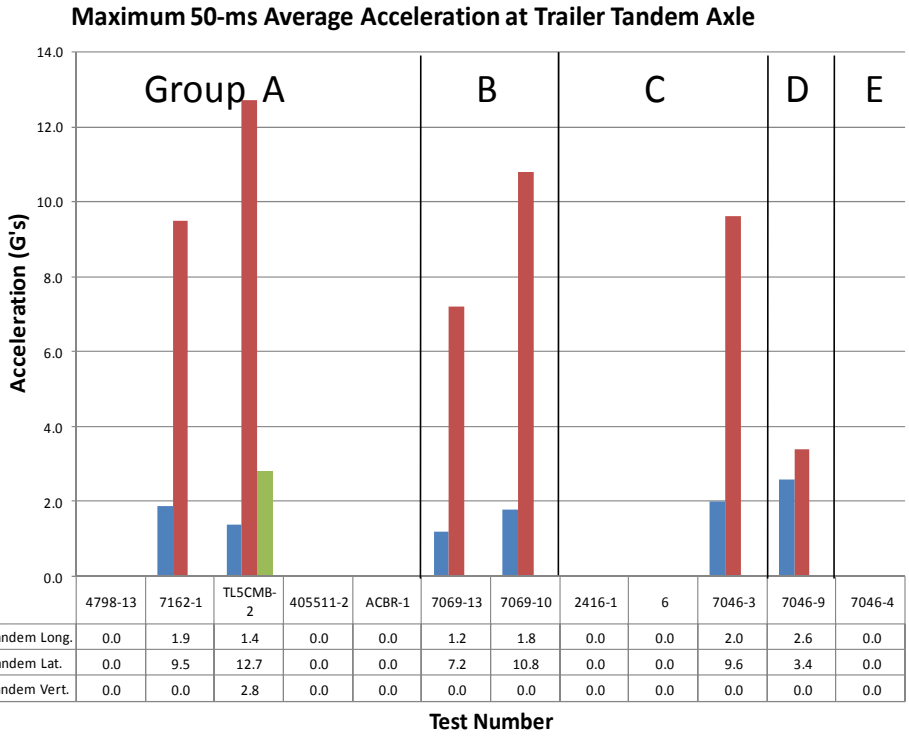

	4798-13	7162-1	TL5CMB-2	405511-2	ACBR-1	7069-13	7069-10	2416-1	6	7046-3	7046-9	7046-4
Trailer Tandem Long.	0.0	1.9	1.4	0.0	0.0	1.2	1.8	0.0	0.0	2.0	2.6	0.0
Trailer Tandem Lat.	0.0	9.5	12.7	0.0	0.0	7.2	10.8	0.0	0.0	9.6	3.4	0.0
Trailer Tandem Vert.	0.0	0.0	2.8	0.0	0.0	0.0	0.0	0.0	0.0	0.0	0.0	0.0

Figure 11. Chart. Summary of peak 0.050-seconds average accelerations from accelerometer located near the trailer tandem axle.

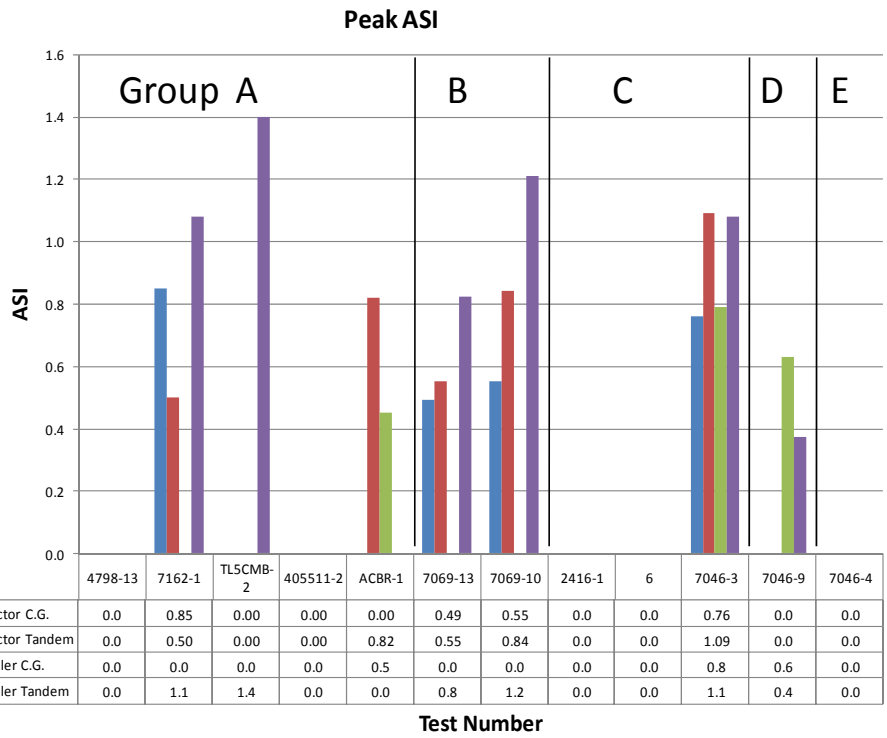

	4798-13	7162-1	TL5CMB-2	405511-2	ACBR-1	7069-13	7069-10	2416-1	6	7046-3	7046-9	7046-4
Peak ASI Tractor C.G.	0.0	0.85	0.00	0.00	0.00	0.49	0.55	0.0	0.0	0.76	0.0	0.0
Peak ASI Tractor Tandem	0.0	0.50	0.00	0.00	0.82	0.55	0.84	0.0	0.0	1.09	0.0	0.0
Peak ASI Trailer C.G.	0.0	0.0	0.0	0.0	0.5	0.0	0.0	0.0	0.0	0.8	0.6	0.0
Peak ASI Trailer Tandem	0.0	1.1	1.4	0.0	0.0	0.8	1.2	0.0	0.0	1.1	0.4	0.0

Figure 12. Chart. Summary of peak ASI values computed from accelerometer data.

Table 9. Summary of the Highest, Lowest and Average of the Peak Values for Each Test Group at each Accelerometer Location.

Group	Peak ASI											
	Tractor Cabin			Tractor Fifth-Wheel			Trailer Ballast C.G.			Trailer Ballast C.G.		
	High	Low	Mean	High	Low	Mean	High	Low	Mean	High	Low	Mean
A	0.85	-	0.85	0.82	0.50	0.66	0.50	-	0.50	1.40	1.10	1.25
B	0.55	0.49	0.52	0.84	0.55	0.70	-	-	-	1.20	0.80	1.00
C	0.76	-	0.76	1.09	-	1.09	0.80	-	0.80	1.10	-	1.10
D	-	-	-	-	-	-	0.60	-	0.60	0.40	-	0.40
E	-	-	-	-	-	-	-	-	-	-	-	-

Table 10. Summary of the Highest, Lowest and Average of the Peak Values for Each Test Group at Each Accelerometer Location.

Tractor Cabin

Group		Longitudinal			Lateral			Vertical		
		high	low	mean	high	low	mean	high	low	mean
A	0.010-sec. average acc.	5.0	4.8	4.9	10.0	6.9	8.5	9.1	-	9.1
	0.050-sec. average acc.	1.9	1.6	1.8	5.9	4.4	5.2	4.0	3.2	3.6
B	0.010-sec. average acc.	6.7	5.3	6.0	7.1	6.9	7.0	7.2	5.4	6.3
	0.050-sec. average acc.	3.3	2.1	2.7	4.7	3.7	4.3	3.4	3.1	3.3
C	0.010-sec. average acc.	3.6	-	3.6	14.4	-	14.4	-	-	-
	0.050-sec. average acc.	1.7	-	1.7	6.7	-	6.7	-	-	-
D	0.010-sec. average acc.	5.0	-	5.0	14.1	-	14.1	7.3	-	7.3
	0.050-sec. average acc.	2.4	-	2.4	6.8	-	6.8	1.6	-	1.6
E	0.010-sec. average acc.	-	-	-	-	-	-	-	-	-
	0.050-sec. average acc.	-	-	-	-	-	-	-	-	-

Tractor Fifth-Wheel

Group		Longitudinal			Lateral			Vertical		
		high	low	mean	high	low	mean	high	low	mean
A	0.010-sec. average acc.	6.3	4.0	4.9	15.0	11.6	12.8	4.8	-	4.8
	0.050-sec. average acc.	6.5	1.2	2.6	8.2	3.1	6.6	9.3	3.0	4.8
B	0.010-sec. average acc.	7.1	4.4	5.8	11.4	10.4	10.9	-	-	-
	0.050-sec. average acc.	2.2	1.6	1.9	7.5	4.9	6.2	-	-	-
C	0.010-sec. average acc.	3.9	-	3.9	15.5	-	15.5	-	-	-
	0.050-sec. average acc.	3.2	1.7	2.3	9.7	5.5	7.0	-	-	-
D	0.010-sec. average acc.	4.6	-	4.6	19.6	-	19.6	-	-	-
	0.050-sec. average acc.	2.9	-	2.9	9.1	-	9.1	-	-	-
E	0.010-sec. average acc.	-	-	-	-	-	-	-	-	-
	0.050-sec. average acc.	2.1	-	2.1	12.3	-	12.3	-	-	-

Trailer Ballast C.G.

Group		Longitudinal			Lateral			Vertical		
		high	low	mean	high	low	mean	high	low	mean
A	0.010-sec. average acc.	3.1	-	3.1	11.1	-	11.1	5.7	-	5.7
	0.050-sec. average acc.	1.3	0.90	1.1	4.1	1.80	3.0	5.7	1.30	5.7
B	0.010-sec. average acc.	-	-	-	-	-	-	-	-	-
	0.050-sec. average acc.	-	-	-	-	-	-	-	-	-
C	0.010-sec. average acc.	3.5	-	3.5	11.5	-	11.5	-	-	-
	0.050-sec. average acc.	2.1	-	2.1	6.9	-	6.9	-	-	-
D	0.010-sec. average acc.	4.9	-	4.9	17.9	-	17.9	-	-	-
	0.050-sec. average acc.	2.3	-	2.3	5.5	-	5.5	-	-	-
E	0.010-sec. average acc.	-	-	-	-	-	-	-	-	-
	0.050-sec. average acc.	-	-	-	-	-	-	-	-	-

Trailer Tandem Axle

Group		Longitudinal			Lateral			Vertical		
		high	low	mean	high	low	mean	high	low	mean
A	0.010-sec. average acc.	5.8	5.3	5.6	36.7	29.2	33.0	9.2	-	9.2
	0.050-sec. average acc.	1.9	1.4	1.7	12.7	9.5	11.1	2.8	-	2.8
B	0.010-sec. average acc.	5.4	2.5	4.0	29.9	26.5	28.2	-	-	-
	0.050-sec. average acc.	1.8	1.2	1.5	10.8	7.2	9.0	-	-	-
C	0.010-sec. average acc.	3.3	-	3.3	12.6	-	12.6	-	-	-
	0.050-sec. average acc.	2.0	-	2.0	9.6	-	9.6	-	-	-
D	0.010-sec. average acc.	5.0	-	5.0	6.6	-	6.6	-	-	-
	0.050-sec. average acc.	2.6	-	2.6	3.4	-	3.4	-	-	-
E	0.010-sec. average acc.	-	-	-	-	-	-	-	-	-
	0.050-sec. average acc.	-	-	-	-	-	-	-	-	-

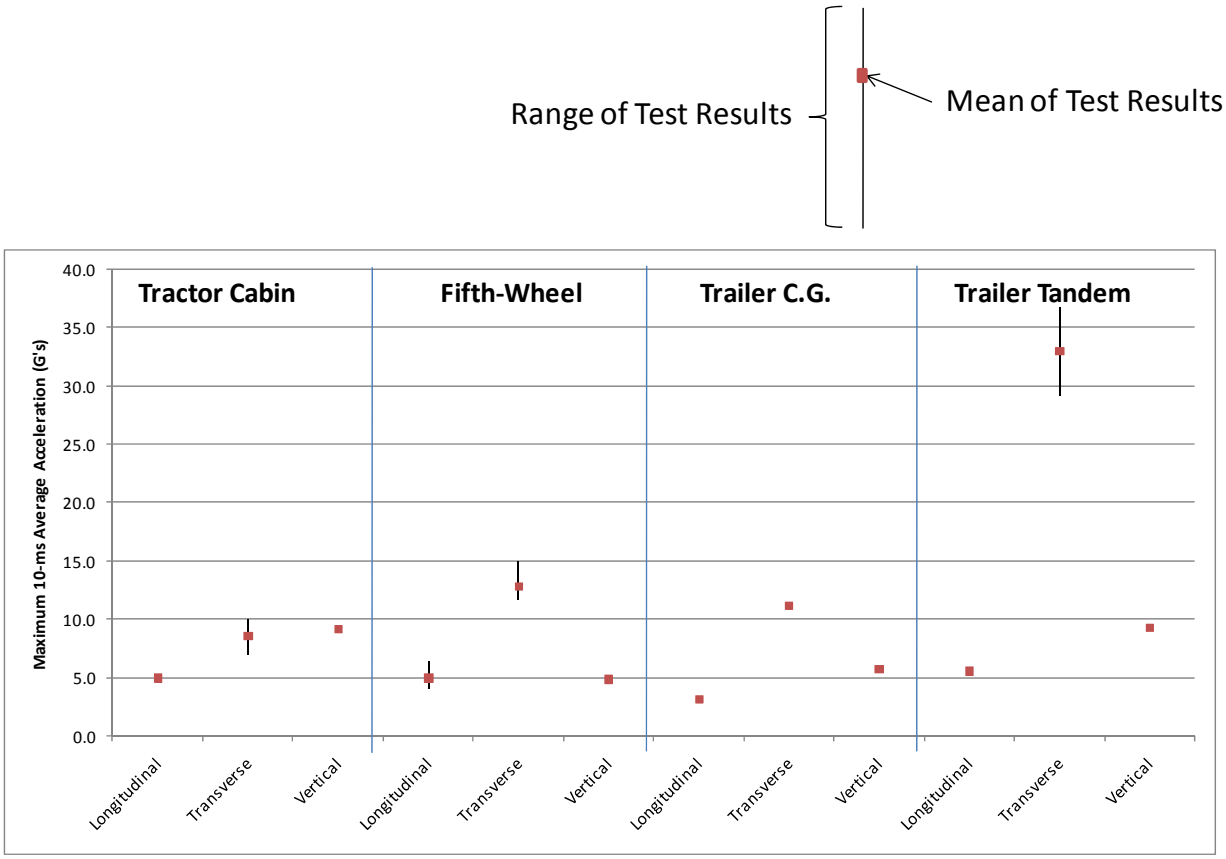

Figure 13. Chart. Summary of peak 0.01-second moving average acceleration from full-scale tests.

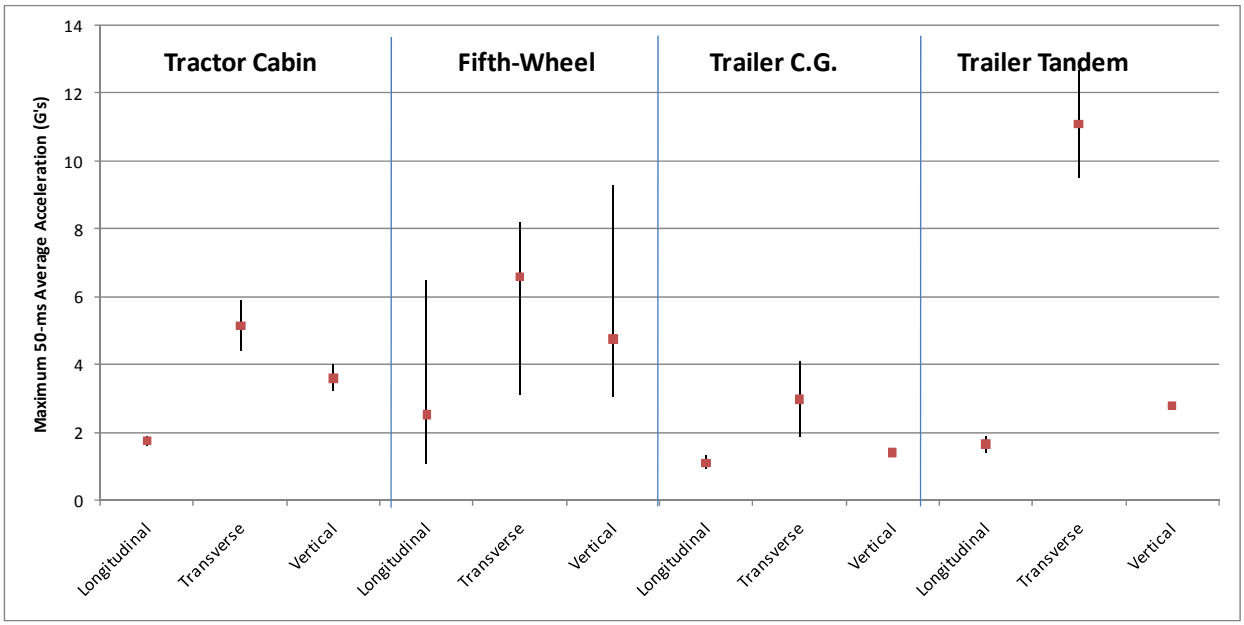

Figure 14. Chart. Summary of peak 0.05-second moving average acceleration from full-scale tests.

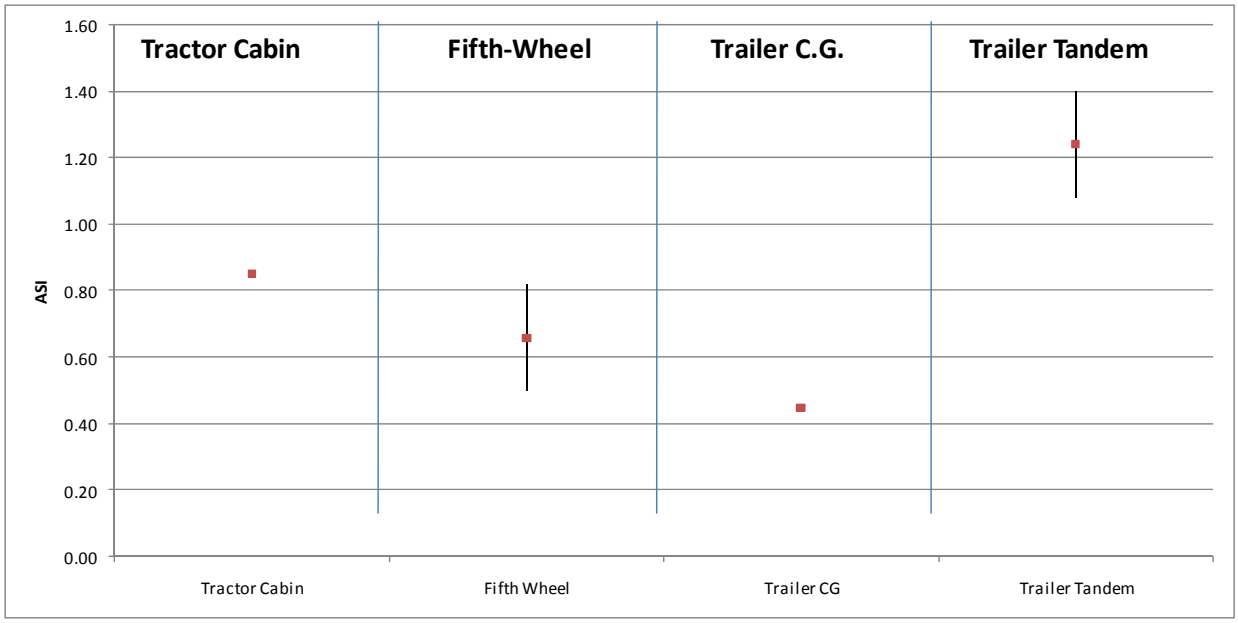

Figure 15. Chart. Summary of peak ASI from full-scale tests.

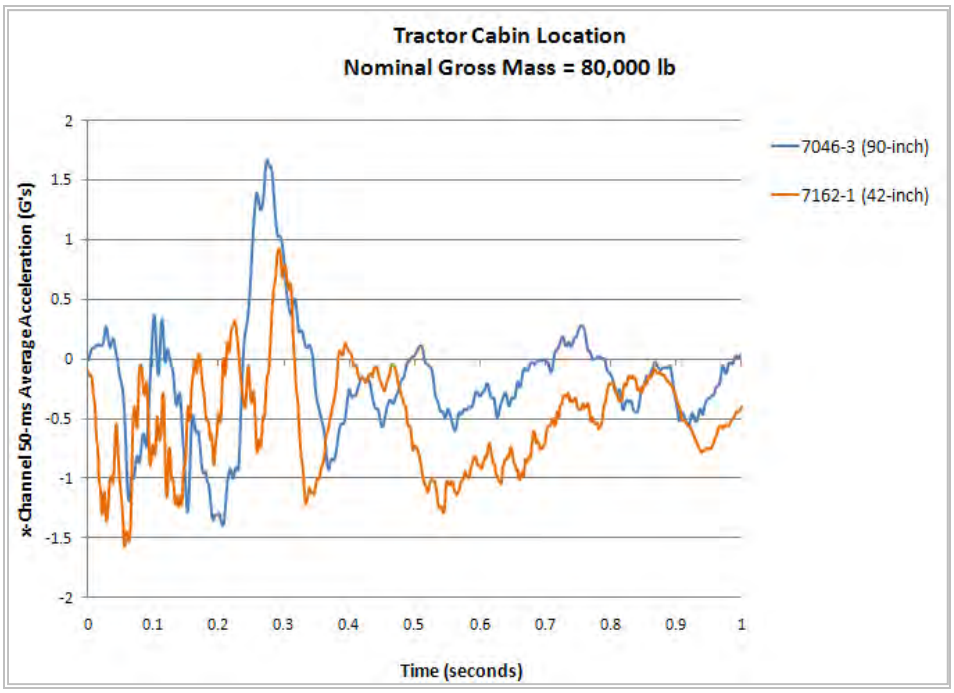

Figure 16. Chart. X-channel 0.050-seconds average acceleration-time history from accelerometer located inside tractor cabin near the tractor center of gravity (for 80,000-lb test vehicles).

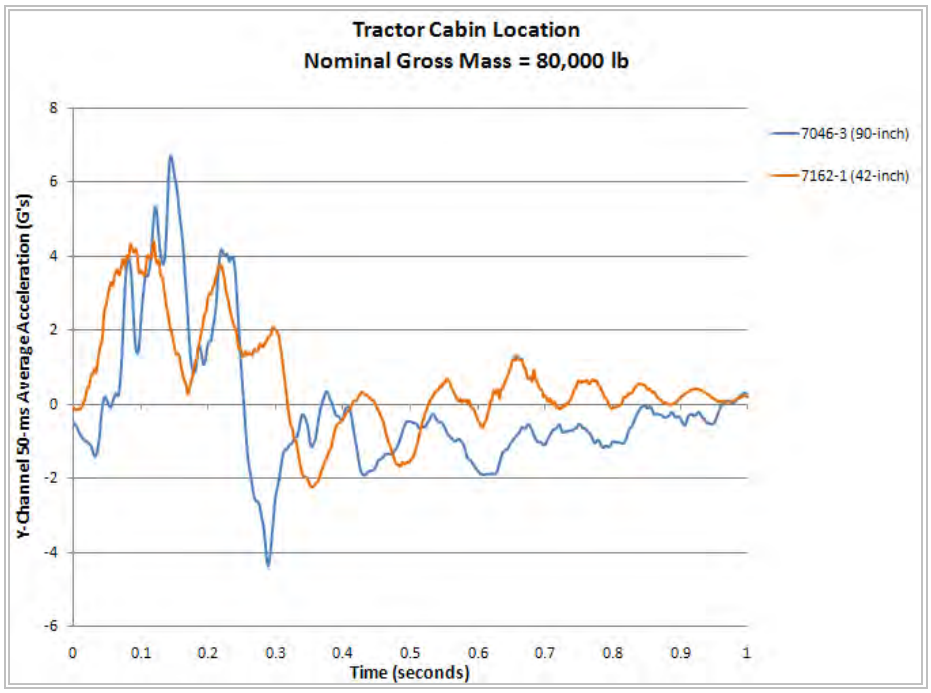

Figure 17. Chart. Y-channel 0.050-seconds average acceleration-time history from accelerometer located inside tractor cabin near the tractor center of gravity (for 80,000-lb test vehicles).

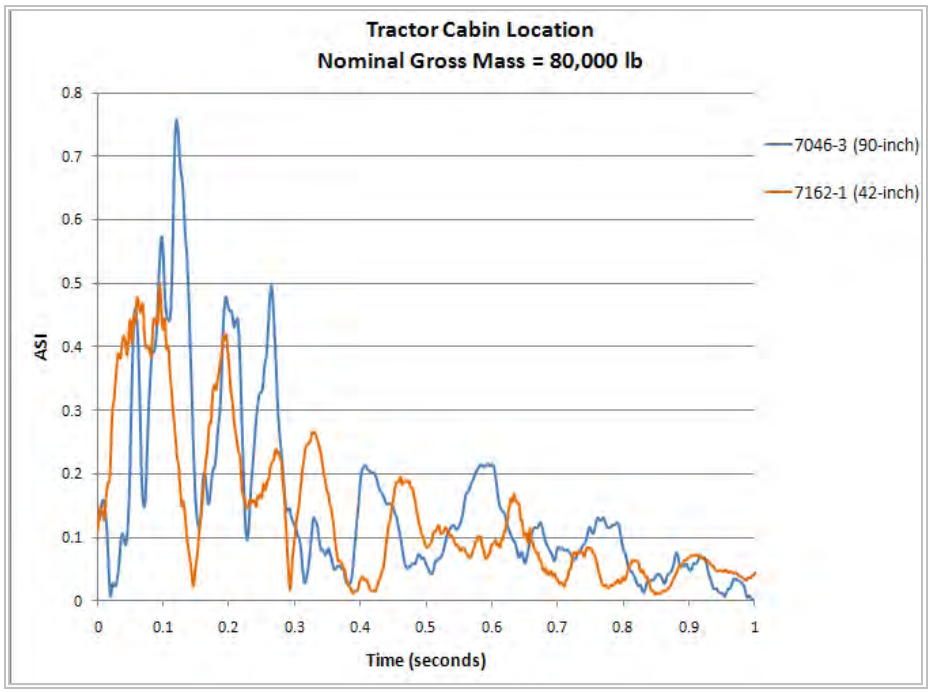

Figure 18. Chart. ASI-time history from accelerometer located inside tractor cabin near the tractor center of gravity (for 80,000-lb test vehicles).

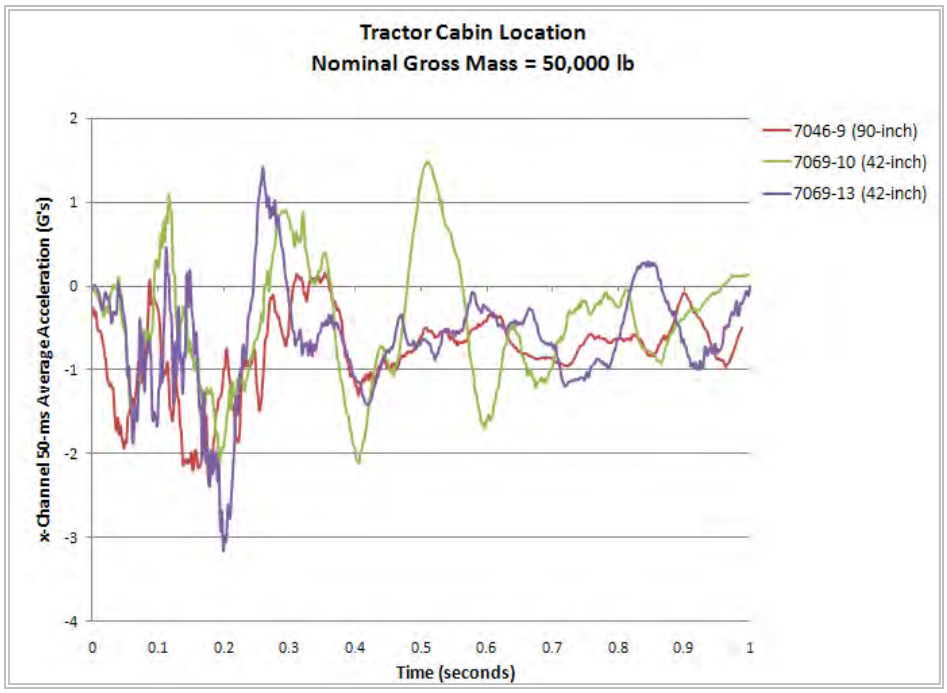

Figure 19. Chart. X-channel 0.050-seconds average acceleration-time history from accelerometer located inside tractor cabin near the tractor center of gravity (for 50,000-lb test vehicles).

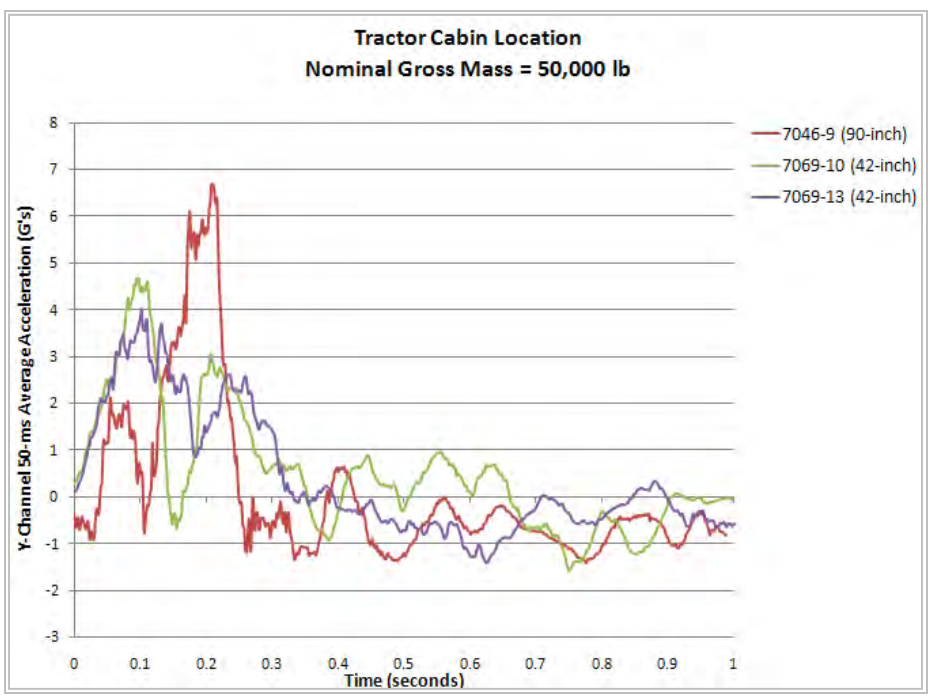

Figure 20. Chart. Y-channel 0.050-seconds average acceleration-time history from accelerometer located inside tractor cabin near the tractor center of gravity (for 50,000-lb test vehicles).

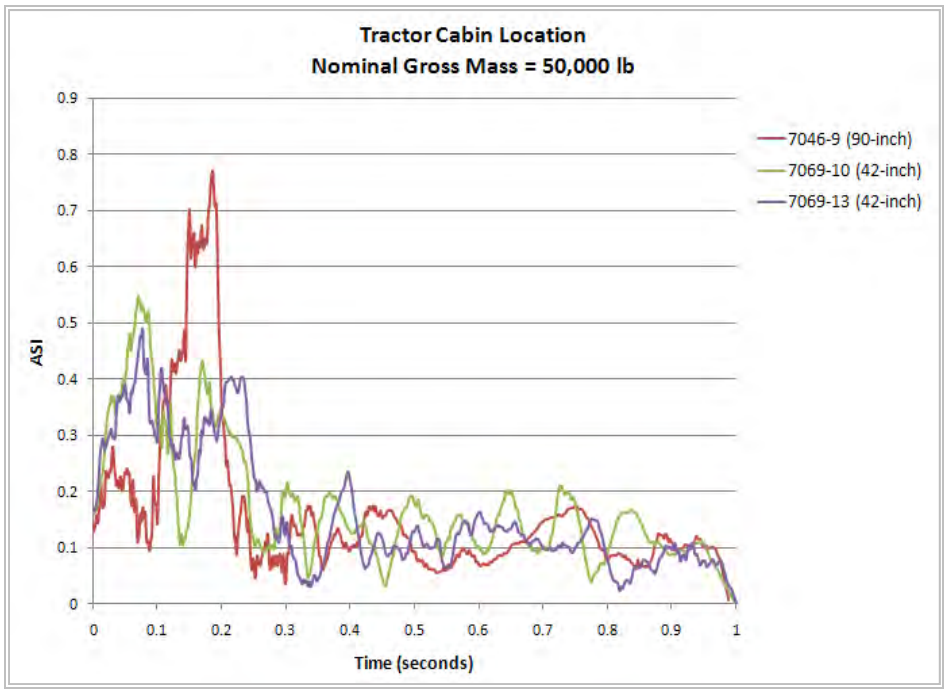

Figure 21. Chart. ASI-time history from accelerometer located inside tractor cabin near the tractor center of gravity (for 50,000-lb test vehicles).

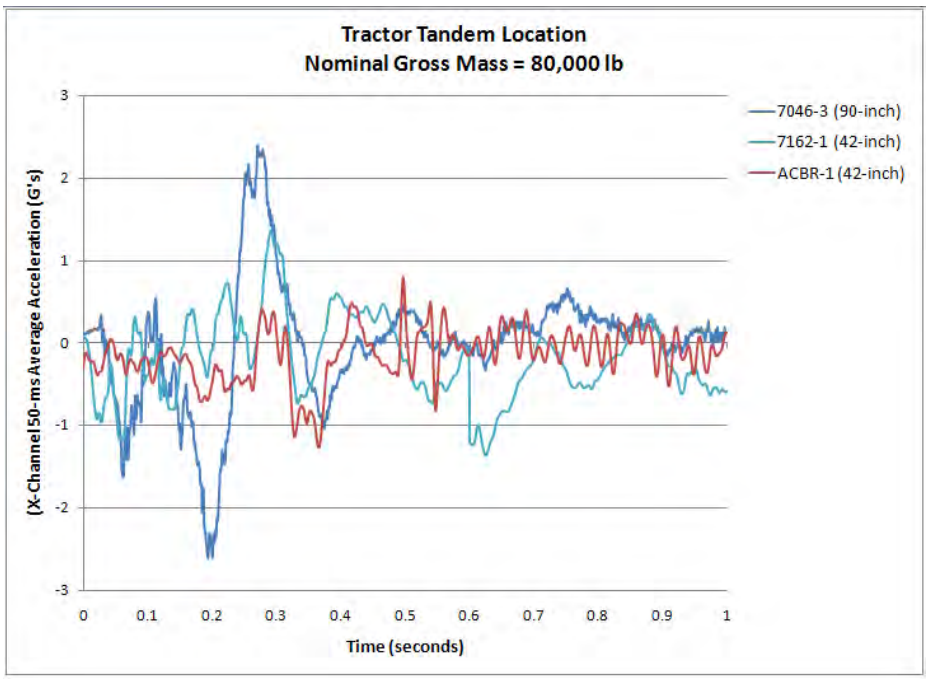

Figure 22. Chart. X-channel 0.050-seconds average acceleration-time history from accelerometer located near the tractor fifth-wheel (for 80,000-lb test vehicles).

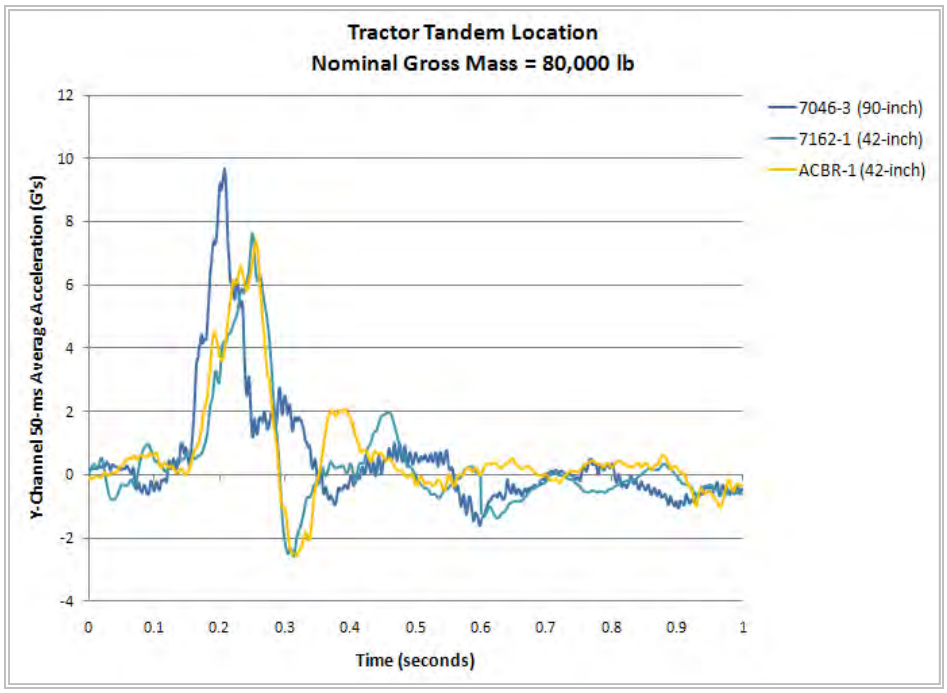

Figure 23. Chart. Y-channel 0.050-seconds average acceleration-time history from accelerometer located near the tractor fifth-wheel (for 80,000-lb test vehicles).

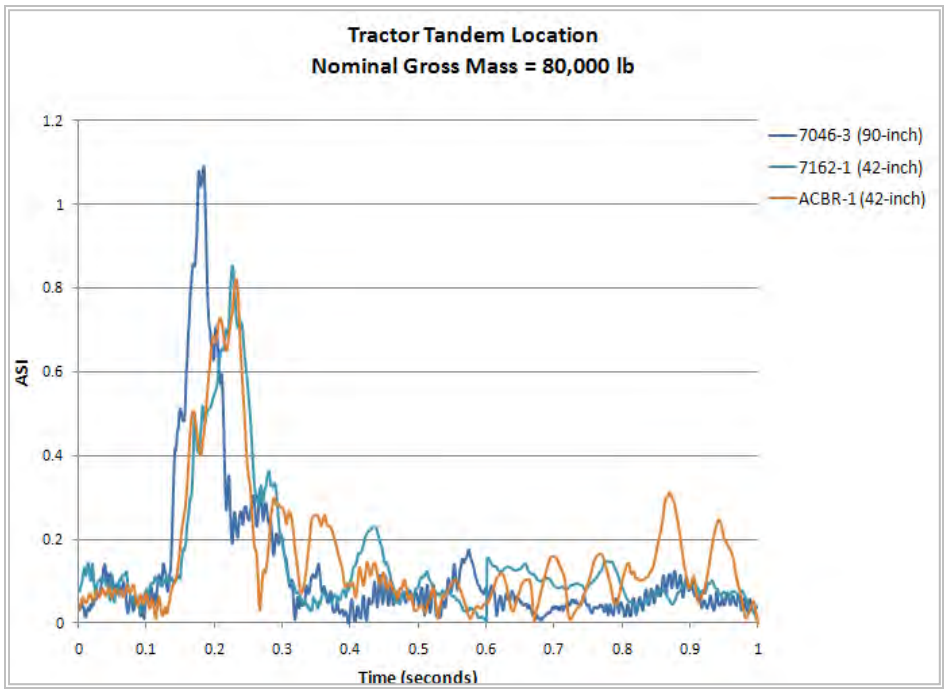

Figure 24. Chart. ASI-time history from accelerometer located near the tractor fifth-wheel (for 80,000-lb test vehicles).

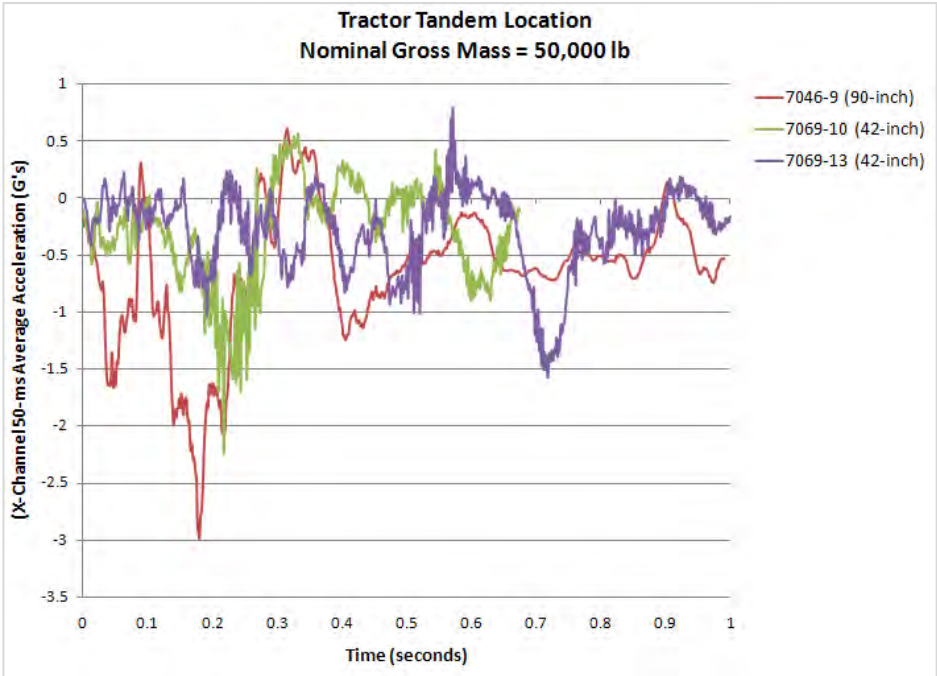

Figure 25. Chart. X-channel 0.050-seconds average acceleration-time history from accelerometer located near the tractor fifth-wheel (for 50,000-lb test vehicles).

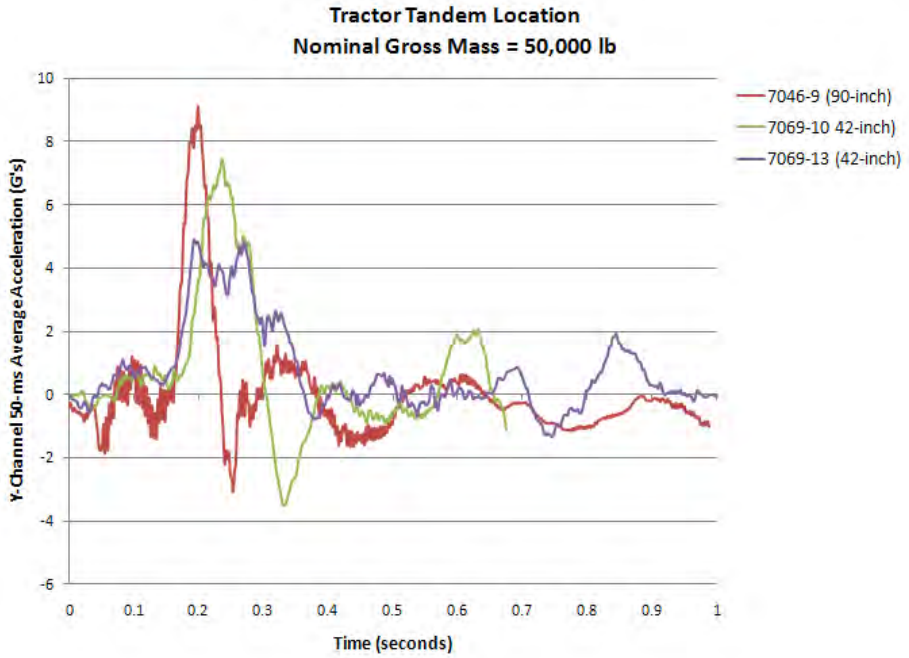

Figure 26. Chart. Y-channel 0.050-seconds average acceleration-time history from accelerometer located near the tractor fifth-wheel (for 50,000-lb test vehicles).

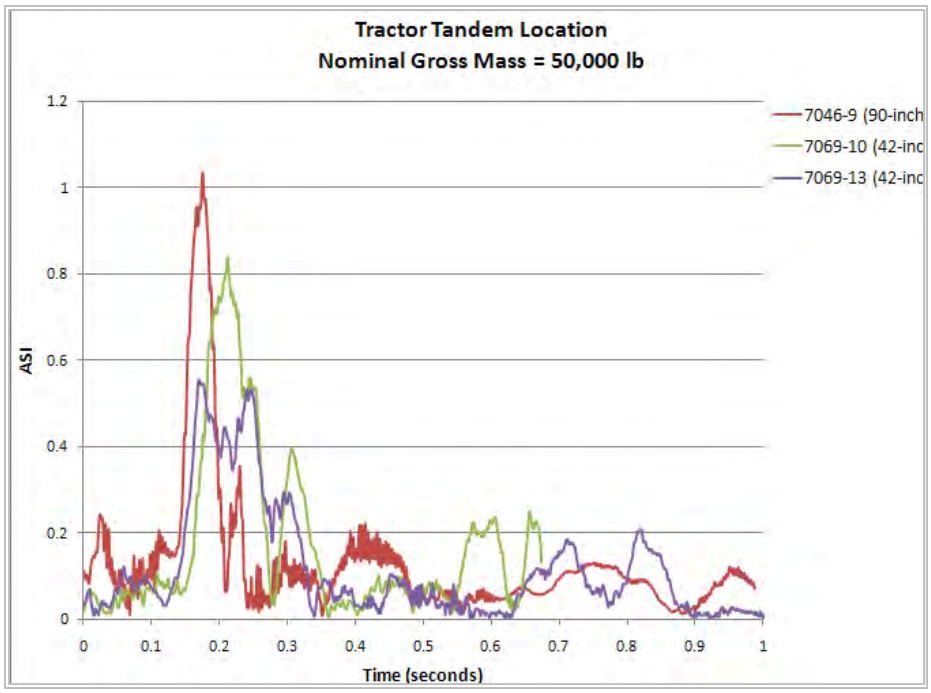

Figure 27. Chart. ASI-time history from accelerometer located near the tractor fifth-wheel (for 50,000-lb test vehicles).

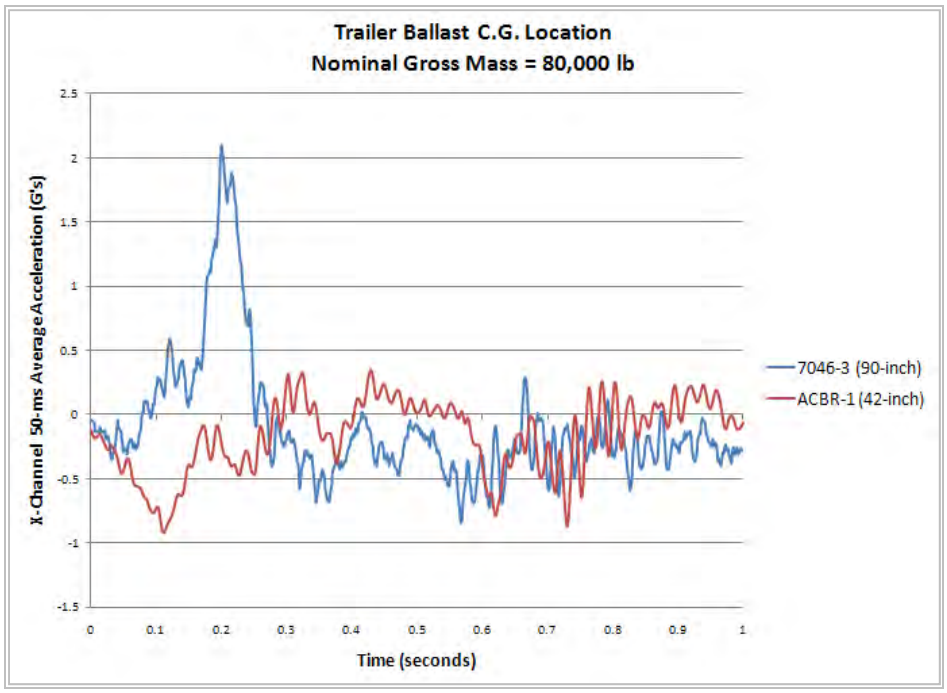

Figure 28. Chart. X-channel 0.050-seconds average acceleration-time history from accelerometer located near the center of gravity of the trailer ballast (for 80,000-lb test vehicles).

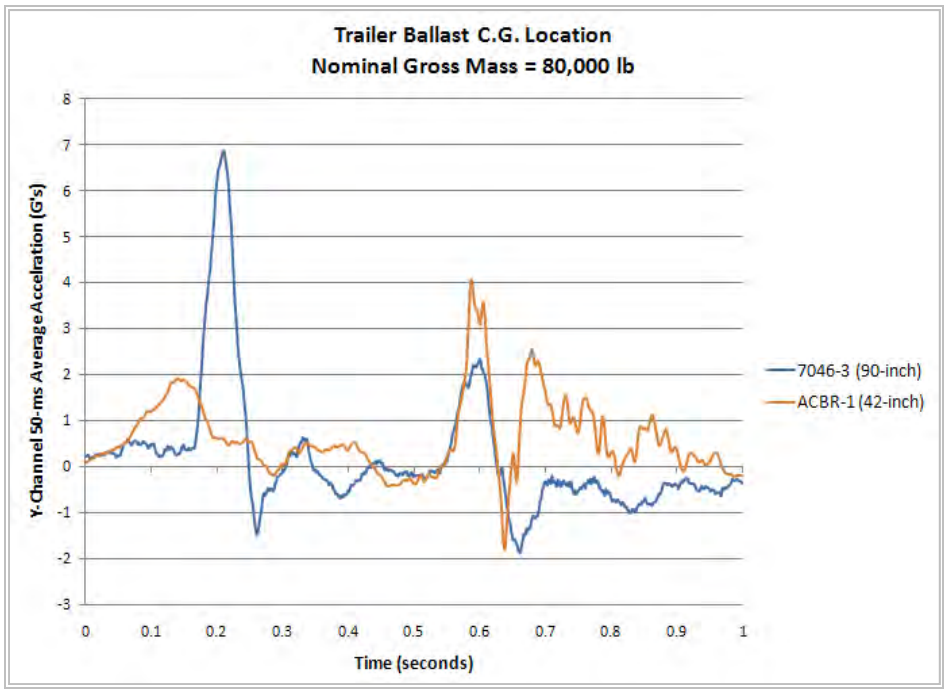

Figure 29. Chart. Y-channel 0.050-seconds average acceleration-time history from accelerometer located near the center of gravity of the trailer ballast (for 80,000-lb test vehicles).

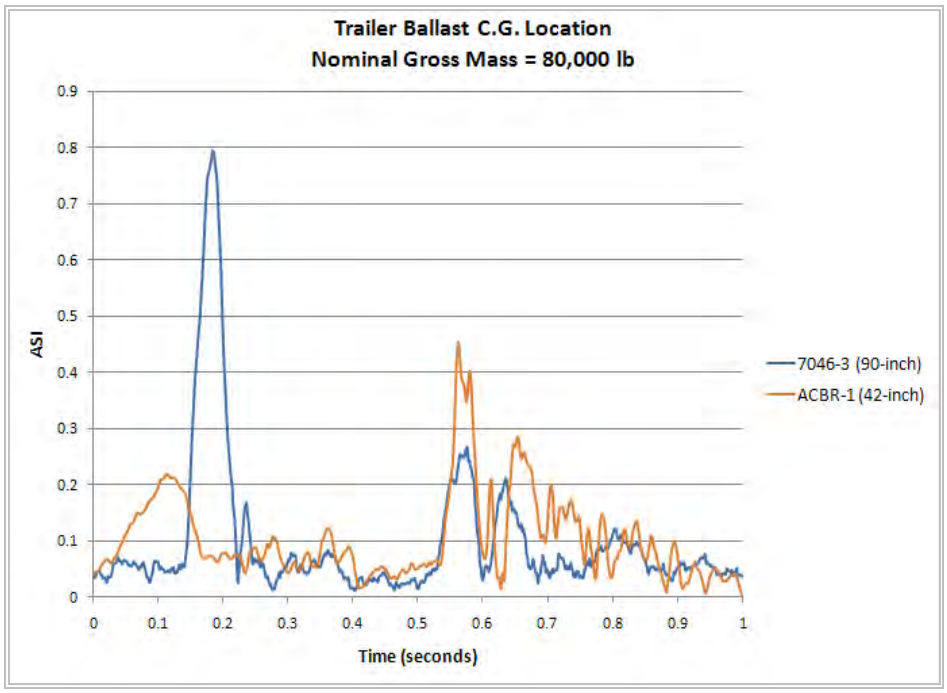

Figure 30. Chart. ASI-time history from accelerometer located near the center of gravity of the trailer ballast (for 80,000-lb test vehicles).

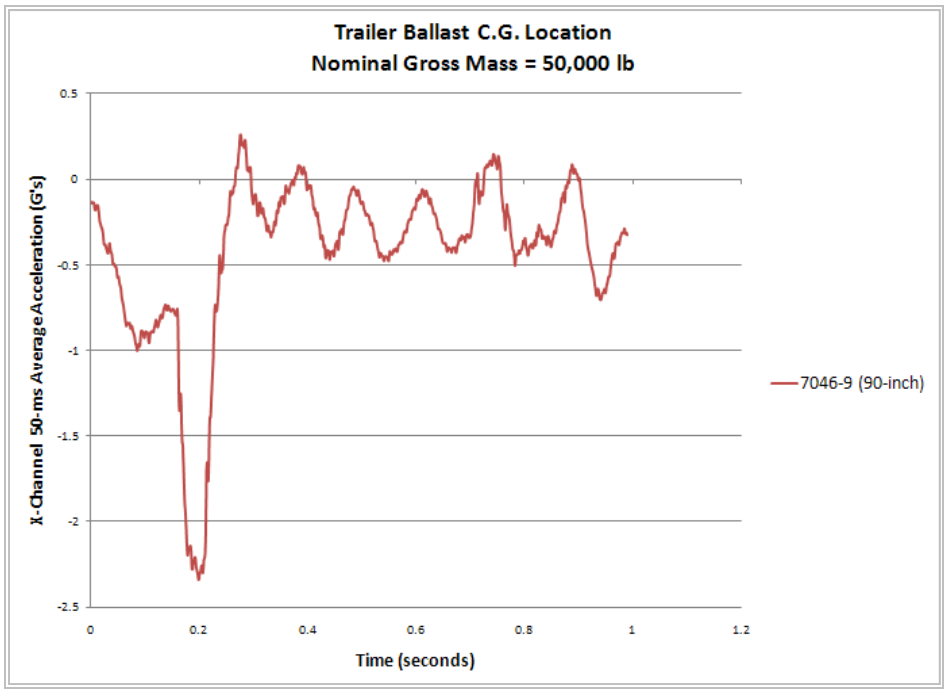

Figure 31. Chart. X-channel 0.050-seconds average acceleration-time history from accelerometer located near the center of gravity of the trailer ballast (for 50,000-lb test vehicles).

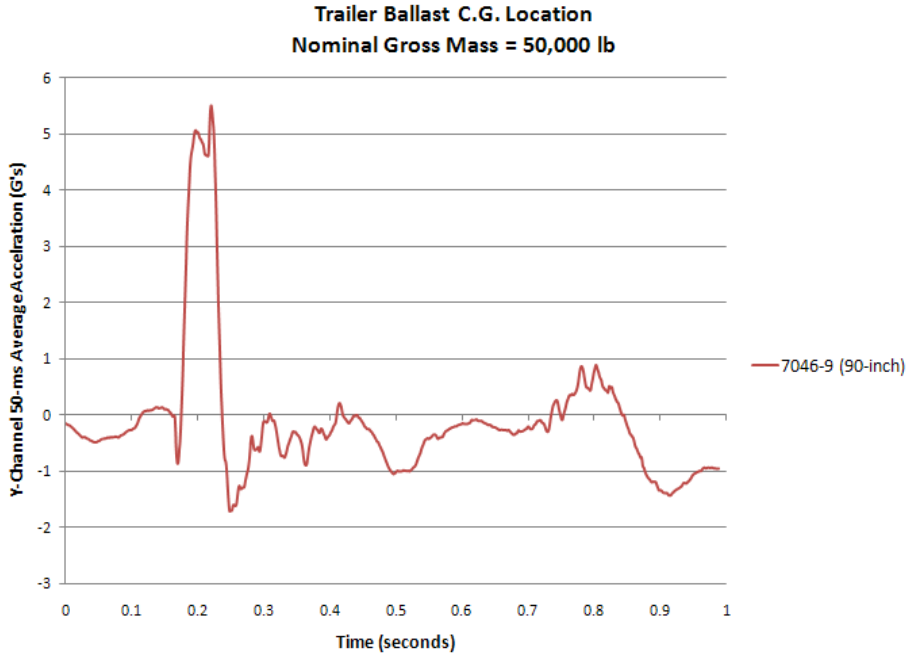

Figure 32. Chart. Y-channel 0.050-seconds average acceleration-time history from accelerometer located near the center of gravity of the trailer ballast (for 50,000-lb test vehicles).

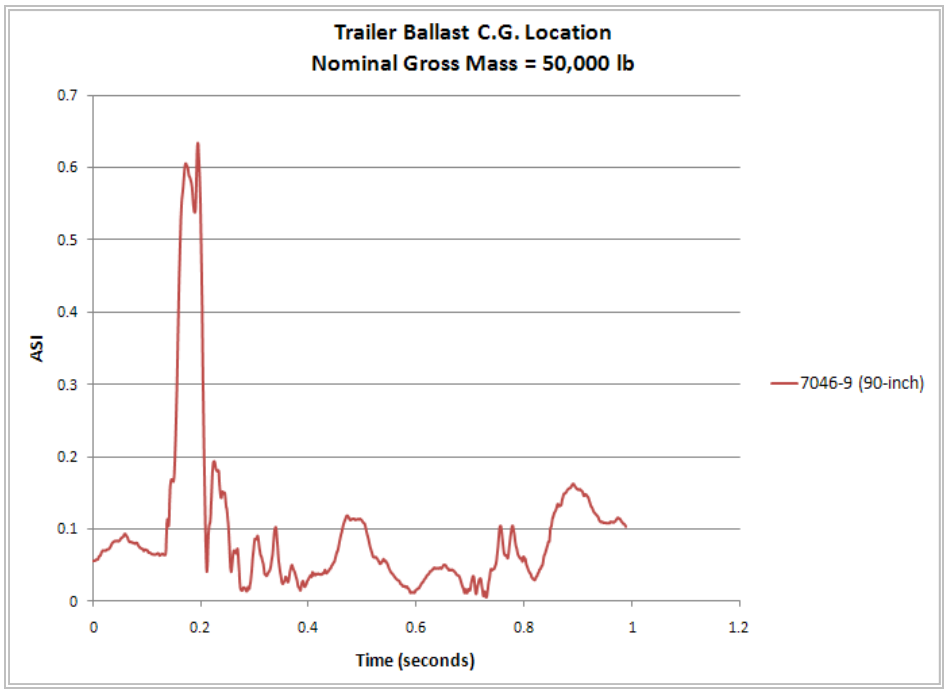

Figure 33. Chart. ASI-time history from accelerometer located near the center of gravity of the trailer ballast (for 50,000-lb test vehicles).

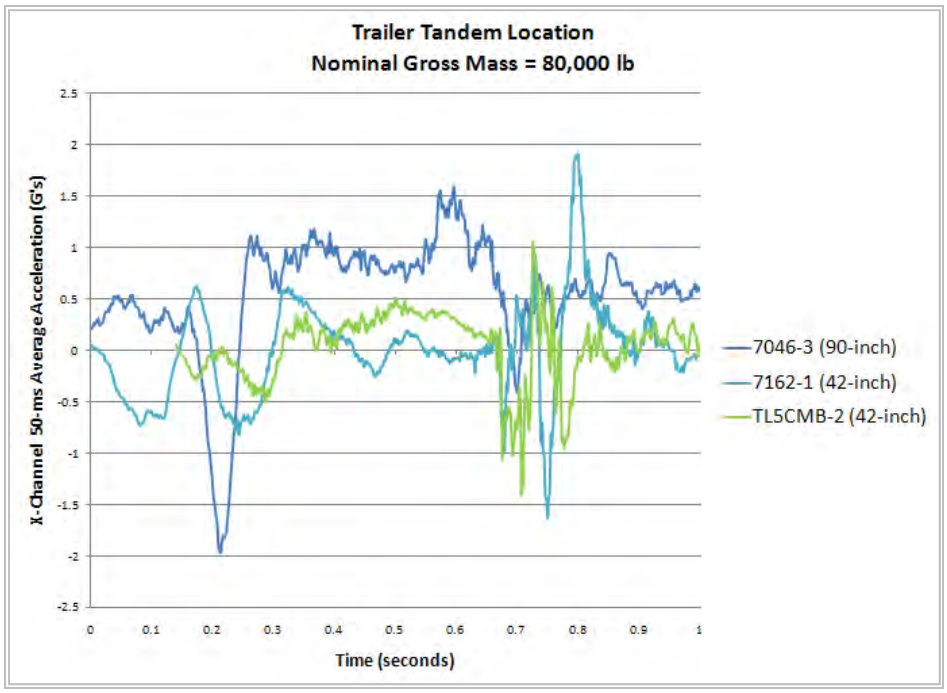

Figure 34. Chart. X-channel 0.050-seconds average acceleration-time history from accelerometer located near the trailer tandem axle (for 80,000-lb test vehicles).

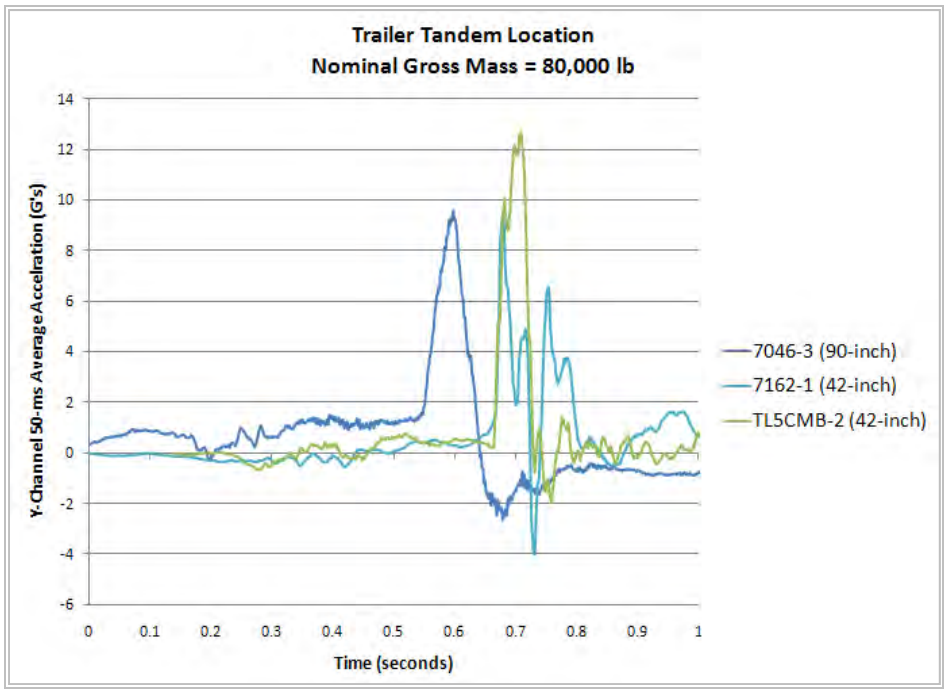

Figure 35. Chart. Y-channel 0.050-seconds average acceleration-time history from accelerometer located near the trailer tandem axle (for 80,000-lb test vehicles).

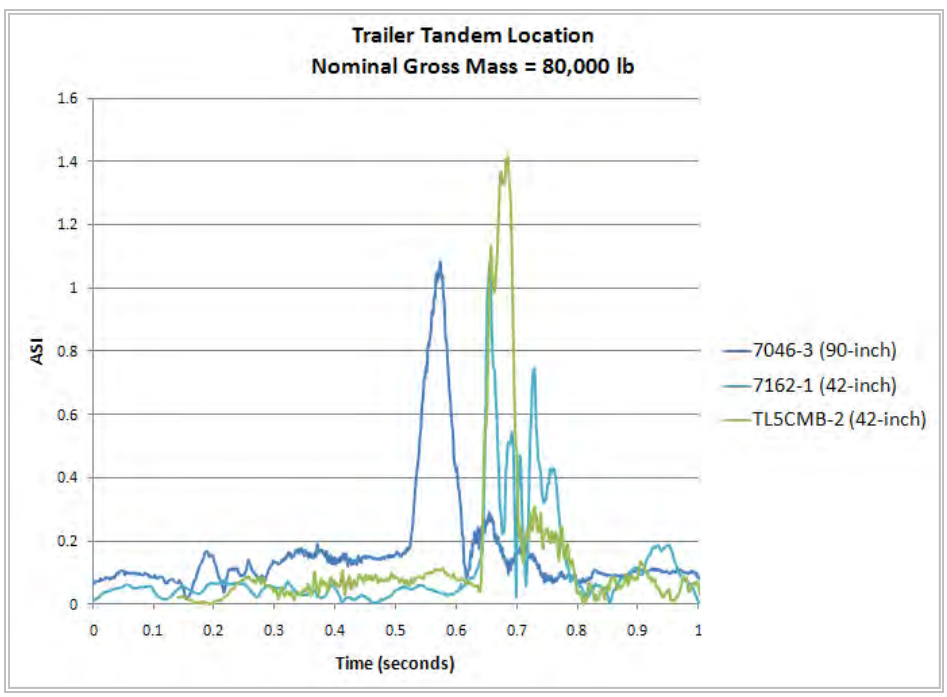

Figure 36. Chart. ASI-time history from accelerometer located near the trailer tandem axle (for 80,000-lb test vehicles).

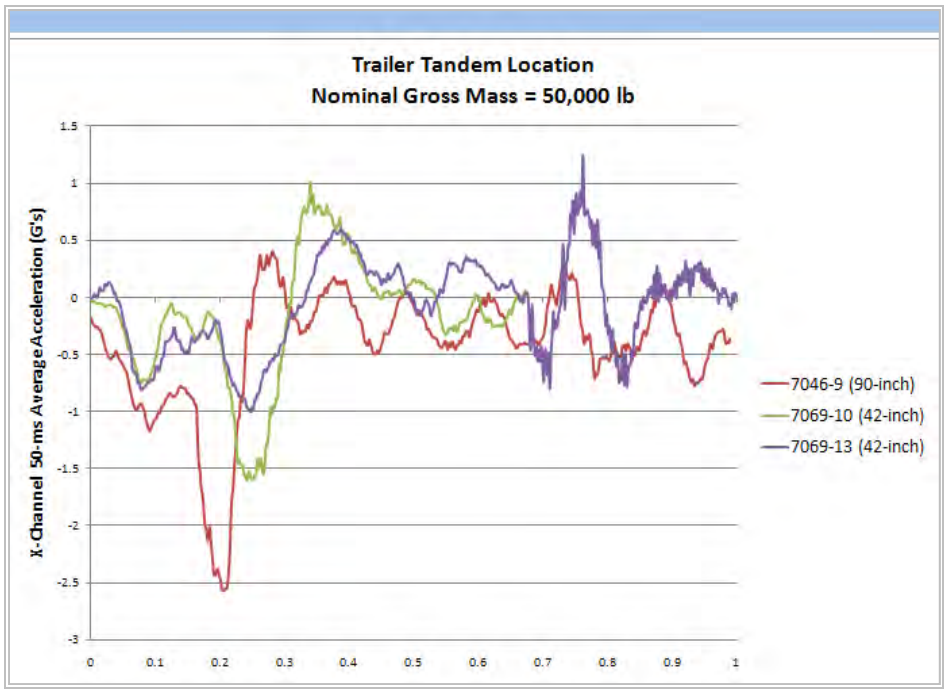

Figure 37. Chart. X-channel 0.050-seconds average acceleration-time history from accelerometer located near the trailer tandem axle (for 50,000-lb test vehicles).

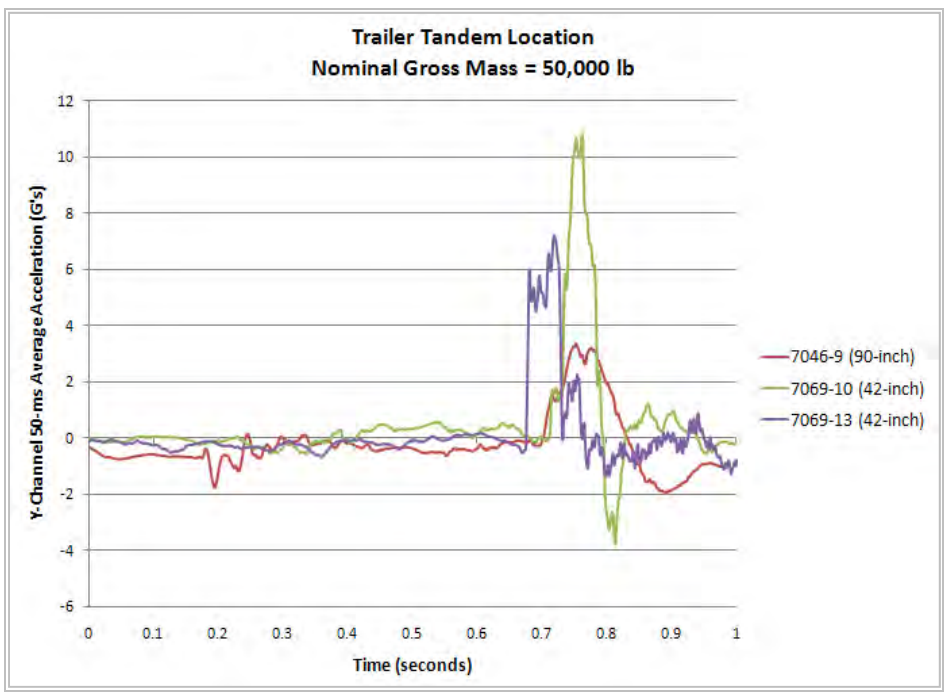

Figure 38. Chart. Y-channel 0.050-seconds average acceleration-time history from accelerometer located near the trailer tandem axle (for 50,000-lb test vehicles).

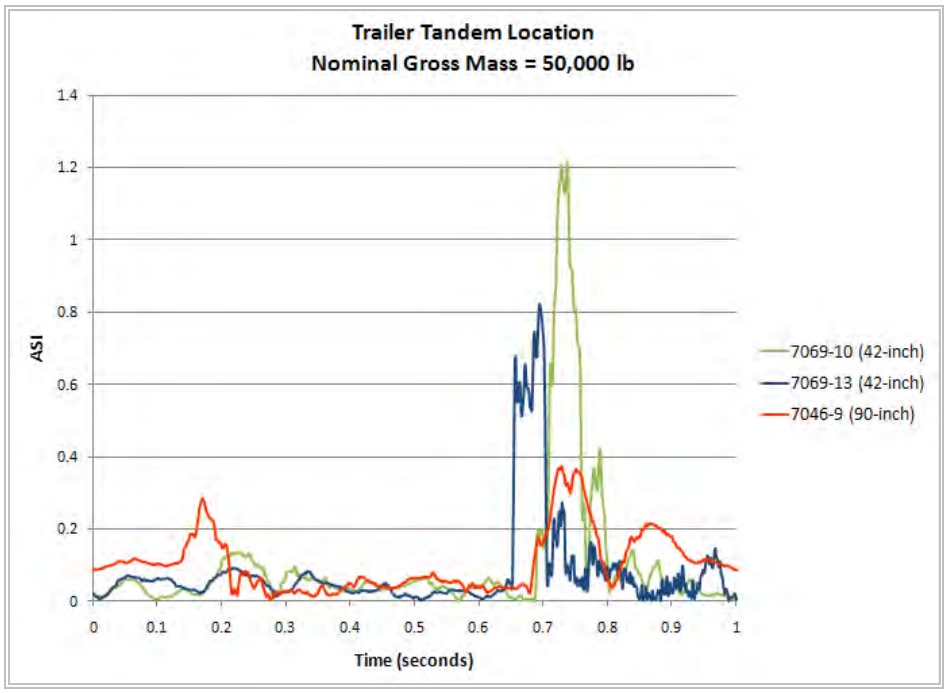

Figure 39. Chart. ASI-time history from accelerometer located near the trailer tandem axle (for 50,000-lb test vehicles).

Chapter 3 – Semitrailer Model Development

The tractor model provided by NCAC did not include a fully compatible trailer. The ultimate usefulness of the tractor FE model, particularly for simulating NCHRP Report 350 Test Level 5 impacts, obviously depends upon the capability to simulate the entire tractor-trailer vehicle. Development of the tractor FE model was started before the trailer FE model because the tractor is much more complex.

The development of a semi-trailer was accomplished during Phase A of this project. The original semi-trailer model developed by NCAC was determined to be inappropriate for use in simulations of NCHRP Report 350 Test Level 5 (TL-5) crash tests, based on comparison of the model's geometry with the requirements specified in Report 350 and with semi-trailers used in previous TL-5 crash tests. A decision was made in Phase A by the NTRCI FEA Research Team, NTRCI, and FHWA to create the new trailer model.

The new trailer model was developed based primarily on the geometry of a 53-ft Stoughton trailer. The CAD geometry was obtained through a collaborative effort between research team and Digimation. Research team staff visited a local Freightliner dealer and surveyed the trailers on their lot. Photographs and measurements were taken and provided to Digimation for use in developing the CAD geometry. This geometry was then used by the research team to develop the FE mesh of the semi-trailer.

While the external appearance of the trailer model developed by the team appeared suitable, it was necessary to make multiple assumptions about the structure and geometry of key components that affect the structural behavior of the trailer. With the agreement of NTRCI, the research team purchased a used box trailer during Phase B and proceeded to disassemble, section, and measure key trailer model components to provide an accurate representation of the trailer. The remainder of this chapter of the Phase B Report is organized into three sections as follows:

- Description of the Physical Trailer Upon Which the Model is Based
- Description of the Trailer FE Model
- Finite Element Meshing and Modeling Approach Details for Major Components.

Description of Physical Trailer Upon Which the Model is Based

The original semi-trailer that was used to obtain detailed physical measurements for the initial FE model developed in Phase A of this project was a 16.2-m (53-foot), dual-tire, tandem axle 2004 Stoughton box trailer located on a Columbus, Ohio Freightliner dealer's lot. The semi-trailer purchased for more detailed FE modeling in Phase B is shown in Figure 40. It was a 14.6-(48-foot), dual-tire, tandem axle 1990 Stoughton box trailer obtained from National Semi-Trailer Corporation in Columbus, Ohio, and was very similar structurally to the original semi-trailer. Both trailers were equipped with Airide suspension systems.

Figure 40. Photograph. Stoughton 14.6-m (48-ft) semi trailer.

The trailers that the FE model was based on had airbag "Airide" rear suspension systems with a moveable wheelset (bogey) with fore-aft position adjustment. This wheelset consists of a longitudinal steel frame with four main crossmembers (called the slider subframe). It has two main axles with four (dual) wheels/tires on each axle and suspension pivot arms to accommodate movement of the airbag "springs" and shock absorbers.

The wheelset is attached to the cargo box via a sliding connection to allow for positioning of the trailer's wheels fore-aft for various loading conditions. This sliding connection is the (nested) interface of the wheelset's subframe (Z-channel) members with the cargo box main longitudinal frame (Z-channel) members. The wheelset is locked into position via two (fore and aft) 25.4-mm (1-inch) diameter round lateral bars on the wheelset subframe that engage indexing holes in the cargo box main longitudinal frame Z-channel members.

The floor of the cargo box is made up of longitudinally oriented oak wood planks bolted to, and supported on, laterally oriented steel I-beams. The main longitudinal cargo box frame that interfaces with the wheelset is welded to the laterally oriented steel I-beams.

The side walls of the cargo box are assemblies of a riveted aluminum (or steel) outer skin, reinforced with galvanized steel vertical "hat-section" beams regularly spaced with 2-foot wide ¼-inch plywood panels between them on the interior of the cargo area.

The front wall is similar in construction to the side walls; a riveted aluminum (or steel) outer skin, reinforced with regularly spaced galvanized steel vertical “hat-section” beams. The vertical beams support one large plywood panel on the interior of the cargo area.

The roof of the cargo box is thin sheet metal skin – typically aluminum, supported on laterally oriented “roof bows” – which are formed, galvanized steel (beam) sections. The roof bows are riveted to the upper side rails, and connected to the roof sheet metal with a flexible adhesive.

Description of the Trailer FE Model

Model Size Data

The trailer FE model size information for version 48_09-0518 is:

- 325,542 Nodes
- 95 Parts
- 233,019 Elements
  - 220,062 shell
  - 12,913 solid
  - 32 beam
  - 108 mass
  - 12 discrete
  - 478 nodal rigid body
- 34 Material Definitions
  - 2 wood
    - Laminated oak
    - Low-grade plywood
  - 24 steel
    - Elastic
    - Rigid
    - ASTM A653/A653M structural quality grade 80
    - CS 1040
    - CS 1095
    - mild steel
    - HSLA Grade 50 SAE950X
    - HSLA Grade 80 SAE980X
    - 4140 Cr-Mo austenized 999C, oil quenched, tempered 399C
    - 4140 Cr-Mo austenized 999C, oil quenched, tempered 199C
    - A500 Grade B Shaped Structural Tubing
    - Leaf Spring Steel 5160 HB 407
    - Leaf Spring Steel 5160 HB 460
    - Malleable cast iron, ferritic

        - Malleable cast iron, whiteheart
        - Malleable cast iron, pearlitic
        - AISI 8630 strength 862 MPa
        - AISI 8630 strength 1034 MPa
        - AISI 8630 strength 1241 MPa
        - Stainless steel rivet 302HQ
        - SAE Grade 5 bolt
        - SAE Grade 8 bolt
        - A148 casting grade 80-50
        - Wheel Rim (Yield 270 MPa)
        - Mat_Spotweld (yield 276 MPa)
    - 7 Aluminum
        - elastic
        - 6061-T6 (JC Model)
        - 6061-T6 (MAT24)
        - A319 casting
        - 3004-H39
        - 3003-H14
        - 2117-T4
    - 1 Rubber
        - Elastic

Time Step

The target minimum time-step specified on the *Control_Timestep card was set to -1.400 microseconds. This minimum time step was specified with the contingency that mass scaling would be used to maintain it. During a recent simulation, there were only about 40 elements that required a smaller time step. Of these 40 elements, the smallest required time step that LS-Dyna calculated was about 1.19 microseconds. With the mass scaling option invoked, the total mass added to the entire model in this simulation was 8.2 kilograms. The element length that corresponds to the specified 1.4 microsecond time step for steel and aluminum is about 7 to 10 mm. The target element size for structural elements is 25 to 100 mm (1.0 to 4.0 inches). To model the geometry everywhere with reasonable accuracy, the actual element sizes in the model ranged from about 8 mm to about 120 mm.

Material Summary

All of the metal parts in the trailer are either aluminum or steel. To avoid repetition in describing these materials in this section, all aluminum parts' elastic material properties were specified with a Young's modulus of 69,000 MPa (10,000,000 psi), density of 2,700 kg/m^3 (0.100 lbs/in^3), and a Poisson's ratio of 0.33. All steel parts' elastic material properties were specified with a Young's modulus of 210,000 MPa (30,000,000 psi), density of 7,850 kg/m^3 (0.289 lbs/in^3), a

Poisson's ratio of 0.30. Refer to the Chapter 4 – Semitrailer Material Properties and Material Models section of this report for more details.

Element Types Used

Shell elements are all specified as type 16. This is a fairly efficient, fully integrated shell-formulation element that will accommodate some warping. Shell elements in areas that were expected to see significant bending were assigned 5 integration points through the thickness. Shell elements in other areas were assigned the default 3 integration points through the thickness.

Solid element type 2, fully integrated/selectively-reduced integration elements, was used to model deformable or geometrically complex solid parts. Solid element type 1, single-integration-point elements, was used for less structurally detailed parts such as spotwelds, accelerometer elements, etc.

In order to maintain an acceptable number of elements and a reasonable time-step, it was necessary to use fully-integrated elements throughout most of the Trailer FE model.

The tradeoff lies in the fact that fully-integrated elements require more calculations per element than reduced integration elements, but under-integrated elements require a minimum of three elements across the width of any planar section, such as a beam flange or web, or in the case of solid elements, multiple elements through a thickness to adequately model bending modes. The level of mesh refinement required to use all under-integrated elements was not possible due to the need to keep the element count reasonable and the time step size manageable.

Connection Schemes Used

In the many areas of the FE model where parts needed to be connected, various methods were used to implement the connections:

Common-Node. Wherever possible, intersecting and adjoining plates were modeled with simple common-node connections that required no further complication.

Constrained Nodal Rigid Bodies (CNRB). CNRBs are a convenient way to connect very dissimilar mesh areas. They were used to connect parts that were more-or-less permanently connected and were not likely to be modified by the user.

CNRBs were used to connect adjoining parts that had mesh-dissimilarities such as different mesh size or element type (shell-to-solid, shell-to-beam, etc.). CNRBs were used to connect:

- Roof bows to upper side rails
- Side-wall vertical beams to upper side rails
- Side-wall vertical beams to lower side rails
- Lateral cross beams to wooden floor
- Front-wall vertical beams to kingpin box

- Landing gear structural members
- Door hinges and latches.

CNRB's were also used in conjunction with kinematic joint elements to create:

- Rotating wheels to axles
- Pivoting suspension control arms
- Kingpin to fifth-wheel pivot point.

Mat_Spotweld. The Mat_Spotweld connection uses solid elements and is a very convenient way to connect parts that might need to be moved relative to each other by the user. They use a tied-interface contact connection method, so if connected parts need to be moved relative to one another, no tedious reconnecting or redefining of the connection elements is necessary. These elements are also easy to create via element move/copy/translate, and no individual node-picking is required to define the connection.

Mat_Spotwelds were used to connect:

- Wheelset subframe to main longitudinal cargo box frame
- Roof bows to roof skin
- Side wall vertical beams
- Front plywood liner to front wall vertical beams.

Accelerometers

Acceleration-time histories and angular rate-time histories were collected using the *Element_Seatbelt_Accelerometer option in Ls-Dyna, which is the preferred method suggested by Ls-Dyna for collecting acceleration data [15]. Only one accelerometer was used on the trailer model. It was connected via a CNRB to the trailer floor at the rear of the cargo box, above the wheelset, at 2122.63 mm forward of the rear bumper in the 48-foot trailer. The time-history data was collected from each accelerometer in a local reference coordinate system which rotates with the accelerometer in the same way that test data is collected from physical accelerometers.

A total mass of 4.8 kg (10.5 lb) was added to the nodes of the CNRB. The purpose of the added mass was to reduce the high frequency response of the accelerometer. For these types of application (vehicle crash analysis), it is not the specific point on the trailer that the accelerometer is connected to that is of interest, but rather the rear section of the trailer in general. Without the added mass, the data from the accelerometer would need to be collected at a frequency of approximately 100 kHz to avoid aliasing of the data. The added mass acts much like a "filter" that reduces the frequency at which data needs to be collected and facilitates data processing. The data was collected at a frequency of 30 kHz which was determined to be sufficient to avoid aliasing of the data.

Model Check Statistics

Jacobian Element Shape Parameter. The Jacobian Element Shape Parameter is a measure of an element's deviation from a perfectly square or cubic shape. The Jacobian parameter varies from 0.0 for badly-shaped elements that will cause the run to terminate to 1.0 for a perfect element. Negative Jacobian values are possible, and simply indicate a mis-connected or inverted element. Jacobian values of 0.70 to 1.0 are considered good elements that will yield acceptably accurate stress results within the limitations of the particular local mesh refinement. Jacobian values in the range of 0.40 to 0.70 will not cause run-time problems, but will have less accurate stress results. Jacobian values in the range of 0.0 to 0.40 are sufficiently misshapen to have inaccurate stiffness or even cause numerical problems.

There are 336 shell elements and 134 solid elements with Jacobian shape parameters less than 0.70. The minimum Jacobian for a shell element is 0.51, and the minimum Jacobian for a deformable solid element is 0.50.

Element Warpage. The maximum warpage in a shell element is 7.3° out of plane, and for a solid element is 2.15° out of plane on an element face.

Aspect Ratio. The maximum aspect ratio for a solid element is 8:1, and for a shell element it is 6:1.

Any Sources of Possible Numerical Instabilities

The most likely sources of numerical instability in the trailer FE model are the typical sources of numerical problems in any FE model:

- Contact
  - Node-tangling
  - Initial penetration
  - Conflicts with tied-contact connections and other constraint methods (e.g., spotweld, CNRB, etc.)
  - Mesh too coarse
- Mesh refinement
  - If the mesh is too coarse in high deformation region in the model, then the elements may become highly distorted during analysis, which would lead to instabilities caused by increased element warping, hourglass modes, poor Jacobian, etc.

Finite Element Meshing and Modeling Approach Details for Major Components

Kingpin Box

The Kingpin box is the heavily reinforced steel weldment at the front of the trailer that provides the structural support and strength for the Kingpin which is the main attachment point for connecting the tractor to the trailer. Since it is half the interface between the tractor and the

trailer, the Kingpin box structural characteristics and stiffness will greatly affect the overall response of the tractor-trailer vehicle. Consequently, this component had to be represented correctly in the FE model. Figure 41 shows an overall view of the Kingpin Box in place in the physical trailer and in the FE model. Figures 42 and 43 show views of the removed Kingpin Box – actual and FE model.

(a) Physical trailer (b) FE model

(a) Physical trailer (b) FE model

Figure 41. Photograph / Illustration. Kingpin box in place in the (a) physical trailer and the (b) FE model.

Figure 42. Photograph / Illustration. (a) Isolated view of the kingpin box after it was removed from the physical trailer and (b) the finite element model of the kingpin box.

(a) Physical trailer (b) FE model

Figure 43. Photograph / Illustration. (a) The kingpin box with material cut away to gain access to the inside structure (b) the finite element model of the kingpin box showing internal structure.

The overall dimensions and plate thicknesses of the Kingpin Box weldment were measured directly. Sketches were made and photographs were taken. The FE model was created directly from this information using HyperMesh. Figure 44 shows the FE model with some elements removed to show mesh detail inside the Kingpin Box.

LS-Dyna Type 16 fully-integrated thin-shell elements were used throughout this component. The element size was nominally 24 mm (1-inch) for all elements in the Kingpin Box Assembly. This size was chosen because it was reasonable for the geometry definition, it would not adversely affect (decrease) the current typical time step size, and it would provide appropriate mesh refinement for contact with the Tractor's fifth wheel.

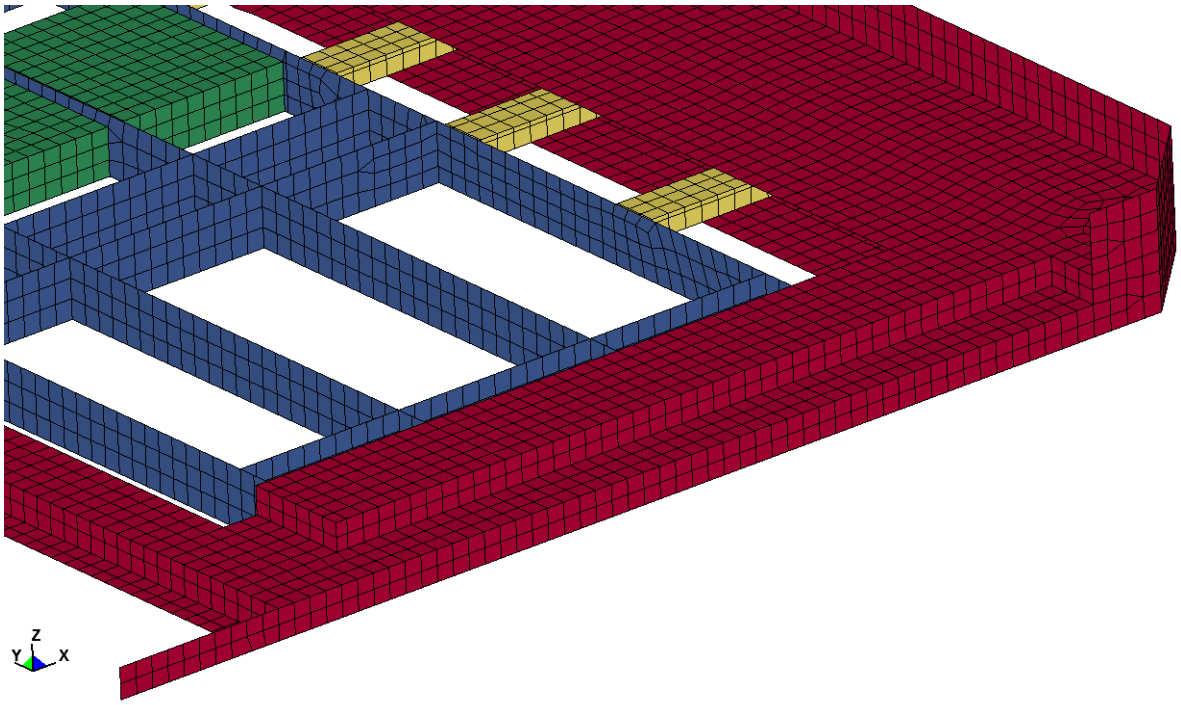

Figure 44. Illustration. Kingpin box showing internal plates and geometric detail.

The connectivity between all individual plates in the assembly was done using common-node connections. Individual plates in the weldment assembly were assigned unique *Part numbers to account for the various thicknesses and/or positions. The shell elements were assigned *Hourglass control type 8.[iii] The Kingpin Box material was characterized as AISI 8630 Steel using *Mat_Piecewise_Linear_Plasticity material model in LS-Dyna with a yield strength of 1,241 MPa. The Kingpin, shown in Figure 41, was specified as rigid material.

Main Lateral Cross-Beams

The main lateral cross beams are 100 mm (4-inch) tall steel I-beams (standard structural shapes) that run width-wise on a 300 mm (12-inch) spacing nearly the entire length of the trailer and support the wooden floor. These lateral cross beams were readily accessible for measurement and did not require dissection to obtain thickness and geometry. Figure 45 shows views of these lateral cross beams in the actual trailer and as implemented in the FE model.

[iii] This particular type of "hourglass control" used in conjunction with this fully integrated element type is actually a method to invoke the element's "full projection warping stiffness" to effect a true shell element formulation.

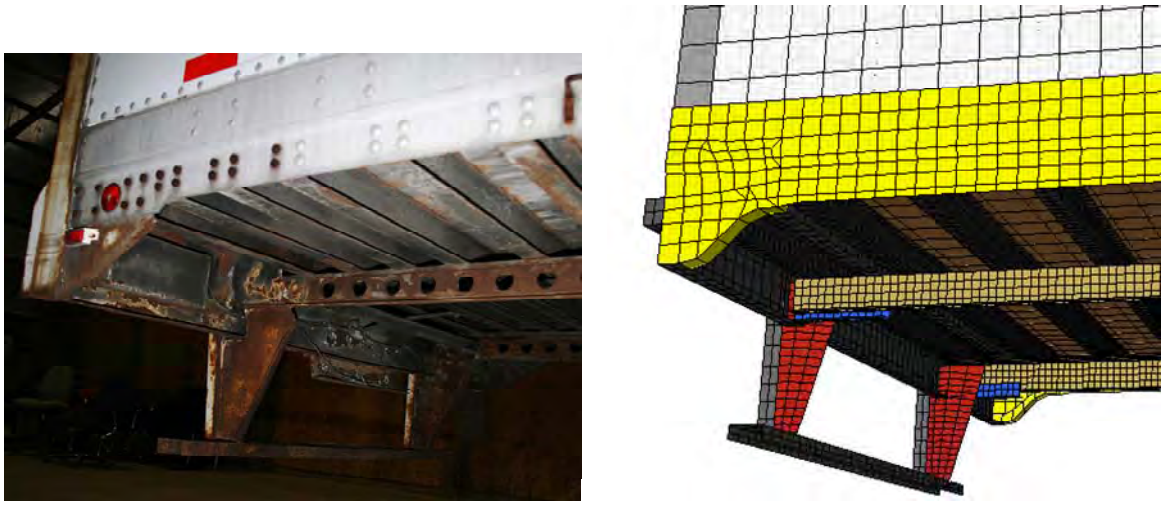

(a) Physical trailer (b) FE model

Figure 45. Photograph / Illustration. View of the lower-rear section of the (a) physical trailer and (b) FE model showing structural detail.

The overall dimensions and plate thicknesses of the Lateral Cross-Beams were measured directly. Sketches were made and photographs were taken. The FE model was created directly from this information using HyperMesh. LS-Dyna Type 16 fully-integrated thin-shell elements were used for the Lateral Cross-Beams. The element size was nominally 25 mm (1-inch) for the flange elements and ~30 mm (1.25-inch) for the web elements. This size was chosen because it was the minimum reasonable size to represent the geometry and it would not adversely affect (decrease) the current typical time step size.

The Lateral Cross Beams shell elements were assigned *Hourglass control type 8.[iii] The material specified for the Lateral Cross Beams was ASTM A653 Grade 80 with a yield strength of 550 MPa using the *Mat_Piecewise_Linear_Plasticity material model in LS-Dyna with no failure. The connectivity between the web and the flange was done with common-node connections. Figure 46 shows the Lateral Cross Beams.

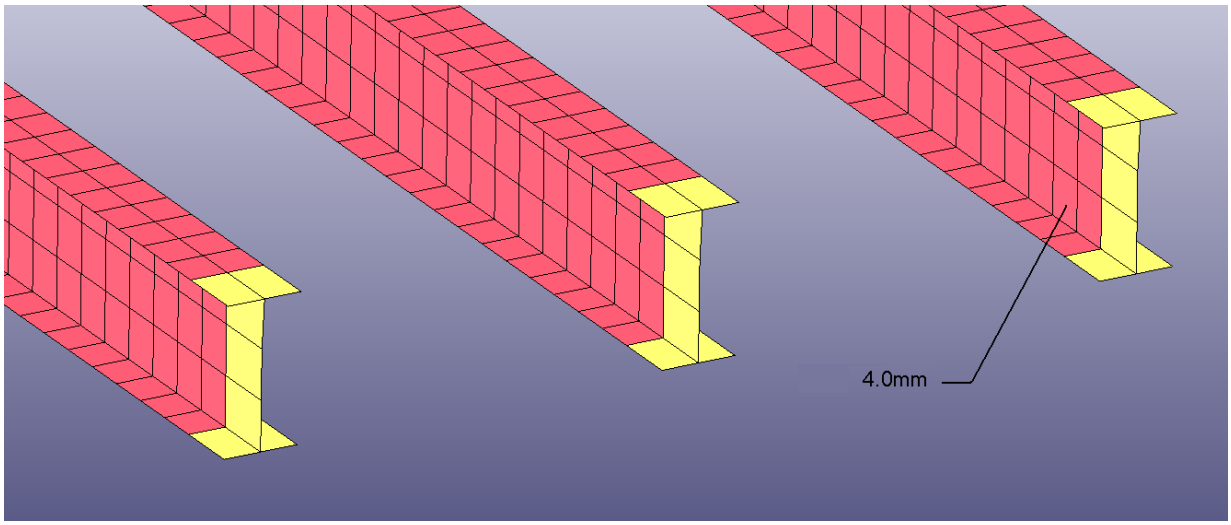

Figure 46. Illustration. Lateral cross beams.

The Lateral Cross Beams are connected to the Lower Side Rails using a tied shell edge contact. Figure 47 shows the orientation of the Lateral Cross Beam's edges to the Lower Side Rails.

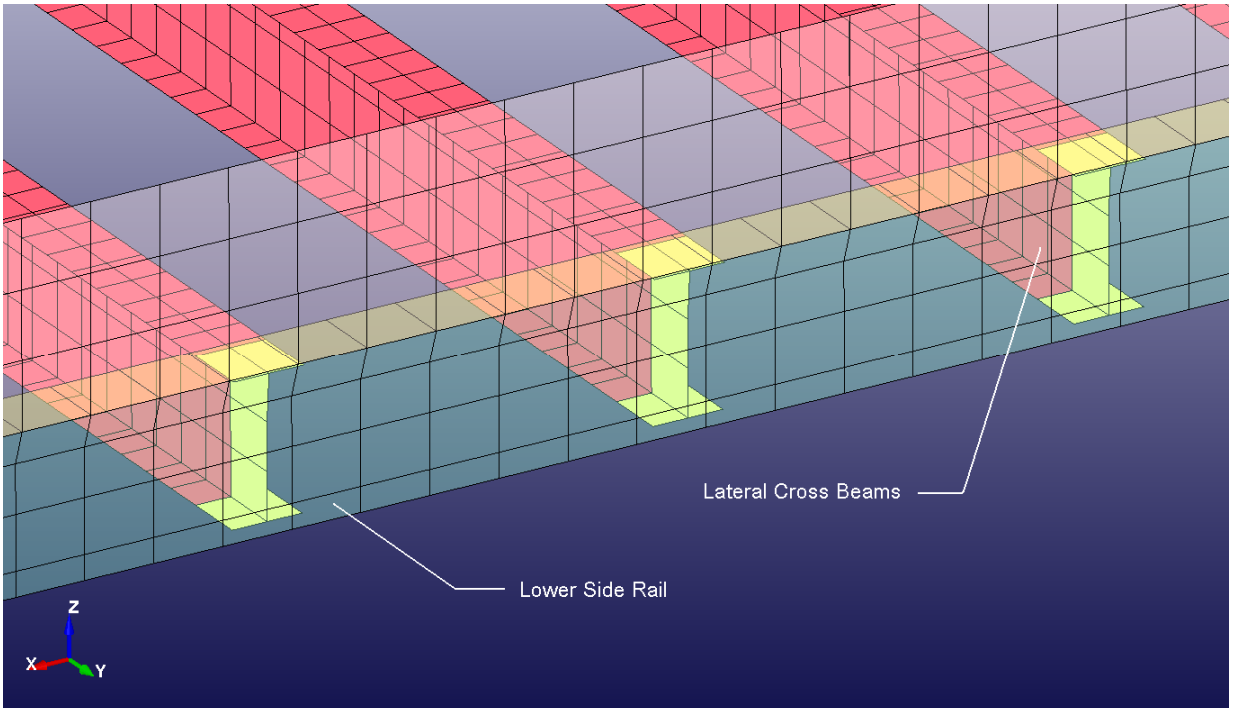

Figure 47. Illustration. Lateral cross beams orientation with lower side rail.

Side-Walls

The side-wall structure is comprised of an outer aluminum "skin", vertically oriented steel formed "hat" beam sections, and multiple vertical plywood panels. The skin, vertical beams, and plywood panels are riveted together. Figure 48 shows the trailer side-wall seen from inside the trailer.

A representative 2-foot by 4-foot section was saw-cut from the side wall. The overall dimensions and plate thicknesses of the side-wall assembly were measured directly. Sketches were made and photographs were taken. The FE model was created directly from this information using HyperMesh. LS-Dyna Type 16 fully-integrated thin-shell elements were used throughout this component. Individual plates in the assembly were assigned unique part numbers to account for the various thicknesses and/or positions. The shell elements were assigned *Hourglass control type 8.[iii] Figure 49 shows the location of the side wall cut and a view of the cut-out section from the actual trailer and from the FE model. Figure 50 is a labeled view of the FE model of the side-wall. Figure 51 shows the side-wall with the aluminum panels removed to reveal detail.

(a) Physical trailer

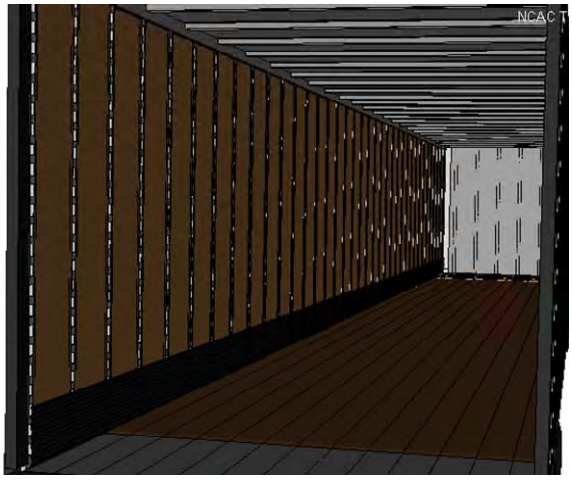

(b) FE model

Figure 48. Photograph / Illustration. View of the inside of the trailer box of (a) the physical trailer and (b) the FE model.

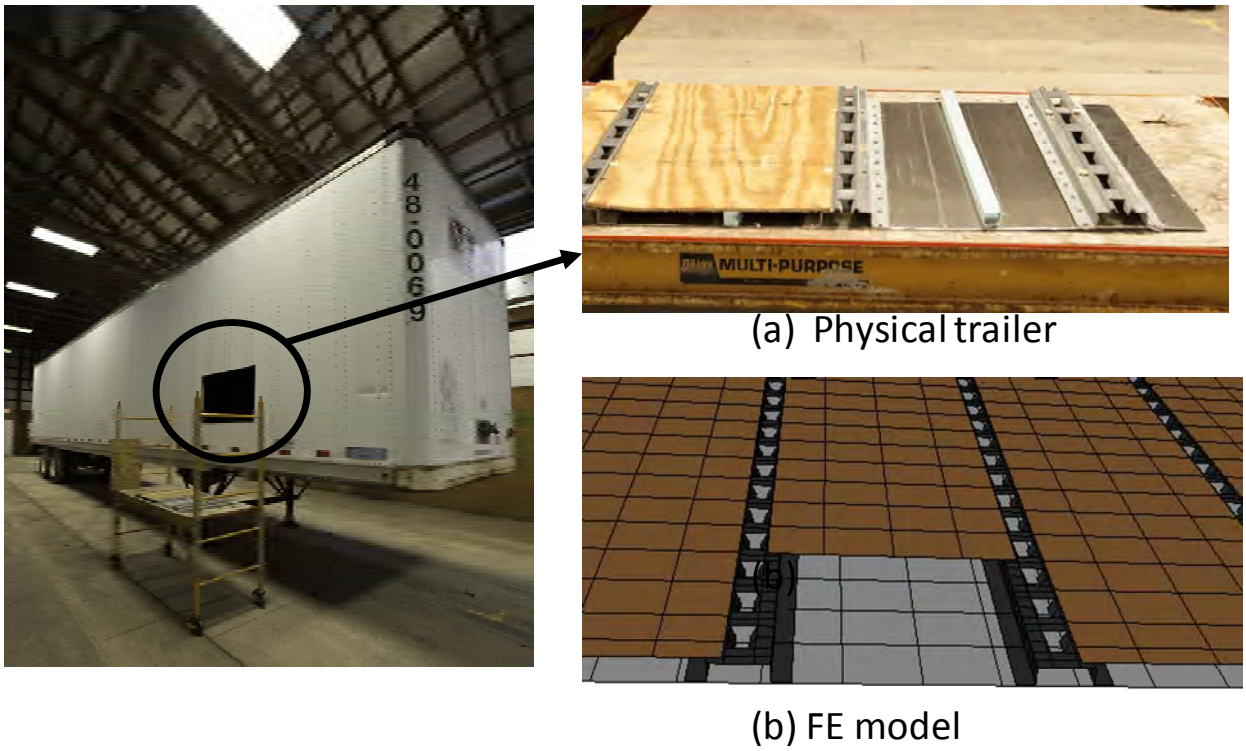

Figure 49. Photograph / Illustration. Cut section of the side-wall showing detail of sidewall components for (a) physical trailer and (b) FE model.

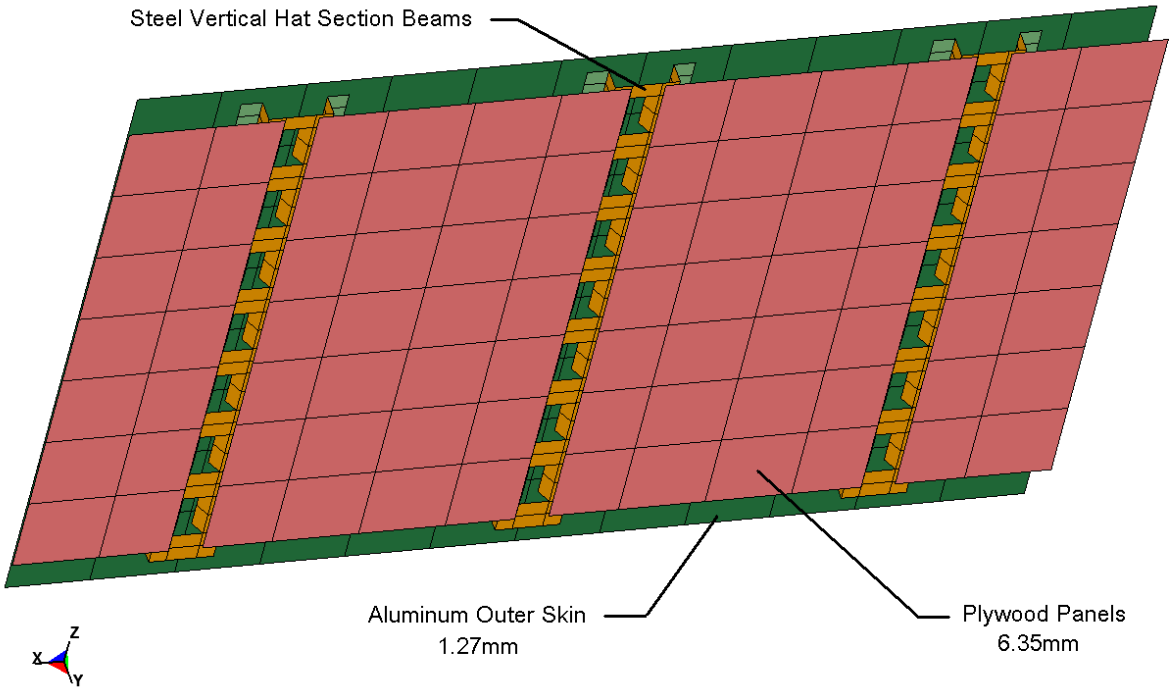

Figure 50. Illustration. Side-wall section detail.

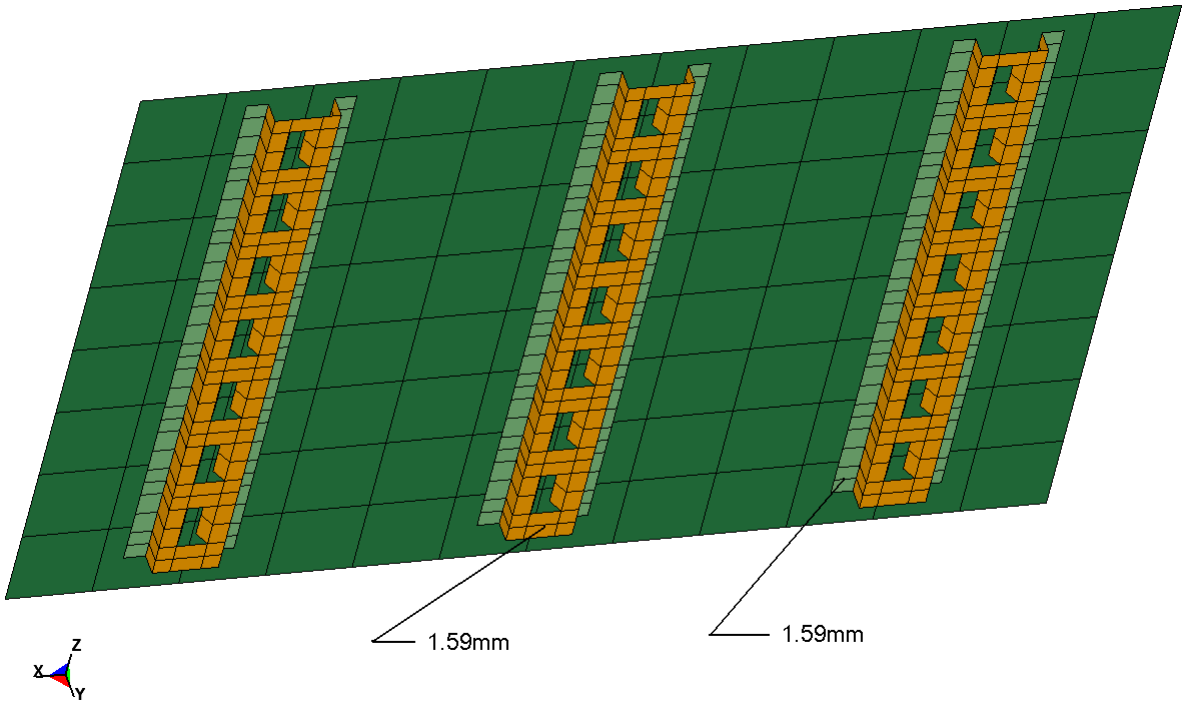

Figure 51. Illustration. Side-wall section detail with plywood removed to show vertical steel hat-sections.

The element size was nominally 100 mm (4-inches) for the elements of the Outer Aluminum skin and the Plywood Panels. The element size was nominally 20 to 40 mm (0.75 to 1.5-inches) for the steel vertical hat-section beams. This element size was chosen because it was reasonable for the geometry definition and it would not adversely affect (decrease) the current typical time step size. These vertical beams were connected to the Outer skin and the Aluminum Panels via "solid weld-elements" using *Mat_Spotweld in Ls-Dyna.

The Aluminum skin was specified as 6061-T6 using the *Mat_Simplified_Johnson_Cook (strain-rate dependent) material model in LS-Dyna with no failure. The plywood panels were modeled using the *Mat_Elastic material model in LS-Dyna with a density of 681 Kg/M^3 (measured) and a Young's Modulus of 12,400 MPa (typical value for wood). The vertical hat-sections were specified as CS1040 steel and were characterized using the *Mat_Piecewise_Linear_Plasticity material model in LS-Dyna with a yield strength of 368 MPa and no failure.

The Side-wall's vertical steel hat-sections are connected to the Upper Side Rails and to the Aluminum outer skin via *Constrained_Nodal_Rigid_Body's (CNRB's). Figure 52 shows a close-up view of this connection.

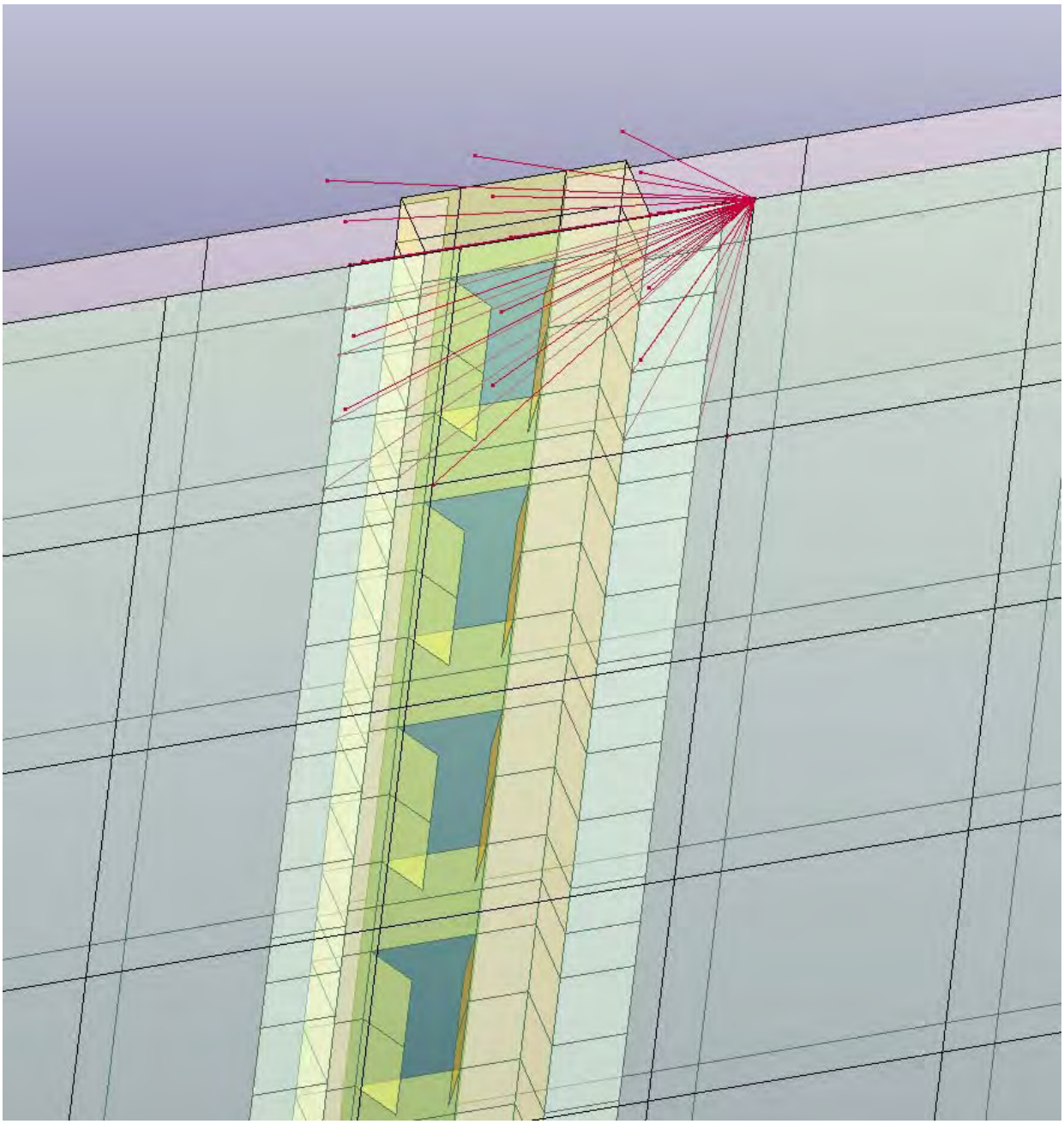

Figure 52. Illustration. Top side-wall connection showing CNRBs.

Upper and Lower Side Rails

The upper and lower side rails are aluminum extrusions that provide the upper and lower longitudinal legs of the cargo box frame for the trailer. They are riveted to the inner and outer skins at the top and bottom of the cargo box. These rails were section-cut to provide access for measuring the details of the geometry of their cross sections so this structural detail could be accurately implemented in the FE model. Figures 53 and 54 show the upper and lower side rails in the actual trailer and the trailer FE model.

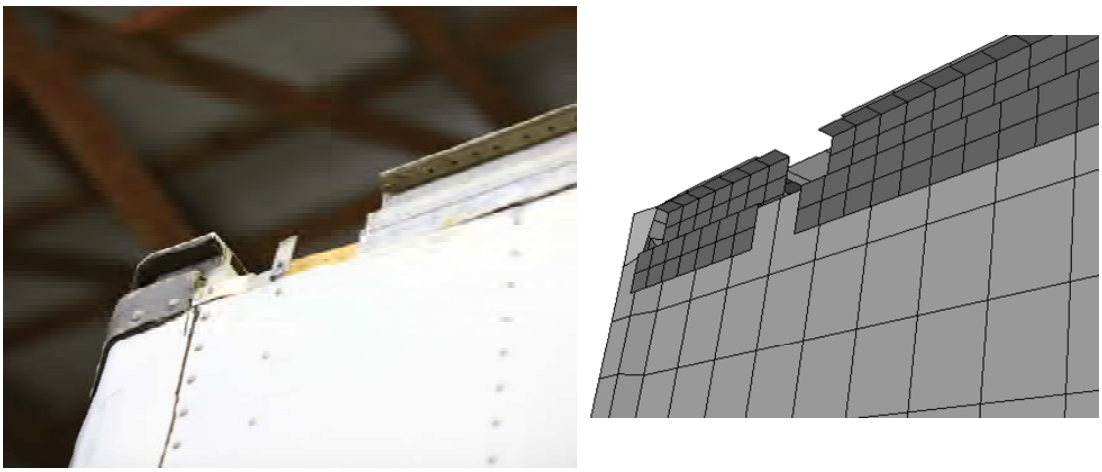

(a) Physical trailer (b) FE model

Figure 53. Photograph / Illustration. Cut section of the upper side rail of the trailer box of (a) the physical trailer and (b) the FE model showing the structural detail and connection methods.

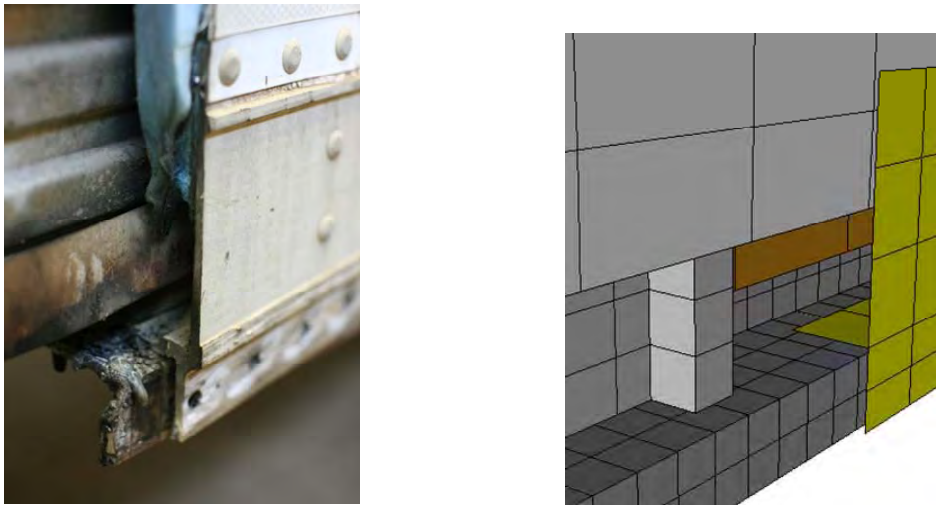

(a) Physical trailer (b) FE model

Figure 54. Photograph / Illustration. Cut section of the lower side rail of the trailer box of (a) the physical trailer and (b) the FE model showing the structural detail and connection methods.

The overall dimensions and plate thicknesses of the upper and lower side rails were measured directly. Sketches were made and photographs were taken. The FE model was created directly from this information using HyperMesh.

The LS-Dyna material model used for the upper and lower side rails was *Mat_Piecewise_Linear_Plasticity. 6061-T6 Aluminum was specified with a yield strength of 276 MPa, and no failure.

LS-Dyna Type 16 fully-integrated thin-shell elements were used to model these components. The element size for the upper side rails was nominally 20 mm to 50 mm (0.75 to 2.0-inch) and 25 mm to 50 mm for elements in the lower side rail. These sizes were chosen because they were the minimum reasonable sizes for geometry definition and they would not adversely affect (decrease) the current typical time step size of the overall FE model.

Figure 55 shows the upper side rail with each *Part of the assembly as a different color. The different parts were defined to define separate thicknesses. Figure 56 shows how the upper side rail is connected to the side-wall assembly via CNRBs.

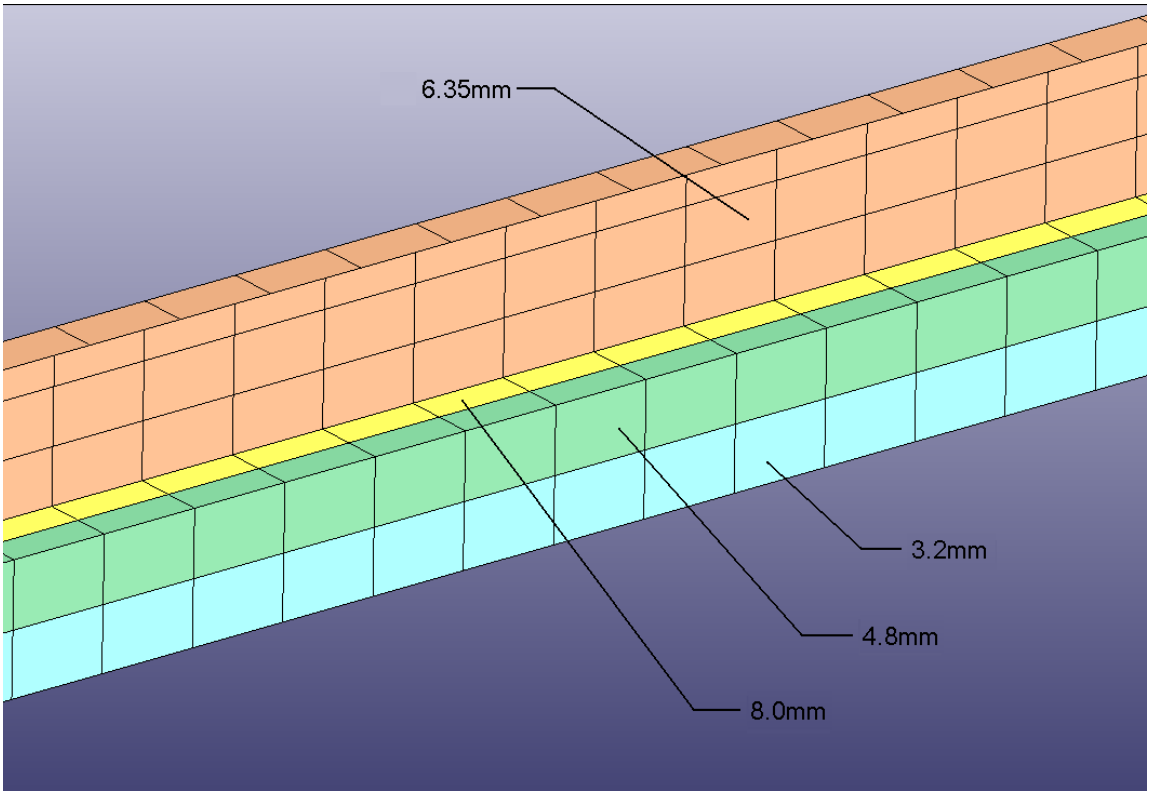

Figure 55. Illustration. Upper side rail model.

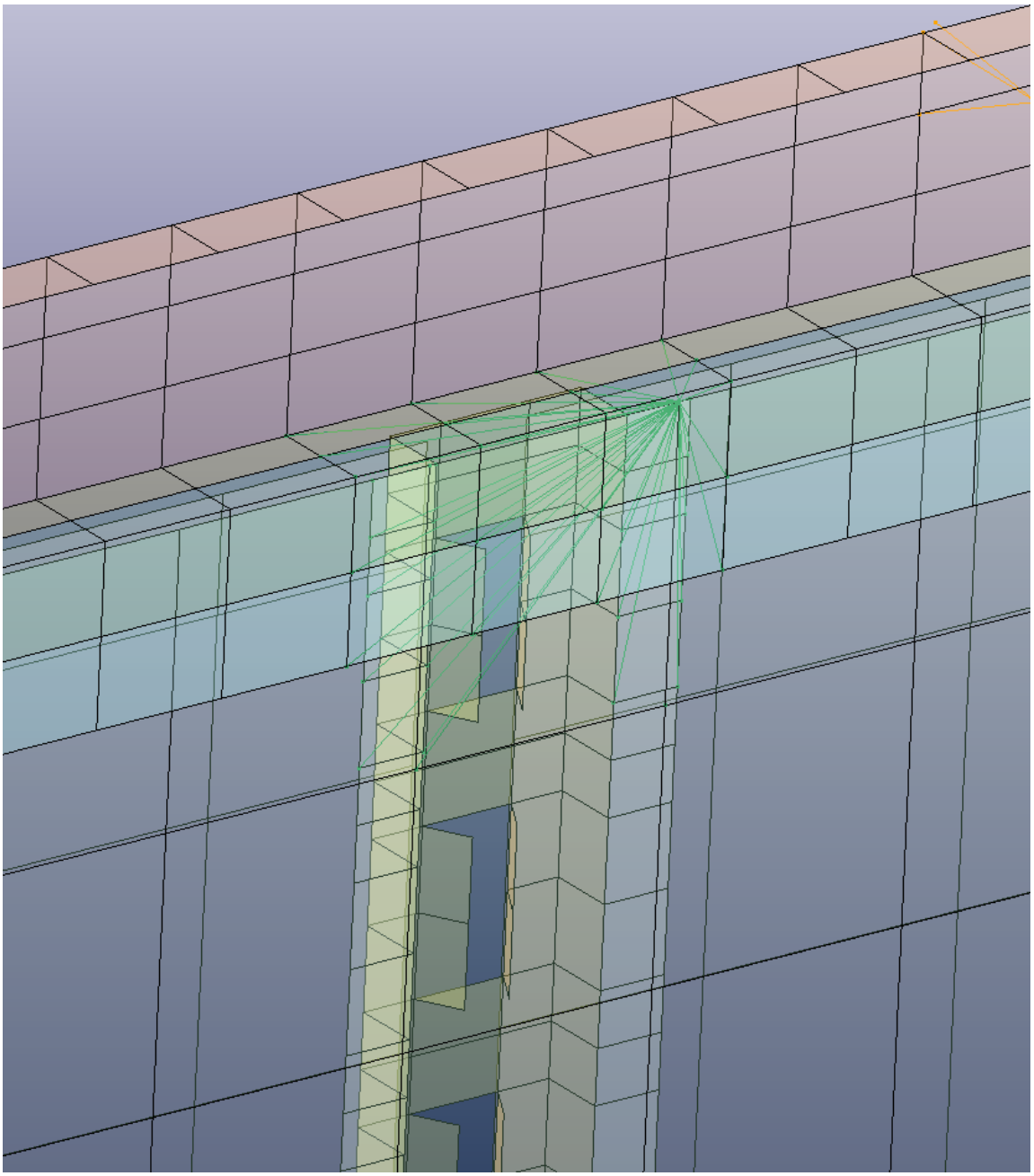

Figure 56. Illustration. Upper side rail to side-wall connection details.

Figure 57 shows the lower side rail with each *Part of the assembly as a different color. The different parts were defined to define separate thicknesses. Figure 58 shows how the lower side rail is connected to the side-wall assembly via CNRBs.

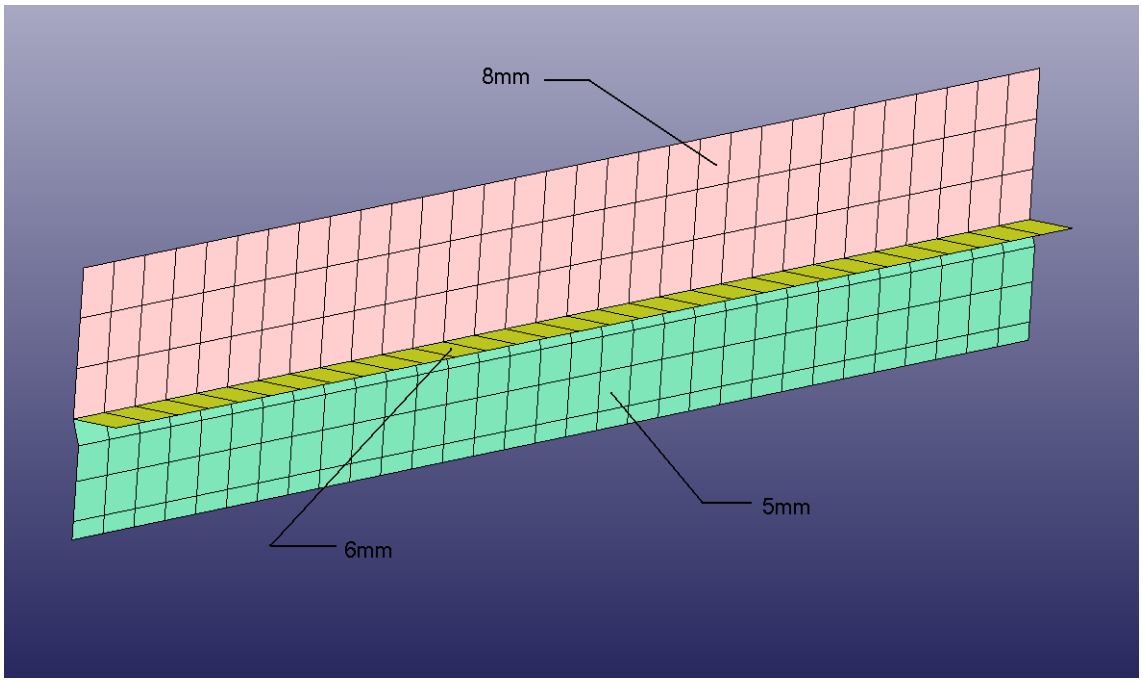

Figure 57. Illustration. Lower side rail model.

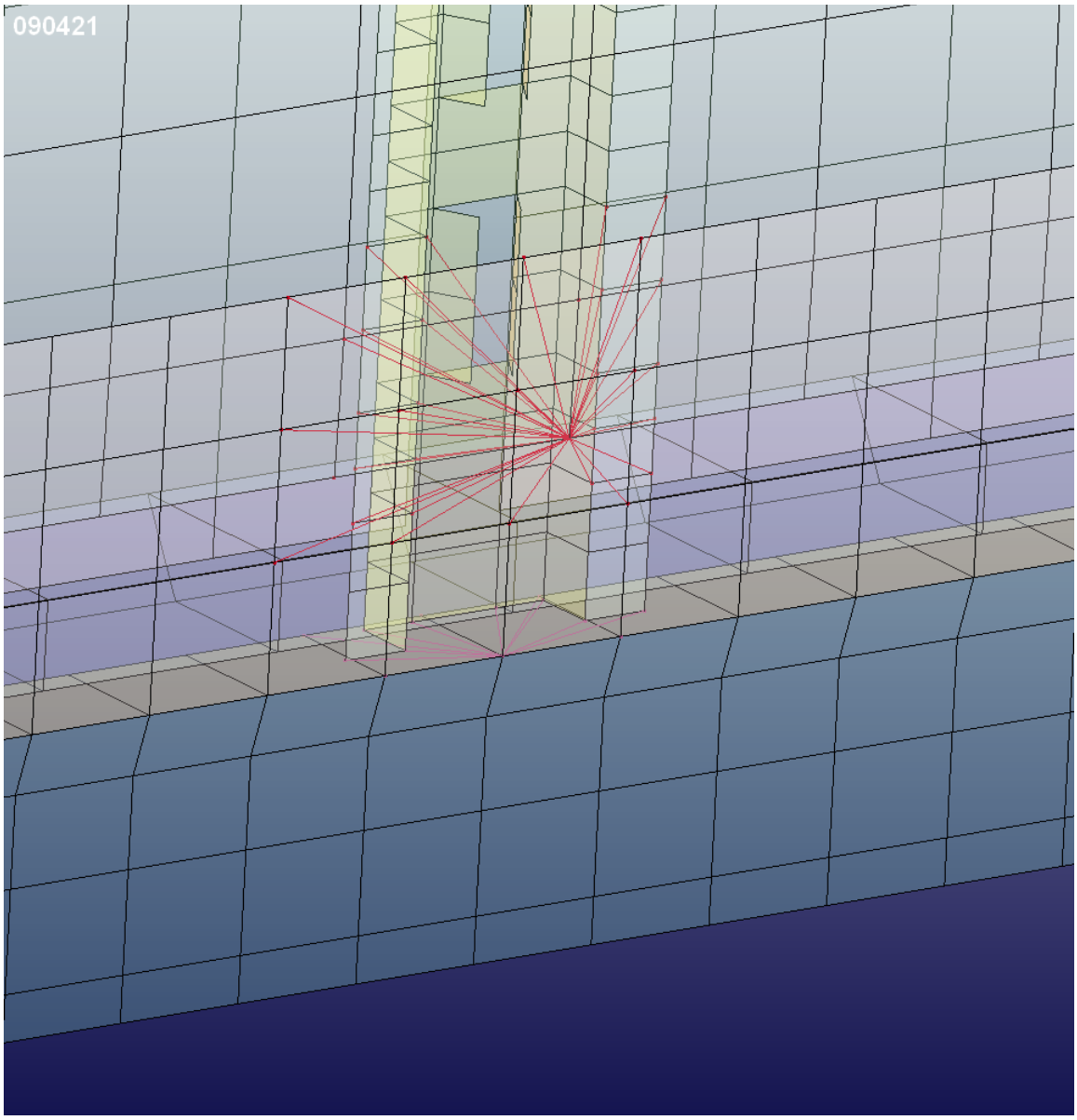

Figure 58. Illustration. Lower side rail to side-wall connection details.

Floor

The wooden floor of the cargo box is comprised of 10-inch wide, 1.25-inch thick laminated oak planks oriented longitudinally across the full width of the trailer. The individual planks are butted together with step-joints and are bolted to the main lateral cross beams. As shown in Figure 59, a section was cut out of the floor to reveal these details.

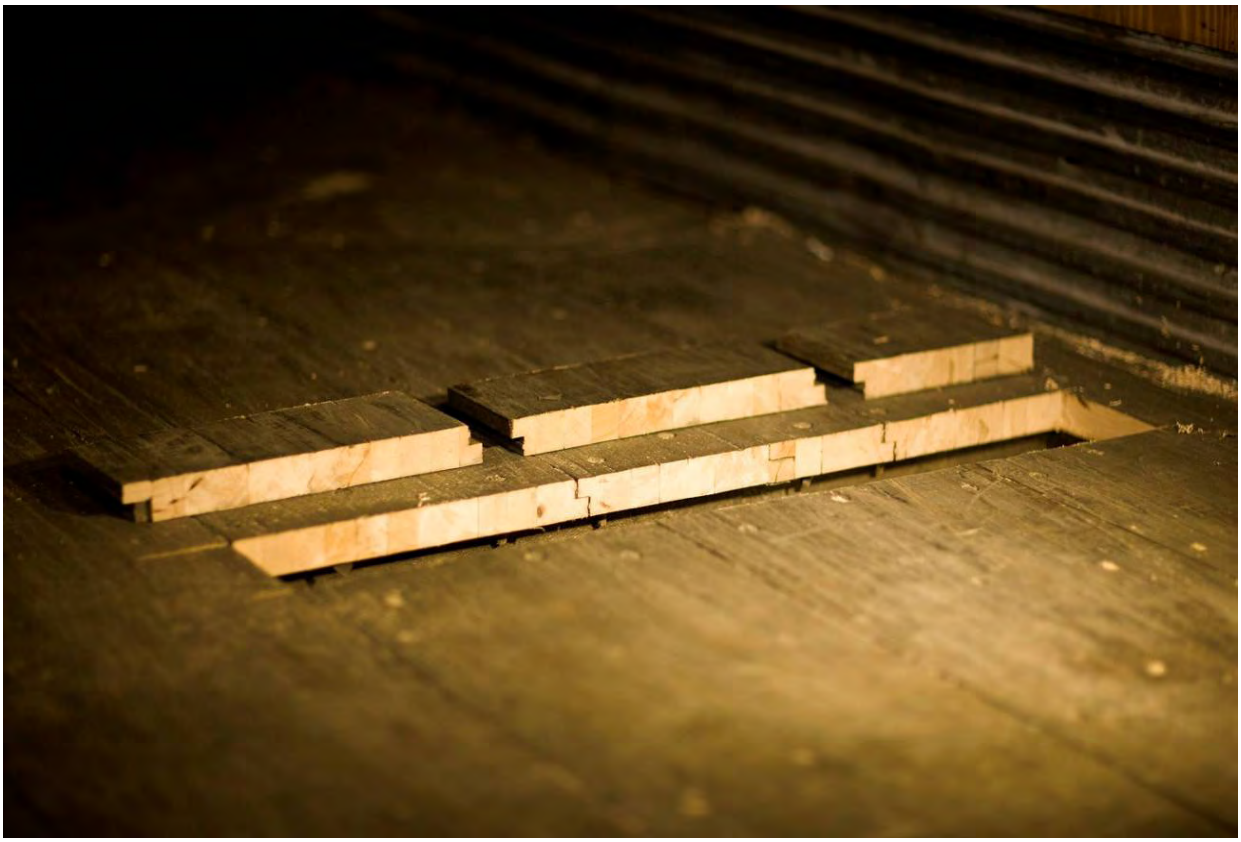

Figure 59. Photograph. Wooden floor cut section.

Figure 60 shows the FE model's individual, longitudinally-oriented oak planks that were modeled as separate pieces in contact with each other with one element through the thickness. The step-joint was simulated with a single slanted interface between the planks as shown in Figure 61.

The oak floor was modeled using the *Mat_Elastic material model in LS-Dyna with a density of 736 kg/m^3 (measured) and a Young's Modulus of 12,400 MPa (typical value for wood).

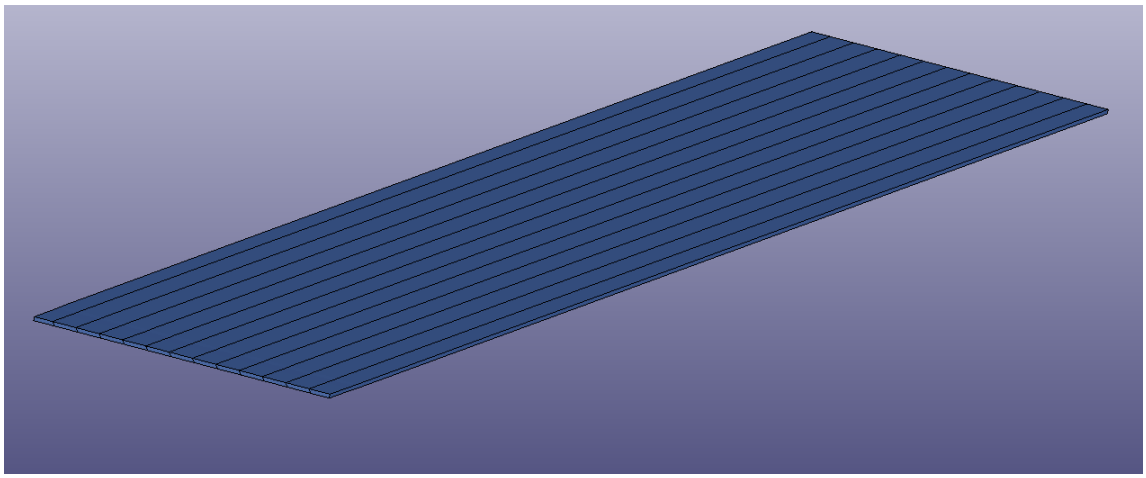

Figure 60. Illustration. Wooden floor FE model.

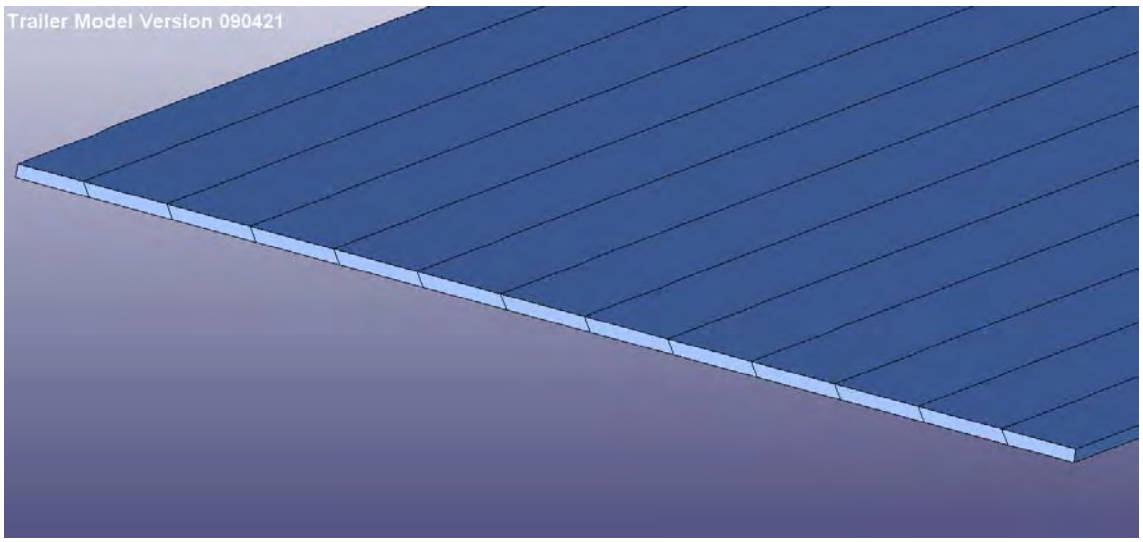

Figure 61. Illustration. Wooden floor FE model showing slanted plank interfaces.

Rear Bumper

The rear bumper (and step) provides significant strength and rigidity to the rear of the trailer. This large weldment assembly was sectioned to obtain detailed geometry information and thickness. Figure 62 shows the rear bumper and one of the sectioned areas. Figure 63 shows the FE model rear bumper area.

Figure 62. Photograph. Rear bumper showing sectioned area.

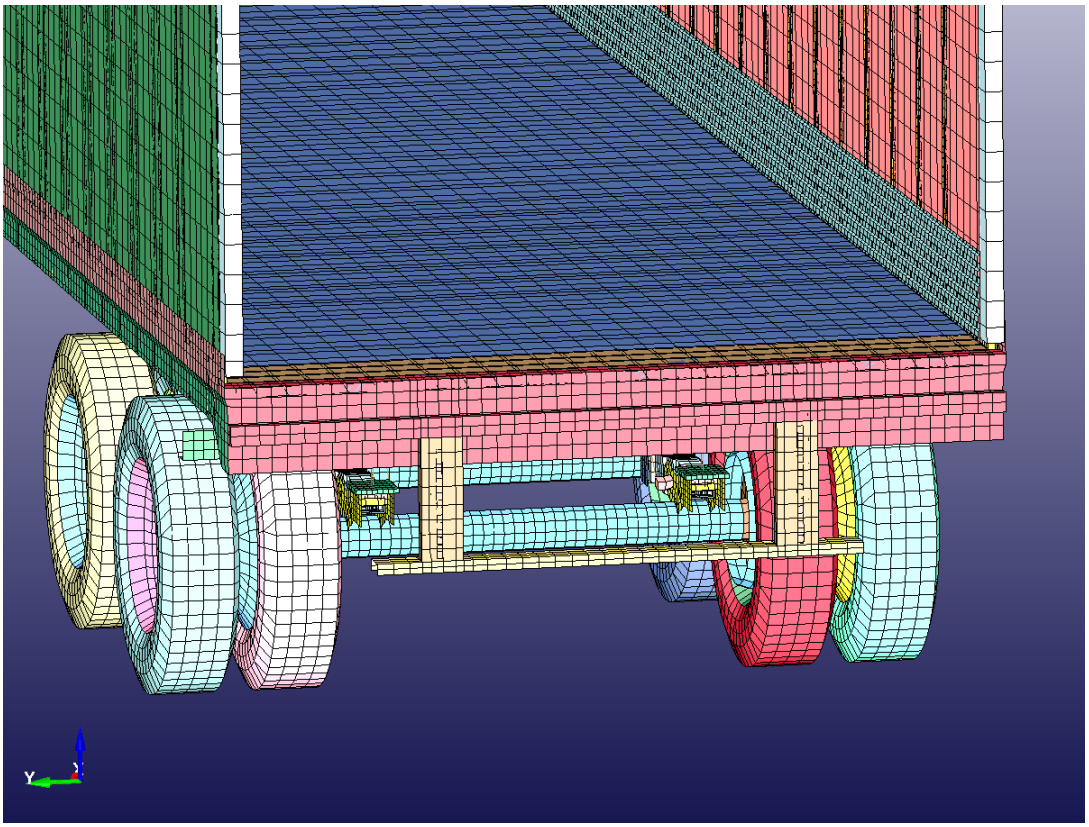

Figure 63. Illustration. Rear bumper area FE model.

The overall dimensions and plate thicknesses of the upper and lower side rails were measured directly. Sketches were made and photographs were taken. The FE model was created directly from this information using HyperMesh.

The material for the rear bumper was specified as SAE980X Grade 80 HSLA steel. The LS-Dyna material model *Mat_Piecewise_Linear_Plasticity was used to characterize the material using a yield strength of 557 MPa and no failure. LS-Dyna Type 16 fully-integrated thin-shell elements were used for all the components in the rear bumper except the weld elements. The element size for the rear bumper parts was nominally 25 mm to 50 mm (1.0 to 2.0-inch). These sizes were chosen because they were the minimum reasonable sizes for geometry definition and they would not adversely affect (decrease) the current typical time step size of the overall FE model.

Figure 64 shows just the rear bumper parts with the trailer frame included to show the connection. Each part of the assembly is shown as a different color. The different parts were separate thicknesses.

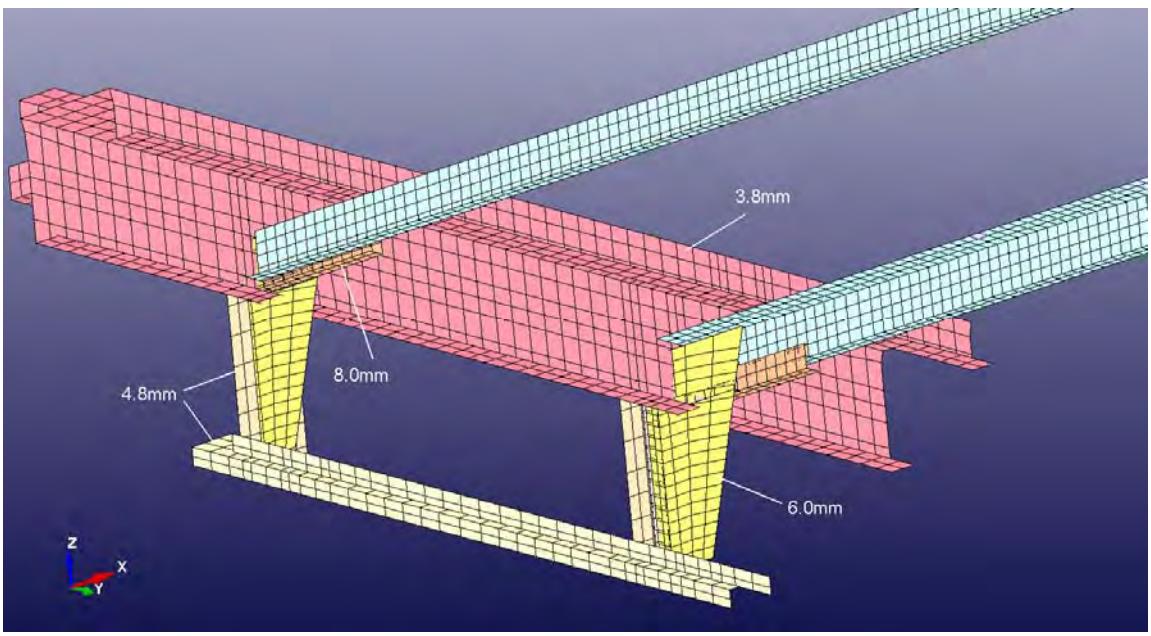

Figure 64. Illustration. Rear bumper area parts only.

The rear bumper components were connected to each other using common-nodes and LS-Dyna weld elements. LS-Dyna weld elements are implemented using solid elements with element connectivity specified to define the normal orientation of the welded connection. The *Mat_Spotweld material model is used to define weld-joint failure mode – if desired. The *Contact_Tied_Surface_to_Surface option is used to define the actual connection of the welded parts. Figure 65 shows the weld elements used to connect the parts in the rear bumper.

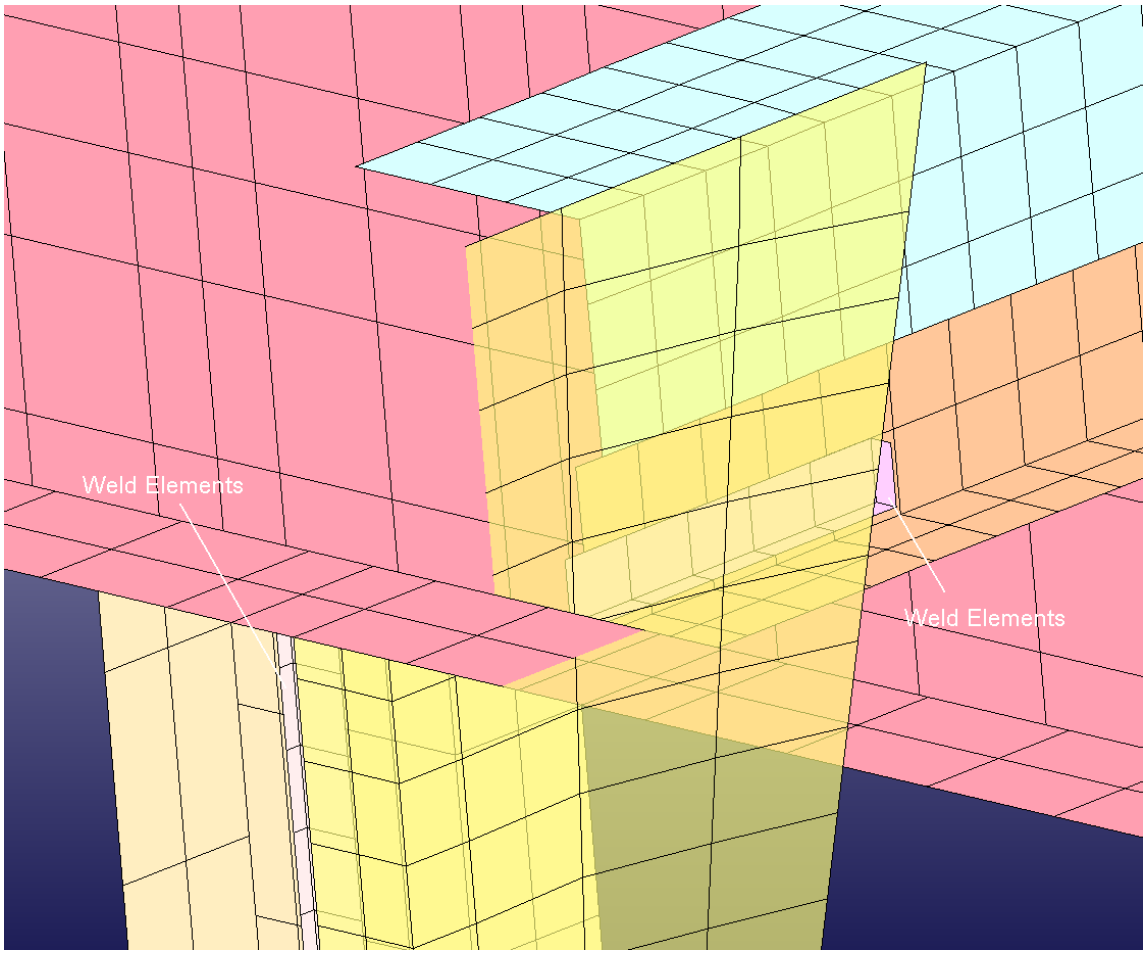

Figure 65. Illustration. *Mat_Spotweld weld elements in rear bumper.

Rear Frame and Bogie

The rear frame is comprised of fixed longitudinal members that are welded to the lateral side beams. The bogie is comprised of the wheels, frame, tires and axles, and the suspension system of the trailer. The bogie is longitudinally adjustable by the driver/operator to accommodate various loading situations. The rear frame and bogie were accessible for measurement and did not require dissection to obtain component thickness and geometry – with the exception of the rear axles. A hole was drilled in one of the axles to obtain the axle tube's thickness. Figures 66 and 68 show views of the rear frame and bogie in the actual trailer and Figures 67 and 69 show the rear frame and bogie as implemented in the FE model.

Figure 66. Photograph. Front view of trailer vehicle frame and bogie.

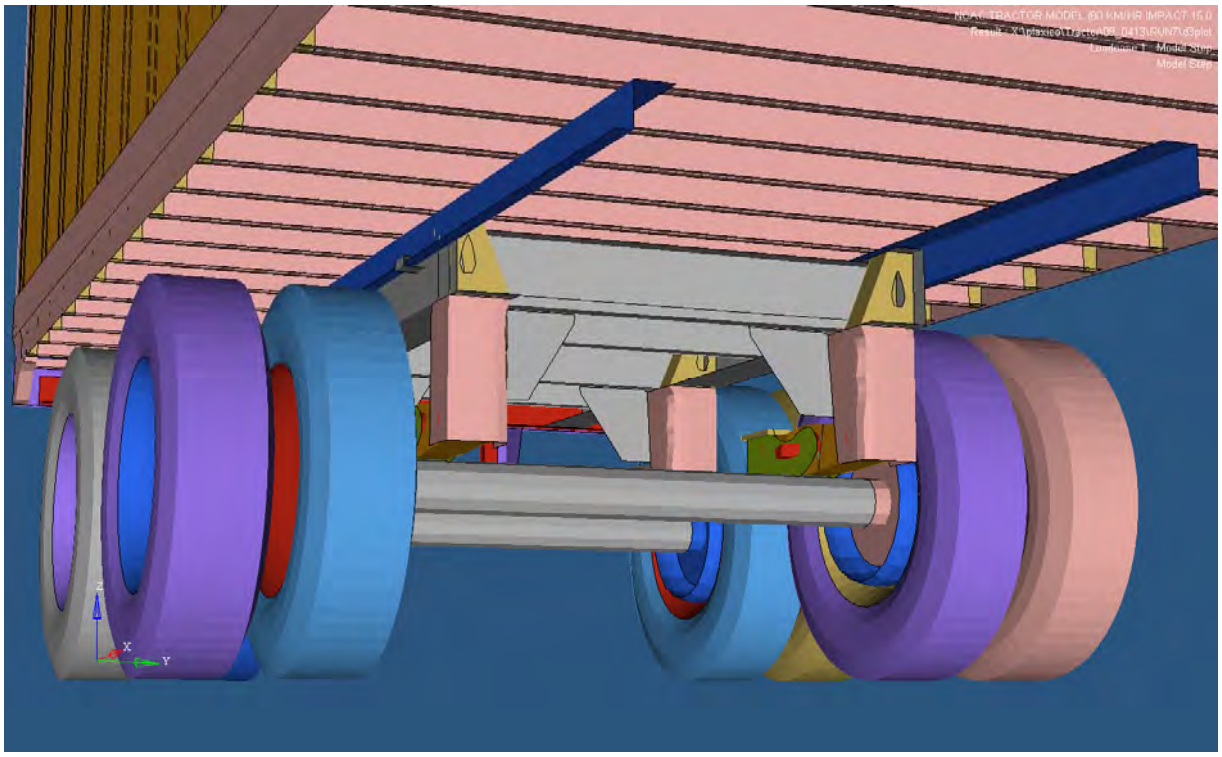

Figure 67. Illustration. Front view of trailer FE vehicle model of frame and bogie.

Figure 68. Photograph. Rear view of trailer vehicle frame and bogie.

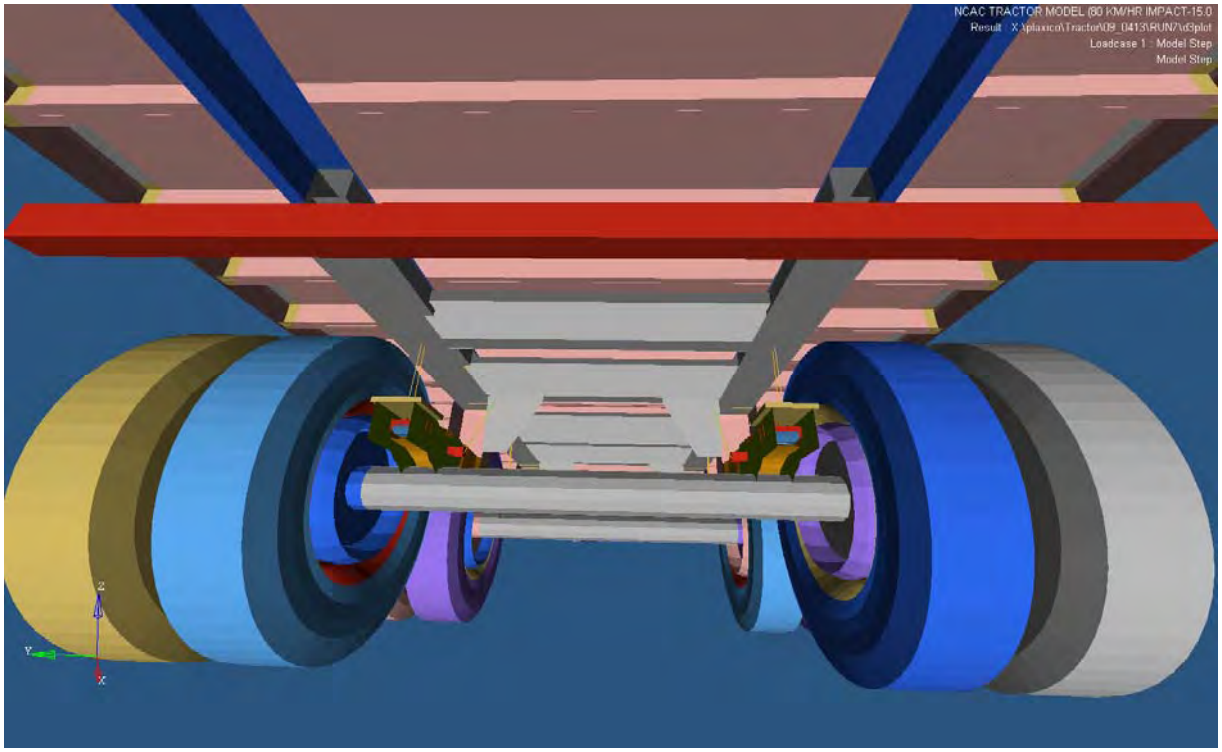

Figure 69. Illustration. Rear view of trailer FE vehicle model of frame and bogie.

The trailer suspension's spring and shock-absorber elements were implemented using LS-Dyna discrete elements (springs and dampers) – the Airide suspension system's air bag's properties and shock-absorber properties were copied from the tractor's suspension system which were obtained by physical testing described in the Phase A final report [1]. Figure 70 shows these elements.

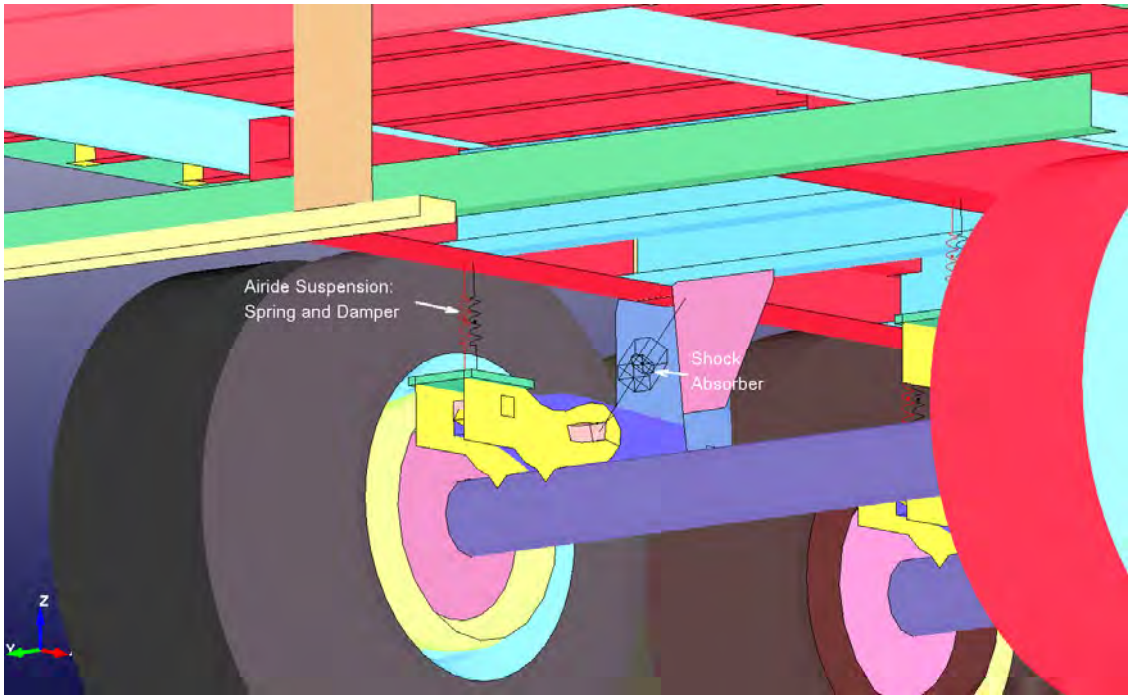

Figure 70. Illustration. Rear view of trailer suspension airbag and shock elements.

The overall dimensions and plate thicknesses of the rear frame and the bogie components were measured directly. Sketches were made and photographs were taken. The FE model was created directly from this information using HyperMesh. Figures 71 and 72 show the thicknesses of the shell elements of the frame and suspension pivot members of the rear frame and bogie, and Figure 73 shows the thicknesses of the tires and wheels.

LS-Dyna Type 16 fully-integrated thin-shell elements were used for most of the rear frame and the bogie components. Type 1 under-integrated and Type 2 fully-integrated solid elements were used for solid-like parts. The element size was nominally 25 mm (1-inch) for the frame elements, about 38 mm (1.5-inch) for the axle-tube and pivot-arm elements, and 50 mm (2-inches) for the wheel and tire elements. These sizes were chosen because it was the minimum reasonable size in each case to represent the geometry and it would not adversely affect (decrease) the current overall model time step size.

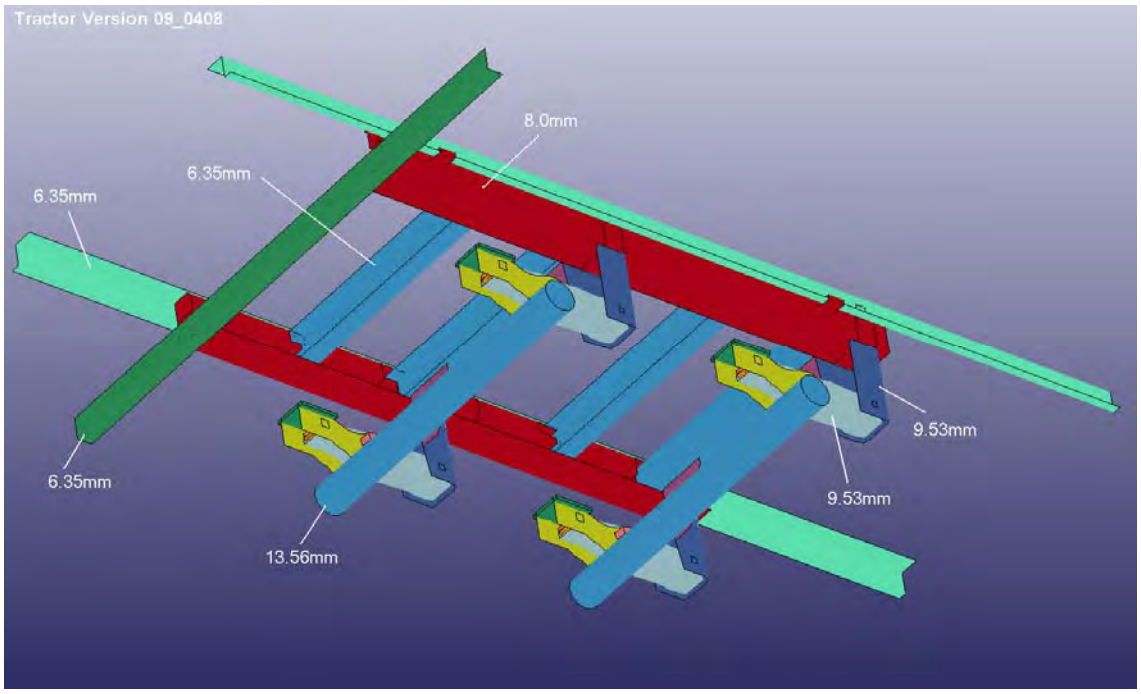

Figure 71. Illustration. Rear frame / bogie part thicknesses.

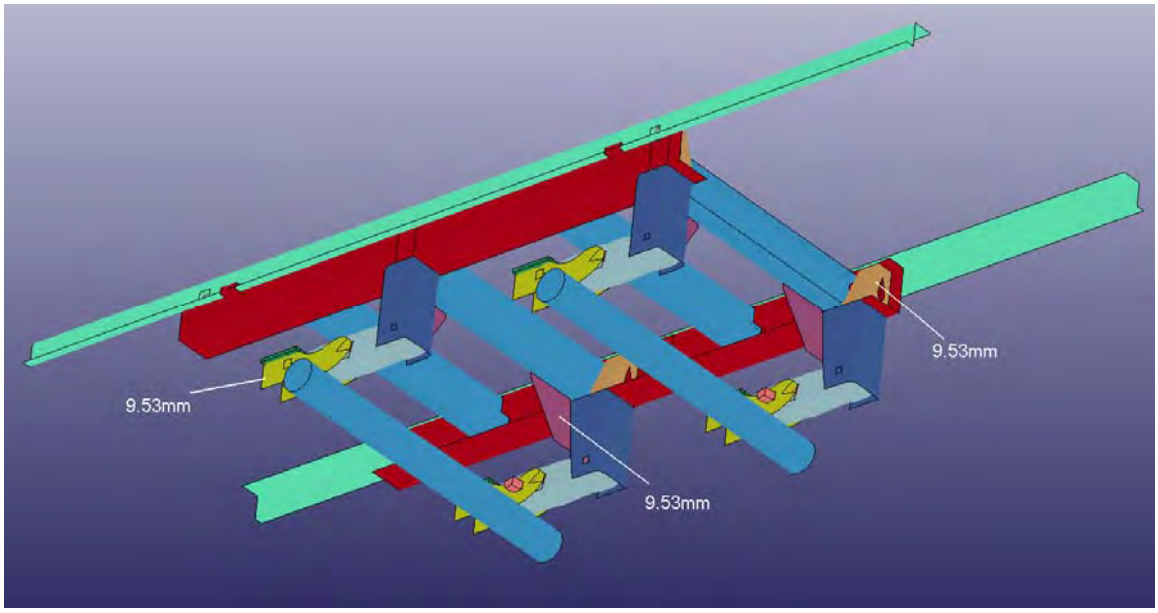

Figure 72. Illustration. Rear frame / bogie part thicknesses.

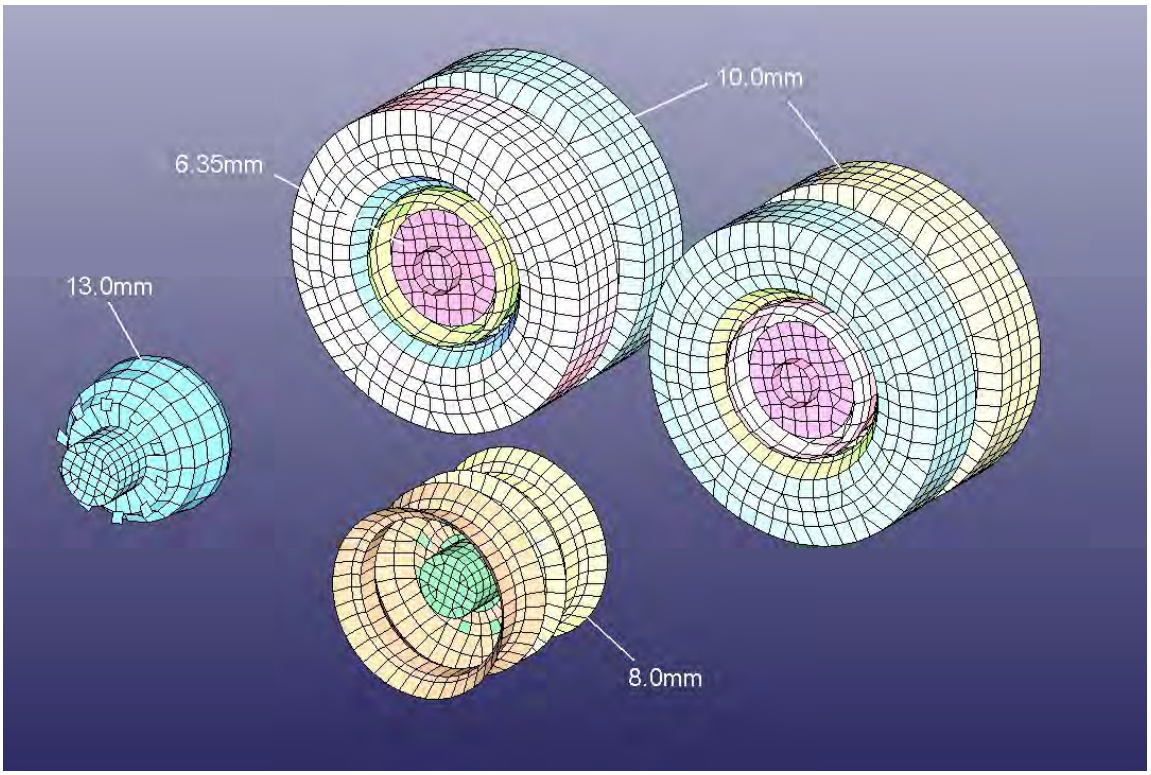

Figure 73. Illustration. Tire and wheel thicknesses.

The shell elements were assigned *Hourglass control type 8[iii] and the solid elements were assigned *Hourglass control type 1.[iii] The material specified for the frame components was SAE 950X HSLA Grade 50 with a yield strength of 340 MPa using the *Mat_Piecewise_Linear_Plasticity material model in LS-Dyna with no failure. The material specified for the axles was A500 Grade B structural steel tubing with a yield strength of 317 MPa using the *Mat_Piecewise_Linear_Plasticity material model with no failure. The material specified for the pivot arms was SAE 1095 steel with a yield strength of 776 MPa using the *Mat_Piecewise_Linear_Plasticity material model with no failure. The material specified for the wheel rims was mild steel with a yield strength of 270 MPa using the *Mat_Piecewise_Linear_Plasticity material model with no failure. The brake drums and the axle-ends / backing plates were specified as rigid materials with steel density. The material specified for the Tires was *Mat_Elastic with an elastic modulus of 2461 MPa. A thickness of 10 mm and a density of 3100 Kg/M^3 were specified to obtain a weight of 53.5 Kg (118 lbs) per tire.

The air pressure in the tires was specified as 0.69 MPa (100 psi). The air pressure in the tires was simulated using the *Airbag_Simple_Pressure_Volume option. Initially, the tire pressure was simulated using the *Airbag_Simple_Airbag_Model option, but was changed to the *Airbag_Simple_Pressure_Volume option for simplicity and better reliability because with the *Airbag_Simple_Pressure_Volume option, the tire pressure can be input directly rather than as a calculated result of multiple parameters. With the *Airbag_Simple_Airbag_Model, the tire

pressure is calculated by LS-Dyna based on: mass flow in, air density, constant volume heat capacity, constant pressure heat capacity, temperature, ambient pressure, and the calculated internal energy. When the original *Airbag_Simple_Airbag_Model option was used with the existing parameters, the air pressure in the Tractor and Trailer tires calculated by LS-Dyna was 0.38 MPa (56 psi). The recommended tire pressure specified by the manufacturer is 0.38 MPa (100 psi).

In general, the connectivity within the rear frame, the wheels, and axles was done with common-node connections. The connection of the fixed-to-movable frames was sliding contact, with spotweld elements at four points fixed to the (moveable) bogie longitudinal frame rails, and in tied contact with the (fixed) trailer longitudinal frame rails. This will allow the user to move the bogie fore/aft without having to re-specify or reconnect CNRBs. The wheels were connected to the axles via spherical joints enabling them to rotate. The pivot arms are connected to the frame components via spherical joints enabling them to rotate.

Chapter 4 – Semitrailer Material Properties and Material Models

The material assignment for the heavy truck trailer model consisted of three steps. The first was to determine the list of structural parts in the trailer and their organization as functional groups. The next was to determine the types of materials and their designation for each of the parts. As different manufacturers have different trailer designs and employ different materials, the first two steps resulted in several part and material assignment schemes. Trailer manufacturers generally do not reveal the specific material grades used for specific parts, so the search had to include original and aftermarket parts suppliers. The third step was to determine elastic and elasto-plastic mechanical properties for each material. The properties were then formatted in the input form for constitutive material models that can be used in LS-DYNA.

As it was not initially specified what type of trailer was going to be used in the simulations, two separate material assignments were developed for Aluminum and for steel trailer bodies. After a steel body trailer was purchased for the model development, the steel assignment was used in the final model.

Dry Freight Trailer Structure

From a structural perspective, designs of dry freight trailers are relatively similar across manufacturers [16, 17, 18, 19, 20, 21]. The top and bottom longitudinal rails at edges of the van are the primary structural components. The rails are connected into a space-frame by the rear frame, the (front) kingpin box, and the corner posts. The side posts, floor cross members, roof beams, and the trailer skin panels complete the box of the trailer and all participate in structural response. To accommodate higher load capacities, manufacturers commonly increase the size of the side rails. Some designs also employ extruded trailer sides [20] with higher rigidity and structural participation.

During the course of the project, a used trailer was purchased to provide more information for the model sub-assemblies. The purchased trailer was a steel dry freight trailer by Stoughton Trailers company [19]. Their web site has an exploded parts diagram [22] that was used for structural part classification and parts nomenclature in the FE model. Other parts suppliers [23, 24] also have vehicle diagrams and material assignments for different trailer configurations, which were used for the Aluminum-model version of the trailer. The exploded parts diagram for a Stoughton dry freight trailer is shown in Figure 74.

This data provided valuable information for conducting further searches on materials for the parts, as now we had the exact terms used by the industry.

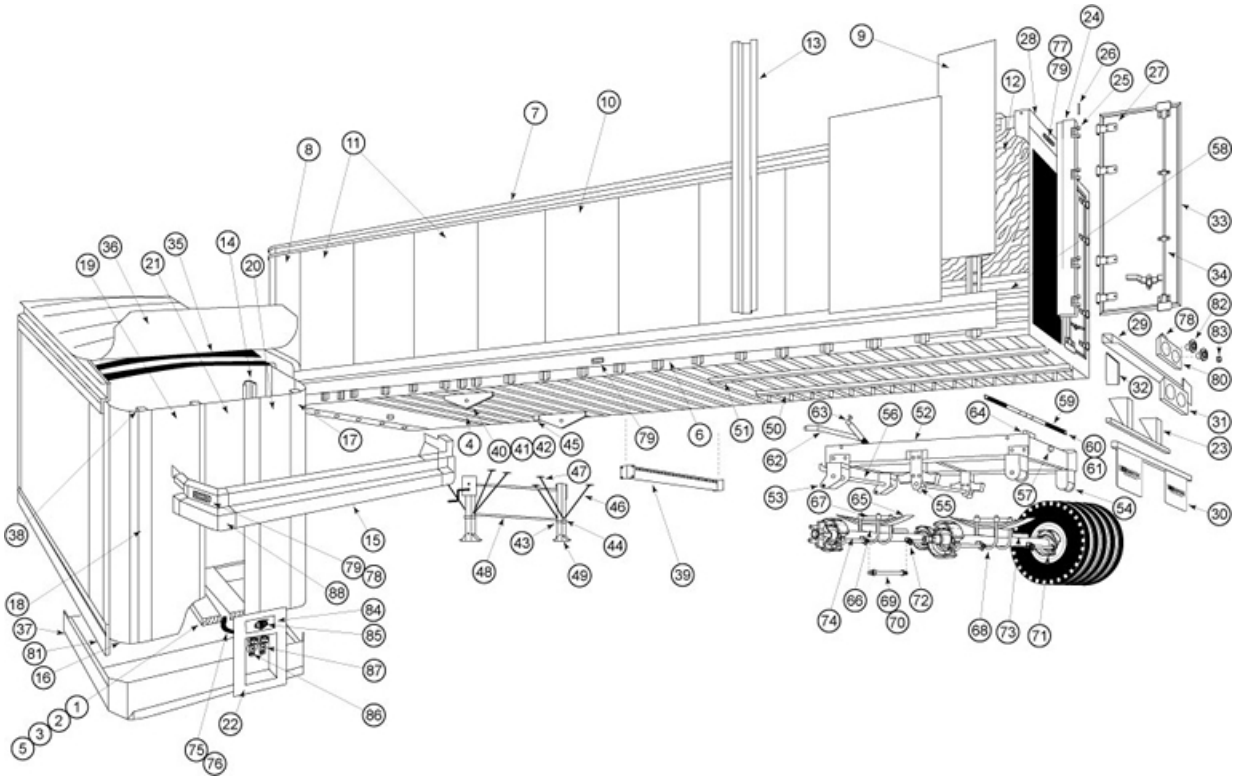

1. Floor Kit Assembly
2. End Board
3. Intermediate Board
4. Hat Section
6. Bottom Rail
7. Top Rail
8. Side Panel
9. Side Panel
10. Side Panel
11. Side Panel
12. Plywood Liner
13. Side Post
14. Nose Post
15. Top Rail, Front Panel
16. Radius Panel - CS
17. Radius Panel - RS
18. Nose Panel
19. Nose Panel
20. Nose Panel
21. Nose Panel
22. Recess Box
23. Step Guard
24. Rear Corner Post, RH (CS), Rear Corner Post, LH (RS)
25. Hinge Butt
26. Hinge Pin
27. Hinge Strap
28. Rear Header Assembly
29. Rear Sill Assembly
32. Bumper Plate
33. Rear Door Assembly, CS, Rear Door Assembly, RS
34. Locking Bar Assembly, CS, Locking Bar Assembly, RS
35. Tension Roof Bow
36. Roof Sheet
37. King Pin Assembly
39. Crossmember Assembly
40. 'H' Frame Assembly
41. Subframe Assembly Landing Gear
42. Gusset, Landing Gear, Mtg., RH/LH
43. Bracket, LG Brace Ear
44. Angle, LG Brace Ear
45. Clip, LG Crank Handle
46. Brace, LG
47. Brace, LG
48. Brace, LG, Horizontal
49. Landing Gear
50. Slider Rail, RH, Slider Rail, LH
51. Slider Stop, Forward and Rear
52. Slider Subframe
53. Front Spring Hanger, RH/LH
54. Rear Spring Hanger, RH/LH
55. Equalizer Assembly
56. Pipe Brace
57. Pipe Crankshaft
58. Scuff Liner
59. Link, Connecting
60. Pin, Locking
61. Spring, Compression
62. Handle, Lock Operating
63. Crank
64. Slider Pad
65. Spring
66. Spring Seat
67. Top Plate
68. 'U' Bolt
69. Torque Arm, Adjustable
70. Torque Arm, Fixed
71. Brake System
72. Slack Adjuster
73. Air Chamber
74. Axle, Front and Rear
88. Aluminum Corner Casting, RH/LH

Figure 74. Illustration. Parts identification for Stoughton trailers.

Material Assignments to Trailer Parts

Several web sites have downloadable parts catalogs with parts dimensions and limited material information [19, 24, 25]. We also obtained a printed parts catalog from a trailer OEM supplier [24] that specified grades of steel and Aluminum for the main structural parts. Great Dane Trailer's [26] web site has product line catalogs that list the suppliers for trailer parts and sub-structures. Web sites of parts suppliers were searched for material assignments to the parts. As an example, various trailer door configurations can be found [27], such as laminated structures with wood or thermoplastic cores, skins made of galvanized steel, Aluminum alloys such as 3003-H14, 3105-H14, 5052-H34, or stainless steel such as 304-2B. Galvanized steel materials were typically "Galavan" – a product of US Steel, which is specified in their product line [28] as ASTM A653 [29] grade 80 structural steel, with minimum yield strength of 80 ksi and minimum tensile strength of 82 ksi.

Trailer rail, posts, corners, roof, and side panel material assignments were determined from reference [24]. In Aluminum trailers, the extrusions (roof bows, side post, corner post, top and bottom rails, rub rails, J-moulding, cross members, front top radius, scuff, flooring) are made of Aluminum alloy 6061-T6. In steel trailers, channel forms are made of HSLA 80 ASTM A656 [30, 31] steel. The Bumper tube [32] and the kingpin box is made of high strength steel with 80 ksi yield stress, HSLA 80 ASTM A656. Aluminum alloys 3105-H14, 3004-H291, 3004, 5052 are used for trailer side sheets. Roof sheets are made of Aluminum alloys 3003-H16, 3103B-H26, and 5052-H33. The Aluminum panels are joined using Aluminum buck rivets made from alloys 2117, 2117-T4, 6053, and 1100 head styles, or solid rivets of type 302HQ (ASTM A 493) for stainless steel panels. The floor panels [17, 19, 25] are usually made of laminated oak or treaded sheet [24] of Aluminum alloys 3003-H22, 3003-H25, and 5086-H32. The kingpin material was listed in on-line brochures of the kingpin and suspension manufacturer [32] as AISI 8630H steel hardened to Brinell Hardness 302-363 BHN.

The suspension of the modeled trailer consists of slider sub frame, different brackets, springs, axles, and wheels. The material for the slider sub frame of the wheelset assembly was listed in manufacturer's brochure [32] as high strength steel with 80 ksi yield, which is most probably HSLA 80 ASTM A656 [30] as this steel is used for frame materials due to the combination of its strength and formability. The standard materials for tractor and trailer leaf springs are heat treated SAE 5160, 1085, and 9260 steels [33, 34, 35]. Leaf spring hangers are made of either formed high strength steel or cast steel [36, 37]. A reference found for trailer axles [38] specifies trailer axle material as ASTM A 500 steel [39].

Several general reference books can be consulted for tractor and trailer parts [35, 37, 40, 41, 42, 43, 44, 45, 46, 47, 48, 49, 50]. These were used to confirm the above assignments and to determine material assignments to parts that were not available from the OEM literature. This particularly pertains to smaller parts of the trailer such as suspension castings, spring hangers,

axle suspension brackets, etc. The most comprehensive assignment information can be found in references [35, 45]. Steel fasteners were listed mostly as SAE Grade 5 and Grade 8 [51].

The comprehensive list of parts and material assignments, including all possible alternative materials are summarized in Table 12. The part names in Table 12 correspond to Stoughton parts diagram from Figure 74. The material assignments for the current trailer FE model are summarized in Table 13. The material abbreviations are shown below in Table 11:

Table 11. Material Abbreviations.

Abbreviation	Material
ST	Steel
SST	Stainless Steel
Al	Aluminum
PW	Plywood

Table 12. Material Assignments for Semitrailer Parts.

ID	Part Name	Num. of Possible Mats.	Mat. Class	Mat. Name	Mat. Class	Mat. Name	Mat. Class	Material Name	Mat. Class	Mat. Name	Mat. Class	Mat. Name	Mat. Class	Mat. Name
1	Floor Kit Assembly	5	PW	Laminated Oak	Al	3003-H22	Al	3003-H25	Al	5086-H32	Al	6061-T6		
2	End Board	5	PW	Laminated Oak	Al	3003-H22	Al	3003-H25	Al	5086-H32	Al	6061-T6		
3	Intermediate Board	5	PW	Laminated Oak	Al	3003-H22	Al	3003-H25	Al	5086-H32	Al	6061-T6		
4	Hat Section	5	PW	Laminated Oak	Al	3003-H22	Al	3003-H25	Al	5086-H32	Al	6061-T6		
5	Floor Seal - Foam Tape	0												
6	Bottom Rail	1	Al	6061-T6										
7	Top Rail	1	Al	6061-T6										
8	Side Panel	6	Al	3004-H291	Al	5052-H291	ST	A653/A653M	SST	301PB	SST	430BA	SST	201LN
9	Side Panel	6	Al	3004-H291	Al	5052-H291	ST	A653/A653M	SST	301PB	SST	430BA	SST	201LN
10	Side Panel	6	Al	3004-H291	Al	5052-H291	ST	A653/A653M	SST	301PB	SST	430BA	SST	201LN
11	Side Panel	6	Al	3004-H291	Al	5052-H291	ST	A653/A653M	SST	301PB	SST	430BA	SST	201LN
12	PW Liner	1	PW											
13	Side Post	2	Al	6061-T6	ST	HSLA 80 A656								

Table 12. Material Assignments for Semitrailer Parts (Continued).

ID	Part Name	Num. of Possible Mats.	Mat. Class	Mat. Name	Mat. Class	Mat. Name	Mat. Class	Material Name	Mat. Class	Mat. Name	Mat. Class	Mat. Name	Mat. Class	Mat. Name
14	Nose Post	2	Al	6061-T6	ST	HSLA 80 A656								
15	Top Rail, Front Panel	1	Al	6061-T6										
16	Radius Panel - CS	6	Al	3004-H291	Al	5052-H291	ST	A653/A653M	SST	301PB	SST	430BA	SST	201LN
17	Radius Panel - RS	6	Al	3004-H291	Al	5052-H291	ST	A653/A653M	SST	301PB	SST	430BA	SST	201LN
18	Nose Panel	6	Al	3004-H291	Al	5052-H291	ST	A653/A653M	SST	301PB	SST	430BA	SST	201LN
19	Nose Panel	6	Al	3004-H291	Al	5052-H291	ST	A653/A653M	SST	301PB	SST	430BA	SST	201LN
20	Nose Panel	6	Al	3004-H291	Al	5052-H291	ST	A653/A653M	SST	301PB	SST	430BA	SST	201LN
21	Nose Panel	6	Al	3004-H291	Al	5052-H291	ST	A653/A653M	SST	301PB	SST	430BA	SST	201LN
22	Recess Box	0												
25	Hinge Butt	1	ST	4130										
26	Hinge Pin	1	ST	4130										
27	Hinge Strap	1	ST	4130										
28	Rear Header Assembly	2	Al	6061-T6	ST	HSLA 80 A656								
29	Rear Sill Assembly	2	Al	6061-T6	ST	HSLA 80 A656								

Table 12. Material Assignments for Semitrailer Parts (Continued).

ID	Part Name	Num. of Possible Mats.	Mat. Class	Mat. Name	Mat. Class	Mat. Name	Mat. Class	Material Name	Mat. Class	Mat. Name	Mat. Class	Mat. Name	Mat. Class	Mat. Name
30	Mud Flap - Kant Sail	0												
31	Light Box, RH, Light Box, LH	0												
32	Bumper Plate	1	ST	HSLA 80 A656										
33	Rear Door Assembly, CS, Rear Door Assembly, RS	6	Al	3004-H291	Al	5052-H291	ST	A653/A653M	SST	301PB	SST	430BA	SST	201LN
34	Locking Bar Assembly, CS, Locking Bar Assembly, RS	1	ST	4130										
35	Tension Roof Bow	2	ST	A653/A653M	Al	6061-T6								
36	Roof Sheet	6	Al	3003-H16	Al	5052-H33	ST	A653/A653M	SST	301PB	SST	430BA	SST	201LN
37	King Pin Assembly	1	ST	8630H										
38	Sealer, Foam Tape	0												
39	Crossmember Assembly	2	ST	HSLA 80 A656	Al	6061-T6								
40	'H' Frame Assembly	1	ST	HSLA 80 A656										
41	Subframe Assembly Landing Gear	1	ST	HSLA 80 A656										
42	Gusset, Landing Gear, Mtg., RH/LH	1	ST	HSLA 80 A656										
43	Bracket, LG Brace Ear	1	ST	HSLA 80 A656										

Table 12. Material Assignments for Semitrailer Parts (Continued).

ID	Part Name	Num. of Possible Mats.	Mat. Class	Mat. Name	Mat. Class	Mat. Name	Mat. Class	Material Name	Mat. Class	Mat. Name	Mat. Class	Mat. Name	Mat. Class	Mat. Name
44	Angle, LG Brace Ear	1	ST	HSLA 80 A656										
45	Clip, LG Crank Handle	1	ST	HSLA 80 A656										
46	Brace, LG	1	ST	HSLA 80 A656										
47	Brace, LG	1	ST	4130										
48	Brace, LG, Horizontal	1	ST	4130										
49	Landing Gear	1	ST	HSLA 80 A656										
50	Slider Rail, RH, Slider Rail, LH	1	ST	HSLA 80 A656										
51	Slider Stop, Forward and Rear	1	ST	HSLA 80 A656										
52	Slider Subframe	1	ST	HSLA 80 A656										
53	Front Spring Hanger, RH/LH	4	ST	HSLA 80 A656	Cast ST	A216	Cast ST	A148 80-50	Cast Iron	65-45-12	Cast ST	SAE J2477		
54	Rear Spring Hanger, RH/LH	4	ST	HSLA 80 A656	Cast ST	A216	Cast ST	A148 80-50	Cast Iron	65-45-12	Cast ST	SAE J2477		
55	Equalizer Assembly	3	ST	1038	ST	1045	ST	51CrV4						
56	Pipe Brace	3	ST	1038	ST	1045	ST	51CrV4						
57	Pipe Crankshaft	3	ST	1038	ST	1045	ST	51CrV4						
58	Scuff Liner	2	Al	6061-T6	ST	A653/A653M								
59	Link, Connecting	1	ST	4130										
60	Pin, Locking	1	ST	4130										

Table 12. Material Assignments for Semitrailer Parts (Continued).

ID	Part Name	Num. of Possible Mats.	Mat. Class	Mat. Name	Mat. Class	Mat. Name	Mat. Class	Material Name	Mat. Class	Mat. Name	Mat. Class	Mat. Name	Mat. Class	Mat. Name
61	Spring, Compression	1	ST	5160										
62	Handle, Lock Operating	1	ST	4130										
63	Crank	1	Cast ST	4130										
64	Slider Pad	0												
65	Spring	1	ST	5160										
66	Spring Seat	1	ST	A500										
67	Top Plate	1	ST	5160										
68	'U' Bolt	1	ST	1137	ST	SAE Grade 8								
69	Torque Arm, Adjustable	2	Cast ST	A148 115-95	ST	4130								
70	Torque Arm, Fixed	2	Cast ST	A148 115-95	ST	4130								
71	Wheel	3	Al	6061-T6	ST	1038	ST	1045						
72	Slack Adjuster	0												
73	Air Chamber	0												
74	Axle, Front and Rear	1	ST	A500										
75	Main Harness	0												
76	Front Harness	0												
77	Rear Harness Assembly	0												
78	Light - Marker, Red	0												
79	Light - Marker, Amber	0												
80	Reflector, Red	0												
81	Reflector, Amber	0												
82	Light, Rear	0												

Table 12. Material Assignments for Semitrailer Parts (Continued).

ID	Part Name	Num. of Possible Mats.	Mat. Class	Mat. Name	Mat. Class	Mat. Name	Mat. Class	Material Name	Mat. Class	Mat. Name	Mat. Class	Mat. Name	Mat. Class	Mat. Name
83	Light, License Plate	0												
84	Plate, Electrical Plugs	0												
85	7-way Receptacle	0												
86	Gladhand - Service	0												
87	Gladhand - Emergency	0												
88	Al Corner Casting, RH/LH	1	Al	A319										
89	Nuts and Bolts	4	ST	1137	ST	SAE Grade 5	ST	1152	ST	SAE Grade 8				
90	Rivets	2	Al	2117-T4	SST	302HQ								
91	Weld Suspension to Frame	1	ST	Grade 70										

Table 13. FE Model Part List and Material Assignment

FE Model Part ID	FE Model Part Name	FE Model Material	FE Model Material Type
1	Lateral I-Beams	Steel	ASTM A653/A653M Grade 80
2	Axle Tubes	Steel	A500 Grade B Shaped Structural Tubing
3	Outer Side Wall	Aluminum	6061-T6
5	Rear Door	Aluminum	6061-T6
6	Tension Roof Bow	Steel	ASTM A653/A653M Grade 80
7	Front Spring Hanger	Steel	CS 1095
8	Cross Channel	Steel	CS 1040
9	Step Guard	Steel	HSLA Grade 80 SAE980X
10	Step Guard	Steel	HSLA Grade 80 SAE980X
11	Rear Seal Ass'y	Steel	HSLA Grade 80 SAE980X
12	Suspension Pivot Arm	Steel	CS 1095
13	Airide Bag Support	Steel	CS 1040
14	Pivot Connector Plates	Steel	CS 1095
15	A-Towers	Steel	HSLA Grade 50 SAE950X
16	Shock Attachment Plate	Steel	HSLA Grade 50 SAE950X
17	Plywood Liner	Wood	Low Grade Plywood
18	Nose Panel	Steel	ASTM A653/A653M Grade 80
19	Subframe Ass'y	Steel	ASTM A653/A653M Grade 80
20	Brace	Steel	CS 1040
21	H-Frame Ass'y	Steel	ASTM A653/A653M Grade 80
22	Landing Gear	Steel	HSLA Grade 50 SAE950X
23	Front Stand	Steel	Malleable cast iron, ferritic
24	Tire	Rubber	Elastic
25	Tire	Rubber	Elastic
26	Brake Drum	Steel	Rigid
27	Wheel Rim	Steel	Yield 270 MPa
28	Wheel Rim	Steel	Yield 270 MPa
29	Slider Rail	Steel	HSLA Grade 50 SAE950X
30	Slider Subframe	Steel	HSLA Grade 50 SAE950X
31	Slider Subframe	Steel	HSLA Grade 50 SAE950X
32	Front Lateral Hat Sections	Steel	ASTM A653/A653M Grade 80
33	H Frame Ass'y	Steel	ASTM A653/A653M Grade 80
34	Brace LG	Steel	CS 1040
35	Brace LG Horizontal	Steel	CS 1040

Table 13. FE Model Part List and Material Assignment (Continued)

FE Model Part ID	FE Model Part Name	FE Model Material	FE Model Material Type
36	Floor Kit Ass'y	Wood	Oak
37	Plywood (Door) Liner	Wood	Low Grade Plywood
38	Roof Sheet	Aluminum	6061-T6
39	Rear Floor Step	Steel	CS 1040
41	Door Frame	Steel	HSLA Grade 80 SAE980X
42	Front Stand Connector	Steel	CS 1040
43	Stand Tube	Steel	CS 1040
45	Axle Tube (End)	Steel	Rigid
46	Main Suspension Pivot	Steel	Elastic
47	Main Suspension Pivot	Steel	Elastic
48	Lower Side Rail	Aluminum	6061-T6
52	Tire	Rubber	Elastic
53	Tire	Rubber	Elastic
54	Brake Drum	Steel	Rigid
55	Wheel Rim	Steel	Yield 270 MPa
56	Wheel Rim	Steel	Yield 270 MPa
57	Axle Tube (End)	Steel	Rigid
58	Tire	Rubber	Elastic
59	Tire	Rubber	Elastic
60	Brake Drum	Steel	Rigid
61	Wheel Rim	Steel	Yield 270 MPa
62	Wheel Rim	Steel	Yield 270 MPa
63	Axle Tube (End)	Steel	Rigid
64	Tire	Rubber	Elastic
65	Tire	Rubber	Elastic
66	Brake Drum	Steel	Rigid
67	Wheel Rim	Steel	Yield 270 MPa
68	Wheel Rim	Steel	Yield 270 MPa
69	Axle Tube (End)	Steel	Rigid
71	Lower Side Rail	Aluminum	6061-T6
72	Lower Side Rail	Aluminum	6061-T6
75	Side Posts	Steel	CS 1040
76	Plywood Liner	Wood	Low Grade Plywood
78	Side Post Flanges	Steel	CS 1040
80	Front Posts	Steel	CS 1040

Table 13. FE Model Part List and Material Assignment (Continued)

FE Model Part ID	FE Model Part Name	FE Model Material	FE Model Material Type
82	Kick Plate	Steel	CS 1040
91	Bumper Gusset	Steel	CS 1040
92	Bogie Rail to Gusset	Steel	CS 1040
101	Lateral I-Beam Ends	Steel	ASTM A653/A653M Grade 80
350	Top Rail	Aluminum	6061-T6
351	Top Rail	Aluminum	6061-T6
352	Top Rail	Aluminum	6061-T6
353	Top Rail	Aluminum	6061-T6
354	King Pin Ass’y	Steel	AISI 8630 strength 1241 MPa
355	King Pin Ass’y	Steel	AISI 8630 strength 1241 MPa
356	King Pin Ass’y	Steel	AISI 8630 strength 1241 MPa
357	King Pin Ass’y	Steel	AISI 8630 strength 1241 MPa
358	King Pin Ass’y	Steel	AISI 8630 strength 1241 MPa

Material Properties and Mechanical Models

The main objective of the trailer FE model is in large scale structural crash simulations, so the constitutive material models have to strike a reasonable balance between available information, model accuracy, model characteristics (e.g., element formulations, discretization), and computational cost [52, 53].

Material properties required for the FE model are density, modulus of elasticity, Poisson's ratio, and non-linear elastic-plastic properties (yield stress, strain hardening).

The most commonly-used constitutive model in structural crashworthiness of metallic structures (using crash simulation code LS-DYNA [54]) is the piecewise linear elastic-plastic material model. In this material model, the plastic hardening curve is implemented as a monotonically increasing, piecewise linear curve relating effective plastic strain and effective plastic stress [55]. One of the principal advantages of this model is that data from uniaxial tension or compression experiments can be directly used in the model after being converted to true stress – true strain form. This type of data is easily found in open literature. The data has to be processed to limit the number of linear segments for the desired accuracy and to eliminate spurious regions of strain softening. This material model formulation was used for metallic materials in the trailer FE model.

The material strength properties for the metallic materials used in the trailer FE model were primarily obtained from compilation of stress–strain data [56]. The data for cast iron and steels was retrieved from standards [36, 57], online databases [58], and reference books [43, 48, 59]. The data for Aluminum alloys were taken from references [56, 60, 61]. The data curves were scanned from the references and digitized. The digitized curves were converted into piecewise linear form by using an optimization algorithm [62] that ensures that the resulting form will be within the prescribed error tolerance.

The trailer materials were implemented as a separate file to be included into the overall model. This simplifies material management and provides for reformulation of material properties in the model.

Chapter 5 – Automated Dimensional Adjustments to the Tractor and Trailer Models

The goal of this project is to develop a representative model for Class 8 truck tractor-semitrailer vehicles. Tractors and trailers are available in many different sizes based on model options, so they vary widely in their dimensional, inertial, and impact characteristics. The tractor model developed by the NCAC was based on a "sleeper cab" version of the vehicle that had a relatively long wheelbase, which is outside the NCHRP Report 350 recommended range for the representative vehicle models [2]. The full-scale crash tests available for comparison in this study were all conducted with shorter wheelbase tractors and trailers of various lengths. Those basic dimensional differences make it difficult to compare simulations and experiments.

It would be beneficial for researchers to be able to account for those variations without having to build a new vehicle model from ground up for each new vehicle configuration. A set of model modification scripts called Automated Dimensional Adjustment Program (ADAP) was developed that allows for tailoring of the wheelbase of the tractor and length of the trailer FE models to desired dimensions. This gives researchers more options for simulations and helps to better validate FE models against existing experiments.

The ADAP program is reasonably general and can be used for other FE model modifications. These options have not been pursued as the scope of this project task was to develop tractor wheelbase modification procedures that would set FE model overall dimensions close to overall dimensions of vehicles in the available physical tests. The model generation is executed using scripts, which perform a sequence of basic model modifications through stand-alone programs. Each modification step results in a syntactically valid LS-DYNA input file, which allows for easier procedure development and debugging. The emphasis of the project was not on computational efficiency of the modification process, but on accuracy and flexibility. In any case, the modification is executed in several minutes, which is negligible compared to new model development.

Tractor Model Modification Steps

Several basic operations were developed for LS-DYNA model modifications:

1. Elimination of connections of a (list of) part(s) with other parts in the structure
2. Removal of a (list of) part(s)
3. Cutting of a segment from a (list of) part(s)
4. Scaling of the geometry of a (list of) part(s)
5. Rotation of the geometry a (list of) part(s)
6. Translation of a (list of) part(s)
7. Merging of a (list of) part(s)
8. Joining of parts.

All of the above operations can be applied to the specified part region only. These basic operations are combined to yield the desired geometry through a sequence of steps. Figures 75 through 87 illustrate the basic concept and graphically show the modification steps. The procedure shown here is the modification of the original tractor FE model from a sleeper cab style with an original wheelbase of 203 inches to a day-cab style tractor with a wheelbase of 129 inches. The sequence is shown in the order they were applied to the FE model based on the development of the ADAP program. Figure 75 shows the original sleeper cab tractor model from different viewpoints.

To accomplish a rather substantial wheelbase reduction of 1.6 m (63 inches), the region was cut from a few inches behind the cab door all the way to and including the stand-on plate that connects the two main rails.

The first step was to disconnect from the model and remove parts that were entirely in the cut region and as such were unnecessary for the final model. The FE model configuration after this operation is shown in Figure 76.

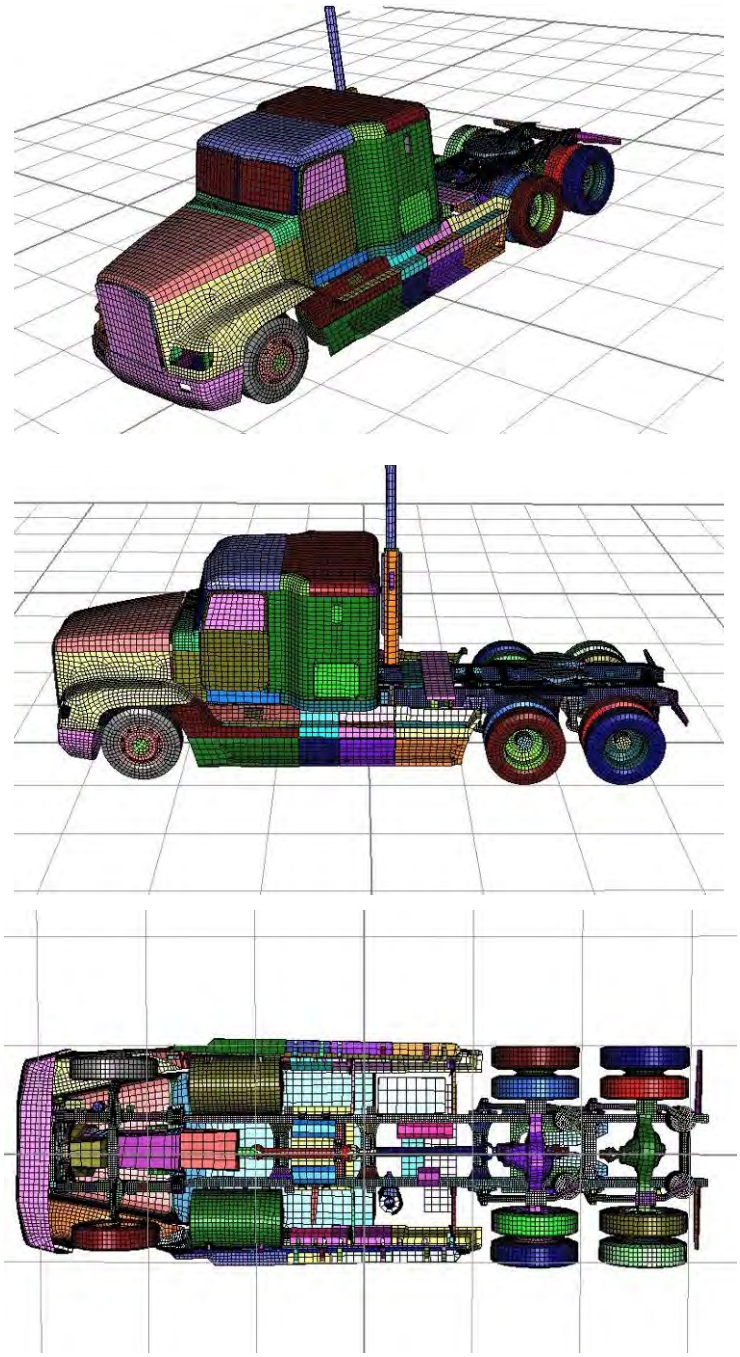

Figure 75. Illustration. Original sleeper-cab style tractor FE model.

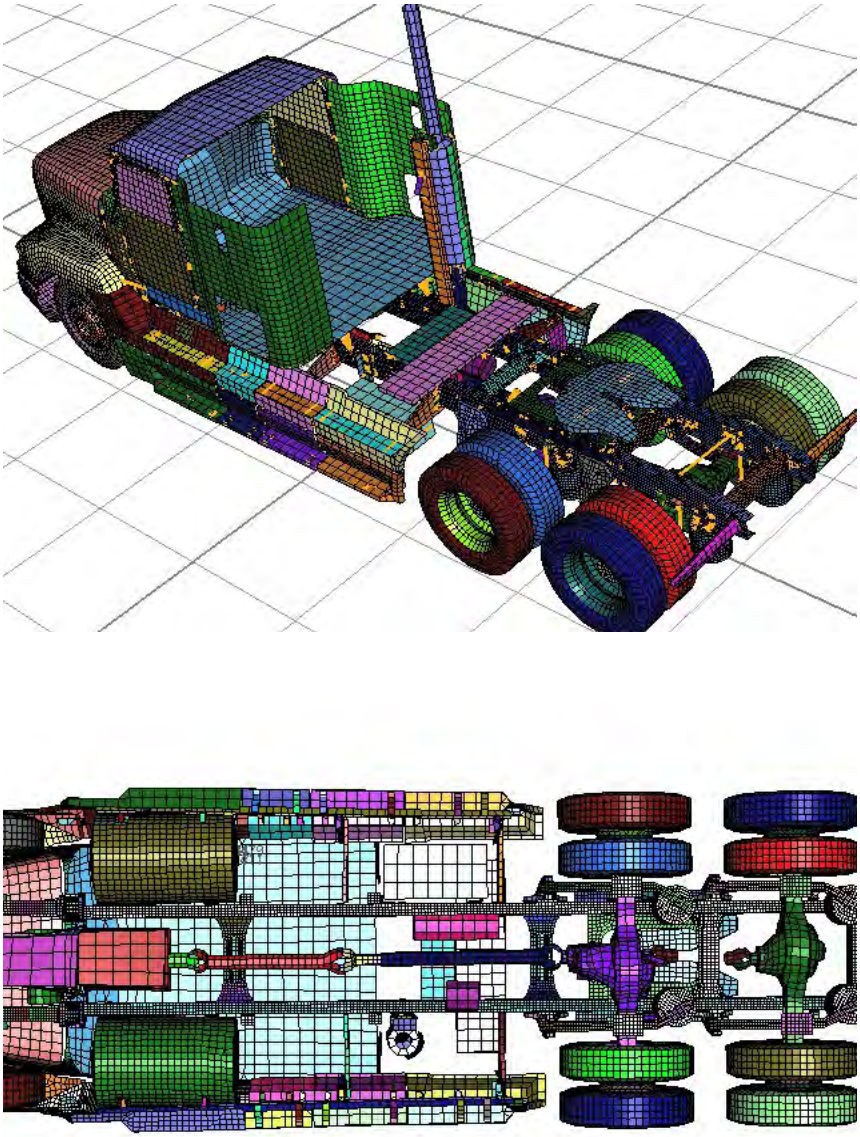

Figure 76. Illustration. Initial removal of parts in the cut region.

The next step was to disconnect and cut the part of the sleeper cab which includes the sides and floor of the cab. The model after this step is shown in Figure 77.

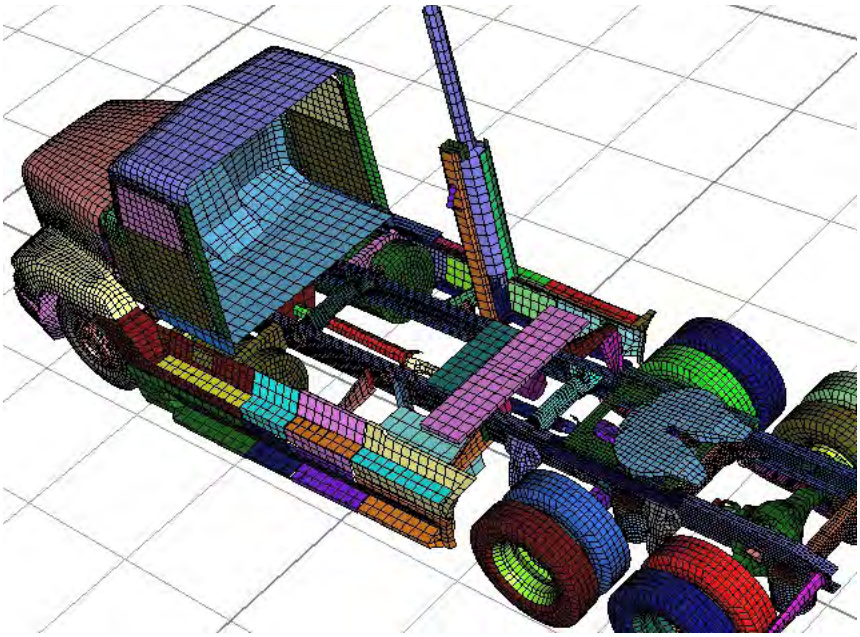

Figure 77. Illustration. Cut sleeper-cab off.

A new geometry to close and complete the day cab was generated and meshed (outside of the modification program) and attached to the model in the next step. The nodes on the perimeter of the new part were merged with nodes of the existing sides, roof, and floor of the cabin. The model after this step is shown in Figure 78 and Figure 79.

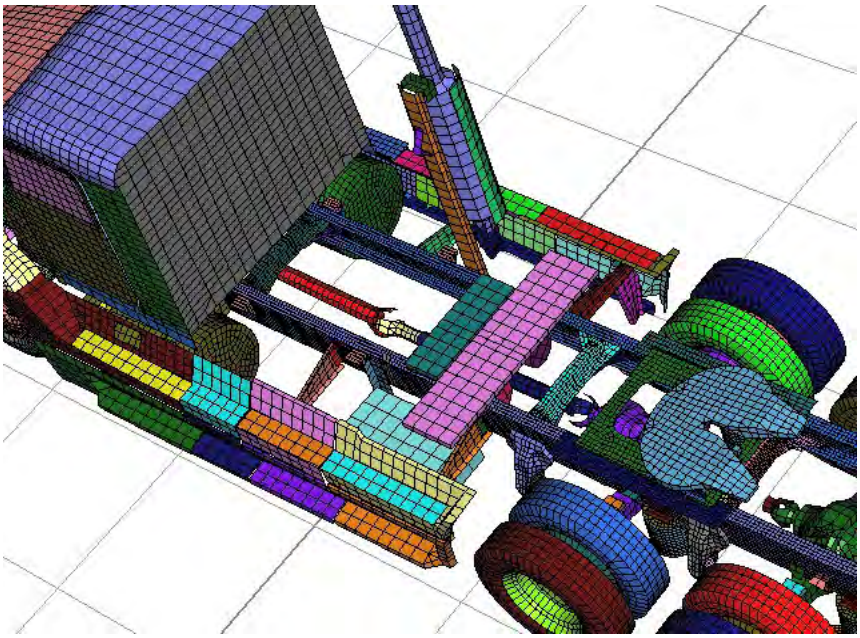

Figure 78. Illustration. Addition of the new back of cabin.

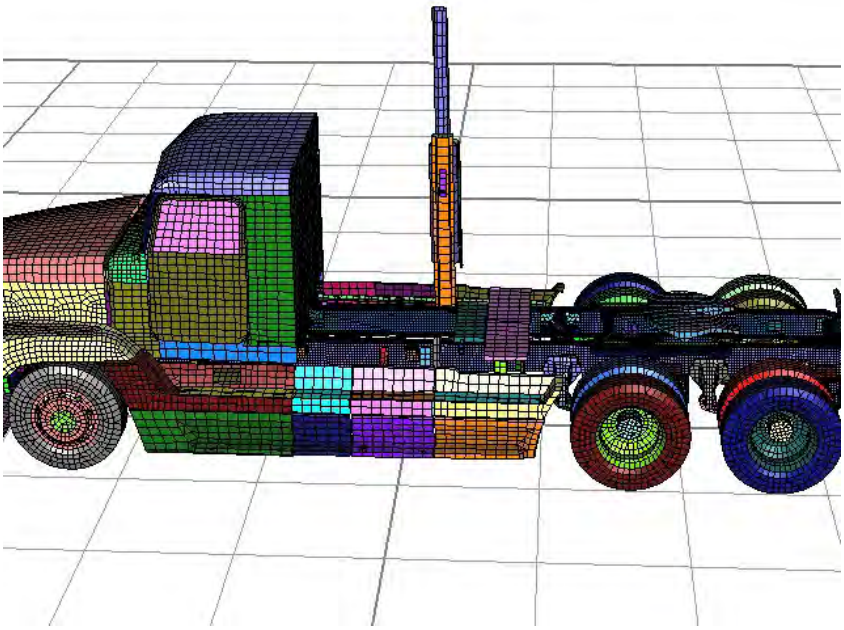

Figure 79. Illustration. Tractor model with new cabin.

The next step was to disconnect two sets of steps/fairings as shown in Figure 80.

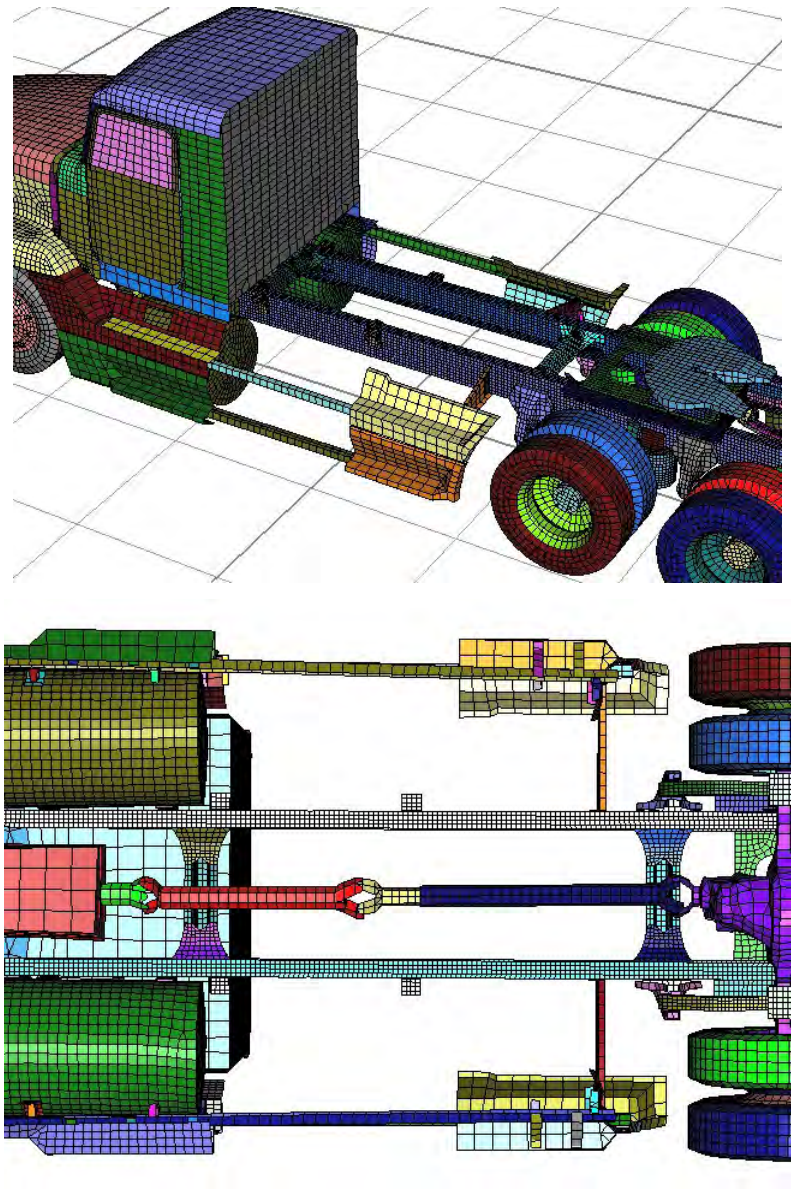

Figure 80. Illustration. Removal of middle set of fairings and exhaust stack.

Each segment of the steps/fairings is independently supported, so it was simpler to completely remove a set than to cut each one partially and adjust the support brackets.

Next, a length of the main rails representing the difference between the current and desired wheelbase was removed as seen in Figure 81.

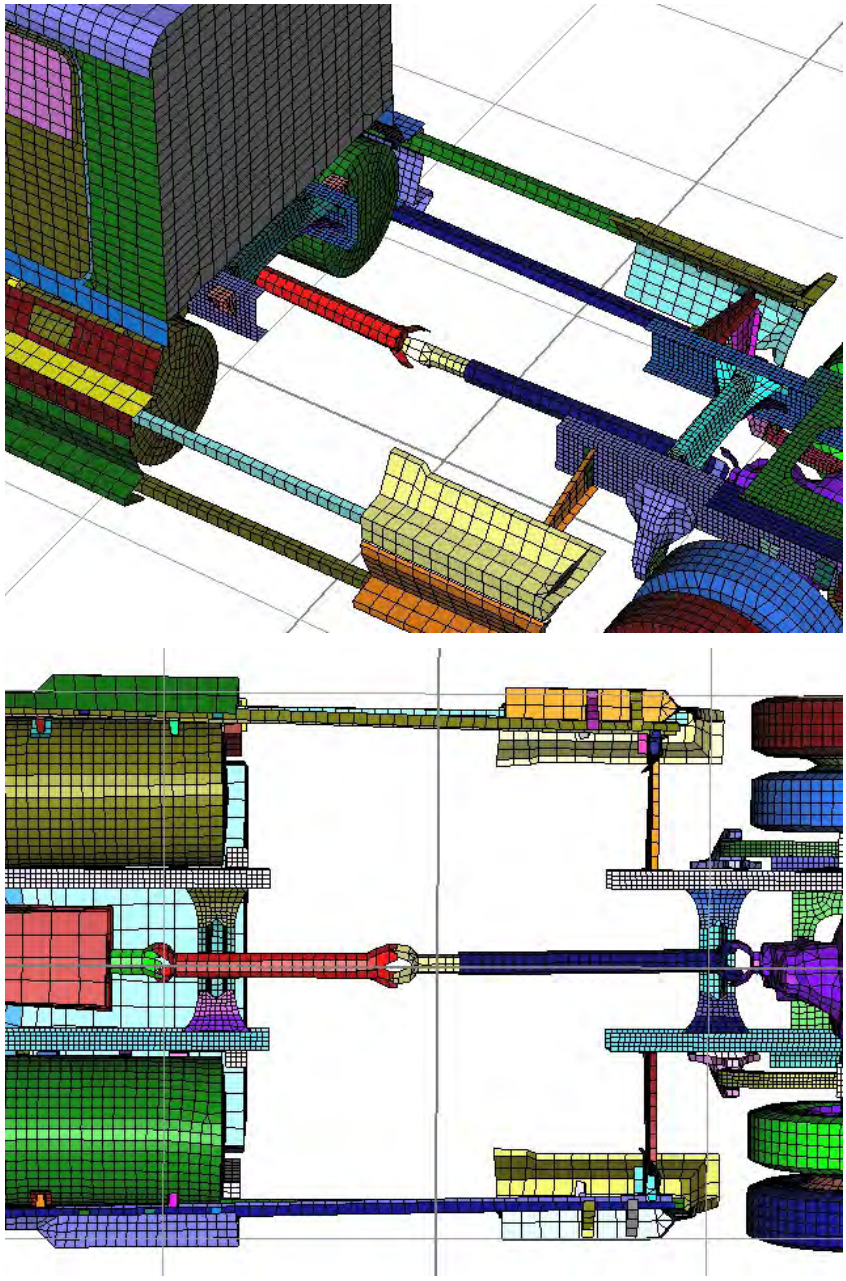

Figure 81. Illustration. Cut frame rails to the desired wheelbase length.

Next, the rear piece of the steps/fairings was cut so that the distance between the edges of the front and rear fairings matches the cut distance of the main rails. The model configuration after this step is shown in Figure 82.

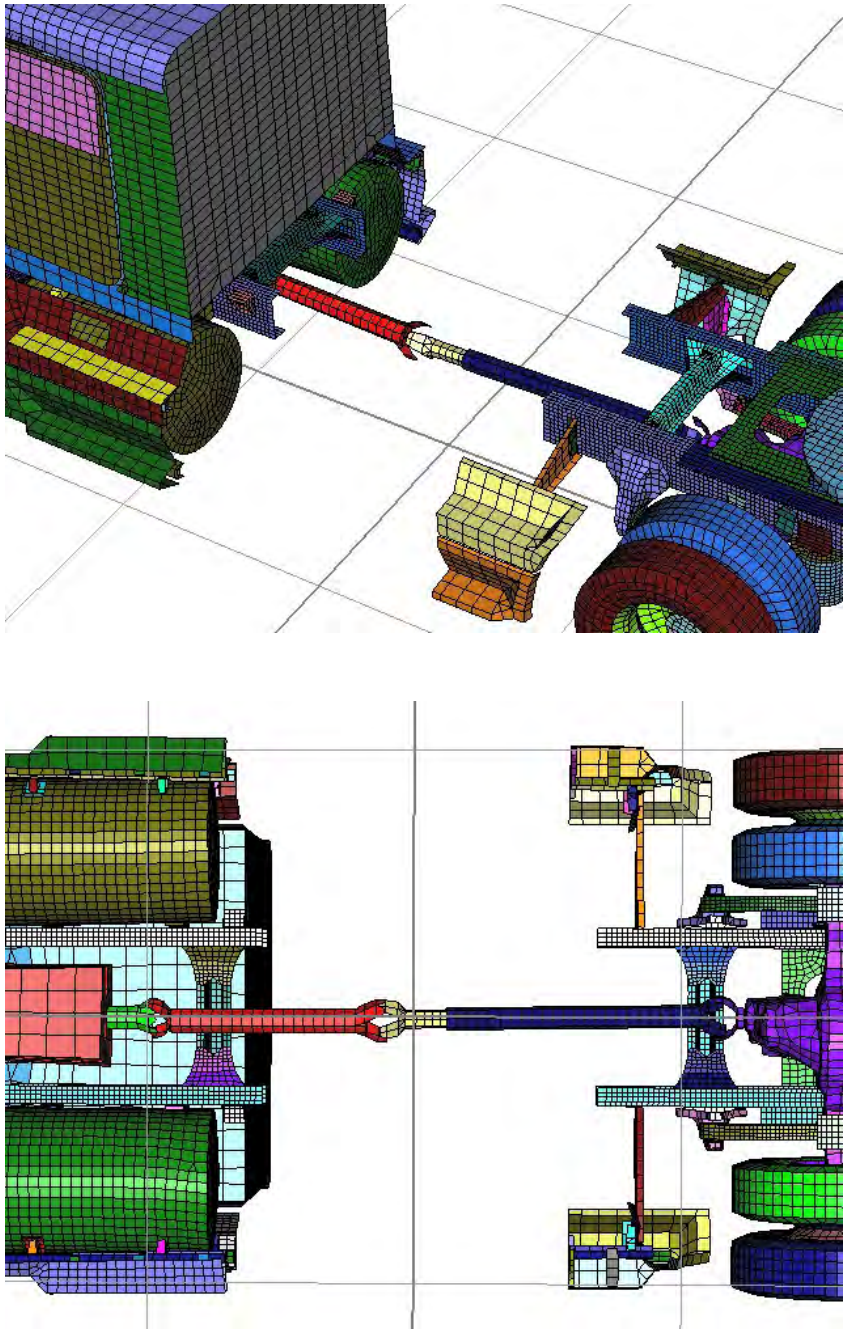

Figure 82. Illustration. Cut fairings to match cut distance of frame rails.

As seen from the above figure, there is a difference in cut plane locations between rails and fairings to accommodate other parts such as fuel tanks and the front rail cross member. Note that the cabin's cut plane is not in the same plane as the frame rail's or steps/fairings' cut plane.

In the next modification step, the drive-shaft parts were shortened/scaled with respect to their front and rear connections (rather than cut and rejoined) as shown in Figure 83.

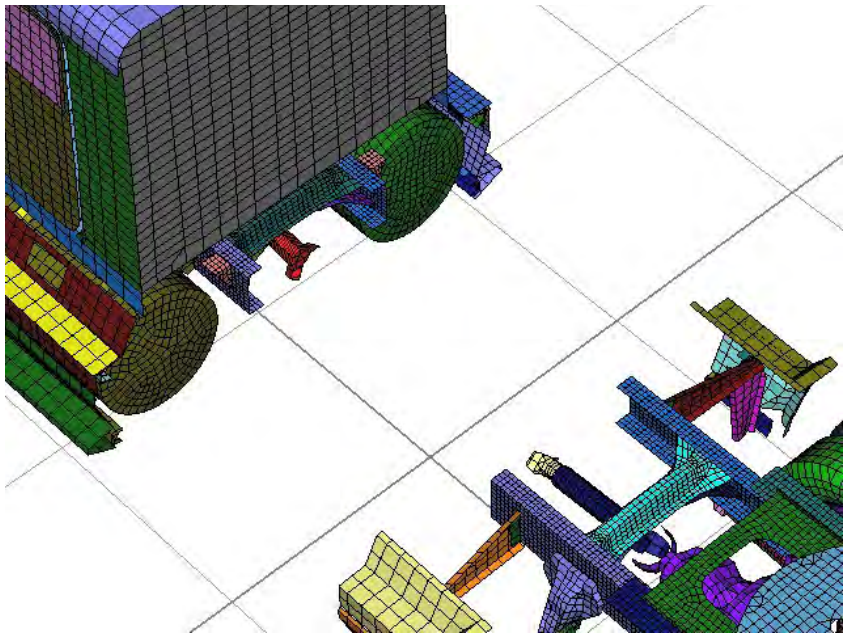

Figure 83. Illustration. Scale (shorten) drive-shaft parts to match cut from frame rails.

The cut-edges of the front and rear steps/fairings do not match exactly, so the rear step/fairing and its support rail were scaled in the lateral and vertical directions with respect to their rear connections to the main rail to match the location of the front edges of the respective parts. The configuration after this step is shown in Figure 84.

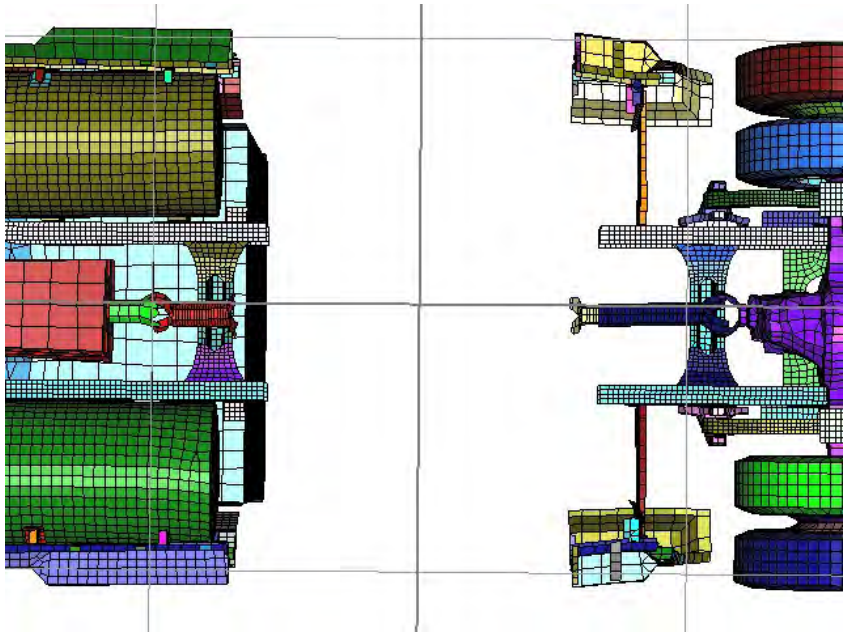

Figure 84. Illustration. Scales fairings and their support rails to match at their front counterparts.

Finally, the front part of the tractor is translated to the rear part over the length of the cut segment. The model after translation is shown in Figure 85.

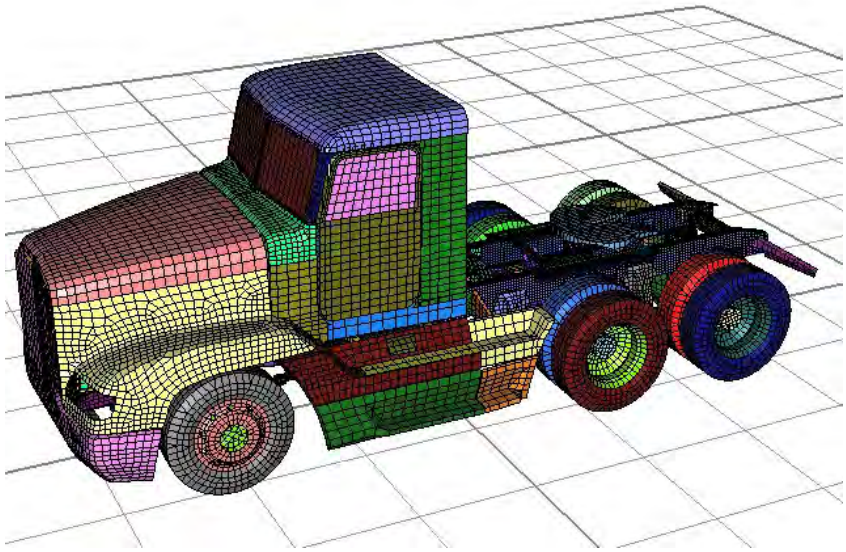

Figure 85. Illustration. Front section translated to meet the back section.

A close-up of the meeting locations of two sides is shown in Figure 86.

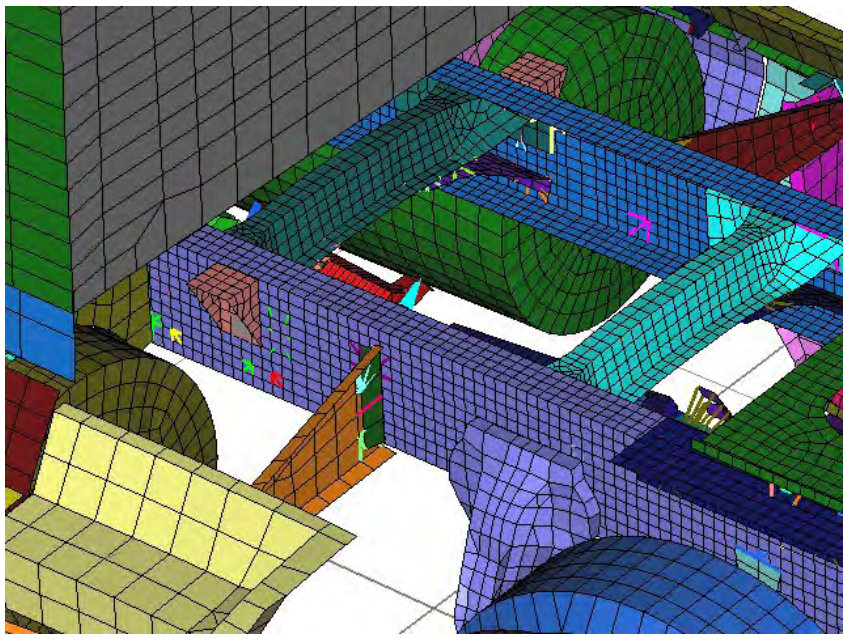

Figure 86. Illustration. Close-up of the model with translated front.

The corresponding parts are node-merged at the cut edges, the exhaust stack is replaced and connected to the main rail and the rear cabin wall. The rear cabin mounts are reconnected to the cabin floor. The final day-cab model is shown in Figure 87. This reduced wheelbase, day-cab style tractor FE model was used for the crash test simulation discussed in Chapter 6 of this report.

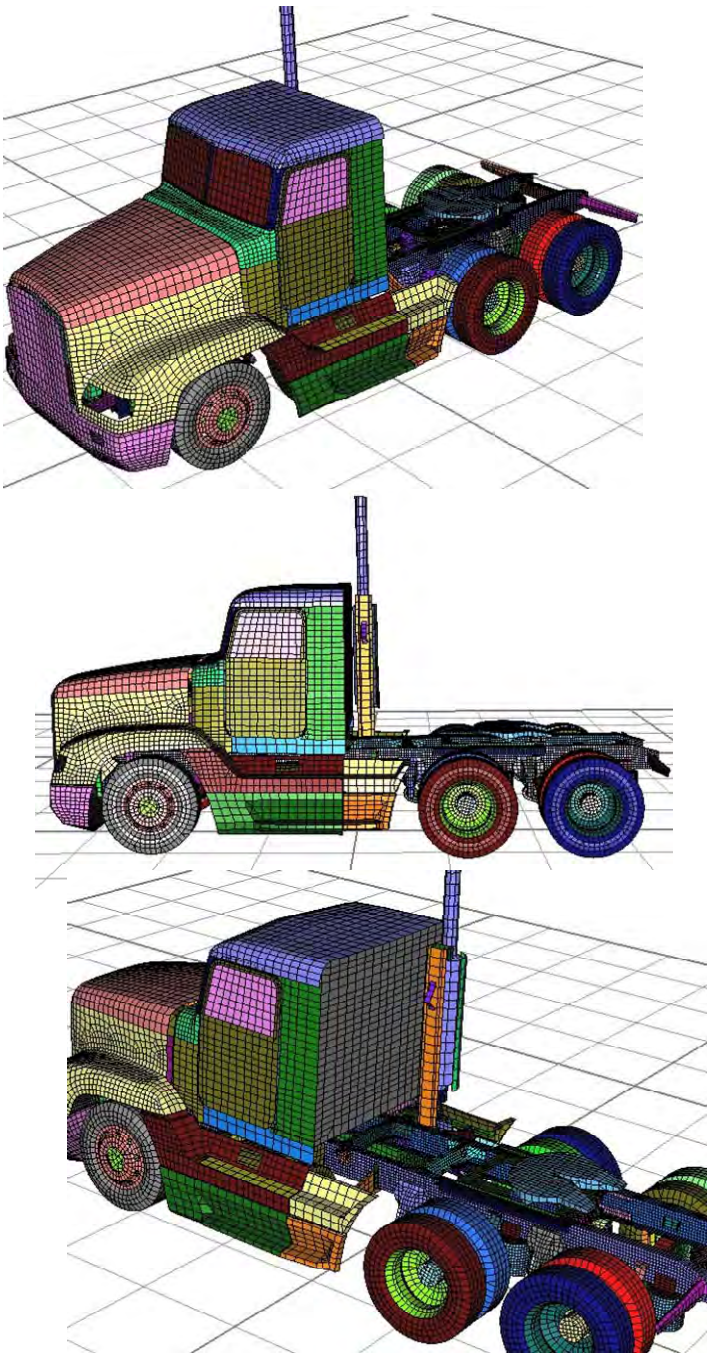

Figure 87. Illustration. Final configuration after merging cut sections and adding the exhaust stack.

The cabin mount connections are shown in Figure 88.

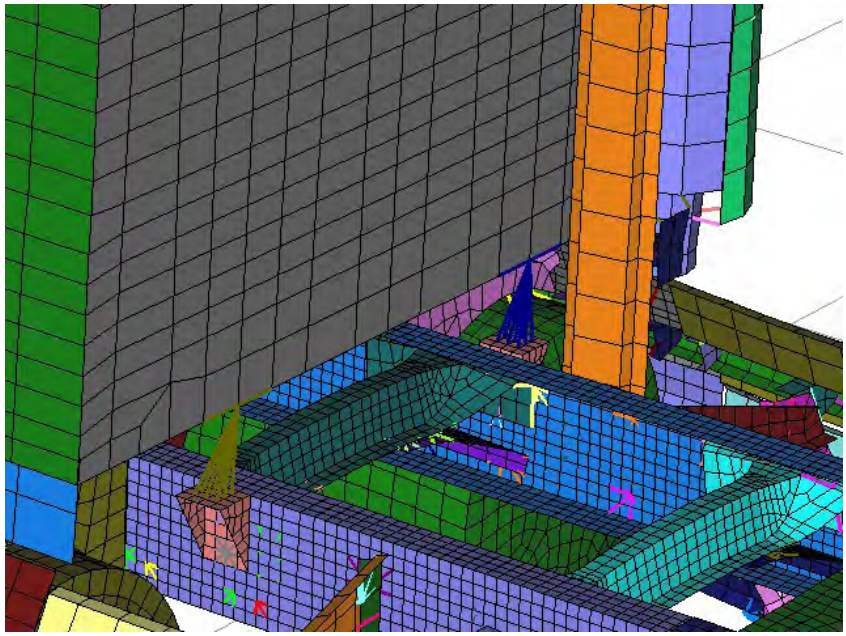

Figure 88. Illustration. Cabin reconnected to frame rails.

Figures 89 to 92 provide some additional views of the final model.

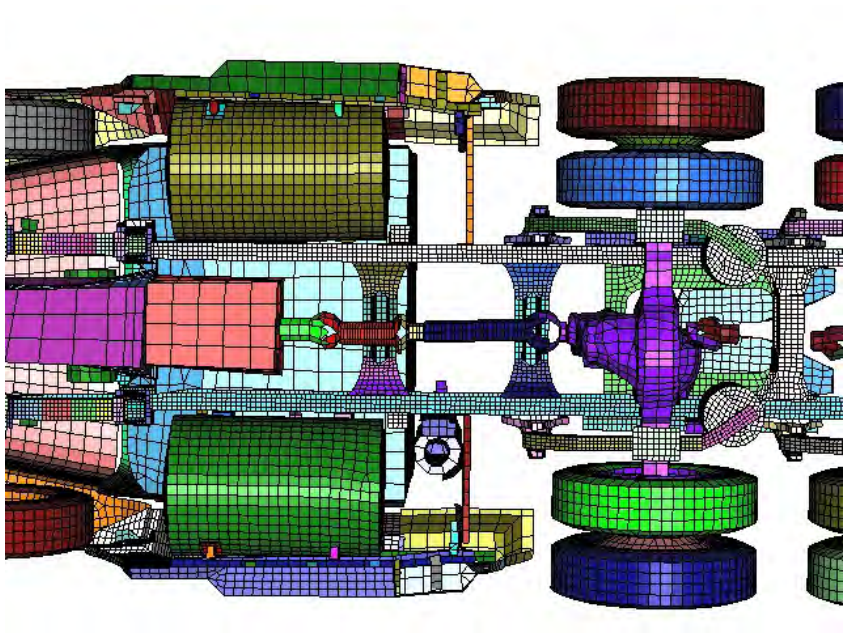

Figure 89. Illustration. Overall bottom view of the final model.

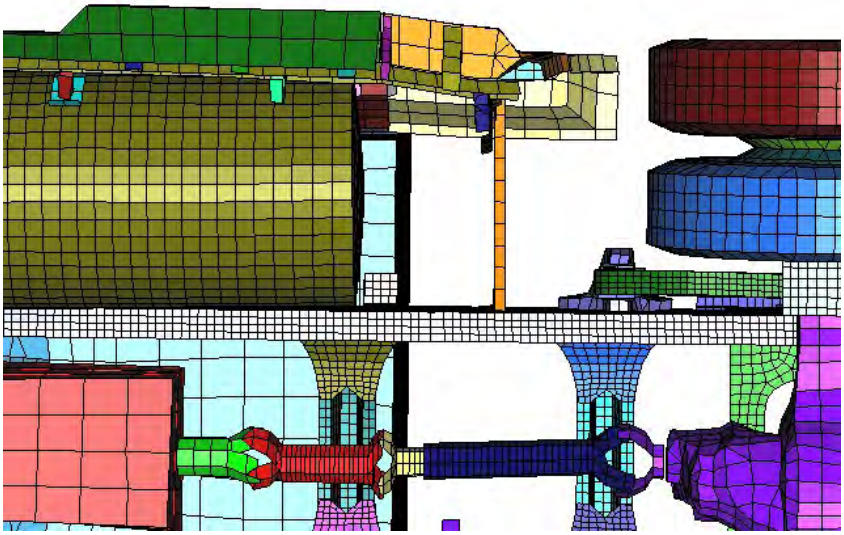

Figure 90. Illustration. Close-Up bottom view of the final model.

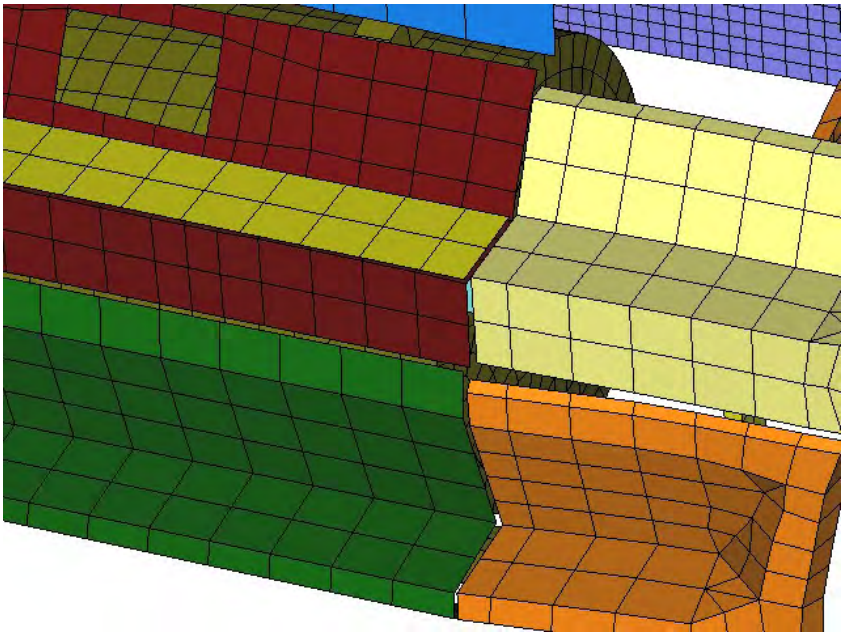

Figure 91. Illustration. Detail view of the fairings fit.

Fairings support rails and brackets can be seen in Figure 92. The connection location is indicated by a slight change in the element size.

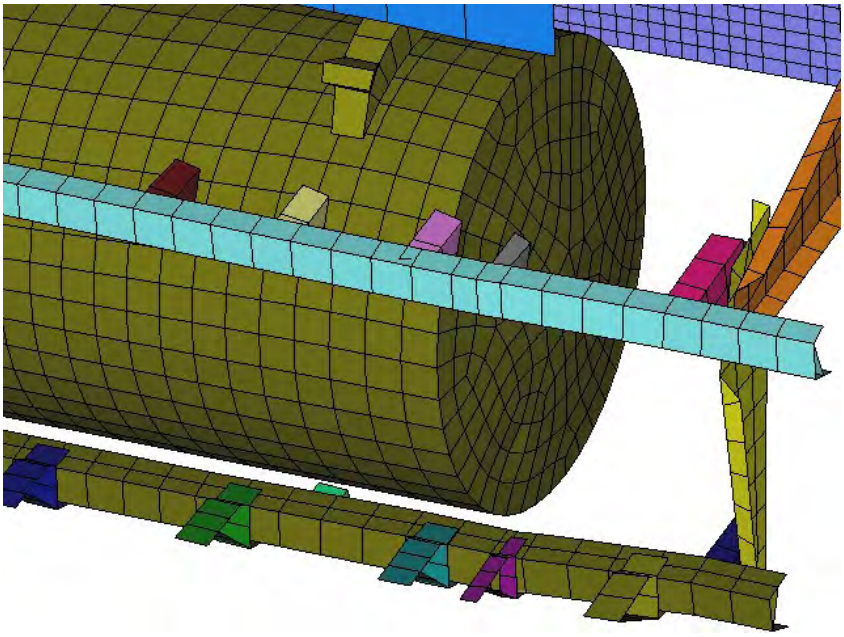

Figure 92. Illustration. Fairing support rails and brackets.

Trailer FE Model Modifications

Similar scripts to modify the trailer length have not been written as yet. They will be much like and patterned after the tractor-modification scripts. The process and algorithms will be very similar and likely less complicated because the trailer structure itself is less complex and is inherently more repetitious. This will be done if needed and if funding is available.

Chapter 6 – Assessment of Tractor-Semitrailer FE Model Simulation Results

The performance of the tractor-semitrailer FE model was assessed in Phase B by comparing simulation results to data obtained from full-scale crash tests. Of the 12 full-scale tractor-semitrailer crash tests identified in the literature summary in Chapter 2, 5 of them involved a day-cab style tractor pulling a 12.2 to 14.6 m (40 to 48-ft) box-trailer impacting a 1,067 mm (42 in) tall barrier at a nominal speed of 80 km/hr at 15 degrees (e.g., Group A in the literature review section) [5, 7, 10, 12, 14]. The most recent of these tests was conducted at the Midwest Roadside Safety Facility on July 12, 2007 (Test No. TL5CMB-2) [14]. For evaluation purposes, the FE analysis was set up to emulate the impact conditions and test vehicle dimensions of that particular test.

The following sections present a summary of the tractor-semitrailer FE model and an evaluation of the results of the model compared to full-scale crash test TL5CMB-2. A quantitative evaluation of the FE model simulations' results is presented; however, the overall evaluation is largely qualitative, since the only quantitative data from test TL5CMB-2 was from a single triaxial accelerometer located on the floor of the trailer near the tandem axle. A general assessment of the models' results is also presented based on a comparison to results of similar tests in the literature. This chapter of the report is organized under the following topic headings:

- Overview Of the MwRSF Crash Test Tl5CMB-213
- Finite Element Model for Tl5CMB-2 Simulation
- Summary Of Key Phenomenological Events from the Tractor-Trailer FE Model Simulation
- Qualitative Assessment of Tractor-Trailer FE Model Simulation Results
  - Qualitative Comparison of Simulation Results with Test Tl5CMB-213
  - Qualitative Comparison of Simulation Results with Other Similar Tests
- Quantitative Assessment of Tractor-Trailer FE Model Simulation Results
  - Quantitative Validation Approach
  - Quantitative Evaluation Results

Overview of the MWRSF Crash Test TL5CMB-2

Test TL5CMB-2 was conducted by MwRSF to evaluate the crash performance of a new concrete median barrier design according to the testing guidelines of NCHRP Report 350 for Test Level 5 impact conditions. The test involved a 36,153-kg (79,705-lb) tractor-semitrailer vehicle impacting a concrete median barrier at 84.9 km/hr (52.7 mph) and impact angle of 15.4 degrees. The test vehicle was a 1991 White GMC tractor with a 1988 Pines 14.6-m (48-ft) semitrailer. The test article was a 1.067 m (42 inches) tall concrete median barrier with an installation length of 60.9 m (200 ft). Figure 93 shows a photograph of the test vehicle and of the barrier with

dimensions labeled. The geometric dimensions and mass inertial measurements of the test vehicle are provided in Figure 94.

The acceleration data from the test was collected using a triaxial piezoresistive accelerometer and the angular velocities were collected using Analog Systems 3-axis rate transducer. The Electronic Recording Devices (ERDs) were mounted at two locations: 1) the primary ERD set was mounted to the trailer floor on the inside of the trailer near the tandem axles of the trailer and 2) the secondary ERD set was mounted near the tractor tandem axles. Unfortunately, data was not recorded for the secondary ERD set due to a premature triggering of the ERD. Four AOS high-speed video cameras with recording speeds of 500 frames/sec and six digital video cameras with recording speeds of approximately 30 frames/sec were used to film the crash test.

(a) Test Vehicle

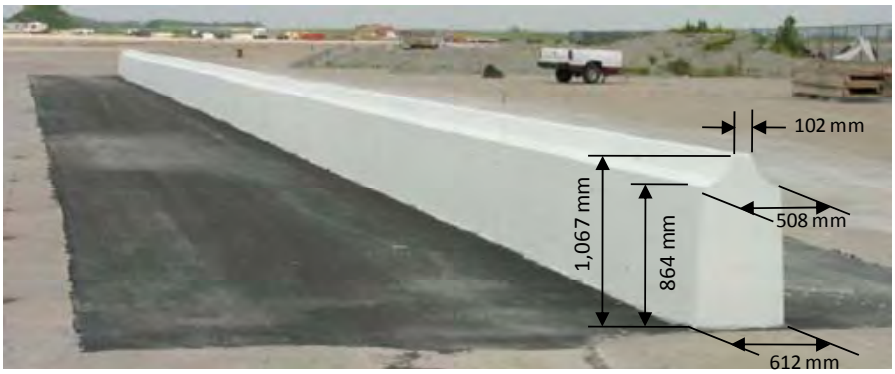

(b) Test Article

Figure 93. Photograph. (a) Tractor-semitrailer vehicle and (b) 1.067 m tall concrete median barrier used in MwRSF Test No. TL5CMB-2.

Date: 7/12/2007 Test Number: MwRSF Test No. TL5CMB-2

Tractor:

VIN No,: 4V1JLBJEGMR810558 Make: White/GMC Model: WG65T

Year: 1991 Odometer: 137548

Trailer:

VIN No,: 1p10748254jka29485 Make: Pines 48' Model: 48' Van

Year: 1988

*All Measurements Refer to Impacting Side

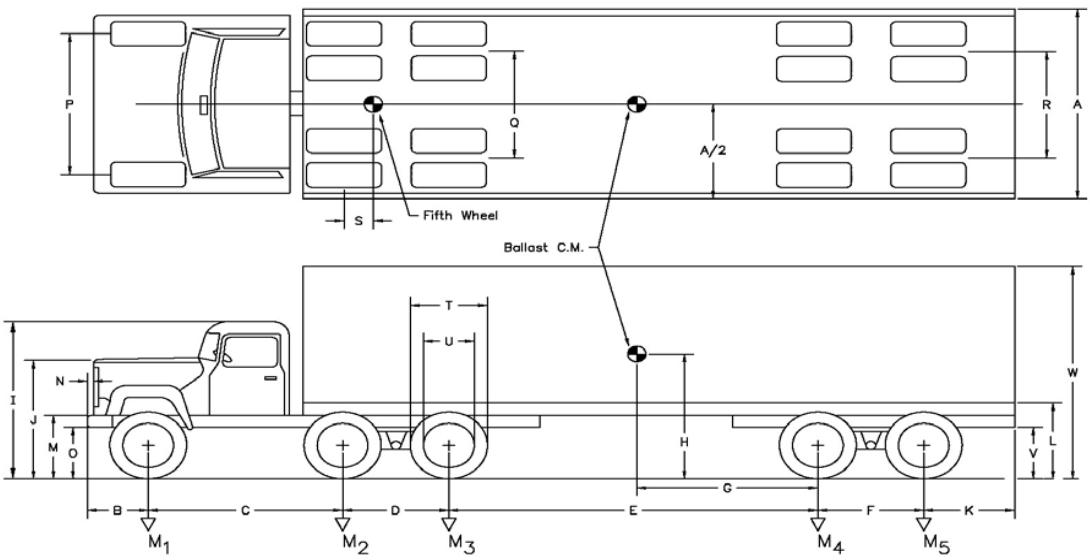

Vehicle Geomerty -mm (in)

A	2,604	(102.5)	G	5,906	(232.5)	N	0	(0.0)	T	1,016	(40.0)
B	1,314	(51.7)	H	1,831	(72.1)	O	584	(23.0)	U	597	(23.5)
C	3,270	(128.7)	J	1,746	(68.7)	P	2,007	(79.0)	V	781	(30.7)
D	1,334	(52.5)	K	1,575	(62.0)	Q	1,842	(72.5)	W	4,064	(160.0)
E	10,185	(401.0)	L	1,156	(45.5)	R	1,981	(78.0)	X	NA	
F	1,257	(49.5)	M	902	(35.5)	S	533	(21.0)			

Mass -Properties		**Curb**		**Test Inertial**		**Gross Static**	
M_1	kg (lb)	3,973	(8,759)	4,441	(9,791)	4,441	(9,791)
$M_2 + M_3$	kg (lb)	5,144	(11,341)	17,017	(37,516)	17,017	(37,516)
$M_4 + M_5$	kg (lb)	3,955	(8,719)	14,696	(32,399)	14,696	(32,399)
M_{Total}	kg (lb)	13,073	(28,821)	36,154	(79,706)	36,154	(79,706)
I_{11}	kg - m^2 (lb-ft^2)		(0)		(0)		(0)
I_{22}	kg - m^2 (lb-ft^2)		(0)		(0)		(0)
I_{33}	kg - m^2 (lb-ft^2)		(0)		(0)		(0)

Figure 94. Illustration. Dimensions of the MwRSF Test No. TL5CMB-2 test vehicle.

Finite Element Model for TL5CMB-2 Simulation

The geometry of the tractor FE model was modified such that the wheelbase of the model was the same as the wheelbase of the test vehicle used in MwRSF Test No. TL5CMB-2. A FE analysis was conducted simulating this test using the tractor-semitrailer FE model (model versions tractor_09-0506 and trailer_09-0518). The friction between the tractor and barrier was set to 0.2, and the friction between the tires and the barrier was set to 0.8. The dimensions of the barrier model were the same as those of the barrier in MwRSF Test No. TL5CMB-2 shown in Figure 93. Since there was negligible deflection of the barrier in the full-scale test, the barrier was modeled as a rigid material with rigid fixity to the ground. The impact conditions for the FE simulation were consistent with those reported in the full-scale crash test (i.e., 84.9 km/hr (52.7 mph) at an impact angle of 15.5 degrees).

The ADAP described in Chapter 6 of this report was developed to aid in the modification of overall vehicle model size and shape parameters (e.g., wheelbase, trailer length). These scripts were designed to operate on the FE model input file directly and were used to modify the tractor model geometry.

In particular, they were used to: 1) make the tractor a day-cab style tractor by removing the sleeper section of the cabin and 2) adjust the wheelbase length of the tractor by removing a section of the frame rails (along with other components in this section of the model). Figure 95 shows a visual comparison between the tractor FE model and the test tractor. The geometric and mass inertial properties of the modified tractor-semitrailer model are shown in Figure 96. A comparison of the dimensional properties of the FE model to the test vehicle is shown in Figure 97. The most notable differences between the test vehicle and modified FE model are listed below:

- *Length dimensions* – The length dimensions of the FE model were all within 2% of the test vehicle dimensions, except for the distance from the front bumper to the center of the front wheel (e.g., dimension “B” in Figure 97), which was 13.5% shorter in the FE model.

- *Trailer box dimensions* – The trailer floor in the FE model was 148 mm (5.8 inches) higher than the test vehicle (e.g., dimension “L” in Figure 97), and the top of the trailer in the FE model was 169 mm (6.7 inches) lower than the test vehicle (e.g., dimension “W” in Figure 97).

- *Ballast center of gravity (c.g.)* – The c.g. of the ballast in the FE model was located 600 mm (23.6 inches) rearward of and 188 mm (4.6 inches) higher than the c.g. location of the ballast in the test vehicle.

- *Trailer suspension* – The suspension system on the FE trailer model was the Airide™ design, and the suspension on the trailer test vehicle was a leaf-spring design.

(a) Test Vehicle

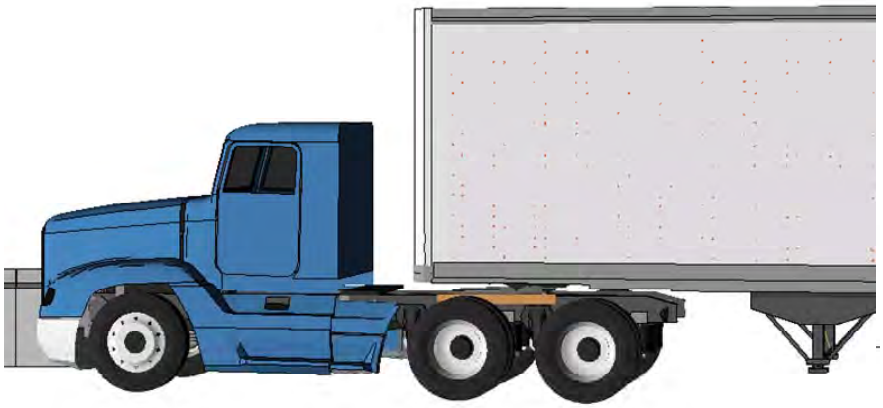

(b) FE Model

Figure 95. Photograph / Illustration. (a) Tractor test vehicle and (b) tractor FE model.

Date: 5/20/2009 Test Number: Battelle Simulation No. TT090518

Tractor:

Model: 01a_Trac_Day_v1a_0900506.k Make: Freightliner Model: FLD120

Year:

Trailer:

Model: 02b_SemiTrailer48_09-0520.k Make: Stoughton Model: 48-ft Box Trailer

Year: 1990

*All Measurements Refer to Impacting Side

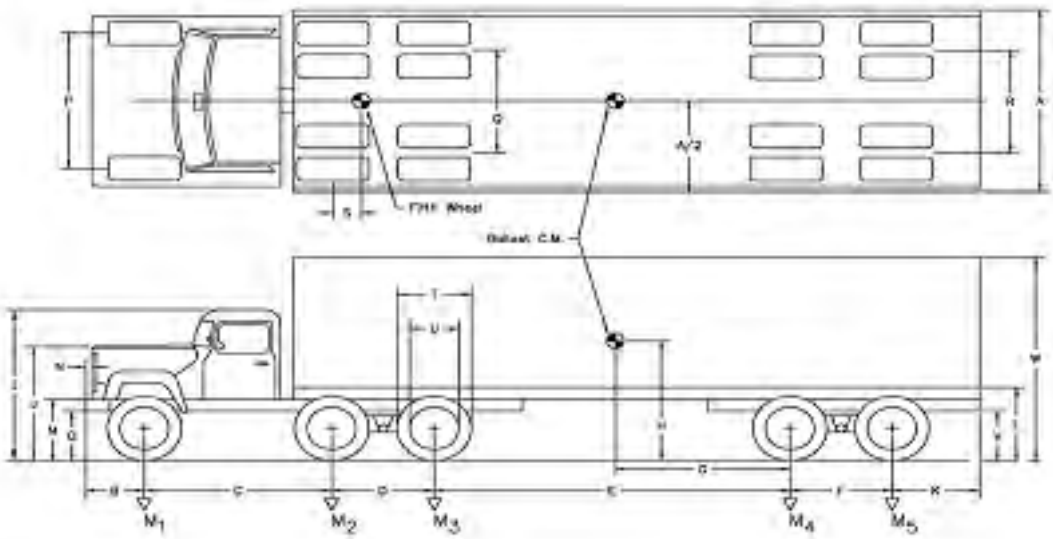

Vehicle Geometry -mm (in)

A	2,636	(103.8)	G	5,307	(208.9)	N			T	1,004	(39.5)
B	1,136	(44.7)	H	1,949	(76.7)	O	518	(20.4)	U	592	(23.3)
C	3,280	(129.1)	J	1,734	(68.3)	P	1,929	(75.9)	V	926	(36.5)
D	1,265	(49.8)	K	1,552	(61.1)	Q	1,906	(75.0)	W	3,895	(153.3)
E	10,188	(401.1)	L	1,304	(51.3)	R	2,046	(80.5)			
F	1,246	(49.0)	M	726	(28.6)	S	460	(18.1)			

Mass -Properties		Curb		Test Inertial		Gross Static	
M_1	kg (lb)		(0)	4,040	(8,907)	4,040	(8,907)
$M_2 + M_3$	kg (lb)		(0)	17,570	(38,735)	17,570	(38,735)
$M_4 + M_5$	kg (lb)		(0)	14,590	(32,165)	14,590	(32,165)
M_{total}	kg (lb)	13,100	(28,881)	36,200	(79,807)	36,200	(79,807)
I_{11}	kg - m^2 (lb-ft^2)	16,020	(115,870)	31420	(227,256)	31420	(227,256)
I_{22}	kg - m^2 (lb-ft^2)	474,300	(3,430,541)	863,200	(6,243,396)	863,200	(6,243,396)
I_{33}	kg - m^2 (lb-ft^2)	473,800	(3,426,924)	866,300	(6,265,818)	866,300	(6,265,818)

Figure 96. Illustration. Dimensions of the tractor-semitrailer FE vehicle model.

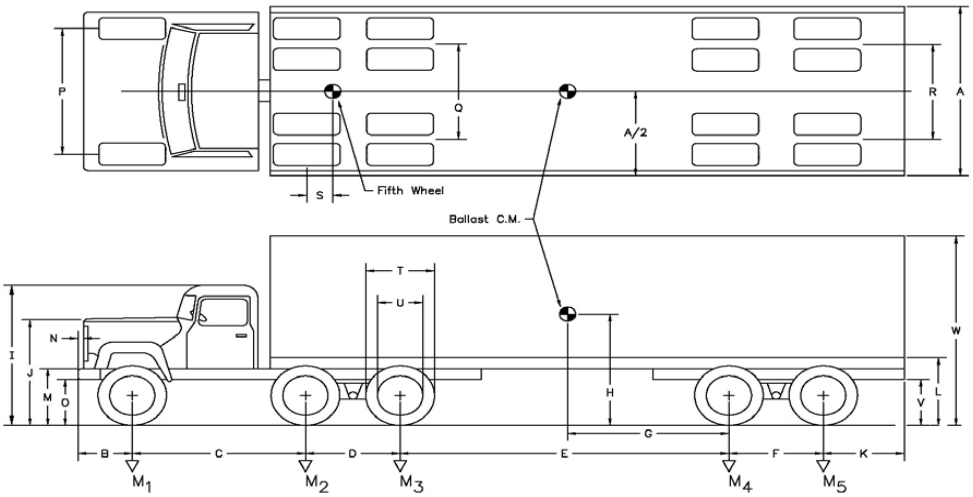

Vehicle Geomerty -mm

	Test Vehicle	FE Model	Error %		Test Vehicle	FE Model	Error %		Test Vehicle	FE Model	Error %		Test Vehicle	FE Model	Error %
A	2,604	2,636	1.2	G	5,906	5,307	-10.1	N				T	1,016	1,004	-1.2
B	1,314	1,136	-13.5	H	1,831	1,949	6.4	O	584	518	-11.3	U	597	592	-0.8
C	3,270	3,280	0.3	J	1,746	1,734	-0.7	P	2,007	1,929	-3.9	V	781	926	18.6
D	1,334	1,265	-5.2	K	1,575	1,552	-1.5	Q	1,842	1,906	3.5	W	4,064	3,895	-4.2
E	10,185	10,188	0.0	L	1,156	1,304	12.8	R	1,981	2,045	3.2				
F	1,257	1,245	-1.0	M	902	726	-19.5	S	533	460	-13.7				

Mass -Properties

		Curb			Test Inertial			Gross Static		
		Test Vehicle	FE Model	Error %	Test Vehicle	FE Model	Error %	Test Vehicle	FE Model	Error %
M_1	(kg)	3,973	-	-	4,441	4,040	-9.0	4,441	4,040	-9.0
$M_2 + M_3$	(kg)	5,144	-	-	17,017	17,570	3.2	17,017	17,570	3.2
$M_4 + M_5$	(kg)	3,955	-	-	14,696	14,590	-0.7	14,696	14,590	-0.7
M_{Total}	(kg)	13,073	13,100	0.2	36,154	36,200	0.1	36,154	36,200	0.1
I_{11}	(kg - m^2)	-	16,020	-	-	31420	-	-	31420	-
I_{22}	(kg - m^2)	-	474,300	-	-	863,200	-	-	863,200	-
I_{33}	(kg - m^2)	-	473,800	-	-	866,300	-	-	866,300	-

Figure 97. Illustration. Comparison of FE vehicle model dimensions to those of the test vehicle.

Although the mass of the test tractor was not reported, it was estimated to be 7,043 kg (15,526 lb) by considering that the total gross static mass of the test vehicle was 13,073 kg (28,819 lb) and that the typical mass of a 14.6-m (48-ft) semitrailer is approximately 6,030 kg (13,300 lb). For comparison, the mass of the FE tractor model was 6,927 kg (15,271 lb). The axle loads of the FE model were within 10% of the axle loads measured on the test vehicle. The total mass of the FE tractor-semitrailer model was 36,200 kg (79,807 lb) which was 0.1% higher than the total mass of the test vehicle.

The analysis was conducted with a time-step of 1.26 microseconds for a time period of 1.87 seconds. The suspension systems on the tractor and trailer models were initialized based on the weight of the model; however, the model was not completely at steady state at the beginning of the analysis. To partially account for this, the tractor-semitrailer model was positioned at

4.7 m upstream of the impact point at the start of the analysis to allow 0.2 seconds for gravity to sufficiently load the suspension of the tractor and trailer prior to impact. So, to avoid confusion in reporting timing of events, the reported time has been shifted -0.2 seconds such that the reported time of impact is 0.0 seconds and the termination time is 1.67 seconds.

Summary of Key Phenomenological Events from the Tractor-Trailer FE Model Simulation

The exact timing of phenomenological events was not possible because simulation results were only collected at 0.01 second intervals throughout the FE analysis. Therefore, a 0.01 second time window corresponding to range of time for which the event could have occurred in the analysis was reported.

The tractor began to yaw between 0.02 seconds and 0.03 seconds. The left-front tires of the tractor lifted off the ground between 0.1 and 0.11 seconds. The right front corner of the trailer contacted the top of the barrier between 0.17 and 0.18 seconds. At 0.19 to 0.2 seconds, the trailer visibly started to roll toward the barrier. The left rear tires of the tractor were lifted off the ground between 0.21 and 0.22 seconds. Both rear trailer tires were lifted off the ground between 0.25 and 0.26 seconds. Between 0.26 and 0.27 seconds the right front corner was vertically coincident with the back face of the barrier.

The tractor became parallel to the barrier between 0.32 and 0.33 seconds. The tractor reached a peak roll angle of 14.6 degrees at 0.295 seconds (computed from the accelerometer at the tractor fifth-wheel). Approximately 15 degrees of roll was measured from the full-scale crash test video. The left front tractor tires returned to the roadway surface between 0.34 and 0.35 seconds, shortly thereafter the left-side front suspension u-bolts failed.

The trailer was parallel to the barrier between 0.63 and 0.64 seconds. The rear trailer tandem wheels impacted the barrier between 0.65 and 0.66 seconds. Between 0.74 and 0.75 seconds the tractor rolled back to level position. The tractor started to roll back toward the barrier between 0.8 and 0.81 seconds.

At 1.2 seconds, the trailer reached maximum roll angle of 42.8 degrees (computed from the accelerometer at the trailer tandem). A maximum roll angle of 42 degrees was measured from the full-scale crash test video. The tractor reached another peak roll angle of 23.8 degrees between 1.16 and 1.17 seconds, compared to approximately 19 degrees measured from the full-scale crash test video. The tractor left-side tandem wheels returned to the roadway surface at 1.53 seconds.

The analysis terminated at 1.66 seconds, at which time

- The roll angle of the tractor was approximately 1.0 degree
- The trailer was rolling back toward level with a roll angle of 16 degrees
- The tractor and trailer were approximately parallel to the barrier and still in contact
- The forward velocity of the tractor was 60.9 km/hr.

Qualitative Assessment of Tractor-Trailer FE Model Simulation Results

Qualitative Comparison of Simulation Results with Test TL5CMB-2

Phenomenological Events

A qualitative assessment was made by comparing sequential snapshots of the full-scale crash test with the results of the simulation to verify vehicle kinematic response, as well as sequence and timing of key phenomenological events. The results from the FE simulation compare reasonably well with the results from full-scale crash test TL5CMB-2. Figures 98, 99 and 100 show sequential snapshots of the impact event from a downstream viewpoint, an upstream viewpoint, and from an oblique (downstream and behind the barrier) view point, respectively.

The FE model simulates the basic kinematic behavior of the tractor-semitrailer reasonably well, and adequately captures the basic phenomenological events that occur during impact. Table 14 provides a list of phenomenological events and their time of occurrence for both the full-scale crash test and the FE simulation.

Acceleration-time histories and angular rate-time histories were collected from several locations in the FE model using the *Element_Seatbelt_Accelerometer option in Ls-Dyna, which is the preferred method suggested by Ls-Dyna for collecting acceleration data [63]. The accelerometers were connected to the tractor-semitrailer model using CNRBs. The time-history data was collected from each accelerometer in a local reference coordinate system which rotates with the accelerometer in the same way that test data is collected from physical accelerometers. The data was collected at a frequency of 30 kHz which was determined to be sufficient to avoid aliasing of the data.

Time = 0.000

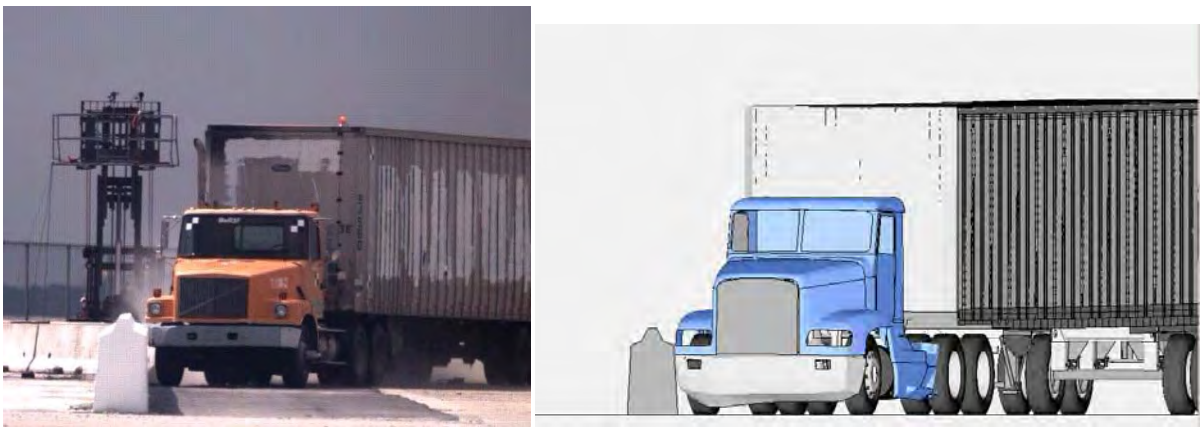

Time = 0.1 second

Time = 0.2 second

Figure 98. Photograph / Illustration. Sequential views of MwRSF Test TL5CMB-2 and FE model simulation from a downstream viewpoint.

Time = 0.3 second

Time = 0.4 second

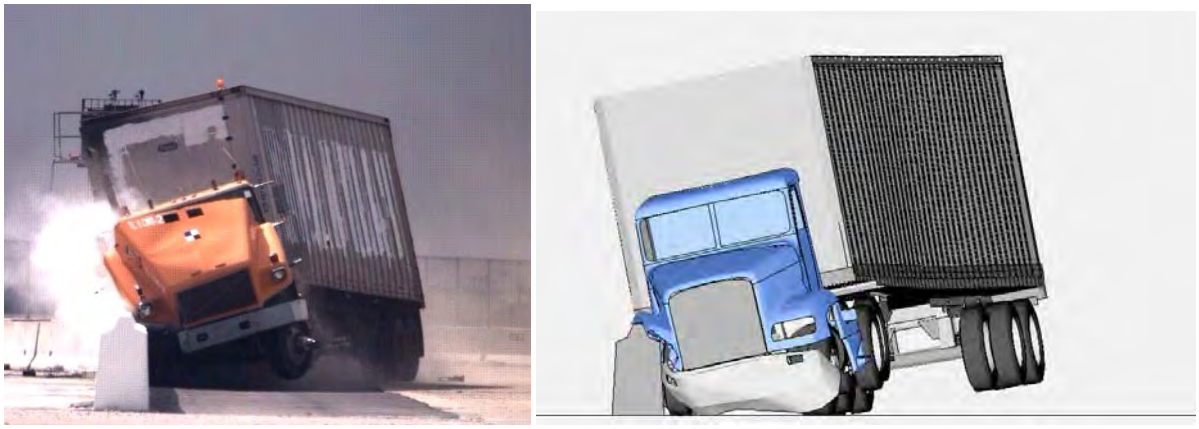

Time = 0.5 second

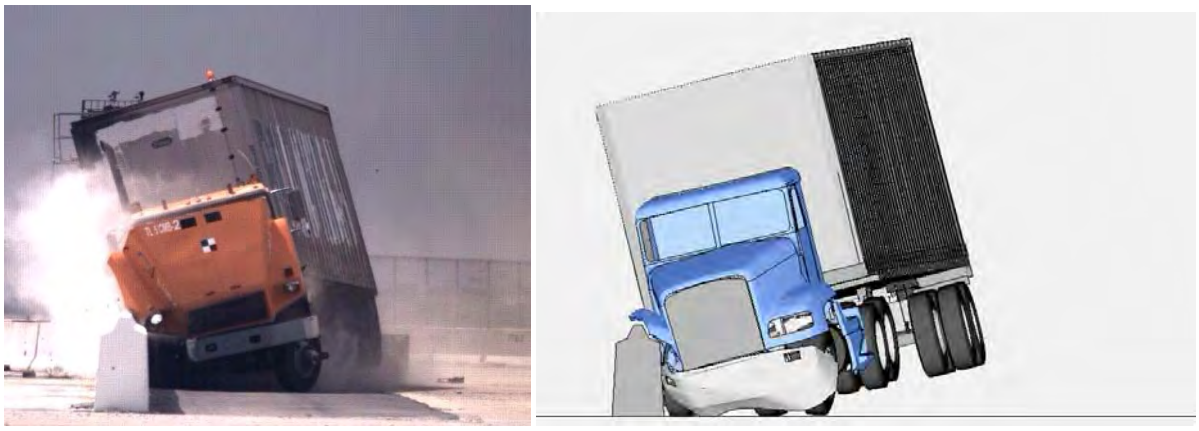

Figure 98. [CONTINUED] Photograph / Illustration. Sequential views of MwRSF Test TL5CMB-2 and FE model simulation from a downstream viewpoint.

Time = 0.6 second

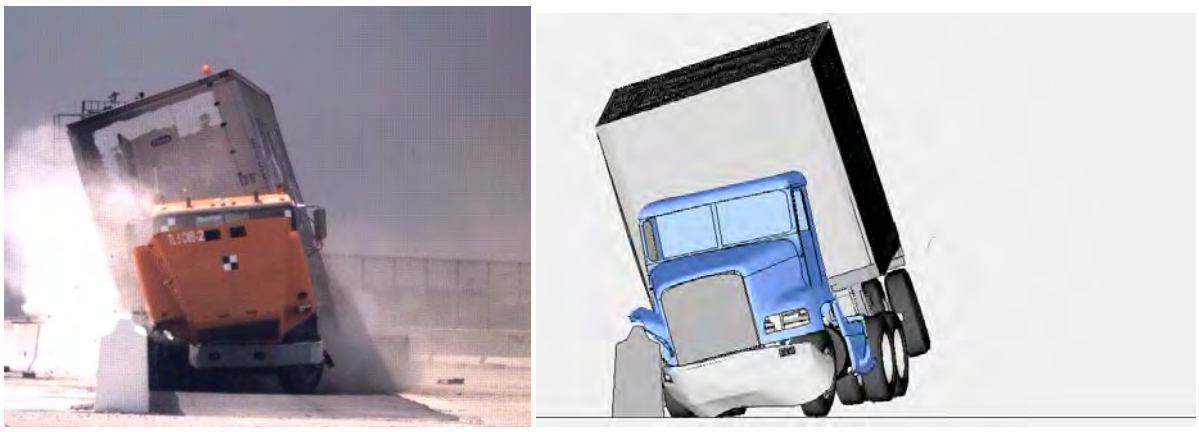

Time = 0.7 second

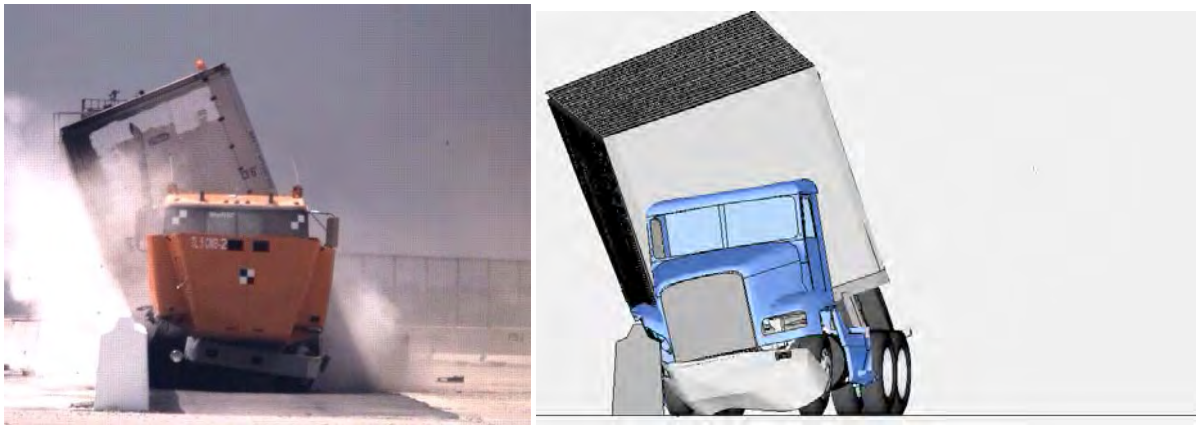

Time = 0.8 second

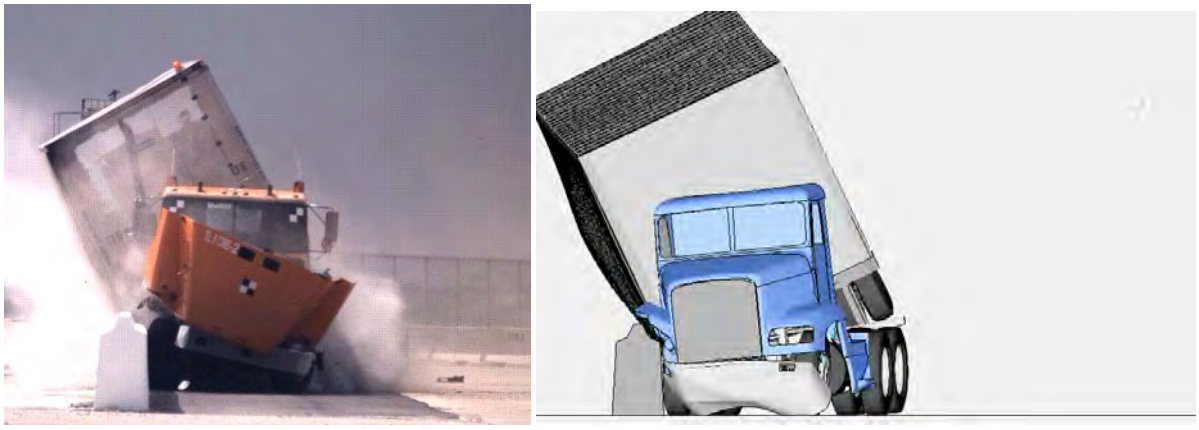

Figure 98. [CONTINUED] Photograph / Illustration. Sequential views of MwRSF Test TL5CMB-2 and FE model simulation from a downstream viewpoint.

Time = 0.9 second

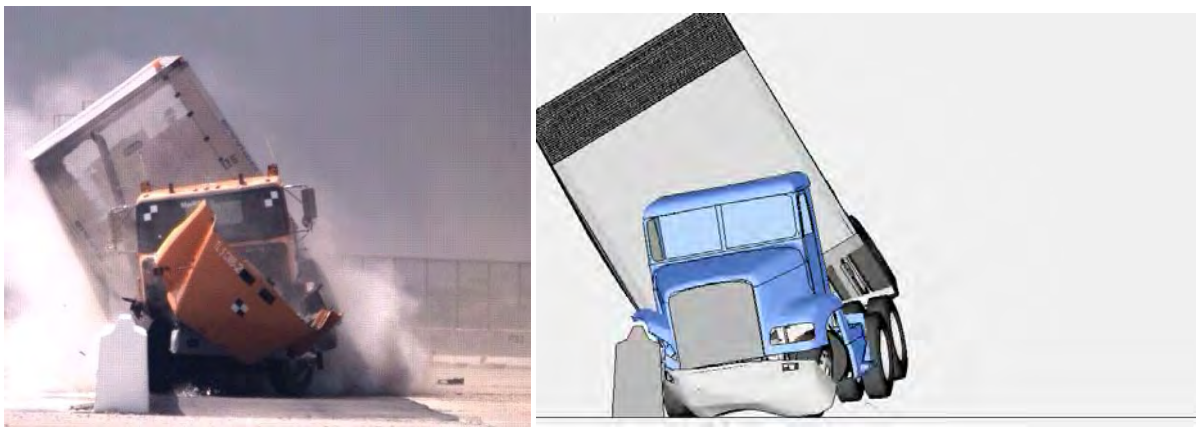

Time = 1.0 second

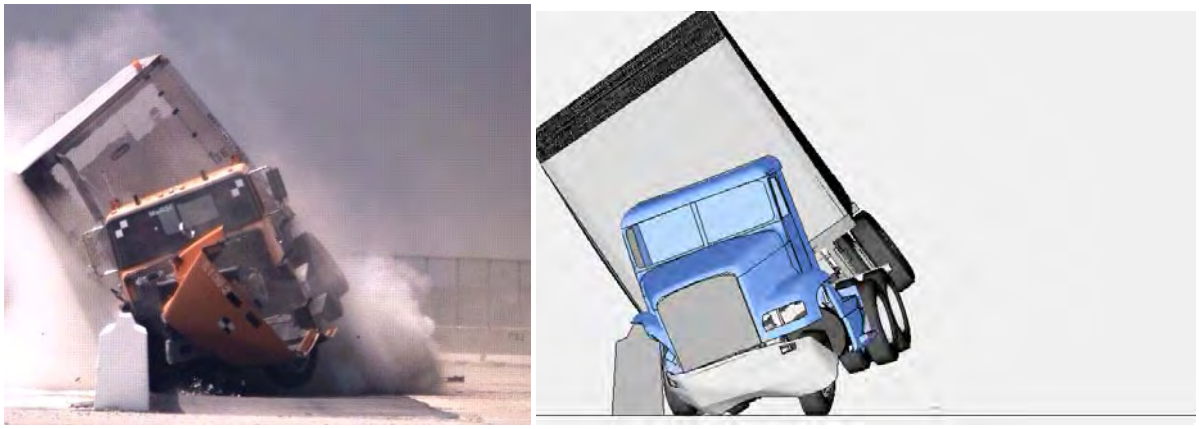

Time = 1.1 second

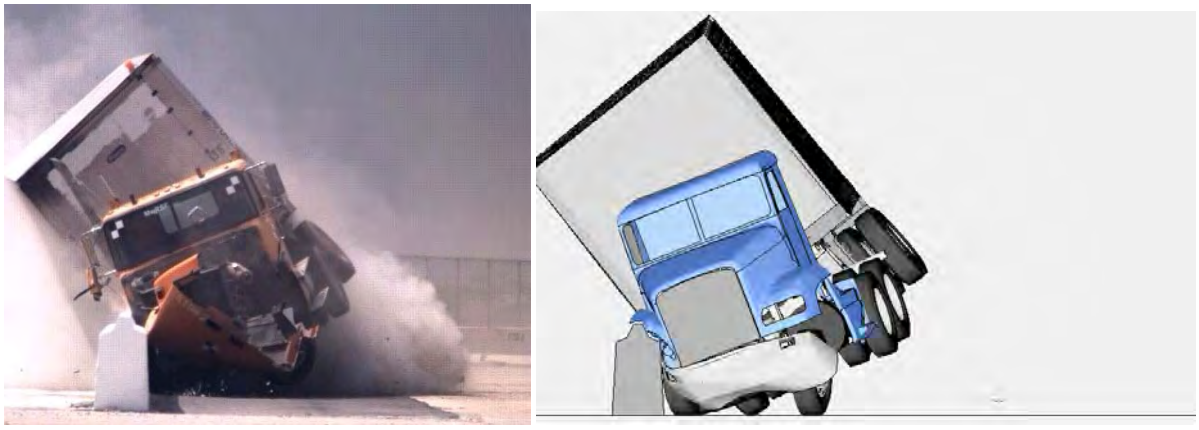

Figure 98. [CONTINUED] Photograph / Illustration. Sequential views of MwRSF Test TL5CMB-2 and FE model simulation from a downstream viewpoint.

Time = 1.2 second

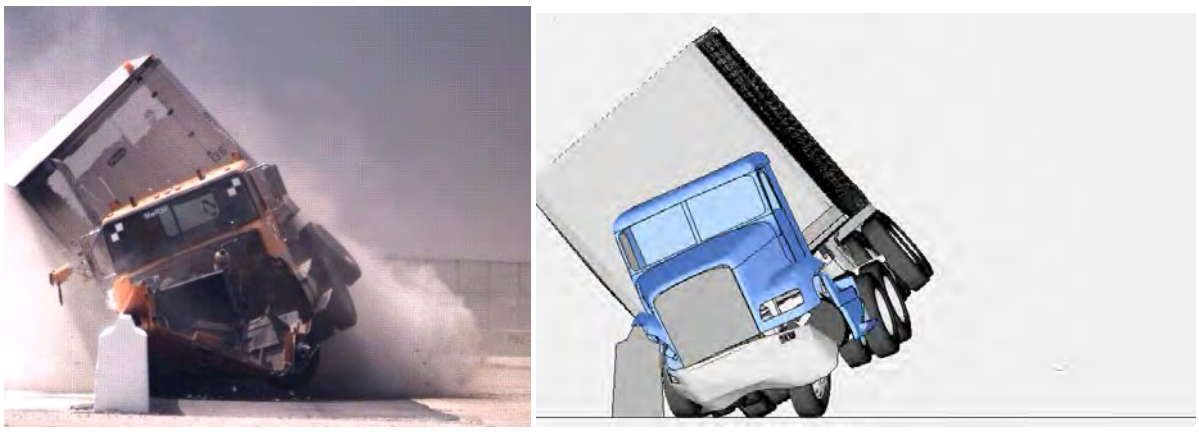

Time = 1.3 second

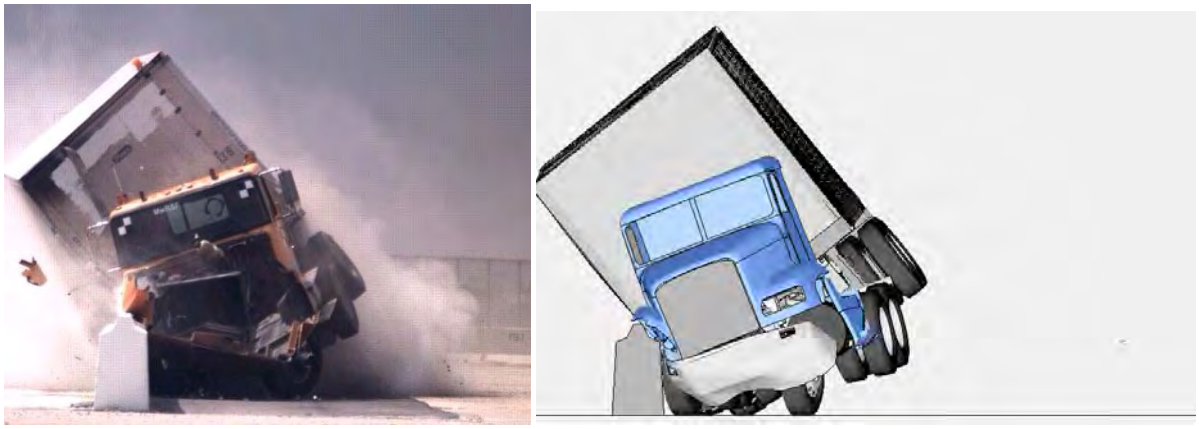

Time = 1.4 second

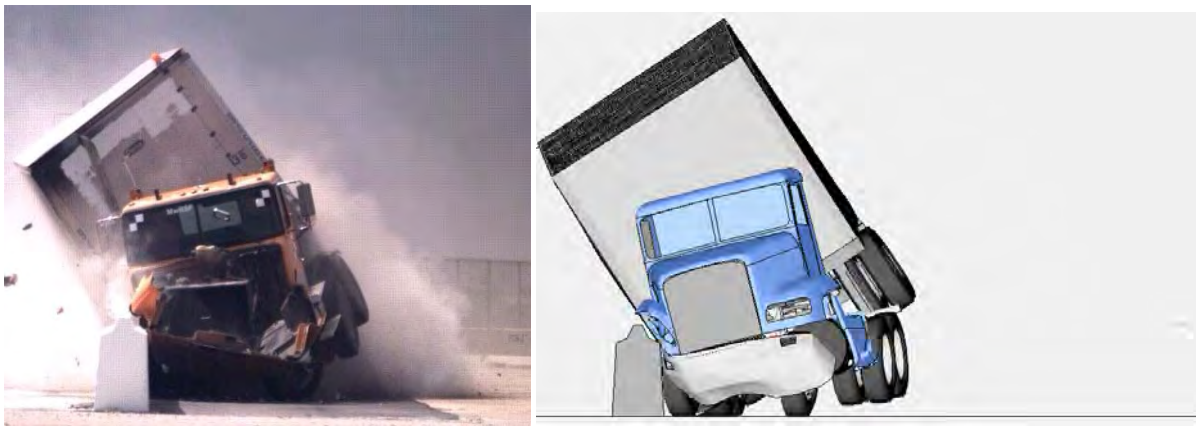

Figure 98. [CONTINUED] Photograph / Illustration. Sequential views of MwRSF Test TL5CMB-2 and FE model simulation from a downstream viewpoint.

Time = 1.5 second

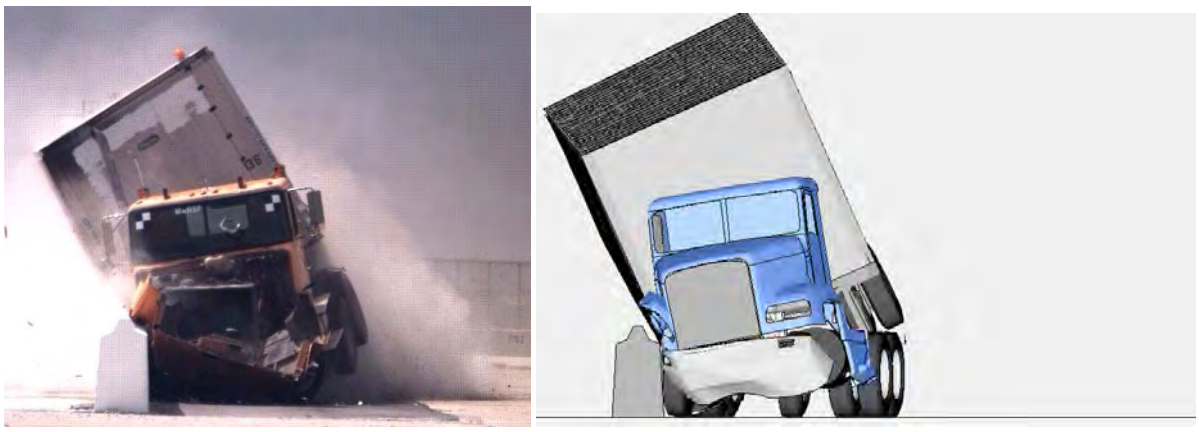

Time = 1.6 second

Time = 1.7 second

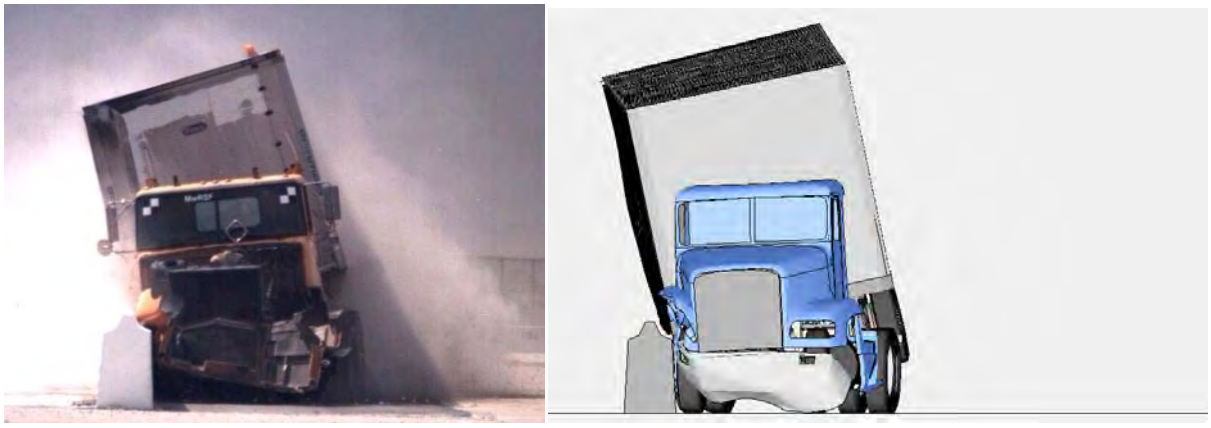

Figure 98. [CONTINUED] Photograph / Illustration. Sequential views of MwRSF Test TL5CMB-2 and FE model simulation from a downstream viewpoint.

Time = 0.000

Time = 0.1 second

Time = 0.2 second

Figure 99. Photograph / Illustration. Sequential views of MwRSF Test TL5CMB-2 and FE model simulation from an upstream viewpoint.

Time = 0.3 second

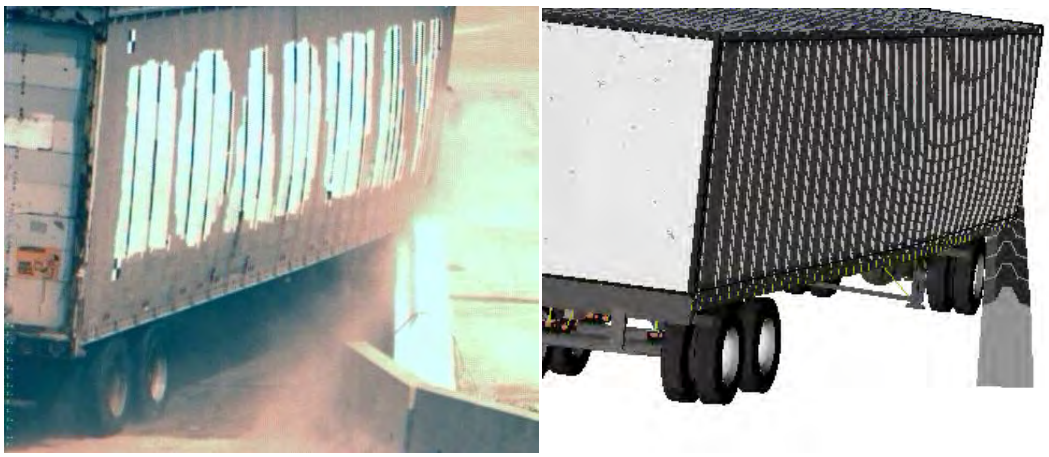

Time = 0.4 second

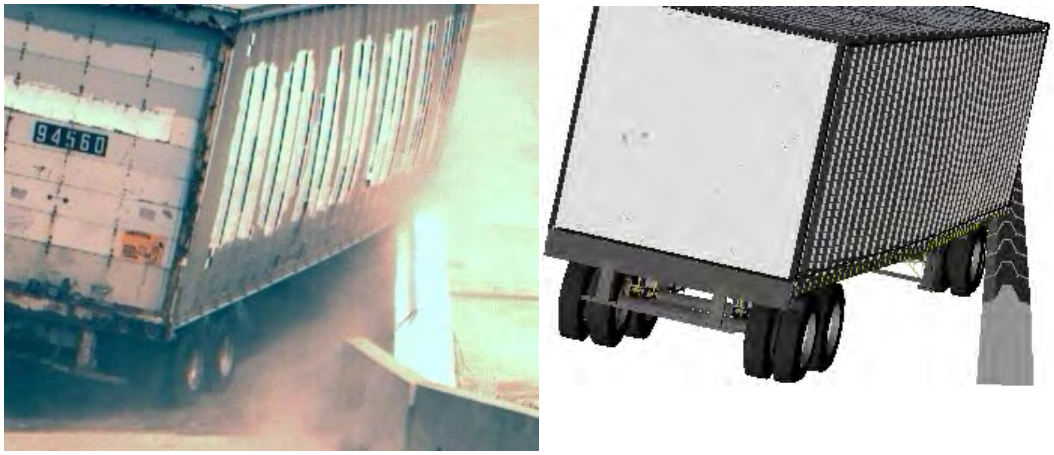

Time = 0.5 second

Figure 99. [CONTINUED] Photograph / Illustration. Sequential views of MwRSF Test TL5CMB-2 and FE Model simulation from an upstream viewpoint.

Time = 0.6 second

Time = 0.7 second

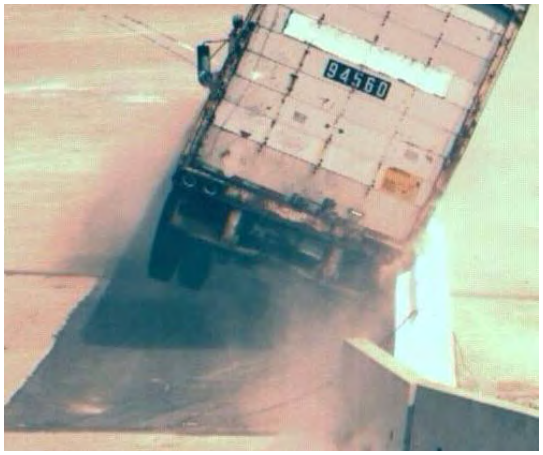

Time = 0.8 second

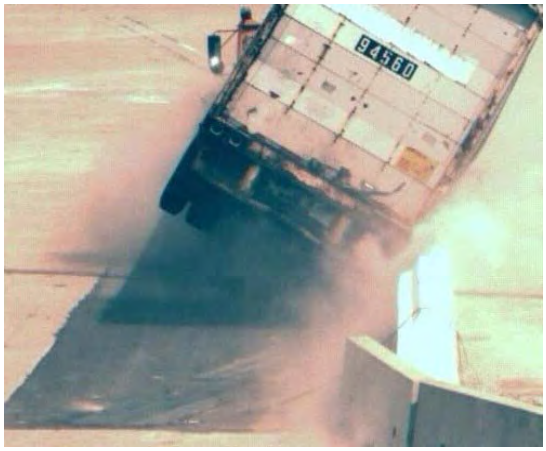

Figure 99. [CONTINUED] Photograph / Illustration. Sequential views of MwRSF Test TL5CMB-2 and FE Model simulation from an upstream viewpoint.

Time = 0.9 second

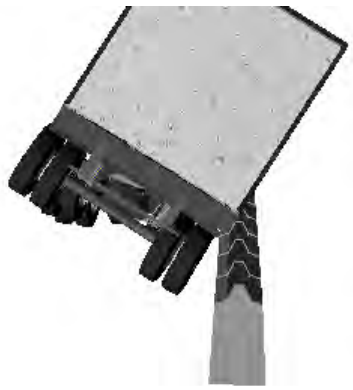

Time = 1.0 second

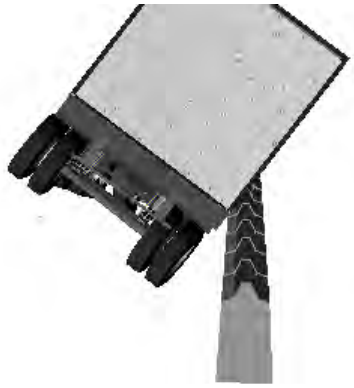

Time = 1.1 second

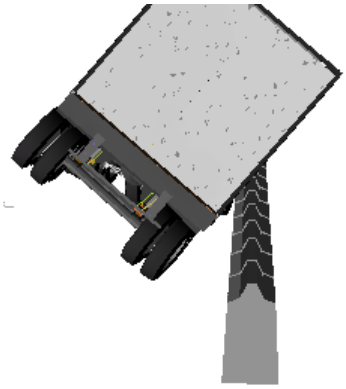

Figure 99. [CONTINUED] Photograph / Illustration. Sequential views of MwRSF Test TL5CMB-2 and FE Model simulation from an upstream viewpoint.

Time = 1.2 second

Time = 1.3 second

Time = 1.4 second

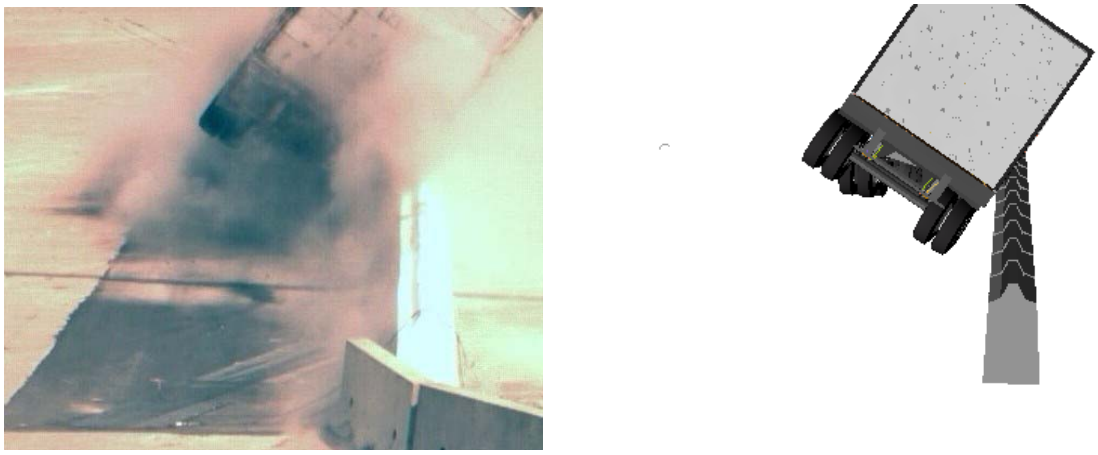

Figure 99. [CONTINUED] Photograph / Illustration. Sequential views of MwRSF Test TL5CMB-2 and FE Model simulation from an upstream viewpoint.

Time = 1.5 second

Time = 1.6 second

Time = 1.7 second

Figure 99. [CONTINUED] Photograph / Illustration. Sequential views of MwRSF Test TL5CMB-2 and FE Model simulation from an upstream viewpoint.

Time = 0.000

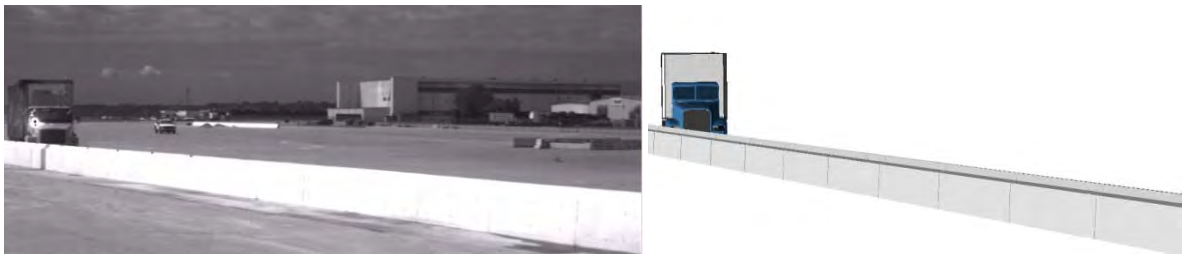

Time = 0.1 second

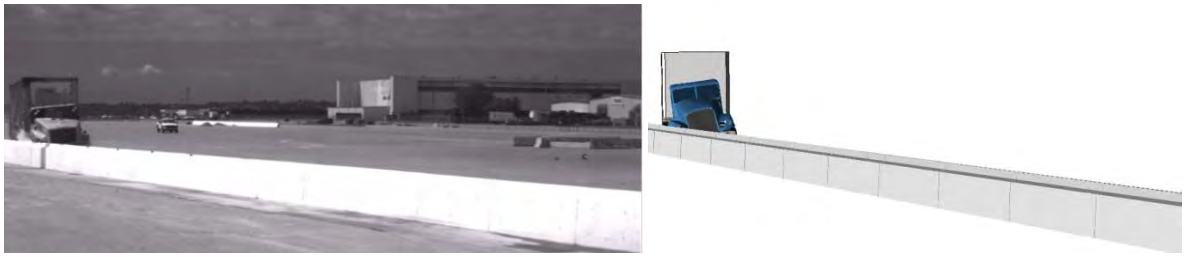

Time = 0.2 second

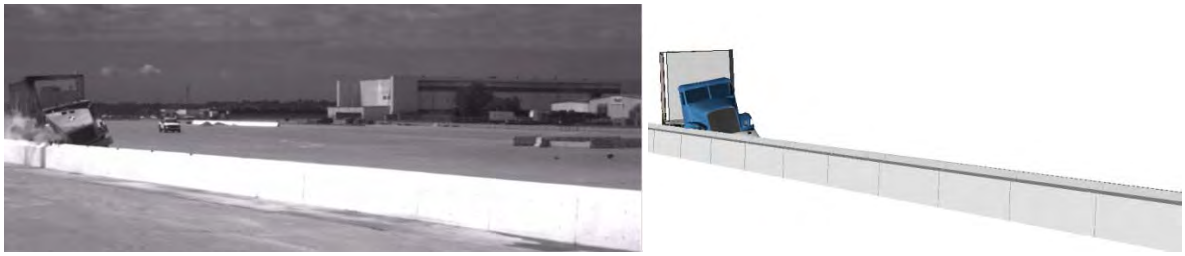

Time = 0.3 second

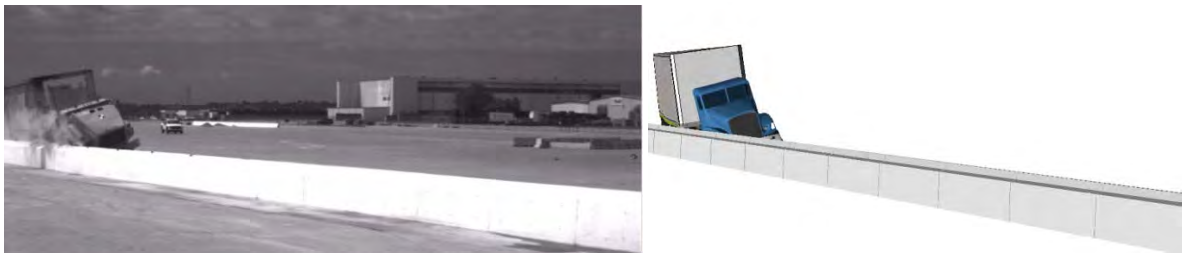

Time = 0.4 second

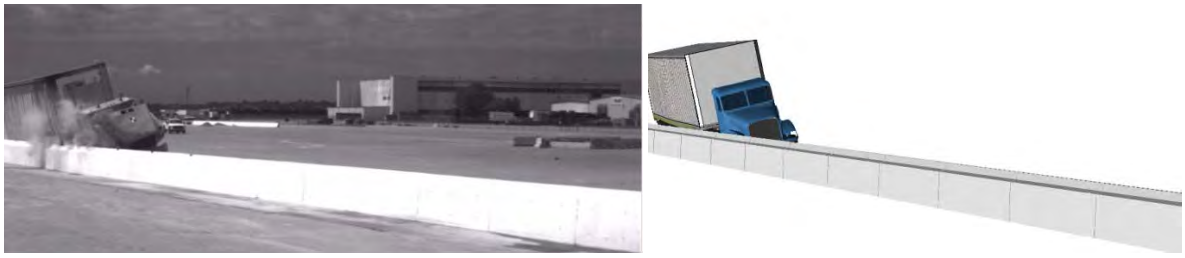

Figure 100. Photograph / Illustration. Sequential views of MwRSF Test TL5CMB-2 and FE model simulation from an isometric viewpoint.

Time = 0.5 second

Time = 0.6 second

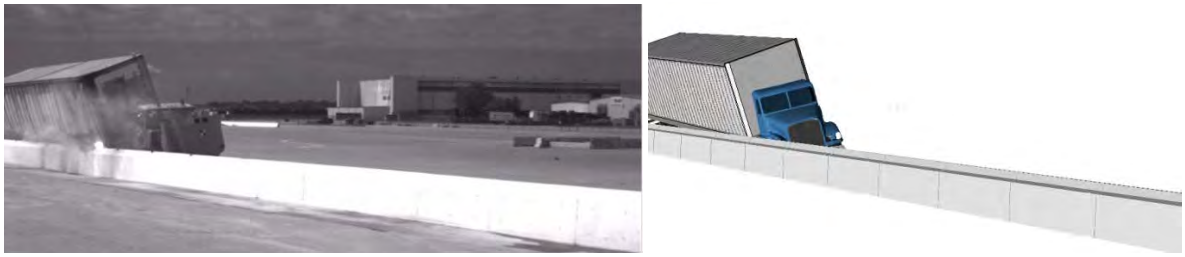

Time = 0.7 second

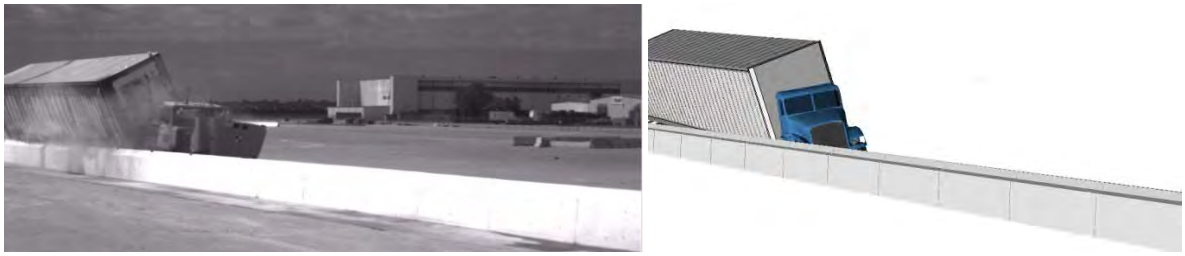

Time = 0.8 second

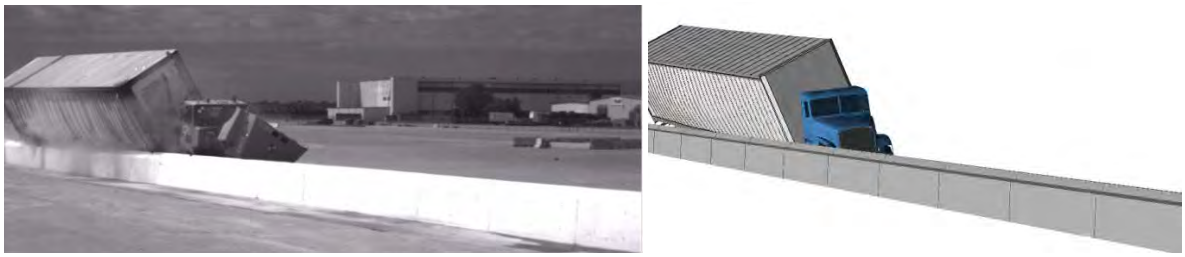

Time = 0.9 second

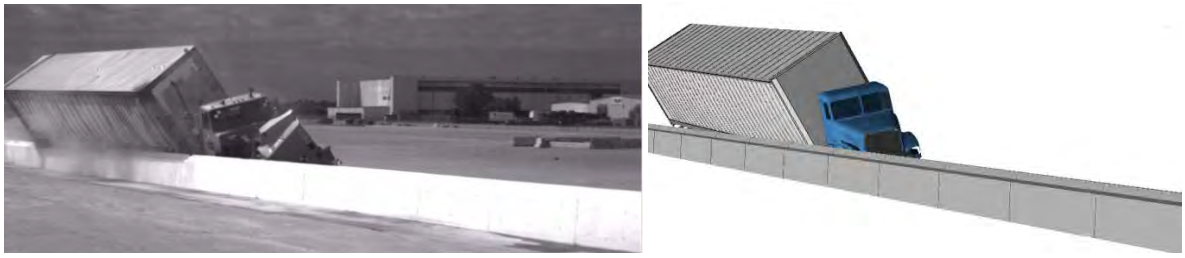

Figure 100. [CONTINUED] Photograph / Illustration. Sequential views of MwRSF Test TL5CMB-2 and FE model simulation from an isometric viewpoint.

Time = 1.0 second

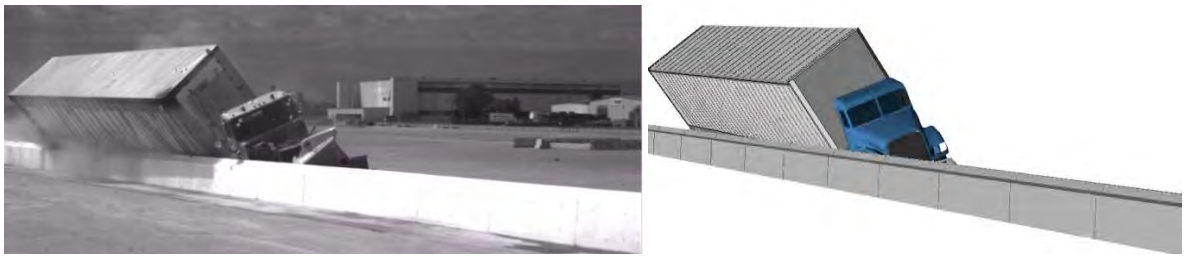

Time = 1.1 second

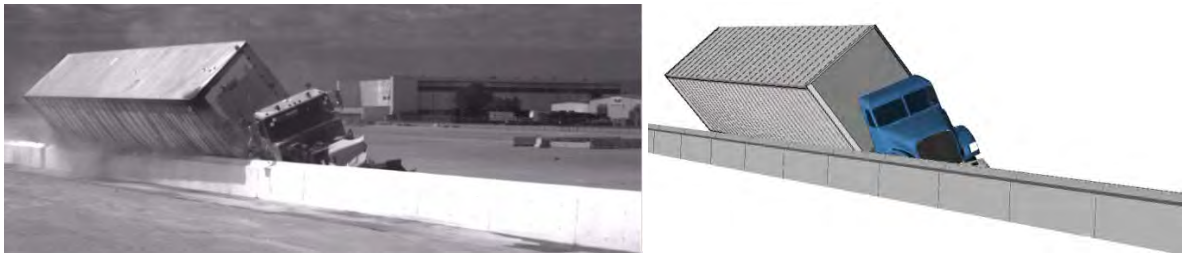

Time = 1.2 second

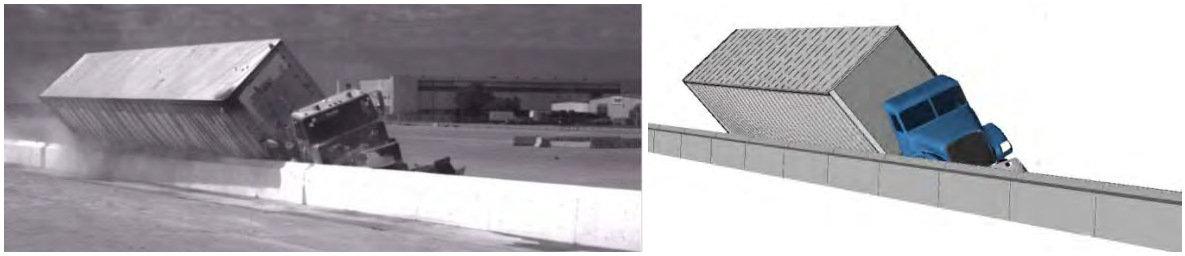

Time = 1.3 second

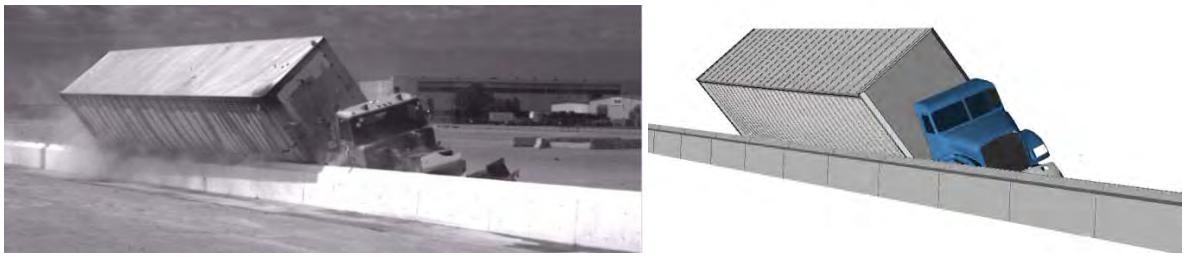

Time = 1.4 second

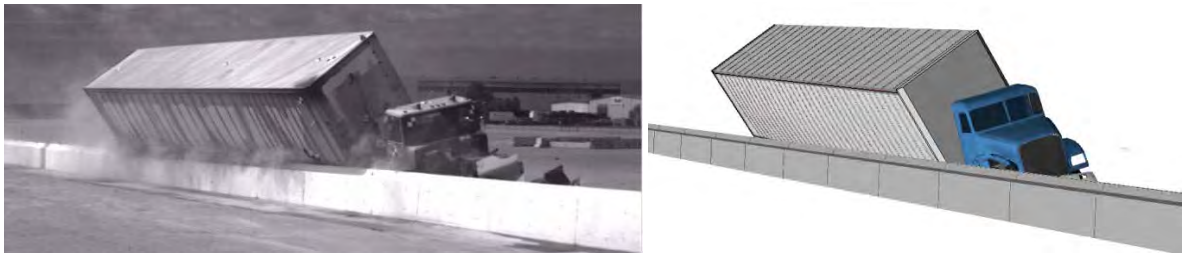

Figure 100. [CONTINUED] Photograph / Illustration. Sequential views of MwRSF Test TL5CMB-2 and FE model simulation from an isometric viewpoint.

Time = 1.5 second

Time = 1.6 second

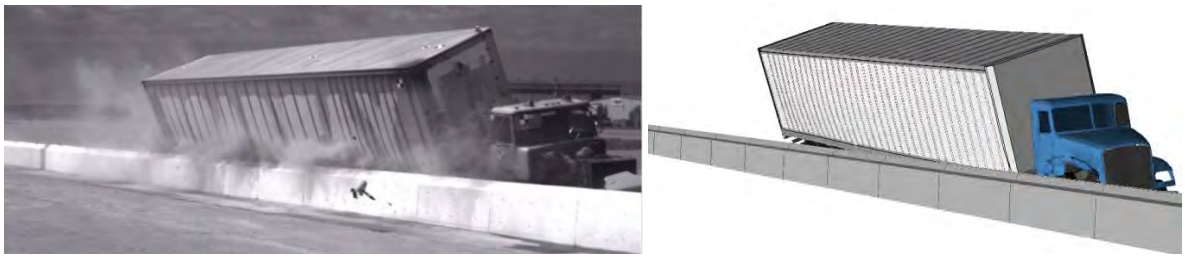

Time = 1.7 second

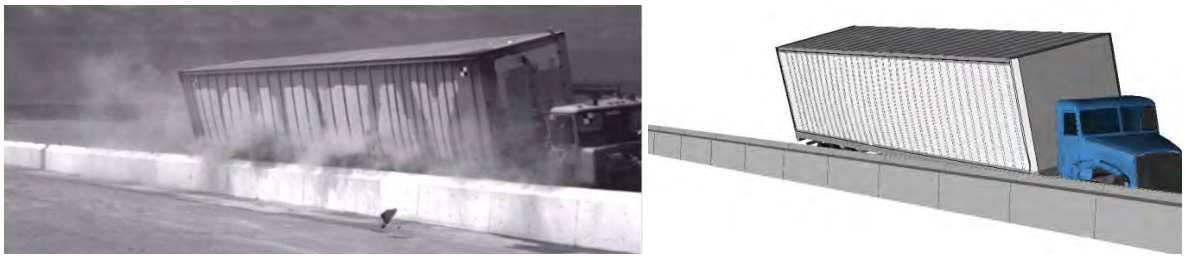

Figure 100. [CONTINUED] Photograph / Illustration. Sequential views of MwRSF Test TL5CMB-2 and FE model simulation from an isometric viewpoint.

Table 14. Summary of Phenomenological Events that Occurred during Full-scale Test and FE Model Simulation

Event	Test (TL5CMB-2) Time (seconds)	FE model Time (seconds)
Tractor begins to yaw	0.024	0.02 - 0.03
U-bolt connecting front axle to right-side leaf spring broke	unknown	0.09 – 0.1
Left-front tire lifts off pavement	0.144	0.10 - 0.11
Right-front corner of trailer contacted the top protrusion of the barrier	0.186	0.17 - 0.18
Trailer started to roll toward the barrier	0.190	0.19 - 0.200
Left-rear tires were lifted off the ground	0.2	0.21 - 0.22
The right front corner of the trailer was vertically coincident with the back face of the barrier	0.260	0.26 - 0.27
Both left-rear trailer tires were lifted off the ground	0.356	0.25 - 0.26
Tractor was parallel to barrier	0.394	0.32 - 0.33
Tractor reached peak roll and began to roll back from the barrier	0.290 – 0.364 (≈15 deg.)	0.29 - 0.30 (14.6 deg.)
Left-front tractor tires returned to roadway surface	0.468	0.34 - 0.35
U-bolt connecting front axle to left-side leaf spring broke	unknown	0.34 - 0.35
Trailer was parallel to barrier	0.648	0.63 - 0.64
Tractor rolled back to level position	0.650	0.74 - 0.75
Rear trailer tandem contacts barrier	0.656	0.65 - 0.66
Time of maximum impact force between trailer tandem and barrier	0.72	0.71 - 0.72
Tractor started to roll toward the barrier	0.776	0.80 - 0.81
Tractor left-front tire again lifted from the roadway	0.956	N/A (u-bolts broken)
Trailer reached maximum roll and began to roll back from the barrier All left side tires were off the ground	1.150 (≈42 deg.)	1.19 - 1.20 (42.8 deg.)
Tractor again reached peak (maximum) roll angle	0.994 (≈19 deg.)	1.16 - 1.17 (23.8 deg.)
Left-front tire returned to the roadway surface	1.294	N/A
Tractor left side tandems returned to roadway surface	1.652	1.52 - 1.53
Analysis Terminated		1.67
Trailer left side tires returned to roadway surface	1.800	-

Comparison of Time-History Data

The tractor-semitrailer FE model was instrumented with 16 accelerometers with 3 accelerometers positioned at locations consistent with typical accelerometer placement in full-scale crash tests. In particular:

- Accelerometer 14 was placed near the center of gravity of the tractor inside the tractor cabin on the cabin floor (e.g., tractor cabin position in full-scale crash test summary section)
- Accelerometer 15 was placed near the fifth-wheel on the cross-beam support for the frame rails at 0.225 m aft of the kingpin (e.g., tractor fifth-wheel position in full-scale crash test summary section).
- Accelerometer 16 was placed near the center of the trailer tandem axle inside the trailer box on the floor (e.g., trailer tandem position in full-scale crash test summary section).

The locations of these accelerometers are shown schematically in Figure 101.

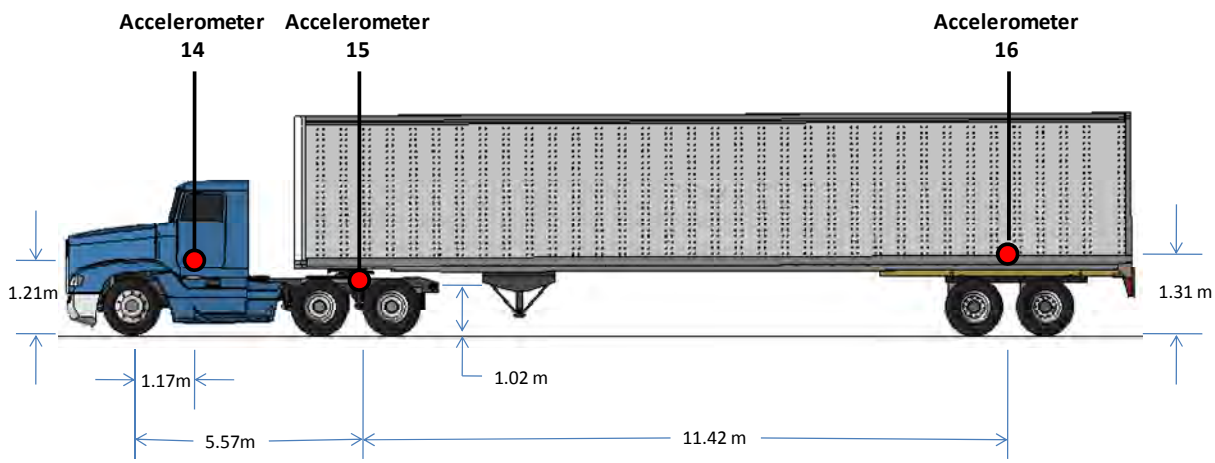

Figure 101. Illustration. Pertinent accelerometer locations in the FE model.

Figures 102, 103, and 104 show the longitudinal, transverse, and vertical acceleration-time histories, respectively, computed from accelerometer 14 located inside the tractor cabin. Figure 105 shows the ASI-time history, and Figure 106 shows the ASI-time history computed using only the longitudinal and transverse channels of acceleration (consistent with the method used to compute the ASI values in the full-scale crash test summary section of this report). Figure 107 shows the roll, pitch, and yaw angles computed at the accelerometer 14 location.

Figures 108, 109, and 110 show the longitudinal, transverse, and vertical acceleration-time histories, respectively, computed from accelerometer 15 located at the tractor fifth-wheel. Figure 111 shows the ASI-time history, and Figure 112 shows the ASI-time history computed

using only the longitudinal and transverse channels of acceleration. Figure 113 shows the roll, pitch, and yaw angles computed at the accelerometer 15 location.

Figures 114, 115 and 116 show the longitudinal, transverse, and vertical acceleration-time histories, respectively, computed from accelerometer 16 located at the trailer tandem axle. Figure 117 shows the ASI-time history, and Figure 118 shows the ASI-time history computed using only the longitudinal and transverse channels of acceleration. Figure 119 shows the roll, pitch, and yaw angles computed at the accelerometer 16 location.

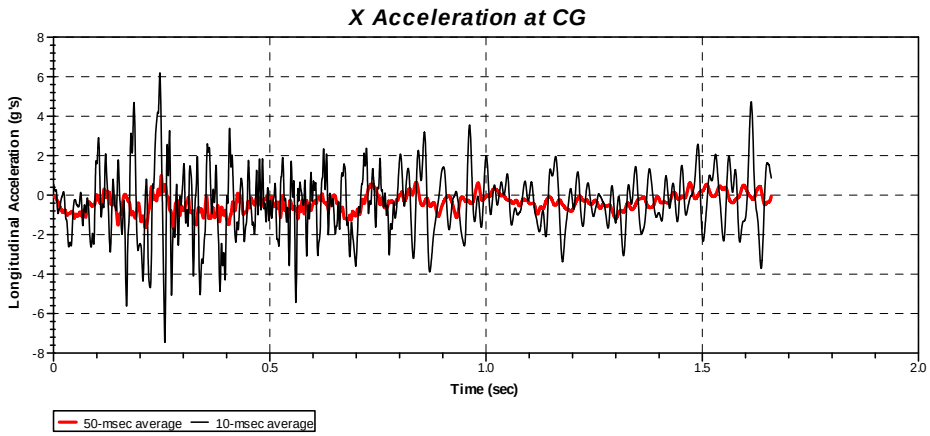

Figure 102. Chart. Longitudinal acceleration-time history plot from *accelerometer 14* inside the tractor cabin (10-millisecond and 50-millisecond moving averages).

Figure 103. Chart. Transverse acceleration-time history plot from *accelerometer 14* inside the tractor cabin (10-millisecond and 50-millisecond moving averages).

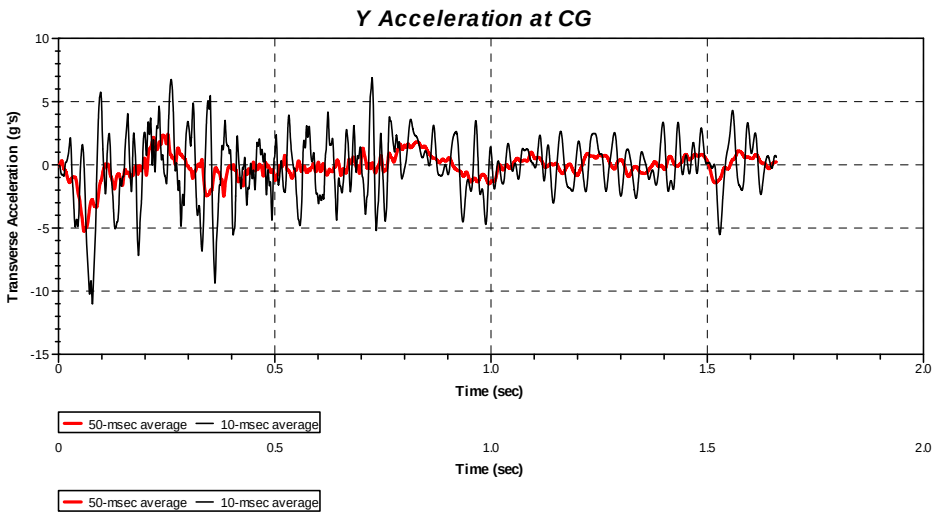

Figure 104. Chart. Transverse acceleration-time history plot from *accelerometer 14* inside the tractor cabin (10-millisecond and 50-millisecond moving averages).

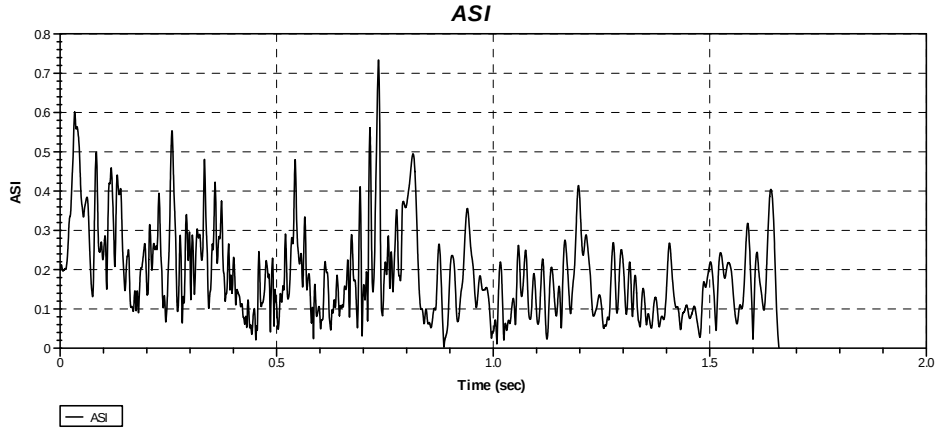

Figure 105. Chart. ASI-time history plot from *accelerometer 14* inside the tractor cabin.

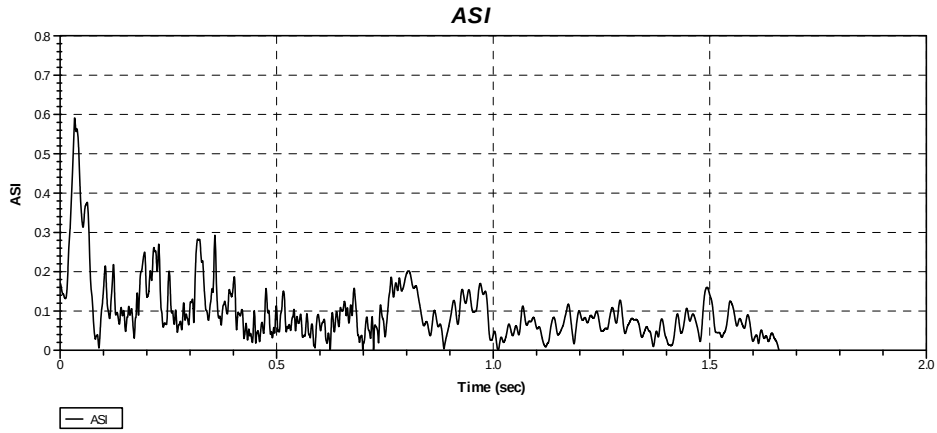

Figure 106. Chart. ASI-time history plot (excluding z-acceleration data) from *accelerometer 14* inside the tractor cabin.

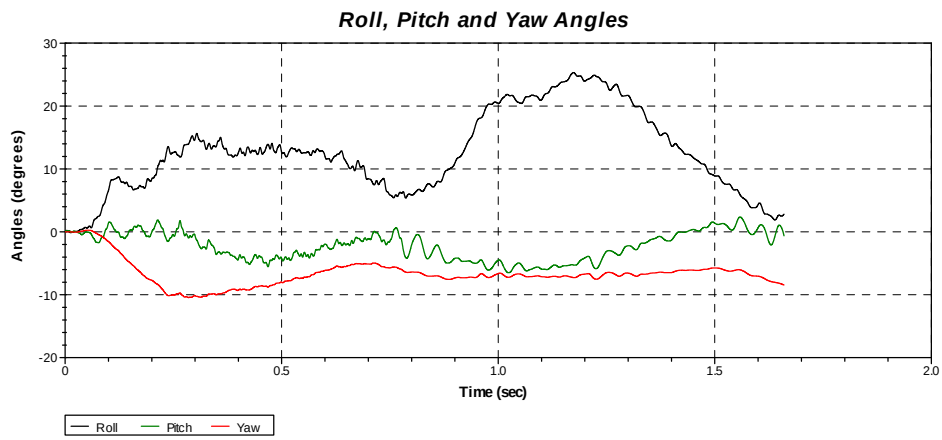

Figure 107. Chart. Roll, pitch and yaw-time history plot from *accelerometer 14* location inside the tractor cabin.

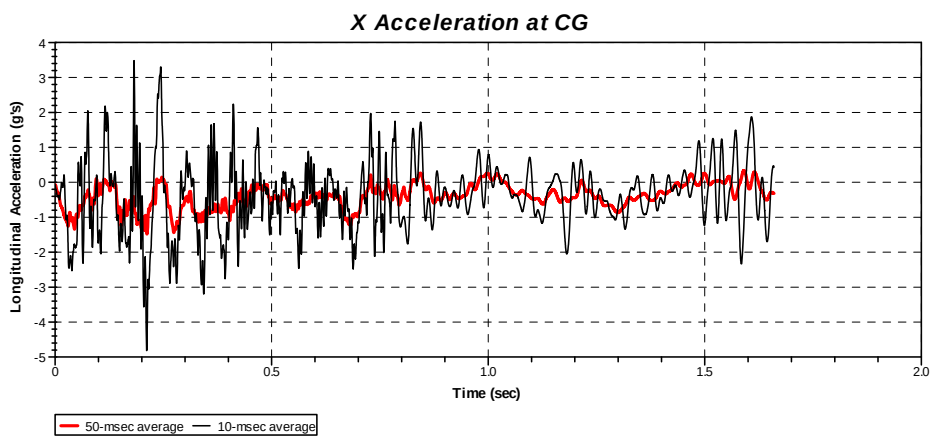

Figure 108. Chart. Longitudinal acceleration-time history plot from *accelerometer 15* near the tractor fifth-wheel (10-millisecond and 50-millisecond moving averages).

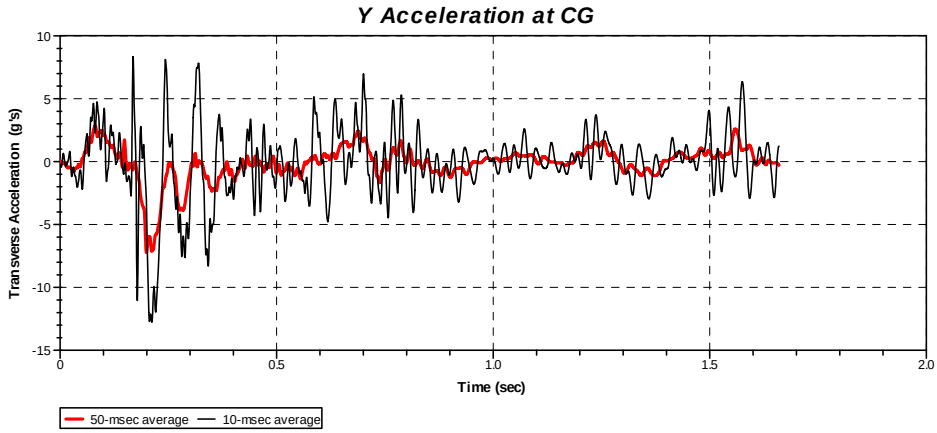

Figure 109. Chart. Transverse acceleration-time history plot from *accelerometer 15* near the tractor fifth-wheel (10-millisecond and 50-millisecond moving averages).

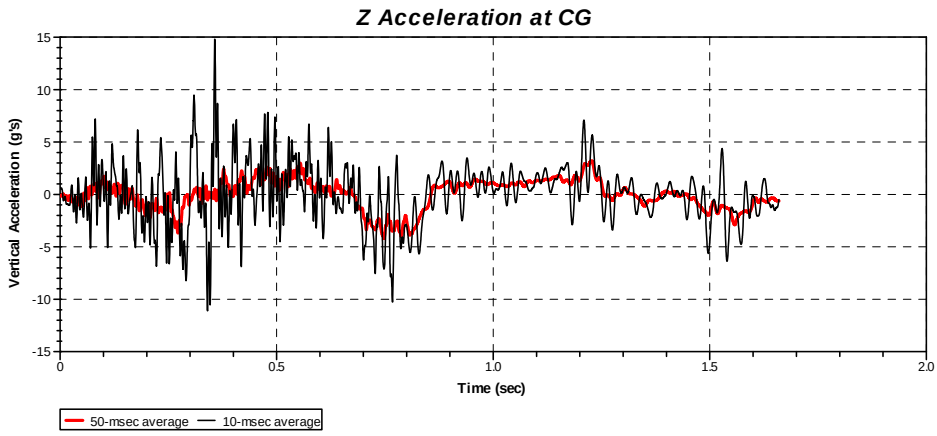

Figure 110. Chart. Transverse acceleration-time history plot from *accelerometer 15* near the tractor fifth-wheel (10-millisecond and 50-millisecond moving averages).

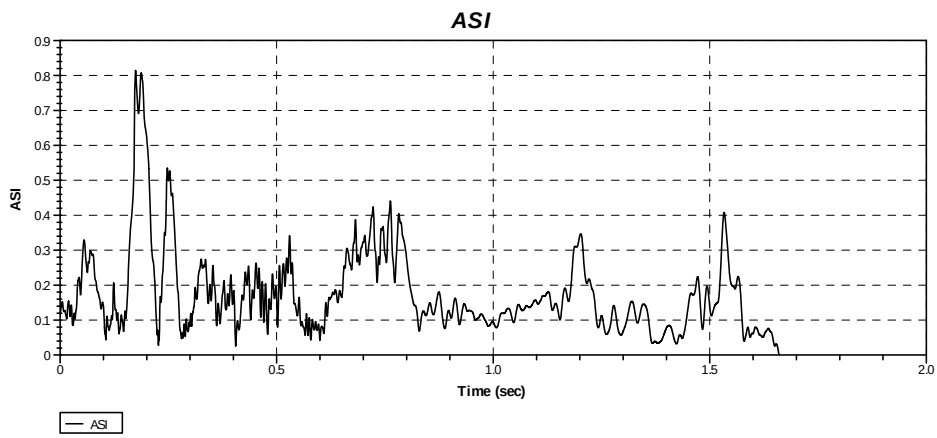

Figure 111. Chart. ASI-time history plot from *accelerometer 15* near the tractor fifth-wheel.

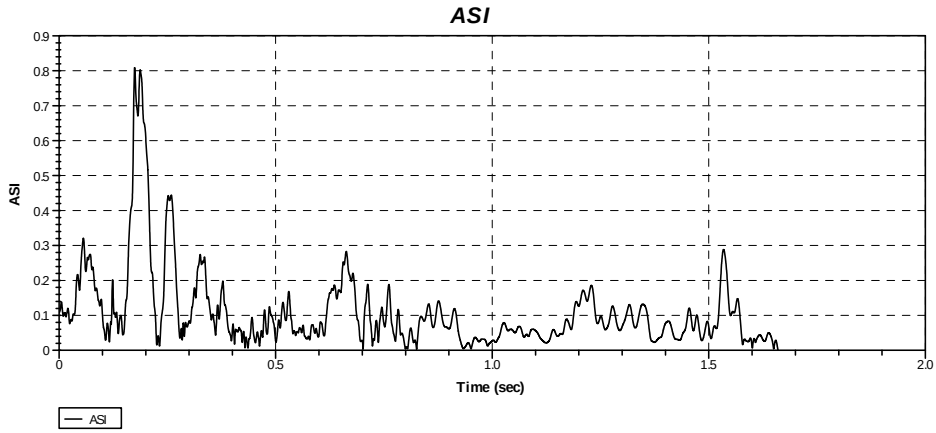

Figure 112. Chart. ASI-time history plot (excluding z-acceleration data) from *accelerometer 15* near the tractor fifth-wheel.

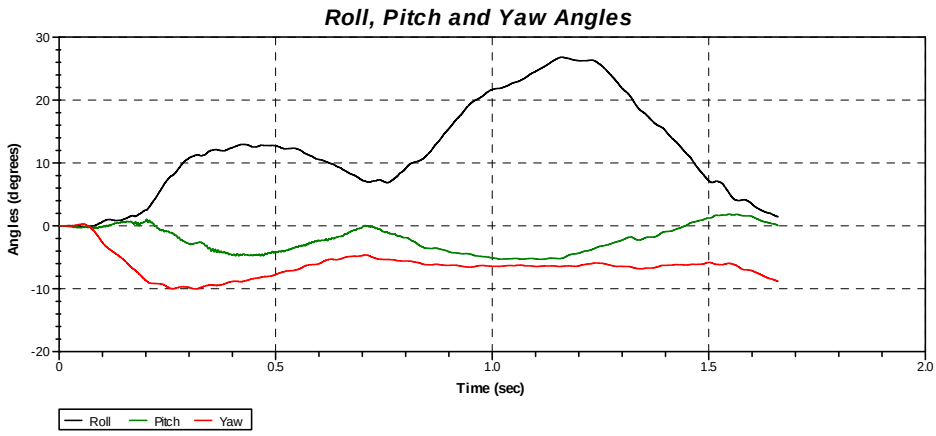

Figure 113. Chart. Roll, pitch and yaw-time history plot from *accelerometer 15* near the tractor fifth-wheel.

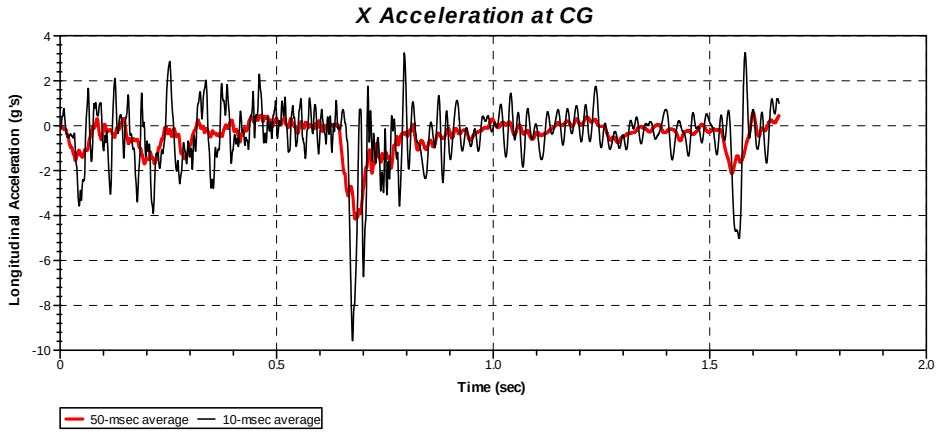

Figure 114. Chart. Longitudinal acceleration-time history plot from *accelerometer 15* near the tractor fifth-wheel (10-millisecond and 50-millisecond moving averages).

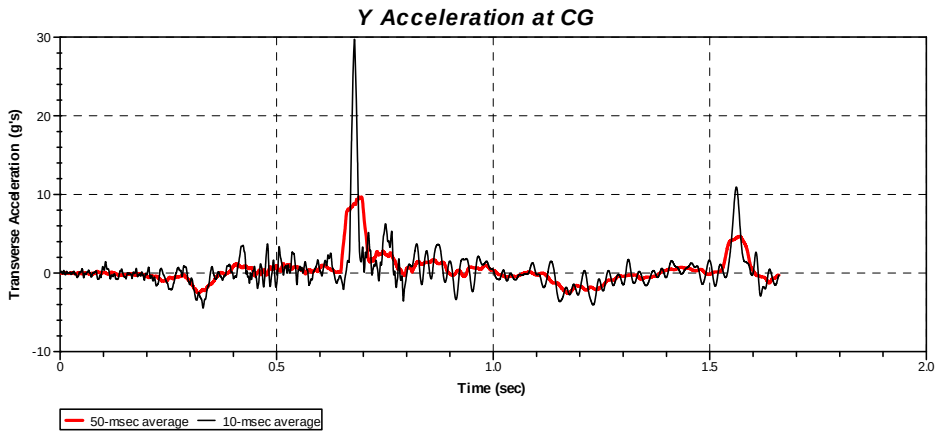

Figure 115. Chart. Transverse acceleration-time history plot from *accelerometer 15* near the tractor fifth-wheel (10-millisecond and 50-millisecond moving averages).

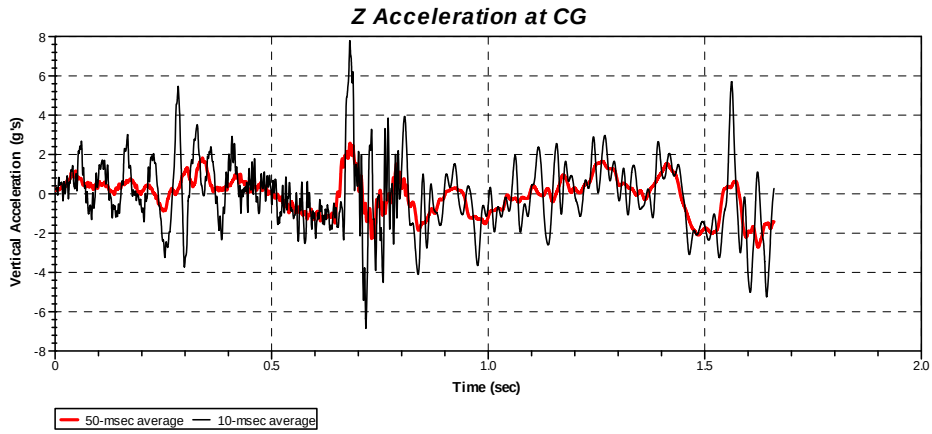

Figure 116. Chart. Transverse acceleration-time history plot from *accelerometer 15* near the tractor fifth-wheel (10-millisecond and 50-millisecond moving averages).

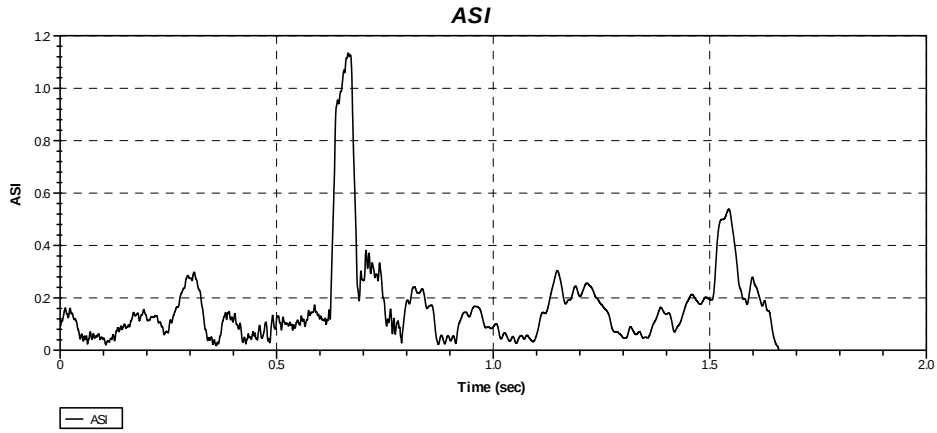

Figure 117. Chart. ASI-time history plot from *accelerometer 15* near the tractor fifth-wheel.

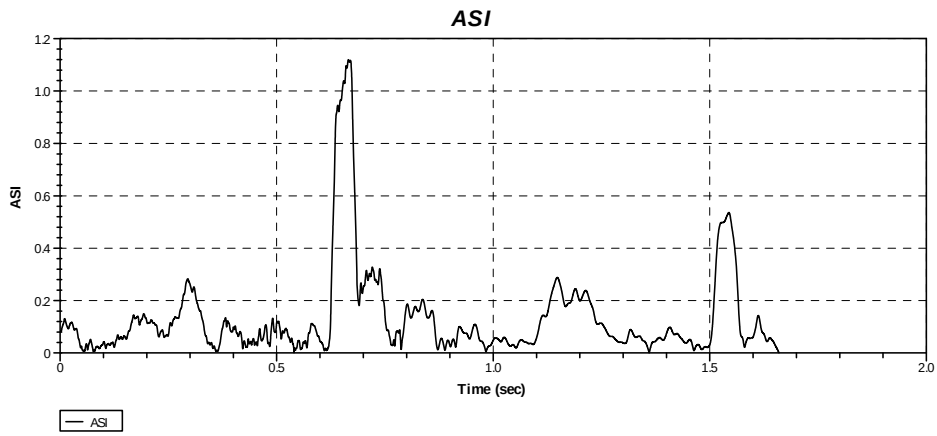

Figure 118. Chart. ASI-time history plot (excluding z-acceleration data) from *accelerometer 15* near the tractor fifth-wheel.

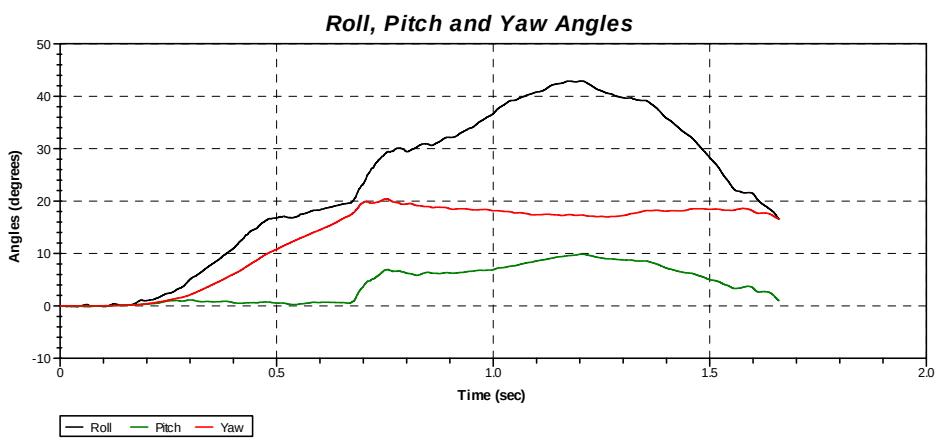

Figure 119. Chart. Roll, pitch and yaw-time history plot from *accelerometer 15* near the tractor fifth-wheel.

Figures 120, 121 and 122 show the 50-millisecond moving average of the longitudinal, transverse, and vertical acceleration-time histories, respectively, comparing the FE analysis results with full-scale test, TL5CMB-2. Figure 123 shows a comparison of the ASI-time history between the FE analysis and full-scale test. Values of the quantitative evaluation metrics are also shown on the time-history plots in Figures 120 through 123. These metrics are discussed in more detail in the Quantitative Assessment later in this chapter.

Figure 121 shows the y-channel (lateral) acceleration at the trailer tandem location annotated with images from the analysis results to help understand the meaning of the peaks in acceleration at key points during the impact event. Each of these is described below:

- The first major peak in lateral acceleration occurred at 0.335 seconds after impact, and was coincident with the time of maximum compression of the right-side trailer suspension.
- The second major peak occurred at 0.72 seconds and corresponded to the maximum impact force between the trailer and the barrier.
- The third major peak occurred at 1.21 seconds as the trailer tandem wheel re-contacted the ground (after being lifted off when the trailer rolled over onto the barrier). When the tires contacted the ground, the trailer tires started to accelerate back toward the barrier as the trailer was rolling back toward level position.
- The fourth major peak occurred at 1.6 seconds and corresponded to a second impact between the trailer tandem and the barrier.

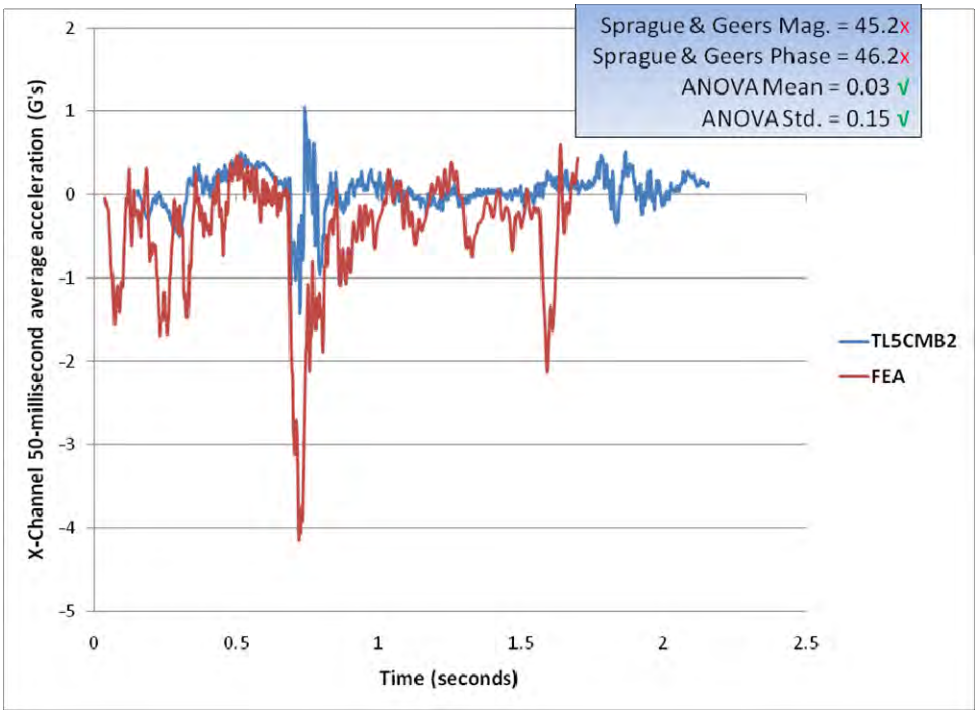

Figure 120. Chart. Longitudinal acceleration-time history plot from the FE simulation and Test TL5CMB-2 from accelerometer at the trailer tandem (50-millisecond moving averages).

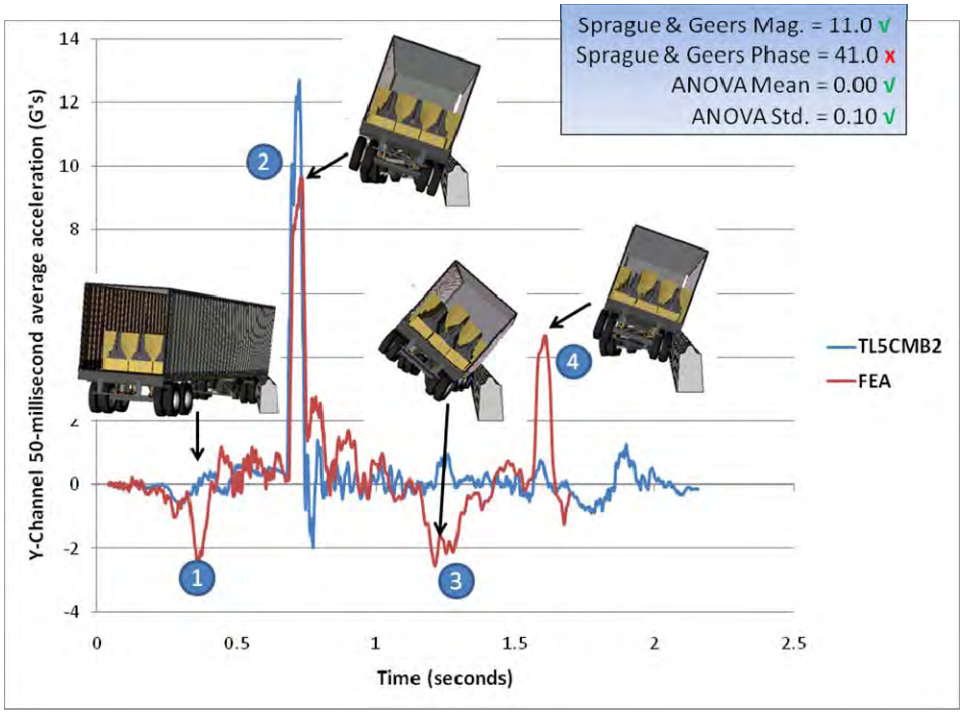

Figure 121. Chart. Lateral acceleration-time history plot from the FE simulation and Test TL5CMB-2 from accelerometer at the trailer tandem (50-millisecond moving averages).

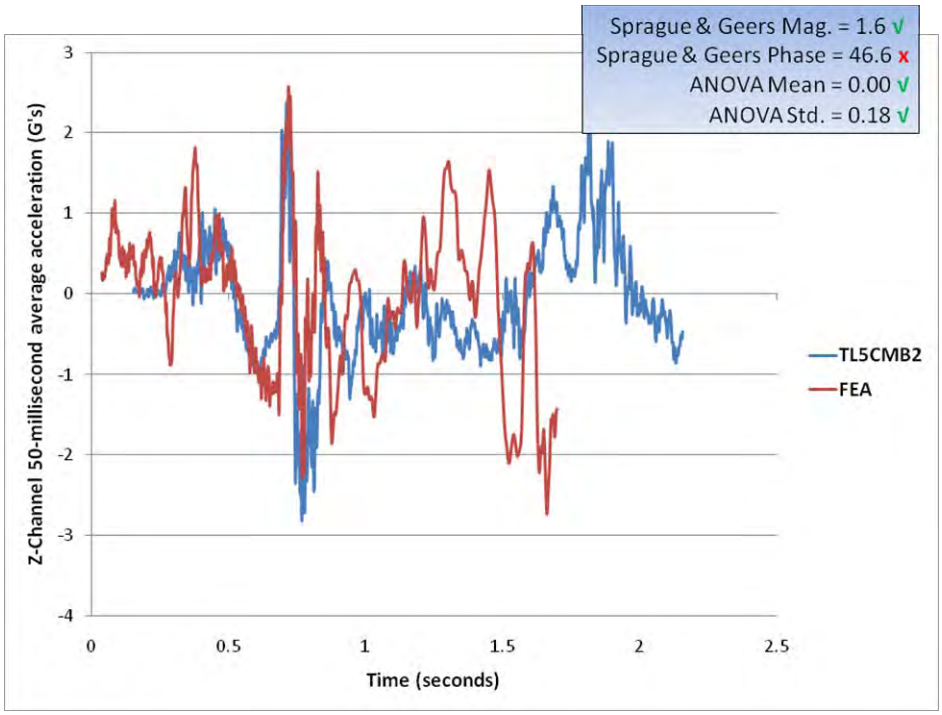

Figure 122. Chart. Vertical acceleration-time history plot from the FE simulation and Test TL5CMB-2 from accelerometer at the trailer tandem (50-millisecond moving averages).

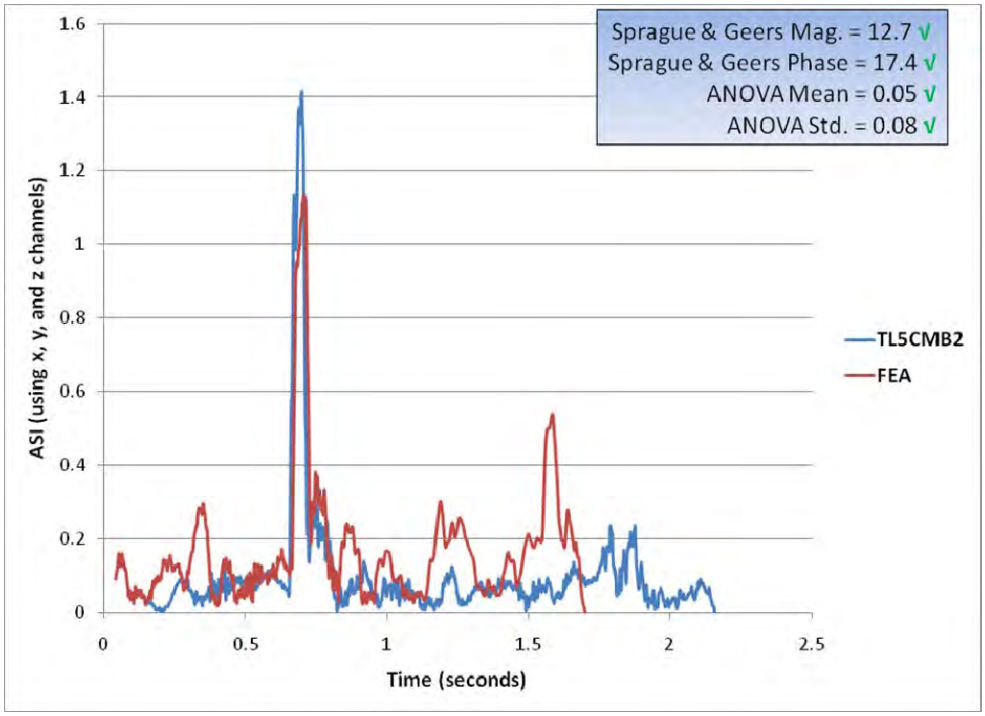

Figure 123. Chart. ASI-time history plot from the FE simulation and Test TL5CMB-2 from accelerometer at the trailer tandem.

Angular-rate data was not collected in test TL5CMB-2. However, the high-speed videos, TL-5 CMB-2 aos3.avi and TL-5 CMB-2 aos-4.avi, from the full-scale test were used to measure the approximate roll-time history of the trailer at time intervals of 0.2 seconds. The roll-time history of the trailer in the simulation compares very well to the roll-time history measured from the high-speed test video, regarding both timing and magnitude, as shown in Figure 124. The analysis terminated prematurely at 1.67 seconds of the impact event, but at the time of termination the simulation was showing approximately the same behavior (e.g., roll position and roll-rate) of the trailer as was measured from the test videos.

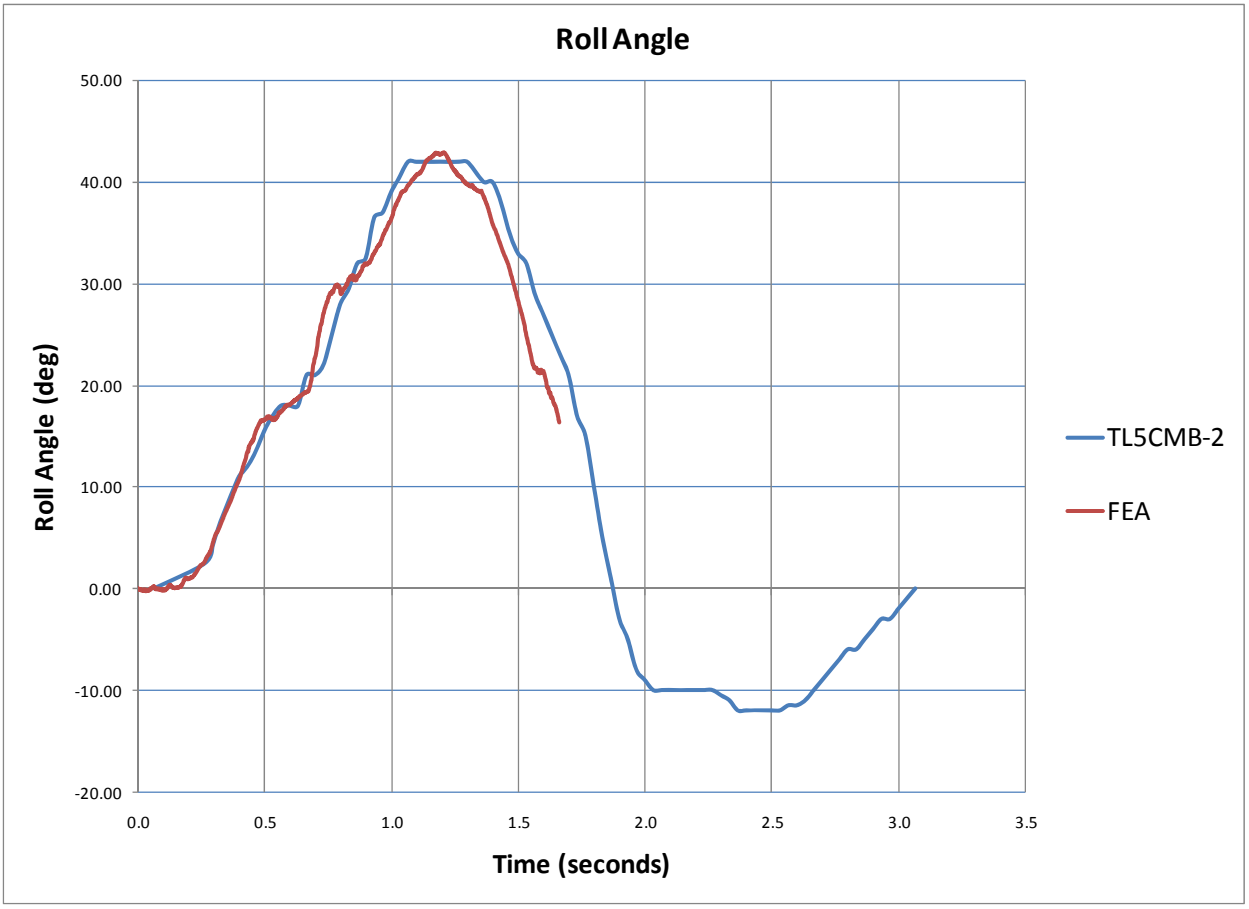

Figure 124. Chart. Roll angle-time history plot of the rear section of the trailer from the FE simulation and Test TL5CMB-2.

Test Vehicle Damage

The damage caused to the tractor during the impact could not be accurately assessed because of a major secondary impact that occurred after the vehicle exited the barrier system. Before the vehicle could be stopped, it impacted another barrier system at a high impact angle which caused further damage to the tractor, as shown in Figure 125.

Figure 125. Photograph. Post test view of test vehicle illustrating excessive damage after secondary impact.

The trailer had scrapes and gouges on its right side that were caused when the trailer rolled over onto the barrier. The scrapes started at the front of the trailer at 533 mm (21 inches) above the bottom and ran all the way down the trailer in a straight line to the back of the trailer to a point 229 mm (9 inches) above the bottom of the trailer. Many of the vertical "ribs" on the impact side of the trailer box were damaged. The impact side of the trailer was bowed outward due to shifting of the ballast during impact as shown in Figure 126. The lower right corner of the bracket at the back of the trailer was fractured and bent.

Figure 126. Photograph. Post test view of the trailer showing damage to sidewall and external ribs.

FE Vehicle Model Damage

Figures 127, 128, and 129 show contour plots of plastic strain which was used to identify areas of the tractor model that suffered damage during the simulated impact event. The damage to the tractor model was limited to the impact side. The most severe damage was to the front bumper, the fender, the side steps, the fuel tank, and the front-right suspension. The high plastic strains on the rear tandem wheel rims also indicate that the tires would likely have debeaded and consequently deflated during the impact, which would affect the kinematics of the vehicle.[iv] There was also moderate plastic strain in components in the support structure for the fifth-wheel.

Figures 130 through 132 show contour plots of plastic strain for the trailer model (note: the aluminum sidewalls were removed from view in Figures 130 through 132). The trailer experienced plastic strains in the top and bottom side rails and in all the vertical ribs attached to the sidewalls. There were also significant plastic strains in the suspension structure and in the connection points of the trailer bogie to the lower cross-beams of the trailer box. The impact side of the trailer was bowed outward slightly due to shifting of the ballast during impact.

[iv] The development of a more realistic tire model was outside the scope of this project.

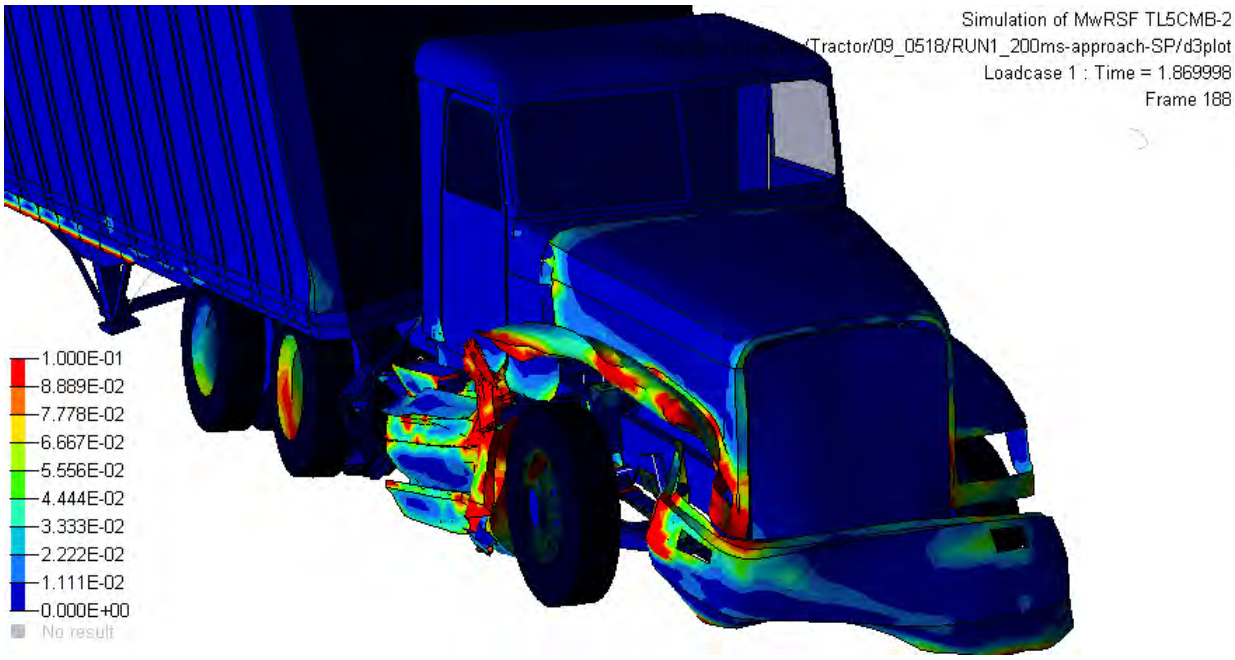

Figure 127. Illustration. Contour of effective plastic strain (with contours cut-off at 10%) used to identify areas of the tractor model that sustained damage during simulated impact.

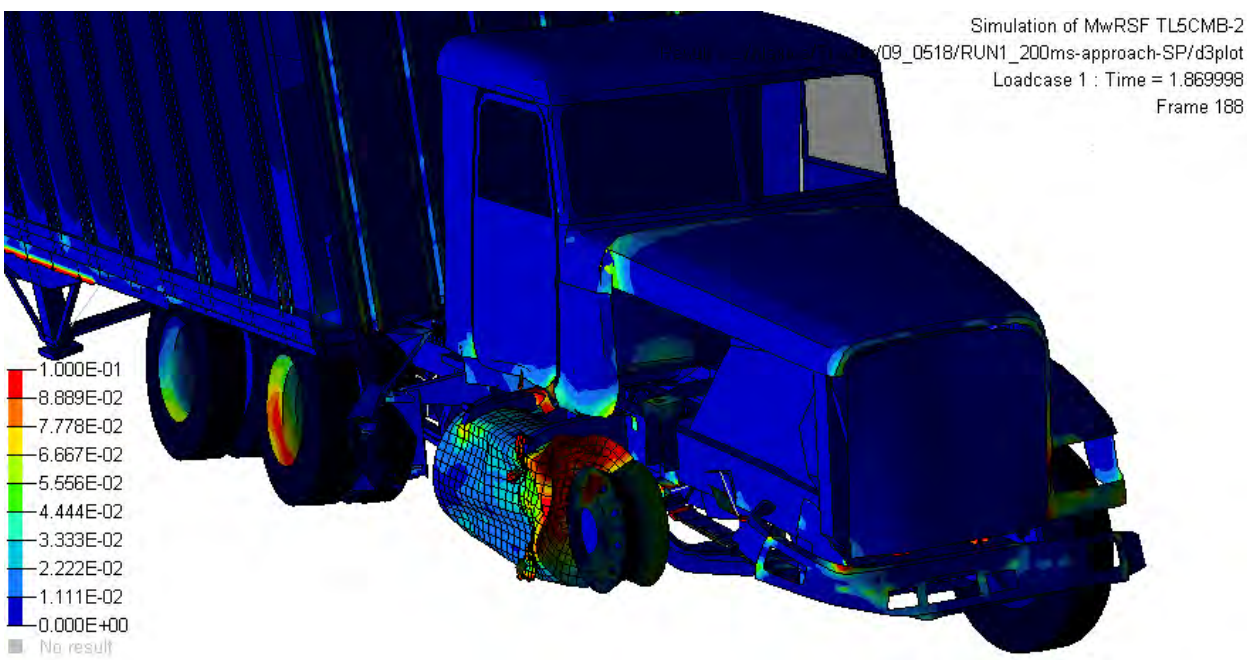

Figure 128. Illustration. Contour of effective plastic strain (with contours cut-off at 10%) used to identify areas of the tractor model that sustained damage during simulated impact.

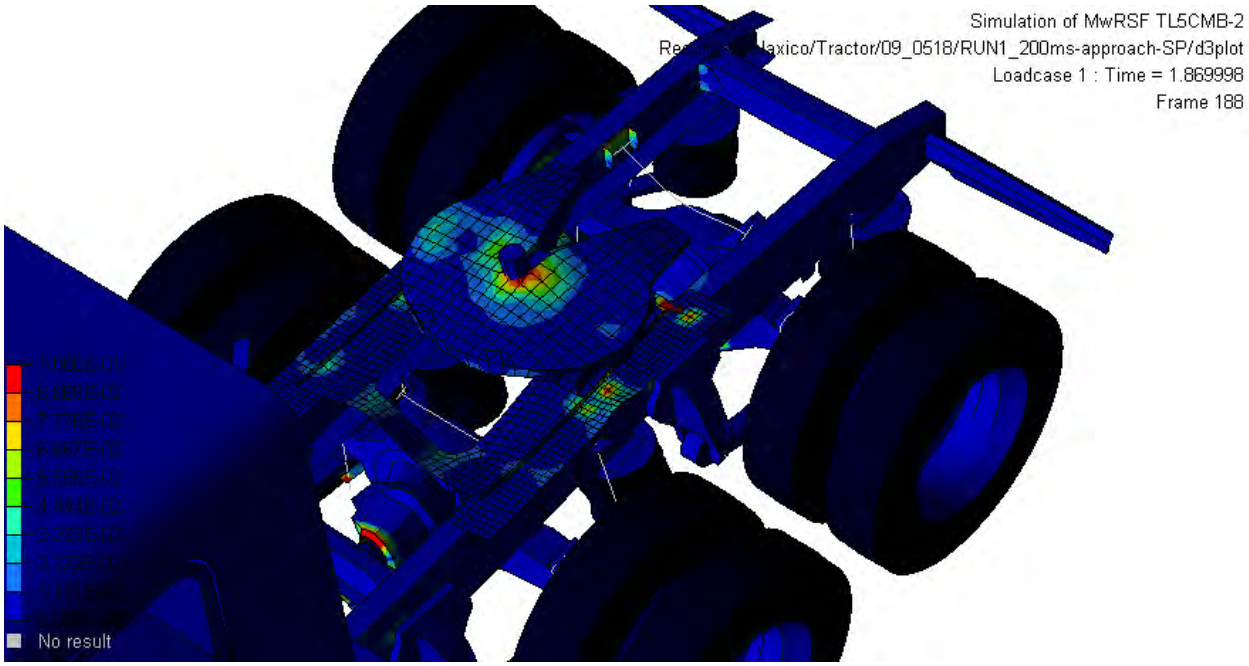

Figure 129. Illustration. Contour of effective plastic strain (with contours cut-off at 10%) used to identify areas of the tractor model that sustained damage during simulated impact.

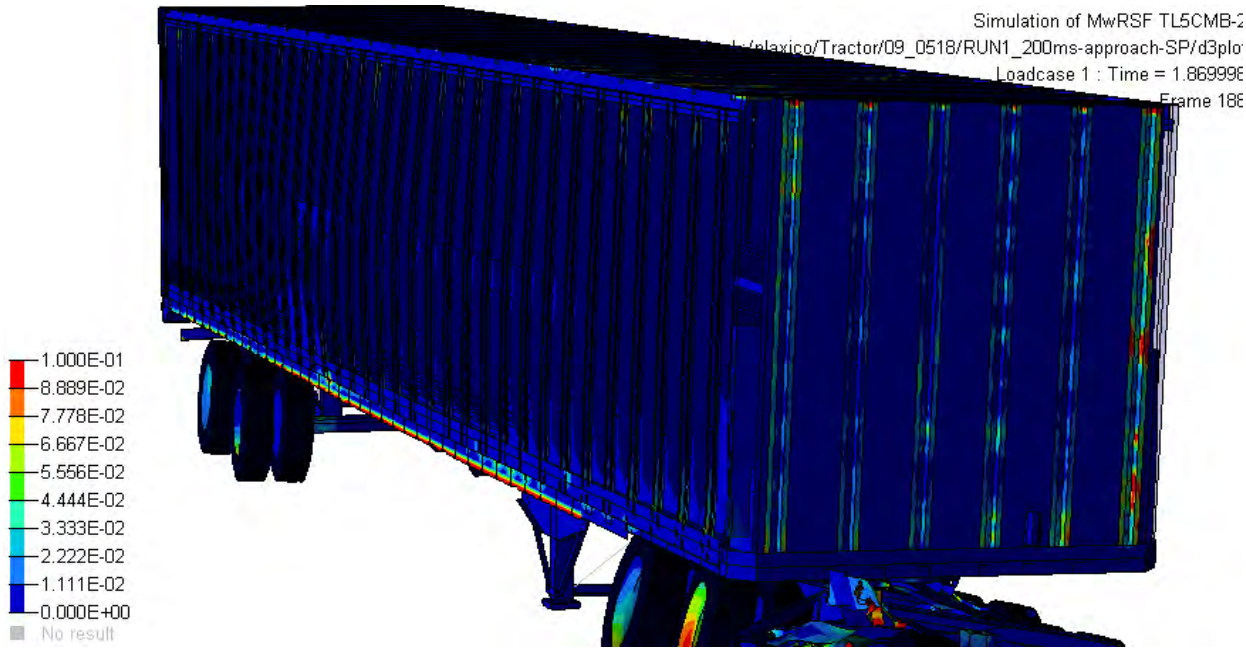

Figure 130. Illustration. Contour of effective plastic strain (with contours cut-off at 10%) used to identify areas of the trailer model that sustained damage during simulated impact.

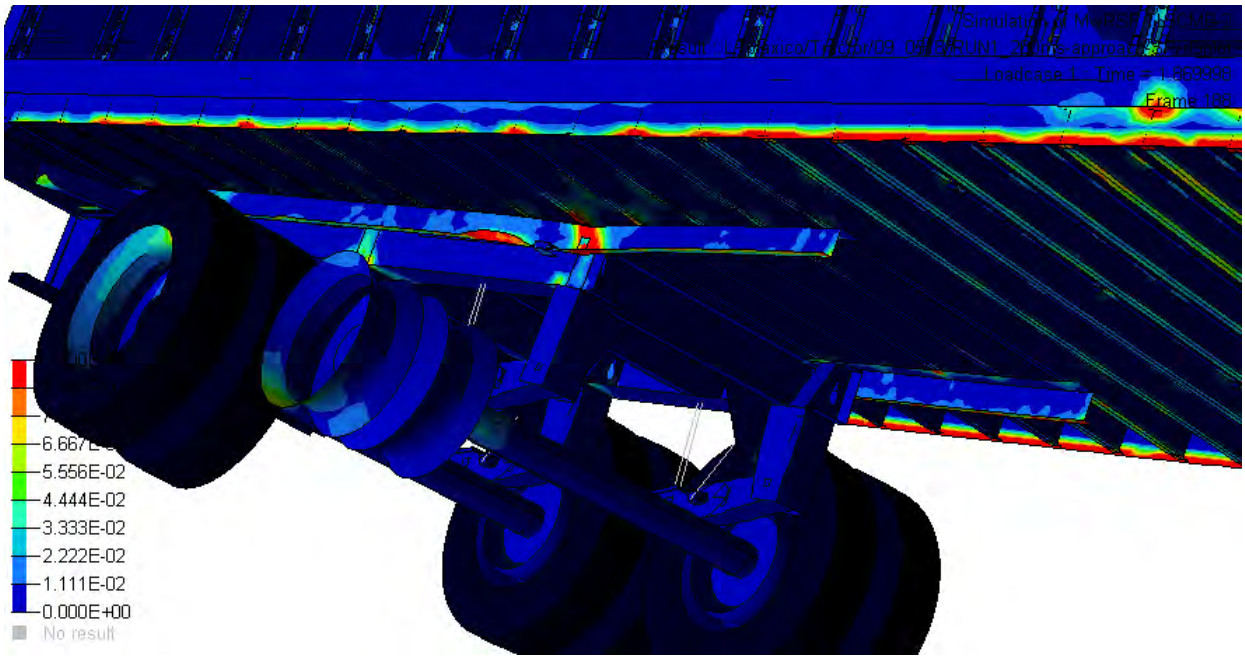

Figure 131. Illustration. Contour of effective plastic strain (with contours cut-off at 10%) used to identify areas of the trailer model that sustained damage during simulated impact.

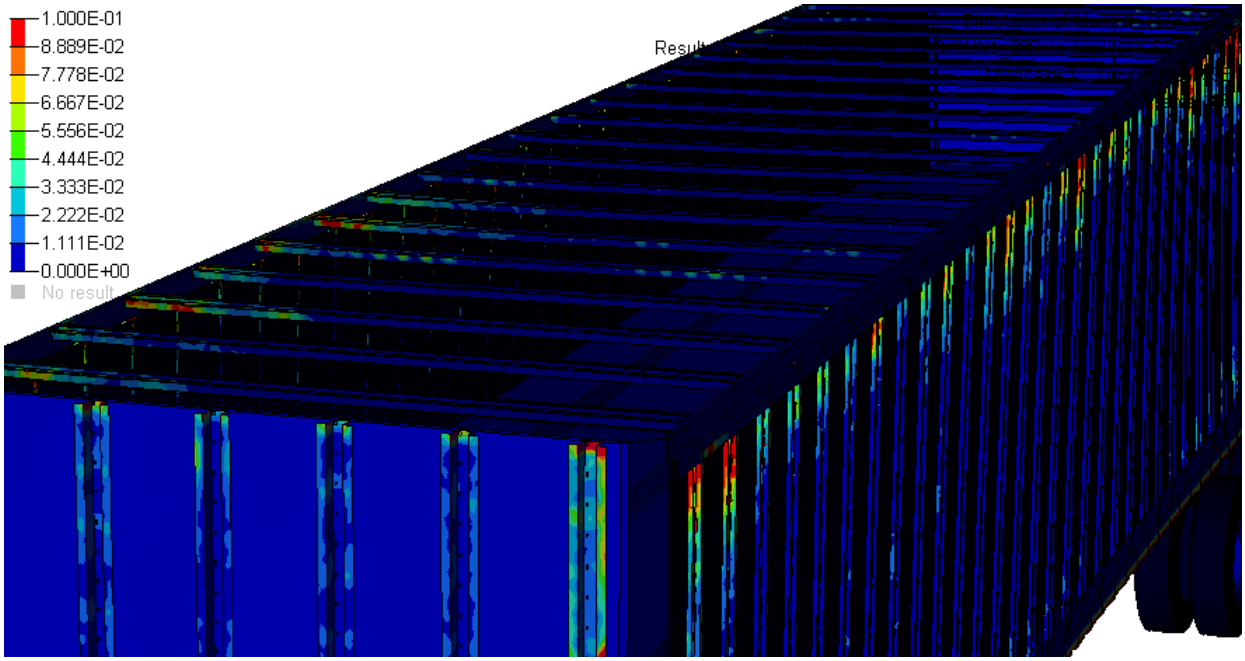

Figure 132. Illustration. Contour of effective plastic strain (with contours cut-off at 10%) used to identify areas of the trailer model that sustained damage during simulated impact.

Qualitative Comparison of Simulation Results with Other Similar Tests

A more general assessment of the models' results was made based on a comparison with similar full-scale tests in the literature. In particular, the model results were compared to tests that involved a tractor with a box-trailer ballasted to a nominal weight of 36,287 kg (80,000 lb) impacting a 1,067 mm (42 inches) tall barrier at a nominal speed and angle of 80 km/hr and 15 degrees (i.e., Group A in the Summary of Full Scale Tests section of this report).

Figures 133, 134, and 135 show the results from the analysis compared with the full-scale tests regarding peak values of acceleration-time histories at three locations on the vehicle. Data was not collected at the center of gravity of the trailer-ballast in the analysis; however, the results from the full-scale tests are shown for convenience. The vertical bar in the plots represents the range of peak values from the test's acceleration-time histories, the red square represents the mean value of the peak values from the test's acceleration-time histories, and the symbol ⊕ denotes the peak value from the analysis results. Refer to the Summary of Full-Scale Tests section for more detail regarding the test data.

Figure 133 shows a comparison of the peak 0.01-second moving average of the three accelerometer channels at four locations on the vehicle. Figure 134 shows a comparison of the peak 0.05-second moving average of the three accelerometer channels, and Figure 135 shows a comparison of the peak ASI computed from the three accelerometer channels. A qualitative assessment of the comparison is provided below:

- Peak 0.01-second moving average acceleration
  - The analysis compared reasonably well for the longitudinal channel at all accelerometer locations.
  - The analysis compared reasonably well for the transverse channel at all accelerometer locations.
  - The analysis did not compare well for the vertical channel at the tractor cabin and the tractor fifth wheel locations; however, there was only one test available for the comparison.
  - The analysis compared well for the vertical channel at the trailer tandem.
- Peak 0.05-second moving average acceleration
  - The analysis compared reasonably well for the longitudinal channel at all accelerometer locations.
  - The analysis compared reasonably well for the transverse channel at all accelerometer locations.
  - The analysis results for the vertical channel did not compare well with the test results at the tractor cabin location, but again only a single test was available for comparison.
  - The analysis results for the vertical channel compared well to all other locations. More data points were available at the tractor fifth-wheel location for the comparison

of the 0.05-second moving average acceleration which showed that the scatter in results was significant at that location.

- Peak ASI value
  - The analysis results for ASI did not compare well at the tractor cabin location; only one test was available for comparison.
  - The analysis results for ASI compared well at the tractor fifth-wheel and trailer tandem locations.

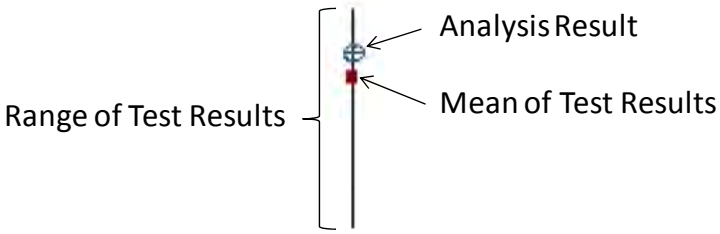

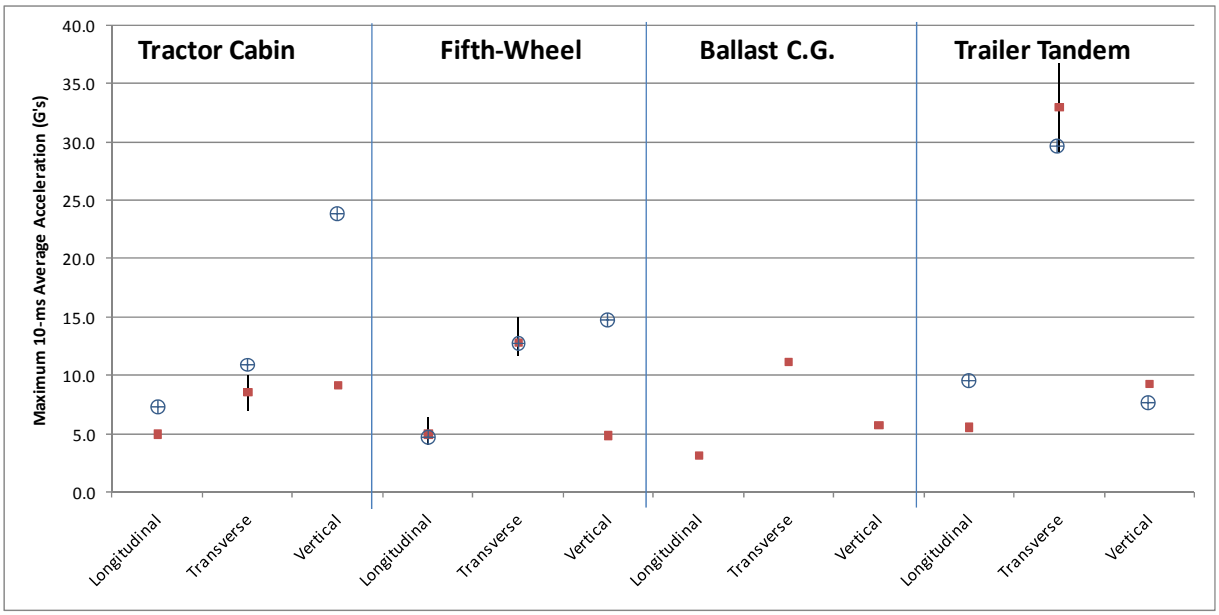

Figure 133. Chart. Results of FE simulation compared to full-scale crash tests regarding peak 0.01-second moving average of the three accelerometer channels at four locations on the vehicle.

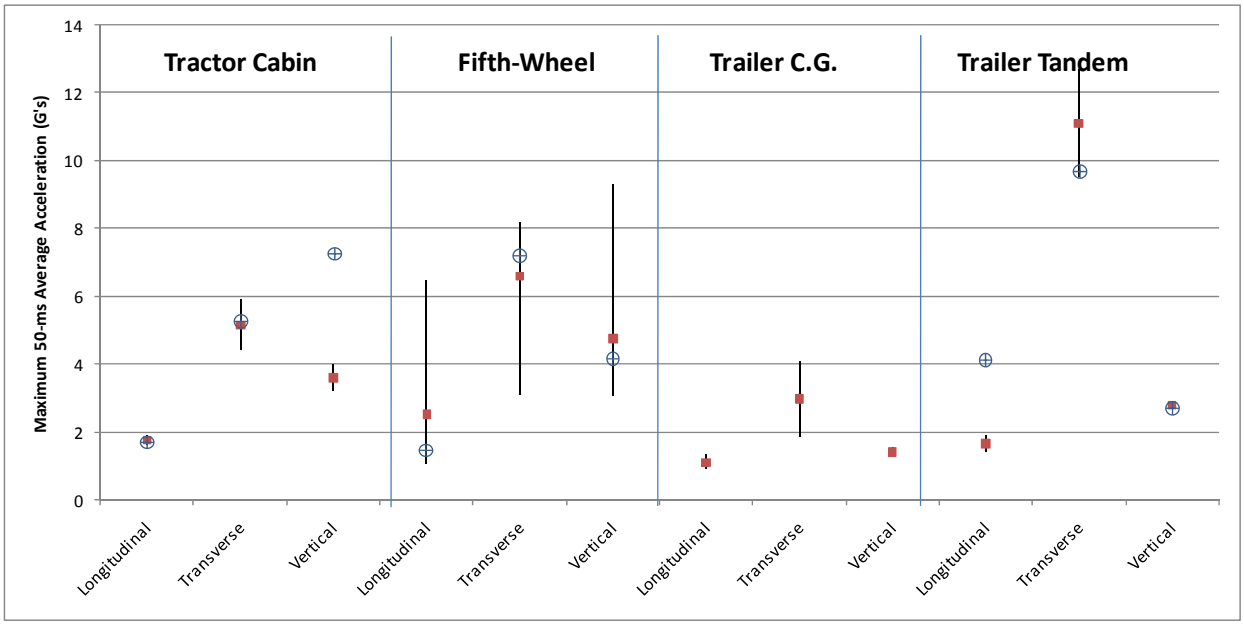

Figure 134. Chart. Results of FE simulation compared to full-scale crash tests regarding peak 0.05-second moving average of the three accelerometer channels at four locations on the vehicle.

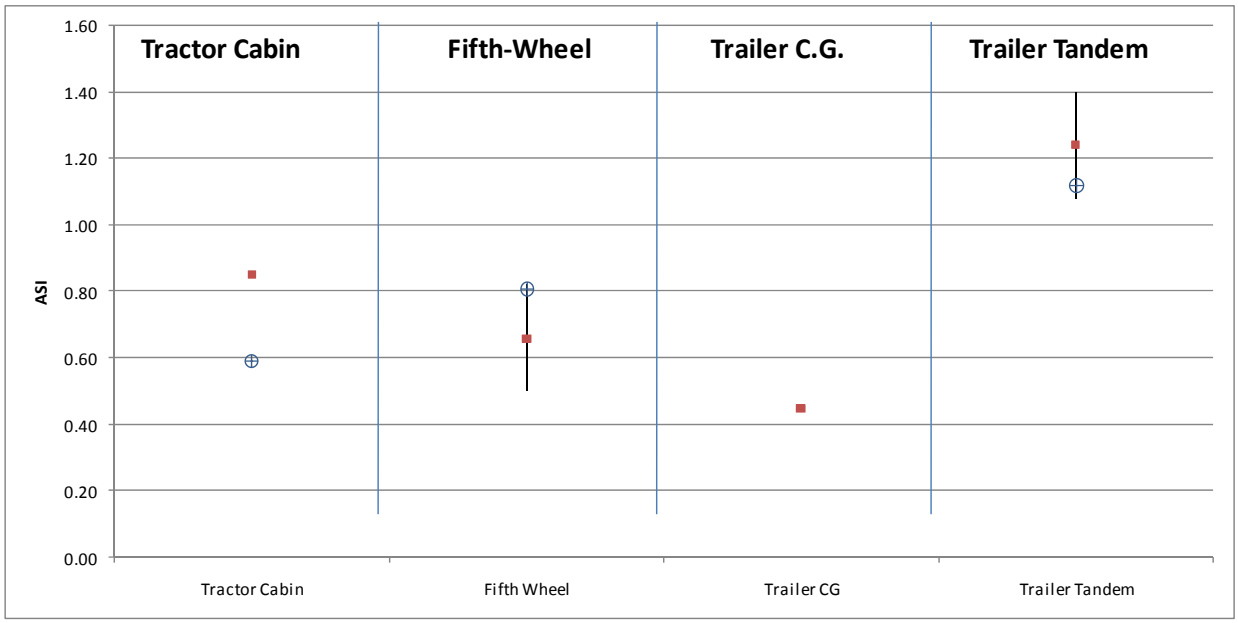

Figure 135. Chart. Results of FE simulation compared to full-scale crash tests regarding peak ASI values at four locations on the vehicle.

Figures 136 through **144** show the 0.05-second moving average acceleration-time histories and the ASI-time histories for the simulation and the full-scale crash tests corresponding to Group A [5, 7, 10, 12, 14].[v]

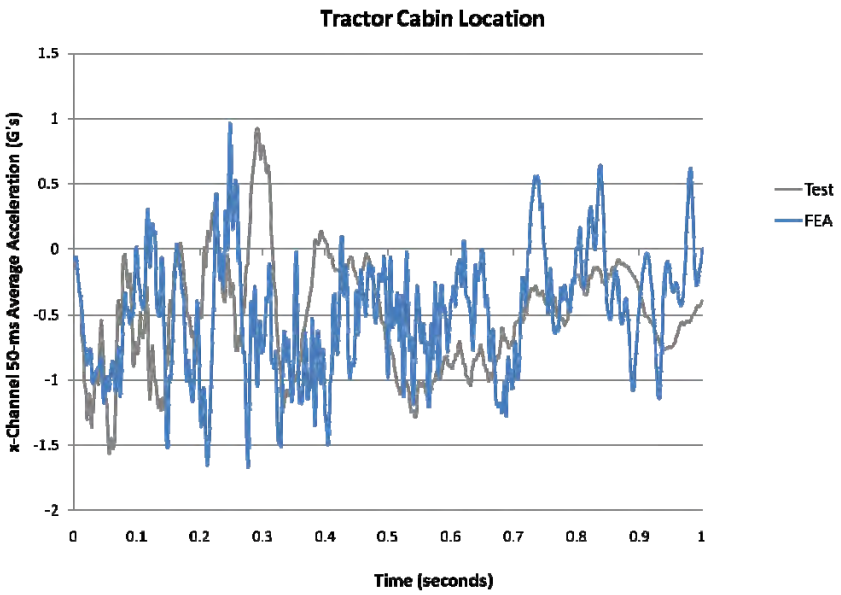

Figure 136. Chart. X-channel 0.050-seconds average acceleration-time history from accelerometer located inside tractor cabin near the tractor center of gravity from simulation and full-scale test Group A.

[v] Plots only include test data that were available in electronic format

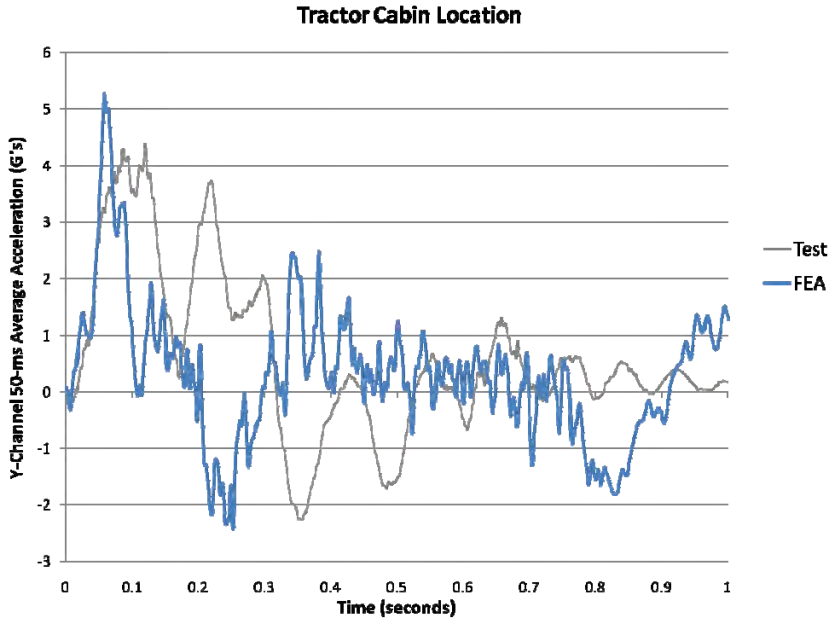

Figure 137. Chart. Y-channel 0.050-seconds average acceleration-time history from accelerometer located inside tractor cabin near the tractor center of gravity from simulation and full-scale test Group A.

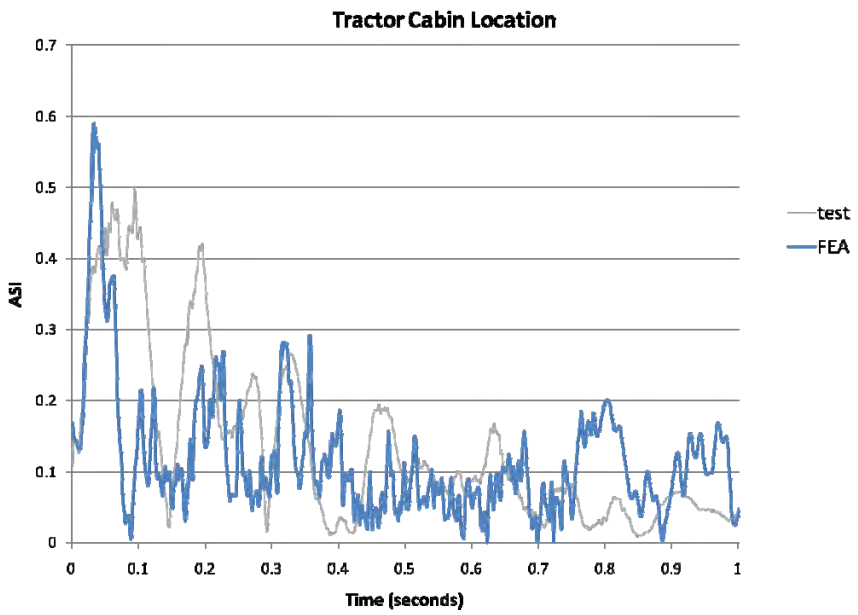

Figure 138. Chart. ASI-time history from accelerometer located inside tractor cabin near the tractor center of gravity from simulation and full-scale test Group A.

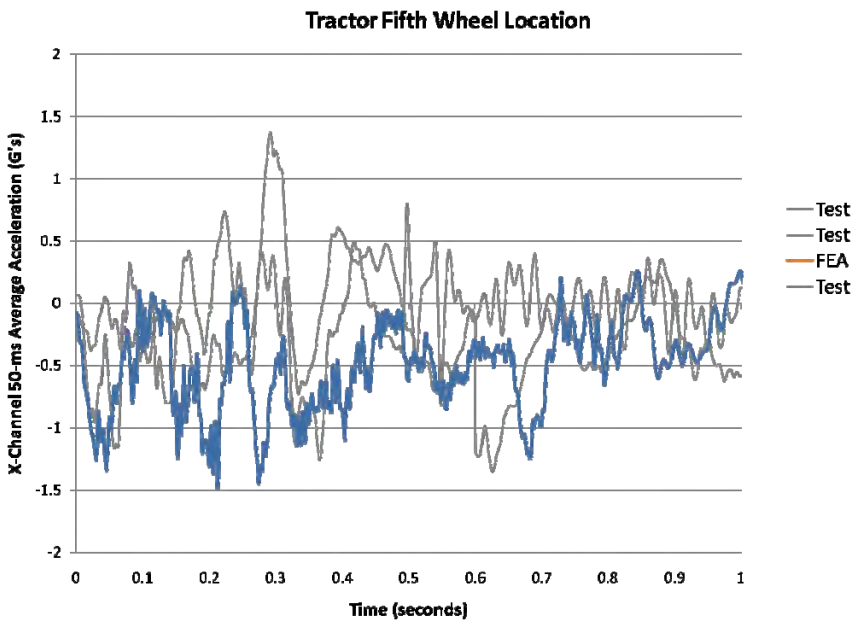

Figure 139. Chart. X-channel 0.050-seconds average acceleration-time history from accelerometer located near the tractor fifth-wheel from simulation and full-scale test Group A.

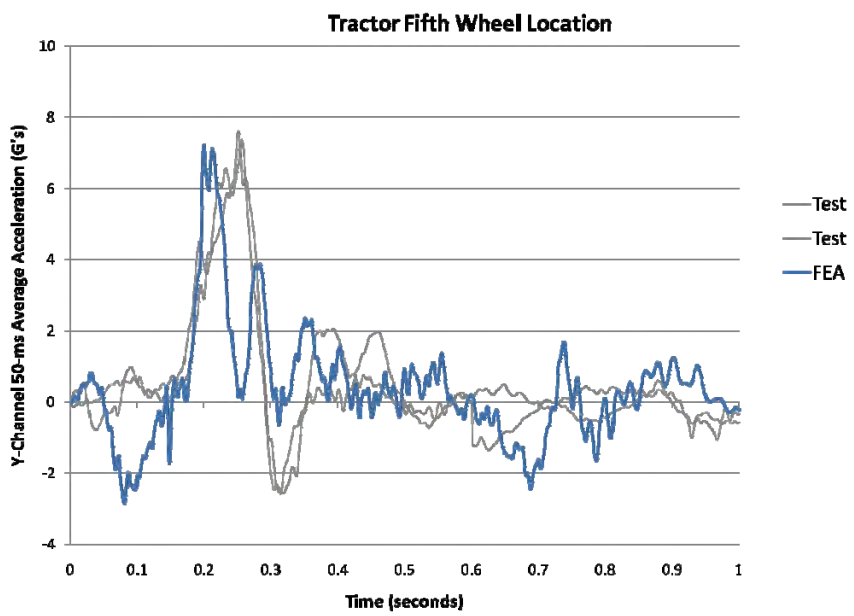

Figure 140. Chart. Y-channel 0.050-seconds average acceleration-time history from accelerometer located near the tractor fifth-wheel from simulation and full-scale test Group A.

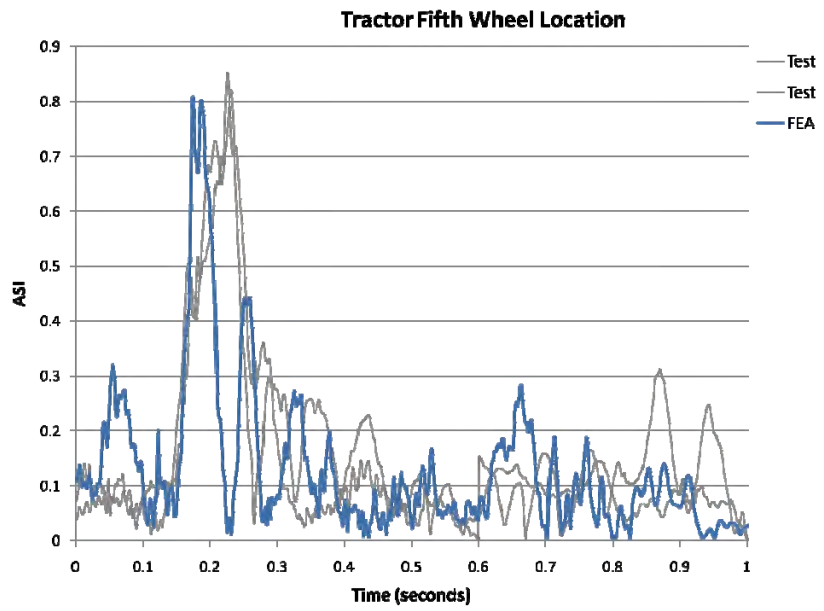

Figure 141. Chart. ASI-time history from accelerometer located near the tractor fifth-wheel from simulation and full-scale test Group A.

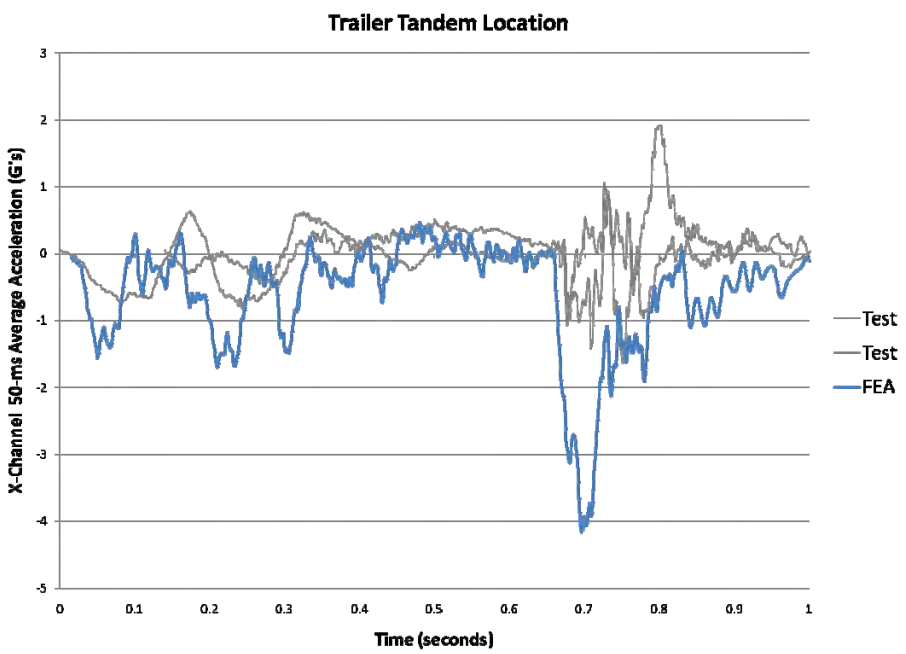

Figure 142. Chart. X-channel 0.050-seconds average acceleration-time history from accelerometer located near the trailer tandem axle from simulation and full-scale crash tests Group A.

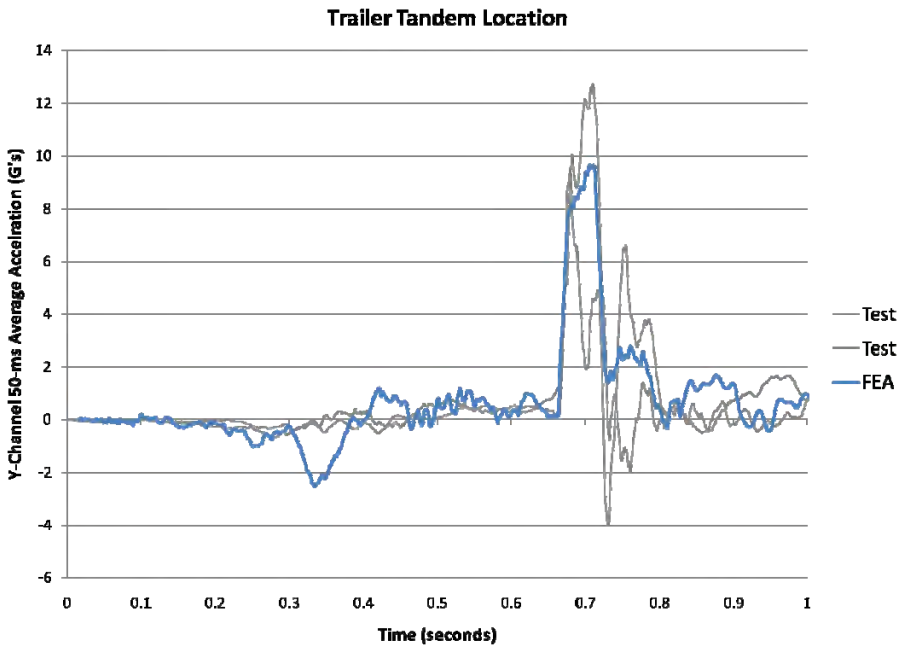

Figure 143. Chart. Y-channel 0.050-seconds average acceleration-time history from accelerometer located near the trailer tandem axle from simulation and full-scale crash tests Group A.

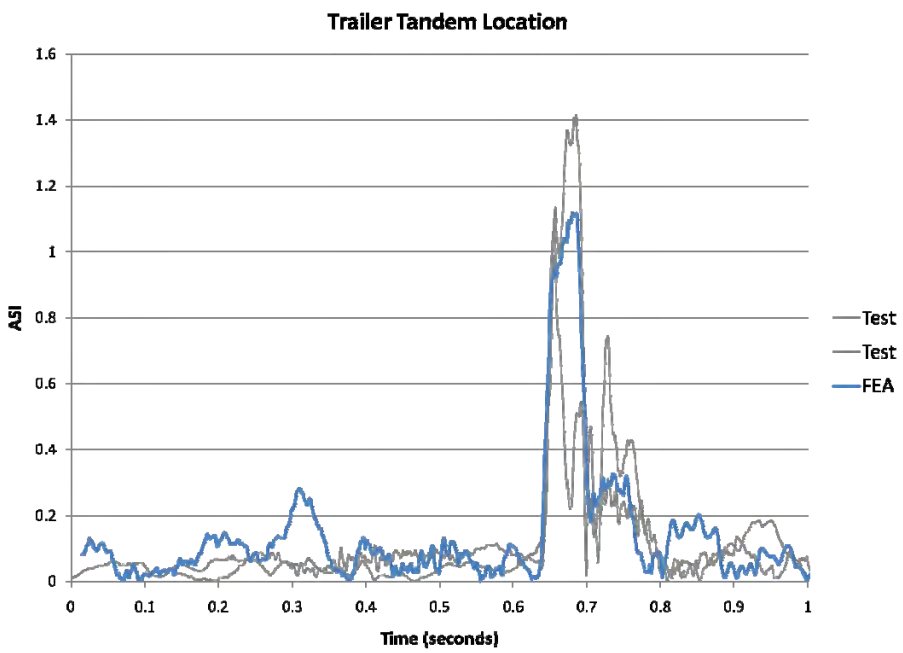

Figure 144. Chart. ASI-time history from accelerometer located near the trailer tandem axle from simulation and full-scale crash tests Group A.

Quantitative Assessment of Tractor-trailer FE Model Simulation Results

Quantitative Validation Approach

The *quantitative validation* assessment of the model's results was based on validation procedures that are currently under development in a project sponsored by NCHRP under project number 22-24 titled "Recommended Procedures for the Verification and Validation of Computer Simulations used for Roadside Safety Applications" [64]. The NCHRP 22-24 project is scheduled to be completed in the latter part of 2009. The objective of NCHRP 22-24 is to develop guidelines for verification and validation of FE analysis models for crash simulations of roadside safety features. The focus of these guidelines is to establish accuracy, credibility, and confidence in the results of crash test simulations that are intended to support policy decisions, and to be used for approval of design modifications to roadside safety devices that were originally approved with full-scale crash testing.

The tractor-trailer FE model is one of several models that are being used as "benchmark cases" for the NCHRP 22-24 project. This quantitative validation will reflect those recommended procedures, but because these procedures are still under development, the results from this quantitative validation should be considered tentative at this point.

The validation procedure has three steps:

1. Solution verification: Indicates whether the analysis solution produced numerically stable results (ensures that basic physical laws are upheld in the model).

2. Time-history evaluation: Quantitative measure of the level of agreement of time-history data (e.g., x, y, z accelerations and roll, pitch, and yaw rates) between analysis and test.

3. Phenomena Importance Ranking Table: A table that documents the types of phenomena that a numerical model is intended to replicate and verifies that the model produces results consistent with its intended use.

Following is a discussion of the time-history evaluation metrics, their acceptance criteria, and the Phenomena Importance Ranking Table.

Time-History Evaluation

A major task in the NCHRP 22-24 project is the development of a computer program that will allow the user to select one or more validation metrics as a basis to compare results from a computational model to the results from physical tests. The validation program is called RSVVP, after the acronym for "Roadside Safety Verification and Validation Procedures." The metrics computed in RSVVP provide a mathematical measure that quantifies the level of agreement between the shapes of time-history data obtained from simulations and tests such as acceleration, velocity, and displacement at specific sensor locations. There are currently 14 methods in the RSVVP software that are available for computing quantitative comparison

measures. All the metrics are deterministic shape-comparison metrics and are classified into three main categories. These are listed below and are described in detail in the Interim Report for the NCHRP Report 22-24 project and in the literature [65, 66, 67, 68]. The methods are"

Magnitude Phase Composite (MPC) metrics

1. Geers
2. Geers CSA
3. Sprague & Geers
4. Russell
5. Knowles & Gear

Single Value Metrics

6. Whang's inequality
7. Theil's inequality
8. Zilliacus error
9. RSS error
10. Weighted Integrated Factor
11. Regression coefficient
12. Correlation Coefficient
13. Correlation Coefficient (NARD)

Analysis of Variance (ANOVA)

14. Ray

The MPC metrics treat the magnitude and phase of the curves separately and combine them into a single value comprehensive metric. The single-value metrics give a single numerical value that represents the agreement between two curves. The ANOVA metric is a statistical assessment of whether the variance between two curves can be attributed to random error.

Another important task in the NCHRP 22-24 project includes determining which of the metrics are the most effective for comparing results of roadside safety impact events and developing acceptance criteria (e.g., what value of the metric indicates that the curves are statistically the same).

The current metrics that have been suggested by the NCHRP 22-24 project team for comparing time-history traces from full-scale crash tests and/or simulations of crash tests are the Sprague & Geers metrics and the ANOVA metrics. The Sprague & Geers metrics assess the magnitude and phase of two curves while the ANOVA examines the differences of residual errors between them. The definitions of these metrics are shown below:

Sprague & Geers

$$\text{Magnitude}\,(M) = \sqrt{\frac{\Sigma c_i^2}{\Sigma m_i^2} - 1}$$

$$\text{Phase}\,(P) = \frac{1}{\pi}\cos^{-1}\frac{\Sigma c_i m_i}{\sqrt{\Sigma c_i^2 \Sigma m_i^2}}$$

$$\text{Comprehensive}\,(C) = \sqrt{M^2 + P^2}$$

Equation 2. Equations for calculating the Sprague & Geers metrics

ANOVA

$$\text{Residual Error}\,(\bar{e}^r) = \frac{\Sigma(m_i - c_i)}{m_{\max}} \cdot \frac{1}{n}$$

$$\text{Standard Deviation}\,(\sigma) = \sqrt{\frac{1}{n}\Sigma(m_i - c_i - \bar{e}^r)^2}$$

Equation 3. Equations for calculating the ANOVA metrics

Where,

c_i = calculated quantities

m_i = measured quanties

$m_{\max}$ = maximum measured experimental value

$\bar{e}^r$ = relative average residual error

σ = relative standard deviation

Time-History Evaluation Acceptance Criteria

Once a measure of comparison is obtained using a quantitative metric, it is necessary to establish an acceptance criterion for deciding if the comparison is acceptable. Because of the highly nonlinear nature of crash events, there are often considerable differences in the results of essentially identical full-scale crash tests – this was shown in the NCHRP study. Likewise, a computational model may not match "exactly" the results of a physical test, but the difference should be no greater than what is expected between physical tests. The approach taken in the NCHRP study was to determine the realistic variation in the deterministic shape comparison metrics for a set of identical physical experiments and use that variation as an acceptance criterion. For example, if a series of physical experiments result in a shape comparison metric that is within some specific range, a mathematical model of the same phenomena should fall within that same range.

The current acceptance criteria is based on the results of a quantitative comparison of ten essentially identical full-scale crash tests that were performed as part of the ROBUST project involving small car impact into a vertical rigid wall at 100 km/hr and 25 degrees [69, 70]. The

purpose of the ROBUST project was to assess the repeatability of full-scale crash tests and the consistency of data processing among different test agencies. There were two sets of tests carried out by five independent test laboratories. The first set involved the same vehicle make, model and year. The second set of tests involved a variety of vehicle makes and models but, in all cases, the test vehicle corresponded to the standard small-car test vehicle specified in the European crash test standards, EN 1317 [71]. A rigid barrier was intentionally chosen to limit the scatter of the results by isolating the energy of the event to strain energy and kinetic energy in the test vehicle. In all cases, the three components of acceleration were measured at the center of gravity of the vehicles.

The comparison metrics were used to compare the similarity of the time histories of the tests and to determine acceptance criteria based on those results. The original raw time histories from the 10 tests were filtered, re-sampled, and synchronized so they could be directly compared to each other. The statistics derived from the analysis of the residuals confirmed that the errors were normally distributed and were thus attributable to normal random experimental error. The expected error between the tests was shown to be approximately 40 percent based on the Sprague-Geers metrics. The average residual error component of the ANOVA metric was generally very close to zero for all the crash tests. The standard deviation of the residual errors was as high as 31 percent and, like all the other metrics, the standard deviation of the standard deviation of the residuals doubled in the second set of tests where the vehicles were similar but not identical.

In a much earlier study, Ray proposed an acceptance criterion of a mean residual error less than 5 percent of the peak and a standard deviation of less than 20 percent of the peak test acceleration based on an evaluation of the ANOVA metrics for a series of six identical frontal rigid pole impacts [68]. The redirection impacts in the ROBUST project resulted in greater error than this between the test data because, as discussed earlier, redirection tests are highly nonlinear. While the impact conditions may be essentially identical in redirection tests, uncontrollable variations in the experiment, such as the suspension or steering system response, can significantly affect the overall result.

A similar multi-vehicle study should be carried out to compare the results of full-scale tractor trailer tests. It is expected that a comparison of essentially identical tractor-trailer tests, where there are many aspects of the vehicle that could influence the results (e.g., suspension response, suspension failure, friction between tire and pavement, vehicle articulation), would result in higher level of expected error between tests.

Based on the results of the NCHRP 22-24 study, comparisons must be made using acceleration-time histories and/or angular rate-time histories with the following time-history acceptance criteria:

- Sprague & Geers
  - Magnitude should be less than 40 percent
  - Phase should be less than 40 percent
- ANOVA metrics
  - Mean residual error should be less than 5 percent
  - Standard deviation should be less than 35 percent.

Phenomena Importance Ranking Tables (PIRT)

FE models, like all mathematical models, are idealized representations of physical systems. The model developer must make assumptions about what is important in the model and what phenomena should be represented in the mathematical model. Unfortunately, these assumptions are generally not apparent to those reviewing the results of the model. A PIRT provides a quick way of documenting the phenomena that have been included in a mathematical model. The PIRT ranks the importance of those phenomena and assesses the overall verification and validation level of the model, so that subsequent users of the model or reviewers of the results will know what phenomena the model can reasonably be expected to represent.

Roadside safety simulations are generally patterned after the standardized tests in NCHRP Report 350. Each Report 350 test involves a test vehicle, a roadside appurtenance, and initial conditions. Each of these should be represented in a PIRT. For example, vehicle models must, at a minimum, have the correct mass distribution, correct exterior geometry, and realistic structural components. Depending on the application, the vehicle models may also require greater detail in the suspension system, the possibility of tire failure, and other refinements. The PIRT is not a static document and it should be developed based on the model's functionality.

The final format of the PIRT has not yet been finalized. The NCHRP 22-24 team, however, has developed a baseline PIRT that includes evaluation criteria that should be included for TL-5 impacts. The PIRT is patterned after the full-scale crash test evaluation criteria listed in Table 5.1 in NCHRP Report 350. The analyst is asked to report the values for the individual metrics from the full-scale test and the computer analysis and calculate the relative difference. If the relative differences are less than 20 percent, then the phenomena are considered to be replicated.

It is expected that the finalized format of the PIRT will include information regarding quantitative validation of individual components of the model. In the current tractor-semitrailer model for example, physical tests were performed for validating the leaf-spring assembly, shock absorbers, and suspension bump-stop for the front suspension. The simulation data could be compared to the test data using the metrics in RSVVP. A validation form would then be included for each validated component of the model. The collection of all the phenomena that have been validated is the PIRT.

Quantitative Evaluation Results

The quantitative evaluation was based on a comparison of the acceleration-time histories collected in the model to those collected in full-scale crash test TL5CMB-2. The data was obtained from an accelerometer mounted to the floor of the semitrailer near the center of the tandem axle at the rear of the trailer. The results of the quantitative validation are provided in the Verification/Validation Report located in Appendix A. The quantitative evaluation showed mixed results as described below.

Based on the Spague & Geers metrics, a comparison of the individual components of acceleration indicated that the simulation was not in agreement with the test. Whereas, the comparison of the ASI-time history, which is a composite of the x-, y-, and z-accelerations, indicated that the simulation was in very good agreement with the test. The results are summarized below:

- The metrics for the x-acceleration were outside acceptable limits for both magnitude (i.e., M=45.2%) and phase (i.e., P=46.2%), which indicates that the simulation is *not* in agreement with the test.
- The metrics for the y-acceleration were good regarding magnitude (i.e., M=11.2%) but fell just outside acceptable limits regarding phase (i.e., P=41.0%).
- The metrics for the z-acceleration were very good regarding magnitude (i.e., M=1.6%) but fell outside acceptable limits regarding phase (i.e., P=46.6%).
- The metrics for the ASI-time history were M=12.7% and P=17.4% indicating that the simulation was in agreement with the test.

Based on the ANOVA metrics, the simulation was in good agreement with the test regarding comparison of the individual components of acceleration and the ASI-time history.

- The metrics for the x-acceleration were good regarding both the mean residual error (i.e., 3%) and the standard deviation of residual error (i.e., 15%), which indicated that the simulation is in agreement with the test.
- The metrics for the y-acceleration were good regarding both the mean residual error (i.e., 0%) and the standard deviation of residual error (i.e., 10%), which indicated that the simulation is in agreement with the test.
- The metrics for the x-acceleration were good regarding both the mean residual error (i.e., 0%) and the standard deviation of residual error (i.e., 18%), which indicated that the simulation is in agreement with the test.

- The metrics for the x-acceleration were good regarding both the mean residual error (i.e., 5%) and the standard deviation of residual error (i.e., 8%), which indicated that the simulation is in agreement with the test.

The quantitative metrics and the validation criteria used in this assessment are consistent with those *currently* suggested by the NCHRP 22-24 project team. The NCHRP project is still underway, thus the validation procedures used in this report are tentative and will be finalized in Phase C.

Chapter 7 – Summary and Discussion of Results

The work completed in Phase B of the project included completion of the tractor-semitrailer model development and an evaluation of its performance by comparing computer simulation results to full-scale tractor-trailer crash test results from the literature. The impact conditions (e.g., vehicle dimensions, mass, velocity, and impact angle) for the model corresponded to those of MwRSF Test No. TL5CMB-2 and were consistent with the crash testing guidelines specified in NCHRP Report 350 Test 5-12. Test TL5CMB-2 was used for the model evaluation, primarily because of the availability of test data in electronic form (e.g., accelerometer data and high-speed video) and because the dimensions of the semitrailer used in the test were very similar to those of the FE model.

Model Enhancement

The material properties for the various parts of the semitrailer model were derived from the literature. The first task in this process was to organize the list of the trailer's structural parts into functional groups. The next task was to determine the types of materials and their designation for each of the parts. As different manufacturers have different trailer designs that use different materials, the first two steps resulted in several part and material assignment schemes. Trailer manufacturers generally do not reveal the specific material grades used for specific parts, so the search had to include original and aftermarket parts suppliers. The third step was to determine elastic and elasto-plastic mechanical properties for each material.

The analysis results presented were from a simulation involving a modified version of the tractor model (i.e., the dimensions of the baseline tractor FE model were modified to correspond with the test vehicle). The original tractor model was based on the dimensions of a 1992 Freightliner FLD 120 sleeper-cab style tractor with a wheel-base length of 5.5 m (18 feet). The test vehicle used in test TL5CMB-2 was a White/GMC day-cab style tractor with a wheel-base length of 3.9 m (12.9 ft). The wheelbase lengths of the original (baseline) FE model of the tractor and semitrailer are relatively long, so an Automated Dimensional Adjustment Program (ADAP) was developed that operates directly on the LS-Dyna model input file to facilitate reducing these vehicle dimensions. This gives researchers more options for using the model to simulate a wider variety of tractor-semitrailer geometries. ADAP is reasonably general and can be used for other modifications, but the scope of this project task was to develop tractor wheelbase modification procedures that would set FE model overall dimensions close to available test vehicle dimensions. The ADAP is executed as "scripts" (similar to macros) and performs individual model modifications. Each modification step results in a syntactically valid LS-DYNA input file, which allows for easier development and debugging.

In general, ADAP performs the following tasks: 1) determine connections of the part to the rest of the model, 2) remove and store the connections relative to the object, 3) cut the parts at the element level in the selected segment, 4) reconnect the elements that are on both sides of the cut,

and 5) reconnect the part to the model. The cutting was performed in a predefined sequence because of the structural hierarchy of the parts in the model.

The advantage of ADAP is that the FE model can be readily modified to represent the properties of test vehicles from several tests. This allows the research team to simulate multiple tests in order to provide a broader assessment of the model's efficacy, and ultimately provide a better quantification of the model's validity. It is expected that further modifications will need to be made to the model in Phase C as more information is made available for judging its performance. All FE model geometry changes will be made using the baseline model as the starting point. The scripts will expedite the process of re-modifying the geometry and inertial properties to match the particular test vehicle for evaluation of those modifications.

The automated scripts of ADAP were very useful in adjusting the model's dimensions to match those of test TL5CMB-2; however, there were still some notable differences. In particular:

- *Length dimensions* – The length dimensions of the FE model were all within 2% of the test vehicle dimensions, except for the distance from the front bumper to the center of the front wheel, which was 13.5% shorter in the FE model.

- *Trailer box dimensions* – The trailer floor in the FE model was 148 mm (5.8 inches) higher than the test vehicle, and the top of the trailer in the FE model was 169 mm (6.7 inches) lower than the test vehicle.

- *Ballast c.g.* – The c.g. of the ballast in the FE model was located 600 mm (23.6 inches) rearward of and 188 mm (4.6 inches) higher than the c.g. location of the ballast in the test vehicle.

- *Trailer suspension* – The suspension system on the FE trailer model was the Airide™ design, and the suspension on the trailer test vehicle was a leaf-spring design.

Each of these basic differences affects the response of the vehicle in an impact. Ideally, the validation would be based on comparing model results to a test involving the same vehicle that the model is based on (i.e., a 1991 Freightliner tractor pulling a 14.6-m (48-ft) Stoughton trailer). Unfortunately, no such test data is currently available. In order to validate the model against available test data, the geometric and inertial properties of the baseline model were modified to match as closely as possible those of the test vehicle that was used in MwRSF Test TL5CMB-2.

Model Validation

The modified tractor-semitrailer model was used to simulate the full-scale test. The impact conditions (e.g., vehicle dimensions, mass, velocity, and impact angle) for the model corresponded to those of MwRSF Test No. TL5CMB-2 and were consistent with the crash testing guidelines specified in NCHRP Report 350 Test 5-12. In the qualitative assessment, the general response of the modified FE model compared well to test TL5CMB-2; the model results

replicated the basic timing and magnitudes of phenomenological events that occurred in the full-scale test. A comparison of sequential views of the test and simulation showed that the attitudes (e.g., roll and pitch) of both the tractor and the semitrailer models were consistent with the behavior of the vehicle in the full-scale crash test.

The translational accelerations and rotational velocities of the vehicle model were collected at 15 locations on the tractor model and at 1 location on the semitrailer model. Three of the accelerometers in the FE model were placed at locations consistent with typical accelerometer positions in full-scale crash tests: 1) near the center of gravity of the tractor inside the tractor cabin on the cabin floor, 2) near the tractor's fifth-wheel and 3) near the center of the semitrailer tandem axle.

The acceleration time-histories collected at the rear tandem location on the semitrailer model seemed to compare reasonably well to those from test TL5CMB-2, particularly regarding the maximum peak in the lateral acceleration-time-history which corresponded to the highest lateral load on the barrier. However, the simulation showed significant peaks in the lateral acceleration-time-history, that did not appear in the test results. These peaks were related to the tire/suspension response of the trailer.

In the current semitrailer FE model, the Airide™ suspension properties are simply copies of the tractor's Airide™ suspension properties. Due to the significant influence on vehicle kinematics, there was extensive testing and characterizing work done in Phase A of this project on the tractor's front and rear suspension components. For the purposes of Phase B (and for expediency), the general consensus of the project team was that the trailer's Airide™ suspension system should be generally similar enough to the tractor's Airide™ suspension system to warrant using it in the FE model of the semitrailer.

A preliminary gravity-only-load analysis (not included in this report) showed that the semitrailer's suspension was not completely at equilibrium at the start of the analysis. To partially account for this, the tractor-semitrailer model was positioned at 4.7 m upstream of the impact point at the start of the analysis to allow 0.2 seconds for the suspension systems to partially equalize under gravity prior to impact. The results of the FE simulation indicated that this was not enough time to sufficiently bring the models into equilibrium; thus, more needs to be done to ensure that the suspension systems in the FE model are effectively at equilibrium at the start of the analysis. Phase C will include a task that involves laboratory tests to determine the exact force-deflection and deflection-rate response of the semitrailer's Airide™ air-bag suspension.

A more general qualitative assessment of the FE model's results was made based on a comparison with additional similar full-scale tests from the literature. In particular, the FE simulation was compared to tests that involved a tractor with a box-trailer ballasted to a nominal weight of 36,287 kg (80,000 lb) impacting a 1,067 mm (42 inches) tall barrier at a nominal speed

and angle of 80 km/hr and 15 degrees (i.e., Group A in the Synthesis of Tractor-Semitrailer Crash Tests section of this report). In that assessment, the peak values of the 0.05-seconds moving average acceleration compared reasonably well in all locations where data were collected, except for the vertical component of acceleration at the tractor cabin.

The response of the tractor-semitrailer FE model was also assessed by a quantitative comparison of the simulation results with those from test TL5CMB-2 using the computer software RSVVP version 1.5(beta). RSVVP computes validation metrics that quantify the similarity between the "shape" of two time-history curves.

The quantitative evaluation showed mixed results. Based on the Sprague & Geers metrics, a comparison of the individual components of acceleration indicated that the simulation was not in agreement with the test, but the comparison of the ASI (Acceleration Severity Index) time history, which is a composite of the x-, y-, and z-accelerations, indicated that the simulation and test were in very good agreement. The ANOVA metrics also indicated that the simulation was in good agreement with the test regarding comparison of the individual components of acceleration as well as the ASI-time history. The quantitative metrics and the validation criteria used in this assessment are consistent with those *currently* suggested by the NCHRP 22-24 project team. The NCHRP project is still underway, thus the validation procedures used in this report are tentative and will be finalized in Phase C.

Chapter 8 – Conclusions and Recommendations for Future Research

The development of the FE model of a tractor-semitrailer was completed in Phase B. The model has been reasonably validated based on comparison with full-scale crash tests results. More specifically, the general response of the FE model replicates the basic timing and magnitudes of phenomenological events that occurred in full-scale tests of tractor-semitrailer impacts with rigid longitudinal barriers. The quantitative validation, which was based on a comparison of a triaxial accelerometer data at a single location on the tractor-semitrailer vehicle, provided mixed results using the currently suggested metrics of RSVVP [65]. The values of the Sprague & Gears [66, 67] metrics indicated that the simulation was just outside the acceptable values for that metric, while the values of the ANOVA [68] metrics indicated that the comparison was at least as good as would be expected from two identical crash tests (i.e., the error in the acceleration-time histories could be attributed to random experimental error).

All validation so far on this tractor-semitrailer FE model has been done by comparison to redirective impact type crash tests into rigid barriers, e.g., NCHRP Report 350 Test 5-12 through about 1.70 seconds of the impact event. The research team believes that this tractor-semitrailer FE model is reasonably valid for this type of crash simulation, and that it will provide useful results in general barrier design evaluation work regarding impact loads and general vehicle-barrier interaction. However, the model has not been assessed for use in other applications, such as high-energy impacts (e.g., full frontal impact with bridge pier), vehicle dynamics (e.g., vehicle response due to steer maneuvers), or vehicle-to-vehicle impacts to name a few. The model user must critically assess the results obtained from the model in all cases, but especially for applications that the model has not been validated for.

Recommendations for Future Work

The following sections describe additional research that would improve the accuracy, robustness, and applicability of the tractor-semitrailer FE model. Some of these research tasks are proposed to be conducted in Phase C of the program, but funding is not sufficient to conduct all tasks. These tasks are not listed in priority order.

Interactive Tractor-Semitrailer Web Site

An interactive web site dedicated to the tractor-semitrailer FE model is proposed to be created in Phase C that will include:

- FE model downloads area
  - FE models
  - User's Manual
  - Different versions of the models with customizable options for model generation

- Interactive browsing of the model documentation through graphical user interface:
  - Parts
  - Materials
  - Properties
  - Contact
  - Masses and inertias
  - Connections.

The web site will enable users to quickly deploy the model and select the model options best suited to their particular impact scenarios.

Users Handbook

Development of a hard copy User Handbook is proposed for Phase C which outlines model development details, model files content and organization, and model usage advice. This handbook would be made available on the Interactive Tractor-Semitrailer web site.

Part Contact Survey

The tractor-semitrailer FE model has contact specified in hundreds of areas throughout its many parts. Myriad variations and types of contact definition are used in this LS-Dyna FE model. Contact performance is highly sensitive to initial geometric position, relative stiffness, and the constantly changing orientation of contacting parts during a simulation. Contact is known to be a source of run-time errors and numerical instability in any simulation, so great care was taken during the development of the tractor-semitrailer FE model to remedy known bad contact conditions and situations. Nonetheless, at the end of Phase B there were still some outstanding contact issues manifested as higher-than-expected sliding (contact) energies in certain contacting regions that need to be resolved. This effort is also proposed for Phase C of the program.

Trailer Suspension Properties

In the current semitrailer FE model, the Airide™ suspension properties are simply copies of the tractor's Airide™ suspension properties. Due to its significant influence on vehicle kinematics, extensive testing and characterizing work was done in Phase A of this project on the tractor's front and rear suspension components. For the purposes of Phase B, the general consensus of the project team was that because the weight supported by the rear tandem of the tractor is the same as the weight supported by the wheel-set of the semitrailer, the trailer's Airide™ suspension system's properties should be similar enough to the tractor's Airide™ suspension system to warrant using it in the FE model of the semitrailer. The analysis results shows significant peaks in lateral acceleration of the semitrailer model as the trailer was yawing towards the barrier that appeared to be related to the tire/suspension response of the rear trailer tandem. Also, in a preliminary analysis (not documented in this report) of the model under simple gravity load, the rear suspension was not in equilibrium after 1.0 seconds. Thus, a test program similar to that

conducted in Phase A for the tractor suspension is proposed for Phase C to accurately characterize the trailer's suspension properties.

Extended Validation

A more extensive evaluation/validation of the model could be obtained through comparison of simulations with other tests in the literature. The ADAP scripts that were developed in Phase B of this project provide a convenient means of adjusting the tractor-semitrailer dimensional properties to match those other test vehicles. The validation exercise should be conducted using the modified model (via ADAP) to simulate other full-scale tests.

Trailer Materials Testing

The materials specifications for the parts in the semitrailer were obtained from the open literature, from manufacturers' data, and from existing tractor FE model material data. If specific impact scenarios concentrate the structural response into parts that have not been sufficiently characterized, more tests are recommended to provide additional information for the model. In addition, if the critical parts exhibit a response that requires more complex material models than currently implemented (e.g., fracture, localization, anisotropy, strain rate sensitivity, etc.), additional tests would be recommended to obtain the needed information.

Leaf Spring Suspension for Semitrailer Model

The current tractor and semitrailer FE models both have Airide™ airbag type suspension systems on their rear tandems. Some older tractors and semitrailers used for crash testing have leaf-spring type suspension systems. To be more compatible and comparable with crash test data, it is recommended that this suspension be added to provide the option in the FE model to specify either type of suspension system.

Standard Trailer Lengths

A suite of standard-length trailer FE models would be valuable for researchers. Most semitrailers used in crash tests are specific standard lengths such as 45-feet, 48-feet, 50-feet, and 53-feet. It is recommended that ADAP scripts be developed and applied to create ready-to-run LS-Dyna FE models of several different common-length semitrailers.

Model Sensitivity Analysis and Uncertainty Quantification

The current tractor-trailer model is a complex assembly of parts, materials, FE formulations, and modeling approaches. The model will be used by other researchers in combination with equally complex structure models to simulate impact events. Basic questions need to be answered in order for the model to be widely adopted by prospective users, such as:

- Range of model validity and application
- Identification of the model's crucial factors/parameters and the how they affect key output metrics
- Determination of the model's parameters that best match experimental data, etc.

Sensitivity analysis tools such as parameter studies, design and analysis of computer experiments, and general sampling methods are used in these studies in combination with High Performance Computing resources that are necessary to investigate a wide range of parameters and design space. Uncertainty analysis and quantification based on uncertain inputs can help 1) determine variance of outputs and probabilities of outcomes that identify parameter correlations/local sensitivities, 2) identify inputs whose variances contribute most to output variance (global sensitivity analysis) and 3) quantify uncertainty when using the calibrated model to predict outcomes outside the domain of calibration. The above methods were extensively developed in the U.S. Department of Energy weapons programs and can be applied to the current vehicle models from DOT.

More Extensive Literature Review

The synthesis of the full-scale crash tests provided very valuable information regarding the kinematic behavior and impact response of tractor-semitrailer vehicles during impact with roadside safety barriers. Unfortunately, the synthesis is largely incomplete due to the inaccessibility of much of the crash test data. These tests were conducted over a span of 26 years starting in 1981 and the data storage devices that some of the data were recorded on are incompatible with our current data reading devices. Of the 12 crash tests that were identified in the literature, crash data was available for only 6. It is possible that these test data can be found (in a compatible format) in the NCAC crash test repository. It is our understanding that the data in this repository is available to the public for a nominal fee; however, we expect that this fee may be waived when the data is to be used for government-sponsored projects.

A more extensive literature assessment is recommended to provide more additional meaningful crash test data for the program and for assessing the response of the model. This effort would also provide very useful information to the roadside safety community in general for use in design of roadside safety barriers.

Model Evaluation for Other Impact Conditions

Impact events other than the redirective type have not yet been run with the tractor-semitrailer FE model for the purpose of model validation. Impact scenarios such as vehicle-to-vehicle, barrier-head-on, truck-arrestor, etc. could be done to expand the applicability of the tractor-semitrailer FE model. Whether full-scale crash data for another impact scenario can be obtained or not, it would be valuable to use the FE model in a different impact condition to investigate the general level of performance and robustness of the FE model.

Conduct Full Scale Crash Test for FE Model Validation

This program would benefit significantly from conducting a full-scale crash test for FE model validation. A test specifically designed for this purpose would be more beneficial than validating the model only against prior tests. There are two approaches to performing this task. One is to conduct a full-scale crash test of a tractor-semitrailer of the *same* (or very similar) make and model as the current tractor-semitrailer FE models into a rigid barrier for the specific purpose of obtaining validation data for the FE model. The second approach would be to participate in a scheduled full-scale crash test of a tractor-semitrailer being conducted elsewhere during the performance period of Phase C. This project could request and potentially provide additional funding to the other testing agency's budget to support 1) the purchase of a specific make and model tractor and/or semitrailer that would closely match the current FE model, and 2) the implementation of additional electronic data recording devices at points of interest to the FE model validation.

Appendix A – Validation/Verification Report for FE Model Simulation of MwRSF TL5CMB-2

VALIDATION/VERIFICATION REPORT

FOR

A **Report 350 Test 5-12 36,000V Tractor Semitrailer**
(Report 350 or MASH08 or EN1317 Vehicle Type)

Striking a **Rigid (42-in) Concrete Median Barrier**
(roadside hardware type and name)

Report Date: **05-29-2009**

Type of Report (check one)
☐ Verification (known numerical solution compared to new numerical solution) or
☒ Validation (full-scale crash test compared to a numerical solution).

General Information	**Known Solution**	**Analysis Solution**
Performing Organization	MwRSF	WPI/Battelle
Test/Run Number:	TL5CMB-2	TT090518_RUN1_200ms-approach-SP
Vehicle:	1991 White/GMC Tractor 1988 Pines 48-ft Trailer	01aTrac_Day_v1a_090506.k 02aSemiTrailer48_090520.k
Impact Conditions		
Vehicle Mass:	36,154 kg	36,200 kg
Speed:	84.9 km/hr	84.9 km/hr
Angle:	15.5 degrees	15.5 degrees
Impact Point:		

Composite Validation/Verification Score

	List the Report 350/MASH08 or EN1317 Test Number	T3-11
Step I	Did all solution verification criteria in Table 1 pass?	No
Step II	Do all the time history evaluation scores from Table 2 result in a satisfactory comparison (i.e., the comparison passes the criterion)?	No
Step III	The PIRT score from Table 4 is less than 0.20?	0.09
	Are the results of Steps I through III all affirmative (i.e., YES)? If all three steps result in a "YES" answer, the comparison can be considered validated or verified. If one of the steps results in a negative response, the result cannot be considered validated or verified.	No

The analysis solution (check one) ☐ is ☒ is NOT verified/validated against the known solution.

PART I: BASIC INFORMATION

These forms may be used for validation or verification of roadside hardware crash tests. If the known solution is a full-scale crash test (i.e., physical experiment) then the procedure is a validation exercise. If the known solution is a numerical solution (e.g., a prior finite element model using a different program or earlier version of the software) then the procedure is a verification exercise.

Provide the following basic information for the validation/verification comparison:

1. What type of roadside hardware is being evaluated (check one)?
   - ☒ Longitudinal barrier or transition
   - ☐ Terminal or crash cushion
   - ☐ Breakaway support or work zone traffic control device
   - ☐ Truck-mounted attenuator
   - ☐ Other hardware: _____

2. What test guidelines were used to perform the full-scale crash test (check one)?
   - ☒ NCHRP Report 350
   - ☐ MASH08
   - ☐ EN1317
   - ☐ Other: _____

3. Indicate the test level and number being evaluated (fill in the blank). ___3-11_____

4. Indicate the vehicle type appropriate for the test level and number indicated in item 3 according to the testing guidelines indicated in item 2.

   NCHRP Report 350/MASH08

☐ 700C	☐ 820C	☐ 1100C
☐ 2000P	☐ 2270P	
☐ 8000S	☐ 10000S	
☒ 36000V		
☐ 36000T		

   EN1317

☐ Car (900 kg)	☐ Car (1300 kg)	☐ Car (1500 kg)
☐ Rigid HGV (10 ton)	☐ Rigid HGV (16 ton)	☐ Rigid HGV (30 ton)
☐ Bus (13 ton)		
☐ Articulated HGV (38 ton)		

PART II: ANALYSIS SOLUTION VERIFICATION

Using the results of the analysis solution, fill in the values for Table A-1. These values are indications of whether the analysis solution produced a numerically stable result and do not necessarily mean that the result is a good comparison to the known solution.

Table A- 1. Analysis Solution Verification Table.

	Verification Evaluation Criteria	Change (%)	Pass?
	Total Energy of the analysis solution (i.e., kinetic, potential, contact, etc.) must not vary more than 10 percent from the beginning of the run to the end of the run.	17%	**NO**
	Sliding Interface Energy in the vehicle's self-contact was the source of the increase in total energy (likely initial penetration between parts)		
	Hourglass Energy of the analysis solution at the end of the run is less than 5 percent of the total initial energy at the beginning of the run.	0.1	**YES**
	Mass Added to the total model is less than five percent of the total model mass at the beginning of the run.	0.2	**YES**
	There are no shooting nodes in the solution?		**YES**
	There are no solid elements with negative volumes?		**YES**

If all the analysis solution verification criteria are scored as passing, the analysis solution can be verified or validated against the known solution. If any criterion in Table A-1 does not pass one of the verification criterion listed in Table A-1, the analysis solution cannot be used to verify or validate the known solution.

The Analysis Solution (check one) ☐ passes ☒ does NOT pass <u>all</u> the criteria in Table A-1.

PART III: TIME HISTORY EVALUATION TABLE

A) Analysis of each single channel

Using the RSVVP computer program ('Single channel' option), compute the Sprague & Geers MPC metrics and ANOVA metrics using time-history data from the known and analysis solutions for a time period starting at the beginning of the contact and ending at the loss of contact. The Sprague & Geers metrics and the ANOVA metrics must be calculated based on the acceleration time-history and/or angular rate-time history. If all six data channels are not available for both the known and analysis solutions, enter "N/A" in the column corresponding to the missing data. In some cases, an analyst may deem some of the time histories unimportant and may also record "N/A" for those time histories as well. An example would be a breakaway sign support test where the lateral (i.e., Y) and vertical (i.e., Z) accelerations are presumably insignificant to the dynamics of the crash event. Enter the values obtained from the RSVVP program in
Tables A-2a and A-2b and indicate if the comparison was acceptable or not by entering a "yes" or "no" in the "Pass?" column.

In order for the analysis solution to be considered in agreement with the known solution (i.e., verified or validated), all the criteria scored in Table A-2a must pass.

The Analysis Solution (check one) ☐ passes ☒ does NOT pass all the criteria in Table A-2a.

Table A-2a. Roadside Safety Validation Metrics Rating Table – Time History Comparisons.

	Evaluation Criteria	Time interval [0 sec; 1.55 sec])		
O	***Sprague & Geers Metrics*** The MPC metrics comparing the full-scale test and simulation acceleration time-histories at the center of gravity. Values strictly less than 40 are acceptable.	**M**	**P**	**Pass?**
	X acceleration	45.2	46.2	**NO**
	Y acceleration	11.2	41.0	**NO**
	Z acceleration	1.6	46.6	**NO**
	Yaw Rate	N/A	N/A	
	Roll Rate	N/A	N/A	
	Pitch Rate	N/A	N/A	
	ASI (x and y channels)	8.9	20.7	**YES**
	ASI (x, y and z channels)	12.7	17.4	**YES**
P	***ANOVA Metrics*** Using the acceleration time histories of the center of gravity from the full-scale crash test and the simulation, all three of the following criteria must be met: • The mean residual error must be less than five percent of the peak acceleration ($\bar{e} \leq 0.05 \cdot a_{Peak}$) • The standard deviation of the residuals must be less than 20 percent of the peak acceleration ($\sigma \leq 0.20 \cdot a_{Peak}$) The absolute value of the *t* statistic should be less than the critical *t*-statistic for a two-tailed *t*-test at the five-percent confidence level (i.e., $t_{0.005,\infty}$). Normally, $t_{0.005,\infty} < 2.65$	**Mean Residual**	**Standard Deviation of Residuals**	Pass?
	X acceleration/Peak	0.03	0.15	**YES**
	Y acceleration/Peak	0.00	0.10	**YES**
	Z acceleration/Peak	0.00	0.18	**YES**
	Yaw Rate	N/A	N/A	
	Roll Rate	N/A	N/A	
	Pitch Rate	N/A	N/A	
	ASI (x and y channels)	0.04	0.08	**YES**
	ASI (x, y and z channels)	0.05	0.08	**YES**

B) Analysis of multiple channels

Using the RSVVP computer program ('Multiple channel' option), compute the Sprague & Geers MPC metrics and ANOVA metrics using all the time histories data from the known and analysis solutions for a time period starting at the beginning of the contact and ending at the loss of contact. The Sprague & Geers metrics and the ANOVA metrics must be calculated based on the acceleration time-history. If all six data channels are not available for both the known and analysis solutions, enter "N/A" in the column corresponding to the missing data. In some cases, an analyst may deem some of the time histories unimportant and may also record "N/A" for those time histories as well. An example would be a breakaway sign support test where the lateral (i.e., Y) and vertical (i.e., Z) accelerations are insignificant to the dynamics of the crash event. Enter the values obtained from the RSVVP program in Table A-2b and indicate if the comparison was acceptable or not by entering a "yes" or "no" in the "Pass?" column.

In order for the analysis solution to be considered in agreement with the known solution (i.e., verified or validated), all the criteria scored in Table A-2b must pass.

The Analysis Solution (check one) ☐ passes ☐ does NOT pass all the criteria in Table A-2b.

Note: The multi-channel option is currently under development; thus, this information cannot be computed at this time. This section will be updated at a later date.

Table A-2b. Roadside Safety Validation Metrics Rating Table – Time History Comparisons (Multiple channels).

Evaluation Criteria (time interval [0 sec; 1.55 sec])		
Channels (Select which was used)		
☒ **X Acceleration**	☒ **Y Acceleration**	☒ **Z Acceleration**
☐ **Roll rate**	☐ **Pitch rate**	☐ **Yaw rate**

Multi-Channel Weighting Method	☐ **Peaks** ☒ **Area I** ☐ **Area II** ☐ **Inertial**	**Channel Weight Factors** **X Channel**----- **Y Channel**----- **Z Channel**----- **Roll Channel**----- N/A **Pitch Channel**----- N/A **Yaw Channel**----- N/A

		M	**P**	**C**	**Pass?**
O	***Sprague & Geers Metrics*** The MPC metrics comparing the full-scale test and simulation velocity time-histories at the center of gravity. Values strictly less than 10 percent are acceptable.				
P	***ANOVA Metrics*** Using the acceleration time histories of the center of gravity from the full-scale crash test and the simulation, all three of the following criteria must be met: • The mean residual error must be less than five percent of the peak acceleration ($\bar{e} \le 0.05 \cdot a_{Peak}$) • The standard deviation of the residuals must be less than 20 percent of the peak acceleration ($\sigma \le 0.20 \cdot a_{Peak}$) • The absolute value of the *t* statistic should be less than the critical *t*-statistic for a two-tailed *t*-test at the five-percent confidence level (i.e., $t_{0.005,\infty}$). Normally, $t_{0.005,\infty} < 2.65$	**Mean Residual**	**Standard Deviation of Residuals**		Pass?

PART IV: PHENOMENA IMPORTANCE RANKING TABLE

The following table is similar to the evaluation tables in Report 350 and MASH08. For the test number identified in Part I, circle all the evaluation criteria applicable to that test in Table A-3. Some of the Report 350 evaluation criteria have been removed (i.e., J and K) since they are not generally useful in assessing the comparison between the known and analysis solutions.

Table A- 3. Evaluation Criteria Test Applicability Table.

Evaluation Factors		Evaluation Criteria	Applicable Tests
Structural Adequacy	A	Test article should contain and redirect the vehicle; the vehicle should not penetrate, under-ride, or override the installation although controlled lateral deflection of the test article is acceptable.	10, 11, 12, 20, 21, 22, 35, 36, 37, 38
	B	The test article should readily activate in a predictable manner by breaking away, fracturing or yielding.	60, 61, 70, 71, 80, 81
	C	Acceptable test article performance may be by redirection, controlled penetration or controlled stopping of the vehicle.	30, 31,, 32, 33, 34, 39, 40, 41, 42, 43, 44, 50, 51, 52, 53
Occupant Risk	D	Detached elements, fragments or other debris from the test article should not penetrate or show potential for penetrating the occupant compartment, or present an undue hazard to other traffic, pedestrians or personnel in a work zone.	All
	E	Detached elements, fragments or other debris from the test article, or vehicular damage should not block the driver's vision or otherwise cause the driver to lose control of the vehicle. (Answer Yes or No)	70, 71
	F	The vehicle should remain upright during and after the collision although moderate roll, pitching and yawing are acceptable.	All except those listed in criterion G
	G	It is preferable, although not essential, that the vehicle remain upright during and after collision.	12, 22 (for test level 1 – 30, 31, 32, 33, 34, 35, 36, 37, 38, 39, 40, 41, 42, 43, 44)
	H	Occupant impact velocities should satisfy the following:	10, 20, 30,31, 32, 33, 34, 36, 40, 41, 42, 43, 50, 51, 52, 53, 80, 81
		Occupant Impact Velocity Limits (ft/s)	
		Component / Preferred / Maximum	
		Longitudinal and Lateral / 30 / 40	
		Longitudinal / 10 / 15	60, 61, 70, 71
	I	Occupant ridedown accelerations should satisfy the following:	10, 20, 30,31, 32, 33, 34, 36, 40, 41, 42, 43, 50, 51, 52, 53, 60, 61, 70, 71, 80, 81
		Occupant Ridedown Acceleration Limits (g's)	
		Component / Preferred / Maximum	
		Longitudinal and Lateral / 15 / 20	
Vehicle Trajectory	L	The occupant impact velocity in the longitudinal direction should not exceed 40 ft/sec and the occupant ride-down acceleration in the longitudinal direction should not exceed 20 G's.	11,21, 35, 37, 38, 39
	M	The exit angle from the test article preferable should be less than 60 percent of test impact angle, measured at the time of vehicle loss of contact with test device.	10, 11, 12, 20, 21, 22, 35, 36, 37, 38, 39
	N	Vehicle trajectory behind the test article is acceptable.	30, 31, 32, 33, 34, 39, 42, 43, 44, 60, 61, 70, 71, 80, 81

Complete Table A-4 according to the results of the known solution (e.g., crash test) and the analysis solution (e.g., simulation). If the result of the analysis solution agrees with the known solution, mark the "agree" column "yes." For example, if the vehicle in both the known and analysis solutions rolls over and, therefore, fails criterion F, the known and the analysis columns for criterion F would be evaluated as "no." Even though both failed the criteria, they agree with each other so the "agree" column is evaluated as "yes." Any criterion that is not applicable to the test being evaluated should be indicated by entering "NA" in the "agree?" column for that row.

Many of the Report 350 evaluation criteria have been subdivided into more specific phenomenon. For example, criterion A is divided into 8 sub-criteria, A1 through A8, that provide more specific phenomena for evaluation. Some of the values are simple yes or no questions while other request numerical values. For the numerical phenomena, the analyst should enter the value for the known and analysis result and then calculate the relative difference. Relative difference is always the absolute value of the difference of the known and analysis solutions divided by the known solution. Enter the value in the "relative difference" column. If the relative difference is less than 20 percent, enter "yes" in the "agree?" column. Otherwise enter "no."

If a numerical model was not created to represent the phenomenon, a value of "NM" (i.e., not modeled) should be entered in the appropriate column of Table A-4. If the known solution for that phenomenon number is "no" then a "NM" value in the "test result" column can be considered to agree. For example, if the material model for the rail element did not include the possibility of failure, "NM" should be entered for phenomenon number T in Table A-4. If the known solution does not indicate rail rupture or failure (i.e., phenomenon T = "no"), then the known and analysis solutions agree and a "yes" can be entered in the "agree?" column. On the other hand, if the known solution shows that a rail rupture did occur resulting in a phenomenon T entry of "yes" for the known solution, the known and analysis solutions do not agree and "no" should be entered in the "agree?" column. Analysts should seriously consider refining their model to incorporate any phenomena that appear in the known solution.

Calculate the PIRT sub-score from Table A-2 by counting all the "yes" values in the "agree" column and all the "no" values in the agree column. Do not include "NA" values in the summation. The score is the number of "no" values divided by the sum of the "no" and "yes" values.

$$TEC_{subscore} = \frac{\mathrm{NO}}{\mathrm{NO} + \mathrm{YES}} = {}^{1}/_{19} = 0.05$$

Enter the PIRT subscore on page 1.

Table A- 4. Roadside Safety Phenomena Importance Ranking Table.

Evaluation Criteria				Known Result	Analysis Result	Relative Diff. (%)	Agree?
Structural Adequacy	A	A1	Test article should contain and redirect the vehicle; the vehicle should not penetrate, under-ride, or override the installation although controlled lateral deflection of the test article is acceptable. (Answer Yes or No)	Yes	Yes		**YES**
		A2	Failure of u-bolt connection of Front Axle to Suspension (Impact Side)	Yes	Yes		**YES**
	B	B1	The test article should readily activate in a predictable manner by breaking away, fracturing or yielding. (Answer Yes or No)				
	C	C1	Acceptable test article performance may be by redirection, controlled penetration or controlled stopping of the vehicle. (Answer Yes or No)				
		C2	The relative difference in maximum system stroke is less than 20 percent.				
		C3	The relative difference in the number of broken or significantly bent posts is less than 20 percent.				
		C4	The rail element did not rupture or tear (Answer Yes or No).				
		C5	There were no failures of connector elements (Answer Yes or No).				

Table A-4. Roadside Safety Phenomena Importance Ranking Table (continued).

Evaluation Criteria				Known Result	Analysis Result	Relative Diff. (%)	Agree?
Occupant Risk	D		Detached elements, fragments or other debris from the test article should not penetrate or show potential for penetrating the occupant compartment, or present an undue hazard to other traffic, pedestrians or personnel in a work zone. (Answer Yes or No)	Pass	Pass		YES
	E		Detached elements, fragments or other debris from the test article, or vehicular damage should not block the driver's vision or otherwise cause the driver to lose control of the vehicle. (Answer Yes or No)				
	F	F1	The vehicle should remain upright during and after the collision although moderate roll, pitching and yawing are acceptable. (Answer Yes or No)				
		F2	The relative difference between the maximum roll of the vehicle is less than 20 percent.				
		F3	The relative difference between the maximum pitch of the vehicle is less than 20 percent.				
		F4	The relative difference between the maximum yaw of the vehicle is less than 20 percent.				
	G	G1	It is preferable, although not essential, that the vehicle remain upright during and after collision. (Answer Yes or No)	Yes	Yes		YES
		G2	The relative difference between the tractor roll is less than 20 percent. (First Peak)	15.0	14.6	3	YES
		G3	The relative difference between the tractor roll is less than 20 percent. (Second Peak)	19.0	23.8	25	NO
		G4	The relative difference between the trailer roll is less than 20 percent.	42	42.8	2	YES
		G5	The frontal axle connection failed (Tests 12 and 22 only).	Yes	Yes		YES
	H	H1	The relative difference in the Occupant impact velocity is less than 20 percent: • Longitudinal OIV (m/s) • Lateral OIV (m/s)				
		H2	• Longitudinal OIV				
		H3	• THIV (m/s)				
	I		The relative difference in the Occupant Ridedown Accelerations is less than 20 percent: • Longitudinal ORA • Lateral ORA • PHD • ASI				

Table A-4. Roadside Safety Phenomena Importance Ranking Table (continued).

Evaluation Criteria				Known Result	Analysis Result	Relative Diff. (%)	Agree?
Vehicle Trajectory	L		The occupant impact velocity in the longitudinal direction should not exceed 40 ft/sec and the occupant ridedown acceleration in the longitudinal direction should not exceed 20 G's.				
	M	M1	The exit angle from the test article preferable should be less than 60 percent of test impact angle, measured at the time of vehicle loss of contact with test device.	Yes	Yes		**YES**
		M2	The relative difference in the exit angle at loss of contact is less than 20 percent.	0°	0°	0	**YES**
		M3	The relative difference in the exit velocity at loss of contact is less than 20 percent.	unknown	N/A		
		M4	One or more vehicle tires failed or de-beaded during the collision event (Answer Yes or No).	Yes	N.A.		
	N		Vehicle trajectory went behind the test article (Answer Yes or No)	No	No		**YES**

Appendix B – References

1. Plaxico, C., Kennedy, J., Simunovic, S. and Zisi, N., Enhanced Finite Element Analysis Crash Model of Tractor-Trailers (Phase A), National Transportation Research Center, Inc., Knoxville, TN, 2008.

2. Ross, H.E., Sicking, D.L., and Perrara, H.S., "Recommended Procedures for the Safety Performance Evaluation of Highway Appurtenances," *National Cooperative Highway Research Program Report No. 350*, Transportation Research Board, Washington, D.C., 1993.

3. Hirsh, T.J. and Arnold, A., "Bridge Rail to Restrain and Redirect 80,000 lb Trucks," Report No. FHWA/TX-81/16+230-4F, Texas State Dept. of Highways & Public Transportation, Austin, Texas (prepared by Texas Transportation Institute, College Station, Texas), 1981. [Test No. 6]

4. Hirsch, T.J, Fairbanks, W.L., and Buth, C.E., "Concrete Safety Shape with Metal on Top to Redirect 80,000-lb Trucks," Report No. FHWA/TX-83/ +416-1F, Federal Highway Administration, U.S. Department of Transportation, Washington, D.C. (prepared by Texas Transportation Institute, College Station, Texas), December 1984. [Test No. 2416-1]

5. Campise, W.L. and Buth, C.E., "Performance Limits of Longitudinal Barrier Systems, Volume III – Appendix B: Details of Full-Scale Crash Tests on Longitudinal Barriers," Federal Highway Administration, U.S. Department of Transportation, Washington, D.C. (prepared by Texas Transportation Institute, College Station, Texas), May 1985. [Test No. 4798-13]

6. Mak, King K., Beason, W.L., Hirsch, T.J., and Campise, W.L., "Oblique Angle Crash Tests of Loaded Heavy Trucks into an Instrumented Wall," Report No. DOT HS 807 256, National Highway Traffic Safety Administration, Washington, D.C., (prepared by Texas Transportation Institute, College Station, Texas), 1988. [Test No. 7046-3 and 7046-4]

7. Mak, King K. and Campise, W.L., "Test and Evaluation of Ontario 'Tall Wall' Barrier with an 80,000-Pound Tractor-Trailer," Project No. 4221-9089-534, Ontario Ministry of Transportation, Ontario (prepared by Texas Transportation Institute, College Station, Texas), September 1990. [Test No. 7162-1]

8. Buth, C.E., Hirsch, T.J., and Menges, W.L., "Testing of New Bridge Rail and Transition Designs," Report No. FHWA-RD-93-068, Vol. XI Appendix J: 42-in (1.07-m) F-Shape Bridge Railing, Turner-Fairbank Highway Research Center, Federal Highway Administration, McLean, Virginia, (prepared by Texas Transportation Institute, College Station, Texas), 1993. [Test No. 7069-10]

9. Buth, C.E., Hirsch, T.J., and Menges, W.L., "Testing of New Bridge Rail and Transition Designs," Report No. FHWA-RD-93-067, Vol. X Appendix I: 42-in (1.07-m) Concrete Parapet Bridge Railing, Turner-Fairbank Highway Research Center, Federal Highway Administration, McLean, Virginia, (prepared by Texas Transportation Institute, College Station, Texas), 1993. [Test No. 7069-13]

10. Alberson, D.C., Zimmer, R.A., and Menges, W.L., "NCHRP Report 350 Compliance Test 5-12 of the 1.07-m Vertical Wall Bridge Railing," Report No. FHWA-RD-96-199, Office of Safety and Traffic Operations R&D, Federal Highway Administration, McLean, Virginia, May 1996. [Test No. 405511-2]

11. Marzougui, FOIL Test 03008, National Crash Analysis Center, Ashburn, VA, 2003.

12. Polivka, K.A., Faller, R.K., Holloway, J.C., Rohde, J.R., and Sicking, D.L., "Development, Testing, and Evaluation of NDOR's TL-5 Aesthetic Open Concrete Bridge Rail," Report No. TRP-03-148-05, Midwest Roadside Safety Facility, Lincoln, Nebraska, 2005. [Test No. ACBR-1]

13. Beason, W.L., Hirsch, T.J., and Campise, W.L., *Measurement of Heavy Vehicle Impact Forces and Inertia Properties*, Report No. FHWA-RD-89-120, Performed for the Office of Safety and Traffic Operations R&D, Federal Highway Administration, Performed by the Texas Transportation Institute, Texas A&M University, College Station, Texas, May 1989. [Test No. 7046-9]

14. Rosenbaugh, S.K, Sicking, D.L., and Faller, R.K., "Development of a TL-5 Vertical Faced Concrete Median Barrier Incorporating Head Ejection Criteria," Test Report No. TRP-030194-07, Midwest Roadside Safety Facility, University of Nebraska-Lincoln, 12/10/2007. [Test No. TL5CMB-2]

15. LS-DYNA Keyword User's Manual, Version 971, Volume 1, Livermore Software Technology Corporation (LSTC), Livermore, California, May 2007.

16. Dorsey Trailers. Products Catalog. http://www.dorseytrailer.net, 2008.

17. Great Dane Trailers. Products Catalog. http://www.greatdanetrailers.com, 2008.

18. National Semi-Trailer Corp. Products. http://www.nationalsemi.com/semi-trailers.asp, 2008.

19. Stoughton Trailers. Products Catalog. http://www.stoughton-trailers.com, 2008.

20. Titan Trailers Inc. Products, THINWALL Extruded Panels. http://www.titantrailers.com, 2008.

21. Vanguard National Trailer Corp. Products. http://www.vanguardtrailer.com; 2008.

22. Stoughton Trailers. Exploded Parts Diagram. http://www.stoughton-trailers.com/parts/explodedtrailer.htm, 2008.

23. Asa Alloys. Truck and Trailer Materials. http://www.asaalloys.com/tandtmaterials.html, 2008.

24. Aluminum Line Products Company. ALPCO Product Catalog. http://aluminumline.com, 2008.

25. Truckline Sale. Truck Trailer Body Parts. http://www.truckline-sale.com; 2008.

26. Great Dane Trailers. Product Line Card. http://www.greatdanetrailers.com/parts/GDLineCard.pdf; 2008.

27. Whiting Door Manufacturing Corp. Products, Doors. http://www.whitingdoor.com; 2008.

28. US Steel Corp. North American Flat Rolled Products. http://www.uss.com; 2008.

29. ASTM International. Standard Specification for Steel Sheet, Zinc-Coated (Galvanized) or Zinc-Iron Alloy-Coated (Galvannealed) by the Hot-Dip Process. 2008; A 653/A 653M - 08.

30. ASTM International. Hot-Rolled Structural Steel, High-Strength Low-Alloy Plate with Improved Formability. 2005.

31. Proft, T., editor. Fatigue failure of welded truck cross members: ASM International; 1992.

32. SAF Holland. Products. http://www.safholland.us, 2008.

33. Yamada, Y., and Kuwabara, T., Materials for Springs. Springer-Verlag Berlin Heidelberg, 2007.

34. Clarke, C. and Borowski, G., Evaluation of a leaf spring failure. Journal of Failure Analysis and Prevention. 2005;5(6):54-63.

35. Oberg, E., Jones, F., Horton, H., and Ryffel, H., Machinery's Handbook. Industrial Press, 2004.

36. ASTM International. Standard Specification for Steel Castings, High Strength, for Structural Purposes. 2008;148/A 148M - 08.

37. Wieser, P., Steel Castings Handbook. Steel Founders' Society of America, 1980.

38. Independence Tube. Trailer Axle Tube. http://www.independencetube.com/downloads/axle_tube.pdf, 2008.

39. ASTM International. Standard Specification for Cold-Formed Welded and Seamless Carbon Steel Structural Tubing in Rounds and Shapes. 2007;A 500/A 500M – 07.

40. Cardarelli, F., Materials handbook : a concise desktop reference. Springer-Verlag London Limited, 2008.

41. Davis, J., Metals handbook. ASM International. Handbook Committee, 1998.

42. Maykuth, D.J., Structural Alloys Handbook. Mechanical Properties Data Center, Battelle Columbus Laboratories, 1982.

43. Mullins, J., Ductile Iron Data for Design Engineers. Ductile Iron Data Society, Soremetal Technical Services, Rio Tinto Iron & Titanium Inc, 1990.

44. Krauss, G., Steels: heat treatment and processing principles. 1990.

45. Buschow, K.H.J., Cahn, R.W., Flemings, M.C., Ilschner, B., Kramer, E.J., and Mahajan, S., Encyclopedia of Materials – Science and Technology. Elsevier, 2001.

46. Blake, A., What every engineer should know about threaded fasteners: materials and design. CRC Press, 1986.

47. Hood, A., Fastener Materials. Handbook of Bolts and Bolted Joints: CRC Press, 1998.

48. Walton, C., Opar T. Iron Castings Handbook. Iron Castings Society, Inc., 1981.

49. Ductile Iron Society. Ductile Iron Data for Design Engineers, Heavy Truck and Bus Components. http://www.ductile.org, 2008.

50. Specialty Steel Industry of North America. Design Guidelines for the Selection and Use of Stainless Steel. http://www.ssina.com.

51. SAE International. Mechanical and Material Requirements for Externally Threaded Fasteners. 1999;J429.

52. Belytschko, T. and Mish, K., Computability in non-linear solid mechanics. Int J Numer Meth Eng. 2001;52:3-21.

53. Crisfield, M., Non-linear finite element analysis of solids and structures. John Wiley & Sons Inc, 1991.

54. Hallquist, J., LS-DYNA Keyword User's Manual Version 970. Livermore Software Technology Corporation. 2003.

55. Hallquist, J., LS-DYNA Theory Manual. Livermore Software Technology Corporation; 2006.

56. Moosbrugger, C., Atlas of Stress--Strain Curves. ASM International, 2002.

57. ASTM International. Standard Specification for Ductile Iron Castings. 2004;A 536 – 84.

58. Automation Creations Inc. MatWeb: material property data. http://www.matweb.com, 2008.

59. Blair, M. and Stevens, T., Steel Castings Handbook. Steel Founders' Society of America, 1995.

60. Hoge, K., Influence of strain rate on mechanical properties of 6061-T6 aluminum under uniaxial and biaxial states of stress. Experimental Mechanics. 1966;6(4):204-211.

61. Nicholas, T., Tensile testing of materials at high rates of strain. Experimental Mechanics. 1981;21(5):177-185.

62. Wilson, D., Piecewise linear approximations of fewest line segments. ACM Transactions on Mathematical Software. 1972;40:187 - 198.

63. LS-DYNA Keyword User's Manual, Version 971, Volumes 1 and 2, Livermore Software Technology Corporation (LSTC), May 2007.

64. Ray, M.H., Mongiardini, M., Atahan, A.O., Plaxico, C.A., and Anghileri, M., "Recommended Procedures for the Verification and Validation of Computer Simulations used for Roadside Safety Applications," Interim Report –Revision 1.3 March 2009, Project No. 22-24, National Cooperative Highway Research Program, December 2007.

65. http://civil-ws2.wpi.edu/Documents/Roadsafe/NCHRP22-24/RevisedInterimReport.pdf

66. Geers, T.L., "An Objective Error Measure for the Comparison of Calculated and Measured Transient Response Histories," The Shock and Vibrations Bulletin, The Shock and Vibration Information Center, Navl Research Laboratory, Washington, D.C., Bulletin 54, Part 2, pp 99:107, June 1984.

67. Sprague, M.A. and Geers, T.L., Spectral elements and field separation for an acoustic fluid subject to cavitations," Journal of Computational Physics, pp. 184:149, Volume 162, 2003.

68. Ray, M.H., “Repeatability of Full-Scale Crash Tests and a Criteria for Validating Finite Element Simulations,” Transportation Research Record, Vol. 1528, pp. 155-160, 1996.

69. Road Barrier Upgrade of Standards (ROBUST), “Deliverable 4.1.1 – Full scale test results – An analysis,” ROBUST PROJECT, GRD-2002-70021.

70. Ray, M.H., Anghileri, M., Mongiardini, M., “Comparison of Validation Metrics Using Full-Scale Automobile Crash Tests,” 8th World Congress on Computational Mechanics, Venice, Italy, June 30 – July 5, 2008.

71. European Committee of Standardization, “European Standard EN 1317-1 and EN 1317-2: Road Restraint Systems,” CEN, 1998.